Enzymatic alternatives to permanent hair straightening methods

Candice Lauren Jeanne Ford

Faculty of Engineering

A thesis submitted to the University of Nottingham for the degree of Doctor of Philosophy

March 2023

Acknowledgements

I would like to express my biggest thanks to all the individuals and organisations who have supported me throughout this PhD journey. Firstly, I want to acknowledge my main supervisor, Dr Anca Pordea, without whom this project would not have been possible. Her exceptional support, guidance, and encouragement throughout this journey have been invaluable. I would also like to thank my industrial supervisor, Dr Daniele Parisi, for his help and kindness over the course of my PhD, providing me with the opportunity to conduct valuable experiments within the Croda labs.

I am also very grateful to the Croda team, Dr Mike Hindley, Dr Elizabeth Ryder, Dr Kate Thorton, and Dr Timothy Miller, for their support and valuable contributions towards the industrial aspect of my project. Special thanks also go to my secondary supervisors, Dr Anna Croft and Dr Alex Conradie, for their time, guidance, and constructive feedback. Thank you to the CDT in Sustainable Chemistry team, namely Pete Licence and Peri, as well as the EPSRC and CRODA, for providing me with the opportunity to pursue this PhD.

Moreover, I am deeply grateful to my lab, office and CDT colleagues, including Harry, Simone, Aziana, Andy and Aoife, who have made my PhD journey a lot smoother. Tini, I am so glad our paths crossed and could not be more thankful for the great friendship and support. I would also like to extend my appreciation to Amy, Lifang, and Steve for their technical support.

I am grateful to the great friends I made in Nottingham, Anna, Malte, Sarah, Jose and many others, thank you for the adventures and memories we have shared together. A special mention to Ollie and Irene for being the best flatmates I could have hoped for in the first three years of the PhD. Gemma, thank you for sharing this Bristol to Nottingham journey with me, your encouragements over the past 9 years has been invaluable and I am so proud of us for what we have accomplished! I also wanted to mention Laure, Paul, Charlotte, Laura, Sarah and Kelly, amongst others, thank you for your unwavering support and friendship.

Finally, I would like to express my special thanks to my parents Martin and Francoise, my uncle Giles, my sister Emma, and brother Nicholas, for their ongoing support and encouragement through thick and thin. I would not be where I am today without their love and support. To my partner Richard, thank you for sharing this PhD journey with me from day one, for your relentless support, encouragement, and love; you have made this experience very special.

Abstract

Permanent hair straightening is a highly popular treatment, especially among African hair types. However, current methods rely on the use of harsh chemicals, such as sodium hydroxide or formaldehyde, and are associated with a range of health concerns, including hair breakage, loss and severe scalp disorders. Permanent hair straightening treatments usually involve a disulfide bond-breaking step which allows the opening of the hair structure, followed by mechanical hair straightening and crosslinking, which helps to set the new hair morphology. In recent years, the cosmetic sector has seen the development of a considerable range of biotechnologically-derived active agents, which offer biocompatibility, versatile activity and good performance.

This project explores the feasibility of incorporating enzymes, which exhibit relevant disulfide bond-reducing and crosslinking activities in nature, into milder permanent hair straightening treatments. The thioredoxin system from *Bacillus subtilis* was identified as a potential alternative for breaking disulfide bonds in keratins. The enzymes thioredoxin and thioredoxin reductases were expressed and purified in *E. coli*. Thioredoxin activity was initially assessed on Keratec™ IFP, a solubilised wool keratin substrate bearing a mix of cystine and sulfonated thiol motifs, associated with easier enzymatic keratin penetration than insoluble counterparts. Reduced thioredoxin was regenerated either by DTT or thioredoxin reductase and NADPH, as electron donors. The reduction of S-sulfocysteine and disulfide bonds in soluble keratin by thioredoxin was observed both by Ellman's and NADPH assays, which monitor free thiols and NADPH consumption, respectively. However, disulfide bond reducing activity was not observed using solid human hair keratin, despite attempts to improve substrate availability through treatment with keratinase from *Bacillus licheniformis* and swelling agents, such as urea.

Enzymatic keratin crosslinking was then studied using laccase from *Trametes versicolor*, tyrosinase from mushroom and microbial transglutaminase, all well characterised crosslinking enzymes with activity on proteins and currently used in a range of industries (eg. food, textile). Soluble keratin crosslinking by laccase was observed using size-exclusion chromatography (SEM) and sodium dodecyl-sulfate polyacrylamide gel electrophoresis (SDS PAGE), both in the presence and absence of vanillin and acetosyringone mediators. However, a lack of significant enzymatic crosslinking was noted for solid hair keratin, where no change in tensile strength was observed upon treatment with laccase.

Overall, novel enzymatic reducing and crosslinking modifications were successfully carried out on solubilised keratin. However, challenges remain regarding solid hair keratin, associated with poor substrate availability and enzyme penetration.

Table of Contents

List of Figures

List of Tables

List of abbreviations

ABTS	2,2'-azino-bis(3-ethylbenzothiazoline-6-sulfonic acid)
Bp	Base pair
BCA	Bicinchoninic acid assay
BLAST	Basic alignment search tool
BSA	Bovine serum albumin
C	Cysteine
Cbz-Gln-Gly	Carbobenzoxy-L-glutaminylglycine
CMC	Cellular Membrane Complex
DNA	Deoxyribonucleic acid
DTNB	5,5’-dithiobis-(2-nitrobenzoic acid)
DTT	Dithiothreitol
E. coli	*Escherichia coli*
EDC	1-ethyl-3-(3-dimethylaminopropyl)carbodiimide
EDTA	Ethylenediaminetetraacetic acid
ER	Endoplasmic reticulum
FAD	Flavin adenine dinucleotide
Grx	Glutaredoxin
GrxR	Glutathione reductase
GSH	Reduced glutathione
GSSG	Oxidised glutathione
HCl	Hydrochloric acid

IMAC	Immobilised metal affinity chromatography
IFP	Intermediate filament proteins
IPTG	Isopropyl β-D-1-thiogalactopyranoside
KA	Keratin Azure
kDa	Kilodalton
kerA	Gene for keratinase from Bacillus licheniformis
KerA	Keratinase from *Bacillus licheniformis*
Lac	Laccase
LB	Lysogeny Broth
L-DOPA	l-3,4-dihydroxyphenylalanine
NADPH	Nicotinamide adenine dinucleotide phosphate
NCBI	National centre for biotechnology information
NEB	New England biolabs
PCR	Polymerase chain reaction
PDI	Protein disulfide isomerase
PDO	Protein disulfide oxidoreductases
PLP	Pyridoxal phosphate
PoLac	Laccase from *Pleurotus ostreatus*
SDS-PAGE	Sodium dodecyl sulfate-polyacrylamide gel electrophoresis

SEC	Size-exclusion chromatography
SEM	Scanning electron microscopy
TAE	Tris base, acetic acid & EDTA
TCA	Trichloroacetic Acid
Tg	Microbial transglutaminase
Trx	Thioredoxin
Trx1	Thioredoxin from *E. coli*
trxA	Gene for Thioredoxin from *Bacillus subtilis*
TrxA	Thioredoxin from *Bacillus subtilis*
trxB	Gene for Thioredoxin reductase from *Bacillus subtilis*
TrxB	Thioredoxin reductase from *Bacillus subtilis*
TvLac	Laccase from *Trametes versicolor*
U	Enzymatic activity units
UV	Ultraviolet
Tyr	Tyrosinase from mushroom

1. Literature review

Hair care products allow for the modification of hair shape, length and colour. With companies such as L'Oréal and Unilever, the hair care market is constantly growing and expected to reach $116 billion by 2024.[1] Permanent hair straightening is a popular treatment, especially amongst African hair-types.[2] Indeed, hair relaxing is used by up to 70% of females of black African ancestry, aimed at beauty, ease of daily hair maintenance as well as acceptance against social and environmental pressures.[3–5]

Hair mainly comprises keratin, an insoluble protein with highly crosslinked and tightly packed polypeptide chains.[6] Permanent hair modifications rely on the breaking of disulfide bonds linking keratin chains together. The formation of new crosslinks between those polypeptide chains then helps stabilise the new hair fibre configuration.[7,8] However, current permanent methods rely on the use of harsh chemicals associated with hair breakage and loss, as well as severe scalp disorders, highlighting the need for milder active agents.[3,4,16–18,7,9–15] The chemistry involved in permanent hair straightening (*i.e.* disulfide bond reduction and crosslinking reinstatement) is prevalent in natural enzymatic activities. The development of biotechnologically-derived active agents, which offer biocompatibility, eco-friendly nature, versatile activity, and good performance, therefore, appears to be a fertile area of research.[19,20]

Keratin is a waste-product from various industries such as leather and poultry industries, and it is challenging to manage or degrade due to its highly crosslinked structure.[21,22] In this way, keratin degradation has been extensively studied, and a range of microorganisms with keratinolytic activity, such as *Bacillus subtilis* and *Bacillus halodurans* have been identified.[23–26]

However, the mechanism behind keratin degradation remains unclear, specifically the role of disulfide bond reduction, which has been reported in keratin-degrading organisms.[23,24,26] While most research on keratin degradation has been conducted on whole microorganisms, the use of isolated enzymes presents many advantages, including faster scale-up, more reaction specificity, and easier storage.[27–30] To this end, a range of enzymes have been isolated from these keratin-degrading microorganisms, mainly keratinases, such as KerA from *Bacillus licheniformis*, which catalyses keratin hydrolysis.[25,31,32] Conflicting evidence for the ability of such enzymes to degrade keratin in the absence of concomitant disulfide bond reduction has been described in the literature.[30,33] A disulfide bond reducing-enzyme was also isolated from *Bacillus halodurans* PPKS-2 and constitutes, to our knowledge, the only keratin disulfide bond-reducing enzyme for which sequence information is disclosed.[24] According to the authors, this enzyme belongs to the family of disulfide bond reductases, known to reduce disulfide bonds in folded proteins.

The value of enzymes as crosslinking agents for the setting of macromolecules such as keratin is based on a large body of research exploring the biocatalytic formation of covalent bonds in a highly selective, atom-efficient and biocompatible manner.[34] Indeed, enzymes have evolved over time to catalyse covalent modifications of proteins essential to pro- and eukaryotic cells.[35] In this way, a range of protein-crosslinking enzymes have been identified, including transglutaminases, laccases and tyrosinases, with an abundance of industrial applications (e.g. dairy, textile etc.).[35–37] Commonly described substrates for these enzymes include β-casein, lignin, gelatine, as well keratin.[38–40] However, the formation of keratin-keratin

crosslinks by these enzymes has not yet been investigated using human hair as a substrate.

To address this critical gap in the literature, this project aims to investigate the potential of disulfide bond reducing and crosslinking enzymes towards permanent hair straightening as milder and greener alternatives to harsh chemicals currently used in the market. If successful, the use of enzymes as active agents could lead to a more positive impact on both consumers and the environment, with potential use in fields beyond the hair care industry.

1.1. Human hair structure

Human hair is composed of proteins, mainly hard keratins characterised by high cysteine contents, lipids, water and small amounts of trace elements.[41,42] Keratins are filament-forming proteins classified as α- and β-keratins, which vary in molecular structure.[43] Indeed, depending on its amino acid sequence, the secondary structure of keratin either forms an α-helix (α-keratin), around 45 nm long and organised as coiled-coil heterodimers (2 nm diameter) composed of type I (acidic, 40-50 kDa) and type II (basic, 50-60 kDa) α-keratins - or β-sheets (β-keratin) (Figure 1a-b), which consist of laterally packed (usually antiparallel) β-strands.[44] Repeats of seven amino acids are a prerequisite for the formation of α-helices and coiled-coil heterodimers, which then aggregate into protofilaments, protofibrils and finally intermediate filaments (7-10 nm).[44] On the other hand, β-keratin filaments consist of polypeptide chains which fold to form four β-strands, which link through hydrogen bonding, resulting in β-pleated sheets. Two β-pleated sheets then combine into a filament (3-4 nm diameter, 9.5 nm length).[43] Moreover, the molecular mass of α-keratin ranges from 40 to 68 kDa, compared to 10-22 kDa in the case of β-keratin.[43] Wool, as a representative α-keratin material, has been extensively studied, as well as

feathers as a typical β-keratin material. Human hair is mainly composed of α-keratins.

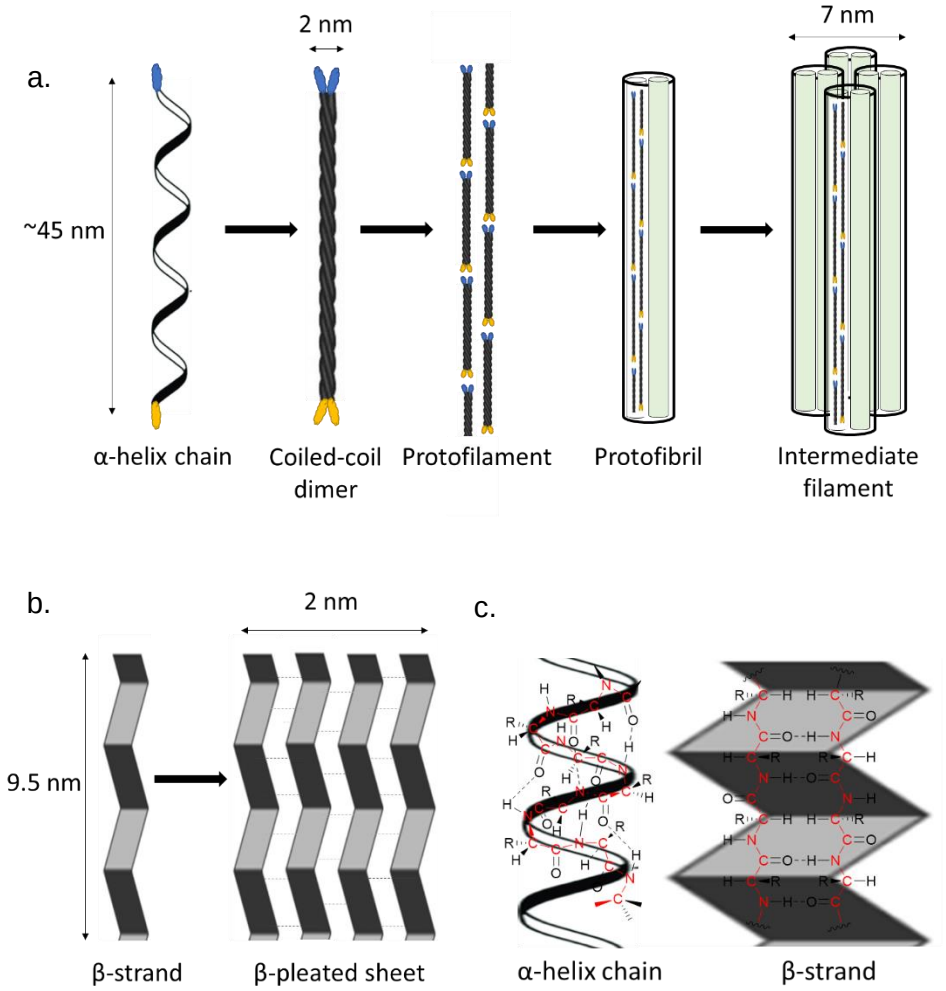

Figure 1. Schematic drawings of α- and β-keratin, a. α-helix chains form coiled-coil dimers which assemble to form protofilaments, protofibrils and finally intermediate filaments, b. one polypeptide chain folds into a four β-strands, which twists to form a β-pleated sheet, two of which assemble into a β-keratin filament, c. α-helix and β-strand polypeptide chains.

Hair fibres are made up of distinct morphological constituents: the cuticle and cortex, as well as a medulla region in thicker fibres (Figure 2a).[45]

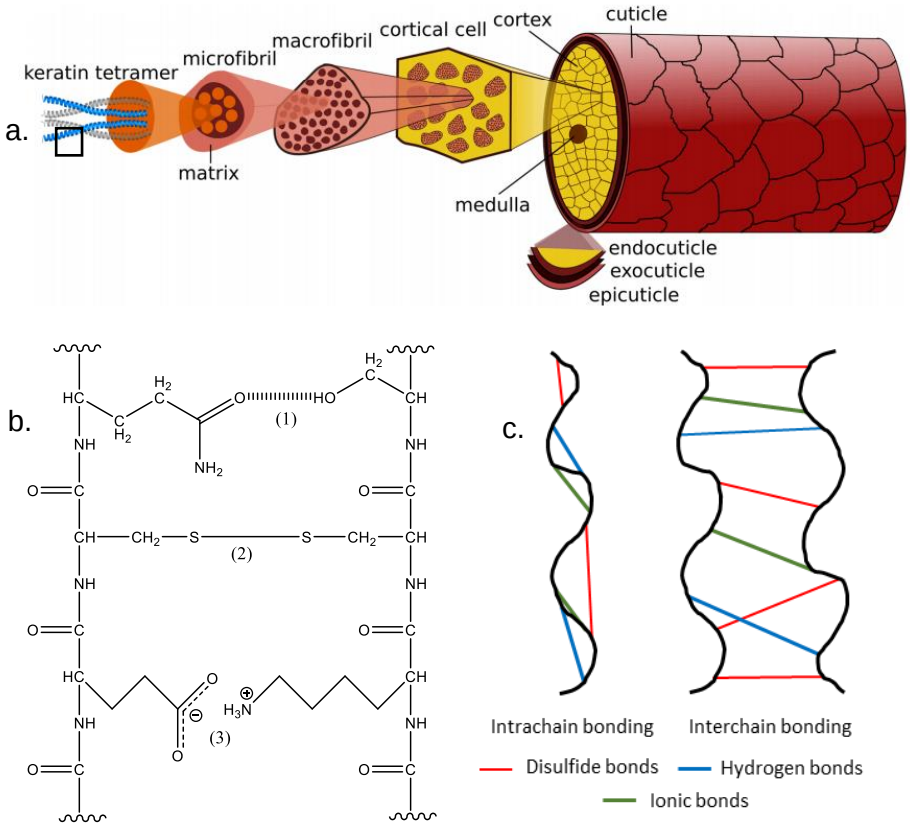

Figure 2. Human hair and keratin structures. a. Schematic cross-section of a hair fibre, reproduced from Cruz *et al*. (2016).[45] b. Keratin stabilisation *via* interactions between chains (1: hydrogen bond, 2: disulfide bond and 3: electrostatic interaction). c. Intra- and interchain interactions in keratin.

The cuticle, which forms a protective barrier over the cortex and holds moisture, is mainly composed of layered β-keratins (β-pleated sheet).[41,46] It contains a lipid layer, including 18-methyl eicosanoic acid (18-MEA) and free lipids, which contribute to hair lubricity and acts as a hydrophobic barrier against hair penetration, as well as an A-layer, and exocuticle and endocuticle keratin layers.[9] The A layer and exocuticle are highly-crosslinked layers with 15-30% cysteine content, responsible for cuticle strength and rigidity, while the endocuticle bears low cysteine levels (3%) and is, therefore, more prone to swelling in water.[5,46] Cuticle cells are held together by the cellular membrane complex (CMC).[45]

The cortex accounts for most of the hair mass and is responsible for hair tensile strength. It is mainly composed of α-keratins (α-helices) and keratin-

associated proteins (KAPs), organised into tightly packed cortical cells.[47] In the case of α-keratins, two right-handed α-helix chains, type I and type II α-keratins interact with each other to form coiled-coil heterodimers.[41,46,48,49] These dimers then aggregate into tetramers, or protofilaments.[50] Two protofilaments then combine into a protofibril, and four protofibrils form an intermediate filament (7 nm diameter).[50] These intermediate filament proteins (IFPs), also called microfibrils, in turn, , constitute macrofibrils which make up cortical cells.[45] IFPs are embedded in an amorphous matrix made of KAPs, also known as γ-keratins (10-25 kDa). KAPs contain high levels of cysteine amino acids (approximately 20%) and hold the cortical cell structure together *via* disulfide bonds, conferring the inertness, rigidity and mechanical strength of keratin fibres.[41,46,48,51] Finally, the CMC binds cortical cells, or cuticle-cortical cells, together.[9]

1.1.1. Chemical interactions within the hair cortex

Within the cortex, keratin filament α-helices are held together by a range of chemical interactions, including ionic forces, hydrogen bonds, Van der Waals forces, hydrophobic bonds (in the presence of water) and disulfide bonds (Figure 2b). These interactions depend on the availability of reactive groups associated with fibre structure. Hydrogen bonds, which are weak and easily broken by water, are the most frequent in hair and form interchain bonds between amide groups essential for α-keratin stability.[7] Ionic bonds, which are held together by coulombic forces, form between acidic and basic side chains and are relatively stable in aqueous environments but highly susceptible to acids and alkalis.[5] Hydrophobic interactions occur between non-polar groups along the keratin and Van der Waals forces are caused by a change in dipole in those non-polar groups.[45] Disulfide bonds link two cysteine amino acids in spatial vicinity together, forming a bridge between

two chains (intermolecular) or two portions of the main chain (intramolecular) (Figure 1c). These bonds, which remain intact in the presence of water permitting the fibre to go back to its original shape, are the main target of permanent hair modifications, allowing α-keratin coils to be stretched when broken.[7–9,45,46,49] The variety of these intra- and interchain interactions provide keratin with a high resistance to degradation.[8]

Beyond the formation of disulfide bonds, other post-translational modifications occur in keratin, which can influence the development of keratin filaments.[44] These include the formation of inter- and intrachain peptide bonds between lysine and glutamyl amino acid residues by transglutaminases, as well as phosphorylation, which affects keratin solubility and interaction with other proteins. Glycosylation, another post-translational modification involving the linking of a sugar moiety to specific amino acid residues, has been shown to alter binding or signalling functions of keratin. Additional post-translational modifications include the deamination of keratin arginine into citrulline by peptidylarginine deiminase, resulting in keratin conformational changes.[44]

1.1.2. Hair structural variations

A range of factors, such as genetic variation, weathering, diet or cosmetic treatments, are associated with structural variations across hair fibres.[7,45] Hair fibre weathering occurs as a result of daily grooming practices and is accentuated upon hair chemical treatment. The removal of 18-MEA, for example, leads to increased inter-fibre friction and renders fibres hydrophilic and, therefore, prone to swelling, while cuticle degradation and cracks are also observed.[9] Moreover, variations in hair fibres can be seen among ethnic groups.[5] While African-type hair presents an elliptical cross-section diameter with variations along the length of the hair fibre, Asian-type hair has the

greatest diameter with circular geometry, and Caucasian hair lies in between. African hair is more susceptible to breakage and frizz due to the small angles of fibre waves, and in this way, Asian-type hair exhibits better mechanical properties than any other ethnic group. Differences in hair curvature have been related to the distribution profile of cortical cells, with fibres varying from straight to heavily crimped.[5] Despite these differences, the amino acid composition of hair across ethnicities is remarkably uniform.[5,9,45,46]

1.1.3. Hair reactivity

Human hair keratin is made up of all 21 known amino acids in different proportions. An estimation of the percentage composition of each amino acid was elucidated by Qiu *et al.* (2020), amongst others (Table 1).[21,52,53] Chao *et al.* (1979) estimated free sulfhydryl in human hair as approximately 14.8 x 10^{17} or 2.46 µmol groups per gram of untreated hair, which was increased between 30 and 200 times upon permanent hair straightening treatment.[54] This confirmed disulfide bonds in hair keratin as targets for such treatments. However, hair reactivity is complex and depends not only on the presence of such reactive groups in the hair fibre but also on their availability, which is affected by fibre morphology and molecular structure.[5,6]

Table 1. Amino acid composition of human hair from Qiu *et al.* (2020).[21]

Amino Acid	Human hair (% w/w)
Alanine	5.2
Glycine	6.6
Isoleucine	3.1
Leucine	7.1
Proline	9.6

Valine	6.2
Phenylalanine	1.9
Tyrosine	1.2
Aspartic acid	7.6
Glutamic acid	11.6
Arginine	4.9
Histidine	1.1
Lysine	3.0
Serine	11.7
Threonine	6.9
Cysteine	10.0
Methionine	2.5

1.1.4. Hair penetration

The penetration of hair by foreign molecules can occur *via* two main pathways: transcellular and intercellular diffusion.[9] The former involves the penetration of highly crosslinked regions (epi-, exo- and endo-cuticle), while the latter requires passing through intercellular cement (CMC), bearing low-sulfur and non-keratin proteins with high swelling potential. While the former may be favoured in the presence of pre-existing mechanical damage, penetration of the hair through the CMC is the main pathway for the delivery of actives into the hair cortex.[9,46] Factors such as cuticle integrity, hair hydrophilicity and porosity affect the penetration of hair by allowing larger amounts of water absorption which as a result, swells and softens the hair by weakening hydrogen bonds and salt bridges.[9,49,55,56] Malinauskyte *et al.* (2020), in agreement with work conducted by Cruz *et al.* (2017), reported the penetration of low-molecular keratin peptides (221 Da) and mid-molecular

weight (2,577 Da) compounds deep into the hair cortex while high-molecular-weight compounds (over 75,000 Da) adsorbed onto the hair surface.[48,57] Hair penetration and amino acid exposition may be increased using a range of methods, including incubation under alkaline conditions, common for permanent chemical hair straightening, at high temperature, or treatment with swelling agents like urea or ethanolamine or detergents like SDS or Tween20.[58–62] These methods allow for the lifting of hair cuticles, commonly observed using Scanning Electron Microscopy (SEM), as well as the breaking of non-covalent bonds, loosening the fibre structure, increasing the availability of reactive groups and facilitating penetration into the hair cortex.[30,57,63–65] Hair delipidation using a combination of methanol and chloroform has also been readily described in the literature for improved active agent access to the cortex.[66–68] In the context of cosmetic treatments, specific formulations may be tailored to facilitate active agent penetration, for example, using a serum.[48]

1.2. Current permanent hair straightening methods and alternatives

While temporary moisture-sensitive hair opening and modifications may be achieved *via* keratin hydrogen bond breaking followed by mechanical straightening, keratin disulfide bonds are the main targets for permanent hair modifications.[5,45] In this way, harsh chemical relaxers are commonly used as active agents, associated with severe health risks to the user and beyond.[3,4,16–18,69,7,9–15]

1.2.1. Harsh chemical active agents

1.2.1.1. Alkaline relaxers

Alkaline relaxers and reducing agents are amongst the most popular chemical relaxers on the market.[9] The former either contain sodium

hydroxide (“lye”) or “no-lye” active agents such as lithium hydroxide, calcium hydroxide or guanidine hydroxide. “No-lye” relaxers were shown the be less irritating to the scalp than their “lye” counterpart.[70,71] High alkaline conditions (pH 9.0-14.0) lead to hair fibre swelling and damage associated with hydrogen bond breaking and electrostatic repulsion, which allows the penetration of hydroxyl ions into the hair fibres. [45,72] Upon contact with the cortex, hydroxyl ions then break disulfide bonds *via* sequential β-elimination and Michael addition leading to the formation of irreversible lanthionines (Figure 3).

Approximately a third of disulfide bonds are in this way converted to lanthionine bonds, along with some peptide bond hydrolysis due to a lack of selectivity.[5,73] No subsequent keratin crosslinking is necessary; however, a neutraliser may be used to return the hair to a neutral pH.[74] Due to high alkalinity, poor selectively and hair fibre weakening as a result of disulfide bond breaking, this highly efficient one-step method has been associated with serious side effects such as scalp burns, cuticle damage, reduced fibre tensile strength and elasticity, as well as hair breakage and hair loss.[3,4,16–18,7,9–15]

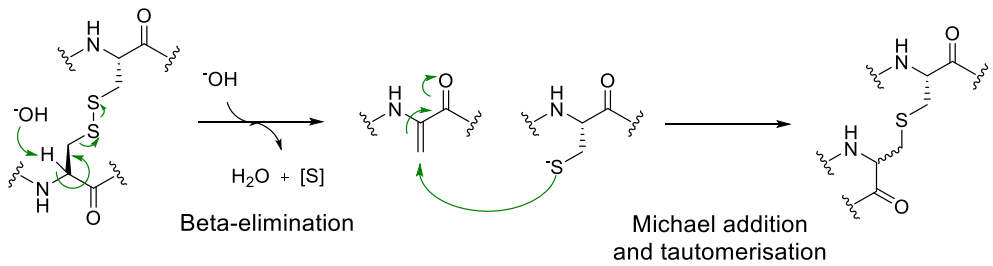

Figure 3. Lanthionisation of hair keratin using sodium hydroxide.

1.2.1.2. Reducing agents

Permanent hair straightening can also be performed using reducing agents, such as ammonium thioglycolate, which selectively reduce disulfide bonds

between cysteine amino acids to sulfhydryl groups under alkaline conditions (Figure 4).[63] The hair fibre is then mechanically straightened before re-oxidation using hydrogen peroxide or sodium bromate.[45,74] This step may not be necessary in the case of high-temperature mechanical straightening due to a process called keratin "super-contraction", where α-helices turn into β-sheets (α-β phase transition) during which hydrogen bonds are reformed.[9] Supercontraction indeed occurs under tensile loading *via* the progressive unravelling of the α-helical coiled-coil domains and the refolding of the stretched α-helices into β-sheets.[43,75] In the case of reducing agents for permanent hair straightening, no lanthionine is formed, and around 90% of the hair cystine content is retained.[9]

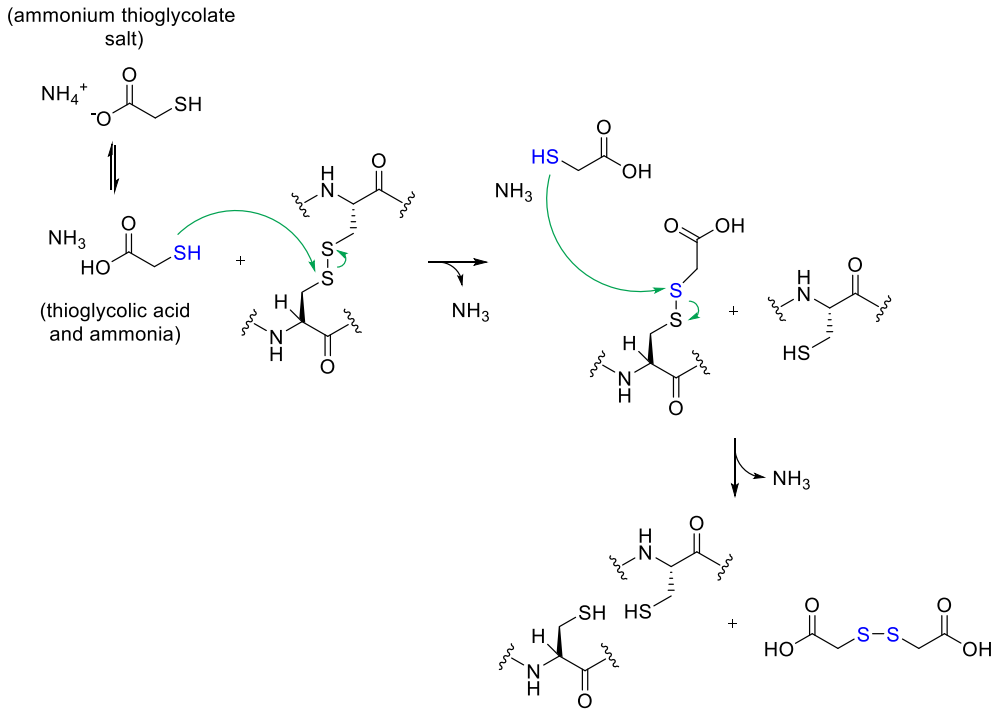

Figure 4. Reduction of disulfide bond by ammonium thioglycolate, where ammonia helps with hair swelling and thioglycolate deprotonation.

Chao *et al.* (1979) interestingly noted that while more sulfhydryl groups are found in the cuticle than in the cortex of virgin hair, thioglycolate distribution

and alkaline relaxation were respectively associated with similar amounts of sulfhydryl in hair cuticle and cortex, or with more sulfhydryl in the cortex.[54] These observations suggest that both methods are associated with active agent penetration within the hair cortex, especially in the case of alkaline relaxation. Overall, hydroxide-based lanthionisation, thio-based reduction, as well as oxidation methods are associated with permanent damage and weakening of hair due to cystine content alterations and peptide bond hydrolysis.[3,4,16–18,63,69,7,9–15]

1.2.1.3. Crosslinkers

Formaldehyde, and more recently glutaraldehyde, have also commonly been used for permanent hair straightening, despite being banned due to their high toxicity, carcinogenicity, and being associated with allergic reactions of the skin, eyes and lungs.[5,18,45,63,76–79] These chemicals operate *via* a very different mechanism, where water initially breaks keratin hydrogen bonds. Formaldehyde then forms crosslinks between side chains of keratin amino acids, such as the amino groups of lysine, arginine, glutamine and asparagine, *via* the formation of a methylene bridge (Figure 5).[9,80,81]

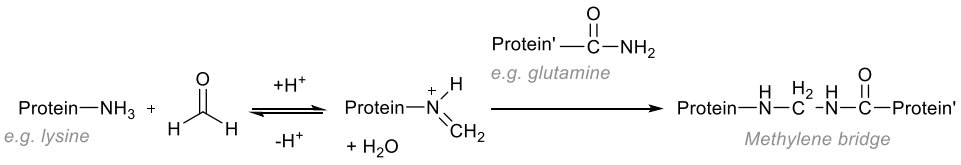

Figure 5. Reaction scheme of formaldehyde with keratin protein.[81]

Formaldehyde releasers, such as glyoxylic acid (GA), which release formaldehyde when subjected to high temperatures, have also been utilised.[71,82] Glyoxylic acid, which remains highly reactive and toxic, penetrates through hair cuticles and acts on hydrogen bonds and tyrosine amino acids of the cortex, forming a polymerised structure in the hair fibre associated with permanent hair straightening.[5,9,71,83] GA-derivatives, such as

glyoxyloyl carbocysteine, have also been used, where carbocysteine is formed *via* the reaction of cysteine and acetic acid. Glyoxyloyl carbocysteine has a pH nearer to human hair and scalp and is, therefore, less damaging than other treatments; however, its straightening effect is not as high.[71,84,85]

Overall, chemical procedures for permanent hair straightening are associated with serious health hazards and severe hair fibre weakening due to cuticle damage and fibre structural distortion.[45] Considering permanent hair straightening treatments need to be repeated every 4-6 weeks as a result of natural growth, their safety is of particular importance.[5] While hair damage can be minimised with correct product usage, there is a clear need for the development of milder and safer alternatives.[45,48]

1.2.2. The emergence of milder alternatives

In an attempt to move away from toxic and environmentally hazardous active agents, safer chemicals such as cysteine and citric acid (obtained from sustainable sources and commonly used in the food industry) have been studied as candidates for permanent hair straightening.[59,86] The effectiveness of cysteine towards the reduction of disulfide bonds in hair keratin was demonstrated in the presence of urea for hair fibre swelling to account for cysteine's poorer penetration into the hair cortex than thioglycolic acid.[59,87] Moreover, citric acid was efficient in crosslinking keratin, restoring the mechanical robustness of hair.[59,86] The combined use of blue light-irradiated riboflavin phosphate, citric acid and polyols for thiol generation, keratin crosslinking and keratin extension was described by Kim *et al.* (2022) as an eco-friendly hair setting method associated with reduced hair damage compared to commercial treatments.[88–90] Cysteine-containing keratin peptides have also been described in the literature as hair straightening modulators with improved elasticity and tensile strength.[48,57,91] The use of

oxidised-sucrose for hair crosslinking was demonstrated by Patil *et al.* (2022); however the straightening effect only lasted up to 4 shampoo cycles.[63] Moreover, Pereira-Silva *et al.* (2022), amongst others, investigated the use of nanomaterials in hair care and treatment to improve the performance of active agents in formulations.[51,92]

The development of biotechnology, which exploits cellular and biomolecular processes of living organisms, has led to a rise in biotechnologically-derived compounds used in cosmetic formulations.[93] Beside their interesting skin and hair care functions, these active agents also offer biocompatibility, eco-friendly nature, versatile activity, and good performance.[19,20] Perhaps the most well-known example is the use of *Clostridium botulinum*-synthesised botulinum neurotoxins (botox) for its paralysing properties, currently exploited to treat a range of serious pathological conditions such as cervical dystonia, strabismus and, more recently, to reduce facial wrinkles.[89,90] The use of isolated enzymes, which offer faster scale-up, more reaction specificity, and easier storage and transport than whole microorganisms, has also been investigated.[30,94] One example is the use of proteases in skin creams to smoothen the skin by peeling off dead or damaged skin.[95,96]

The chemistry involved in permanent hair straightening, namely disulfide bond reduction and crosslink formation, is naturally prevalent amongst enzymes. The development of an enzymatic route for hair straightening, therefore, appears to be a fertile area of research. While the main body of research on enzymatic activities towards keratin has been aimed at its degradation, or keratinolysis, enzymes with the ability to reduce disulfide bonds or crosslink folded proteins have been readily characterised.

1.3. Enzymatic modifications of keratin

Keratin, in the form of feathers, nails, hair, horns etc., is abundantly available in nature as waste. As an example, millions of tons of feathers are generated worldwide annually as by-products of the poultry industry.[97,98] Significant effort has thus been directed towards the valorisation of keratin waste in areas ranging from animal feed to compostable packaging.[60,72,99–102] In this way, a range of methods have been developed for keratin hydrolysis and solubilisation; however, the highly crosslinked nature of keratin makes its dissolution challenging and necessitates harsh and toxic conditions.[72,91,108,109,99–101,103–107]

1.3.1. Chemical methods towards keratin solubilisation

One of the most common chemical methods for keratin extraction is the Shindai method, which involves incubation with 2-mercaptoethanol (2-ME), urea and thiourea, and allows for a high degree of keratin isolation while limiting peptide bond hydrolysis.[91,99,103,108,110] Alkali extraction using sodium hydroxide has also been extensively explored.[72,100,103,104] Both acid and alkali hydrolyses allow for high degrees of keratin isolation associated with significant peptide bond hydrolysis and protein fragmentation.[99] While the former leads to the loss of certain amino acids (e.g. methionine, histidine), the latter is associated with higher protein yield but stronger fragmentation, resulting in lower molecular weight protein fractions.[99,111] With the aim of moving away from these harsh conditions associated with severe keratin degradation and environmental pollution, the use of ionic liquids (ILs) as highly tunable green solvents (low flammability, lack of vaporisation) has been explored for keratin extraction.[100,101,112–117] The combined effect of anions and cations in ionic liquids indeed allows for the breaking of covalent and non-covalent interactions in keratin.[117] Zhang *et al.* (2017) reported that

a minimum of 65% of disulfide bonds in keratin must be cleaved as a requirement for solubilisation in ionic liquids.[106] According to the authors, anions in ionic liquids, in particular acetate and chloride, are responsible for disulfide bond reduction in keratin, while cations are associated with hydrogen bond formation.[100,106,117,118] Imidazolium-based acetate ionic liquids, such as [EMIM]OAc and [BMIM]OAc (Figure 6), were associated with the highest disulfide bond percentage breakage (>92%).[106,119] [BMIM]Cl also led to total wool keratin dissolution, with a disulfide bond breakage of 67.5%, while [BMIM]Br broke only 29% of wool keratin disulfide bonds and led to partial dissolution after 30 minutes.[106]

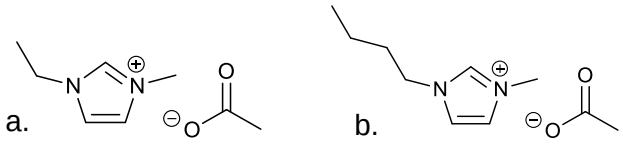

Figure 6. Chemical structures of (a.) 1-Ethyl-3-methylimidazolium acetate ([EMIM]OAc) and (b.) 1-Butyl-3-methylimidazolium acetate ([BMIM]OAc).

Microbial degradation has also gained increasing attention over the years as an environmentally-friendly alternative to waste management associated with the production of high-value products.[29,31,98] While most research on microbial keratin degradation has been done with whole keratinolytic microorganisms, the use of isolated enzymes presents many advantages, including faster scale-up, more reaction specificity, and easier storage and transport.[30]

1.3.2. Microbial keratin degradation mechanism

A range of microorganisms with keratin-decomposing ability, mostly isolated from feather keratin waste heaps, have been identified, including *Bacillus subtilis, Streptomyces* spp and *Bacillus licheniformis*.[25,26,29–31,97,98,120] As an

example, the latter demonstrated complete feather degradation within 24 hours at pH 7.5, making microbial keratinolysis a relatively slow process with potential for improvement *via* enzyme engineering.[121,122] While the exact mechanism by which microorganisms degrade keratin remains unclear, the secretion of extracellular enzymes, keratinases (EC 3.4.21) with concurrent keratin structure opening *via* disulfide bond reduction is generally accepted (Figure 7).[21,30,98,123–126] Qiu *et al.* (2020) reported the sequential activities of endo-, exo- and oligo- keratinases following disulfide bond reduction, where the enzymes respectively degrade keratin, cleave peptide chains from both ends and finally release amino acids or shorter peptides.[21]

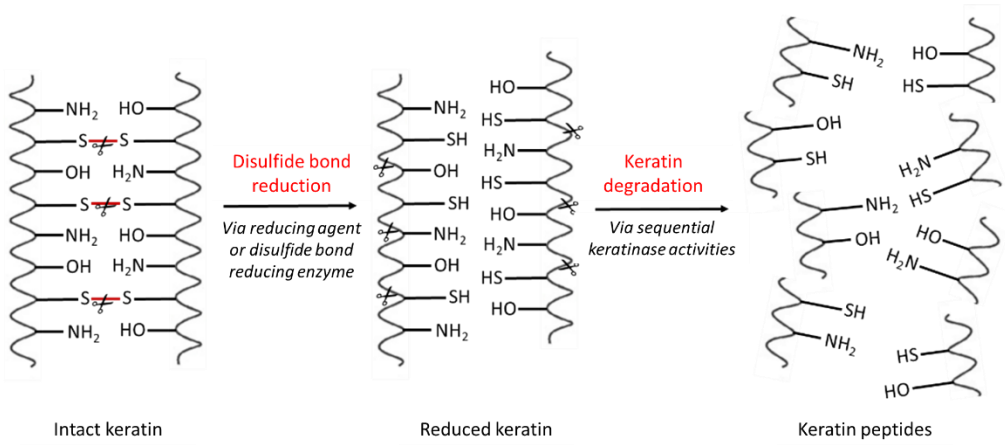

Figure 7. Potential steps towards keratin degradation, with disulfide bond reduction and sequential hydrolyses by keratinases.

1.3.3. Keratinases (EC.3.4.21)

Keratinases are extracellular enzymes belonging to the family of serine proteases, which catalyse the hydrolysis of peptide bonds *via* an aspartic acid, histidine, and serine catalytic triad at the active site. The histidine, which is brought into the correct orientation by aspartic acid and plays the role of both electron donor and acceptor, activates the serine *via* hydrogen transfer.[21] Upon binding of the substrate to the surface of the protease, the

serine performs a nucleophilic attack at the carbonyl carbon of the substrate peptide bond (Figure 8).[21] The covalent enzyme-substrate complex formed in this way is then hydrolysed, resulting in a cleaved peptide bond and regenerated enzyme.[127]

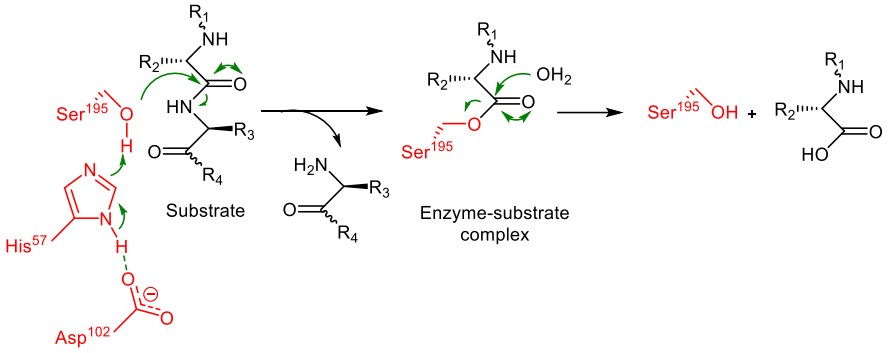

Figure 8. Peptide bond hydrolysis mechanism by serine proteases.

Keratinases are predominantly extracellular enzymes, ranging between 18 and 200 kDa with pH and temperature optima of 7.5-9 and 40-100 °C, respectively.[33,128–132] These enzymes are known to catalyse the hydrolysis (mostly endo-) of recalcitrant keratin substrates, which are of great value towards a range of industrial applications, including animal feed production and leather dehairing.[25,27,136,137,28,31,121,122,128,133–135] However, the exact mechanism behind enzymatic keratin degradation remains unclear, which has affected the development of industrial keratinase formulations.[30] While keratinolysis is believed to involve two steps: sulfitolysis and proteolysis (Figure 5), keratinases do not have disulfide bond-reducing activity, which was confirmed by Ellman's assay.[21,26,30,98,120,126,138]

Keratinase (KerA) from *Bacillus licheniformis* was the first keratinase to be purified and characterised. The nucleotide sequence of the gene encoding for KerA (*kerA)* was determined and disclosed by Lin *et al.* (1995).[31] The enzyme was later cloned, expressed in *E. coli* and assayed by Xu *et al.* (2013).[135,139] The keratinolytic activity of keratinases from a range of

microorganisms has been evaluated both in the absence and presence of concurrent disulfide bond reduction in the form of enzymes or reducing agents.[25,26,142–146,30–32,97,98,139–141] While the mechanism behind keratinolysis is not fully elucidated, a lack of complete enzymatic keratin degradation was observed in the absence of concurrent disulfide bond reduction.[30,33] Enhanced keratinolytic activities were indeed observed with the addition of reducing agents, such as sodium thioglycolate and DTT, or disulfide bond reducing enzymes.[26,30,33,98,120] Navone *et al.* (2018) assayed the keratinolytic activity of commercial keratinase KerA (as part of *Bacillus licheniformis* fermentation solubles) and concluded that the presence of reducing agents was essential for complete keratin degradation.[21,30] The authors observed well-defined stages of hair keratin degradation using both keratinase and reducing agents *via* Scanning Electron Microscopy (SEM), i.e. lifting of the hair cuticle, complete cuticle removal and initial cortex damage, then fracture of the cortex, and in the presence of reducing agents, keratin fragmentation into an amorphous protein material (α-β phase transition).[30] Navone *et al.* (2018) also mentioned enzymatic absorption to the substrate as a potential factor to keratin degradation.[30,147]

Moreover, keratinases have been patented as active agents in a range of cosmetic treatments, including skin whitening, acne treatment as well as depilation.[137,148–151] In addition, gentle but permanent hair relaxation and straightening has been described using KerA from *Bacillus licheniformis,* with peptide bond cleavage allowing the hair fibre to be relaxed and straightened with less damage than traditional straightening methods.[122,152]

1.3.4. Keratin disulfide bond-reducing enzymes

Several hypotheses have emerged towards the path *via* which disulfide bond reduction occurs in keratin-degrading microorganisms, including the

secretion of sulfite through the process of cysteine metabolism.[98]. Another example involves reducing power generation by cell-bound redox reaction systems upon adherence to the surface of the keratin substrate and suggests that whole microorganisms are required for keratin degradation.[98,133,153,154] The concurrent secretion of extracellular disulfide bond reducing enzymes has also been suggested.[25–27,98,120]

Yamamura *et al.* (2002) were the first to isolate and characterise a disulfide bond-reducing enzyme with respect to keratin degradation.[26] The authors indeed identified two extracellular enzymes, protease D-1 and a disulfide reductase-like protein, from the keratin-degrading bacterium *Stenotrophomonas* sp. strain D-1, isolated from deer fur. The latter was found to be around 15 kDa, with an optimum pH and temperature of 7 and 30 °C and an increased activity upon the addition of NADH as electron donor. The enzyme exhibited disulfide bond-reducing activity on resuspended human hair powder, as well as oxidised glutathione and cystine. The authors reported a homology of approximately 50% with a thioredoxin-like protein from *Arabidopsis thaliana*.[26] A disulfide bond reductase from *Bacillus* sp. MTS, shown to greatly enhance chicken feather keratin solubilisation and exhibiting disulfide bond-reducing activity on oxidised glutathione, was also purified.[120]

Moreover, Prakash *et al.* (2010) purified and secreted two extracellular enzymes from the keratin-degradation organism *Bacillus halodurans* PPKS2, one of which showed significant keratin disulfide bond-reducing activity, increased in the presence of NADH, using Ellman's assay on soluble feather keratin and oxidised glutathione.[24] The N-terminal sequence of this 30 kDa disulfide bond-reducing enzyme was determined and constitutes the only sequence available regarding an enzyme with disulfide bond reducing

activity on keratin. The sequence revealed high homology with protein disulfide reductases from a range of microorganisms, including *Bacillus licheniformis*. While the isolated disulfide bond reductase enzymes mentioned above are crucial for keratin degradation and have been shown to greatly enhance keratinase activities, no work has been conducted towards the effect of keratinases on enzymatic disulfide bond reduction.

The potential role of γ-glutamyl transferases (GGT, E.C. 2.3.2.2.) in keratin degradation *via* indirect disulfide bond reduction has also been described in the literature.[155–157] Γ-glutamyl transferase enzymes are essential to maintaining cysteine levels in the body.[158] They are located on the cell surface and are known to catalyse the hydrolysis of extracellular glutathione (GSH), *via* the breaking of the γ-glutamyl bond associated with the release of cysteinyl-glycine (Figure 9), a strong reductant with the ability to break disulfide bonds.[155–158] The resulting γ-glutamyl-enzyme intermediate can then react with either water (hydrolysis) or an amino acid or dipeptide (transpeptidation).[159,160] Threonine has been identified as the catalytic residue in *E. coli* GGT.[161]

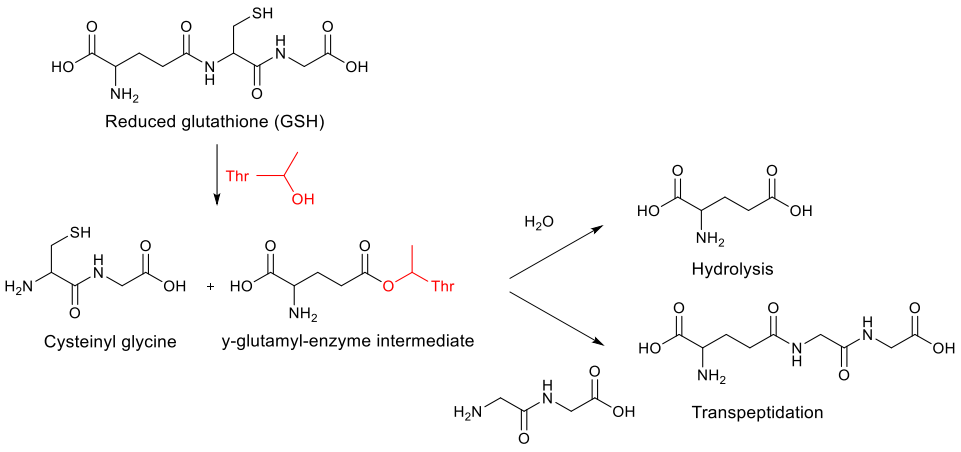

Figure 9. Enzymatic reaction of GTT (*via* threonine residue) with subsequent release of cysteinyl glycine.

It is believed that GGT-GSH plays a role in feather degradation sulfitolysis, using cysteinyl-glycine as the active redox moiety.[156] In this way, GGT have been reported in several feather-degrading organisms, such as *Bacillus subtilis*, where both GGT and reductase enzymes were shown to provide reducing activities for keratin decomposition by the proteases.[162]

1.4. Protein disulfide bond reduction

In vivo, the formation and reduction of disulfide bonds is catalysed by specialised thiol-disulfide exchanging enzymes, known as protein disulfide oxidoreductases.[163] These redox enzymes are involved in a range of intracellular processes, such as iron assimilation and redox sensing.[164–167] Protein disulfide oxidoreductases are highly selective for exposed disulfide bonds in folded proteins and are present in a variety of organisms.[163–165,168,169]

A range of disulfide bond reductases have been identified and characterised, such as thioredoxin (Trx), glutaredoxin (Grx) and protein disulfide isomerase (PDI), typically differing by subunit molecular mass and substrate specificity.[163,165,170,171] Thioredoxins and glutaredoxins catalyse disulfide bond reduction by transferring electrons from NADPH to the disulfide-containing substrate *via* the thioredoxin and glutaredoxin systems, respectively, while protein disulfide isomerases catalyse the formation or rearrangement of disulfide bridges in the protein folding process.[164,165,170,172]

While these enzymes are attractive catalysts for many industrial applications, such as the construction of biosensors and the degradation of environmental pollutants, they, however, rely on expensive cofactors like nicotinamide adenine dinucleotide phosphate (NADPH).[94] Effective regeneration of cofactors is therefore critical to the economic viability of industrial-scale bio-transformations using these enzymes. Sustainable methods of cofactor

regeneration include membrane entrapment and solid-attachment of cofactors.[94] Membrane entrapment allows the use of free cofactors with great mobility and high activity but is compromised by small membrane pore size determined by the size of the cofactor. On the other hand, the use of solid-phase cofactors, where the cofactors are physically entrapped or adsorbed, will lead to mass transfer-limited reaction kinetics. Chemical-entrapment *via* covalent bonding of the cofactor to solid supports allows for more open structures to minimise mass transfer resistance, but the chemical modification may significantly reduce the activity of the catalyst system (reaction-limited kinetic). In an attempt to combine the advantages of membrane entrapment and solid-attachment, Wang *et al.* (2005) designed the micro-capsulation of nanoparticle-attached cofactors.[173]

1.4.1. The thioredoxin system

The thioredoxin system is composed of thioredoxin (Trx), thioredoxin reductase (TrxR, E.C.1.8.1.9.) and NADPH, which constitute a thiol-dependent redox system that can catalyse the reduction of disulfide bonds.[165,167,172,174] Thioredoxins and thioredoxin reductases from a range of organisms, such as *E. coli* and *Bacillus subtilis*, have been expressed and characterised.[84,98,183,184,175–182] Moreover, disulfide bond reduction by the thioredoxin system has been described for a variety of proteins, including insulin, fibrin, cyclophilin and coagulation factor VIII.[185,186] *E. coli* thioredoxin was shown to reduce bovine insulin at least 10,000 times more rapidly than dithiothreitol at pH 7.[186] Tan *et al.* (2010) also demonstrated the ability of the thioredoxin system from *Saccharomyces cerevisiae* to reduce oxidised glutathione, indicating the ability of thioredoxin systems to reduce intermolecular disulfide bonds.[187] Furthermore, a thioredoxin-like protein was used to catalyse the treatment of hair with reduced chemical relaxer

amounts.[152,188] The reduction of S-sulfocysteine to cysteine has also been described in the literature for thioredoxins from *Salmonella typhimurium*, as well as *E. coli.*[189–191]

While thioredoxins can be reduced by photo-reduced ferredoxin *via* an iron-sulfur ferredoxin-thioredoxin reductase system, they are generally reduced enzymatically *via* the thioredoxin reductase/NADPH pathway (Figure 10).[167,171]

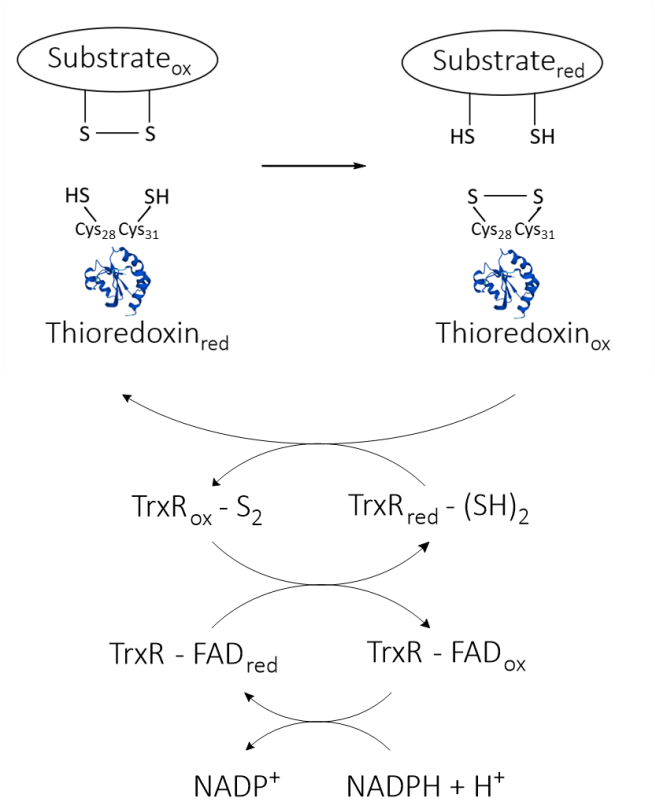

Figure 10. Schematic representation of *Bacillus subtilis* thioredoxin system electron transfer mechanism, from NADPH to thioredoxin reductase (TrxR), and thioredoxin, resulting in substrate disulfide bond reduction.

1.4.1.1. Thioredoxin and thioredoxin reductase characteristics

Thioredoxins are small redox proteins present in all organisms and are involved in maintaining the redox status of sulfhydryl groups inside the cell, amongst other cellular functions.[171,186,192] These proteins usually range between 9-12 kDa and share a common structural fold with glutaredoxins.

The “thioredoxin fold” usually consists of three-helices surrounding a central core of a four-stranded β-sheet (Figure 11), although additional α-helices or β-sheets can be observed in higher organisms, such as humans.[193]

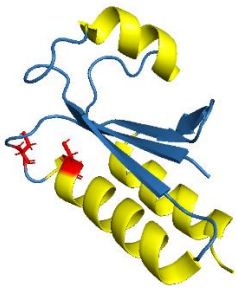

Figure 11. Thioredoxin fold structure of *E. coli* glutaredoxin 1, with the typical three α-helices (yellow) surrounding a central core of a four-stranded β-sheet motif (blue) – the active cysteines are shown in red (PDB accession number: 1EGR).

Thioredoxins and glutaredoxins also share a CXXC sequence motif at their active site (where C corresponds to cysteines and X to any other amino acids), most commonly CGPC and CPYC, respectively.[194] The proline residue at the active site of thioredoxin and glutaredoxin, amongst neighbouring amino acids, is involved in the proteins’ redox and stability properties, affecting the pKa value of catalytic thiols.[185,195] During the catalytic process, the two cysteines undergo reversible oxidation-reduction by shuttling between a dithiol and disulfide form.[170]

Thioredoxin reductases are NADPH-dependent enzymes which play an important role in cell proliferation, with physiological effects comparable to dithiothreitol.[98,196] These enzymes exist either as high molecular weight (55-60 kDa) or low molecular weight (35-40 kDa) homo-dimers, with each subunit containing an FAD (flavin adenine dinucleotide) domain and a redox-active disulfide (Cys-Gly-Pro-Cys).[178,197] Thioredoxin and glutathione reductases divergently evolved from the same ancestral nucleotide-binding protein and acquired their disulfide reductase activities independently, bearing catalytic disulfides at opposite sides of the flavin ring system.[165,174,198,199]

1.4.1.2. Electron transfer within the thioredoxin system

Within the thioredoxin system, NADPH first transfers a hydride to the oxidised thioredoxin reductase flavin nitrogen (Figure 12a). This is followed by a nucleophilic attack of the reduced flavin on the thioredoxin reductase disulfide, resulting in the formation of a flavin-cysteine adduct. Thiol elimination from the adduct leads to an oxidised flavin-cysteine charge-transfer complex, which then binds to thioredoxin and attacks its redox-active disulfide, forming a thioredoxin reductase-thioredoxin mixed disulfide (Figure 12b).[200] The mixed disulfide is then attacked by the thioredoxin reductase charge-transfer thiol, reforming the thioredoxin reductase disulfide and releasing the reduced thioredoxin.[200,201]

Reduced thioredoxin can then, in turn, reduce substrate protein disulfides *via* its active site cysteines, following a dithiol mechanism (Figure 12c). The exposed thioredoxin N-terminal active site thiol has a low pK_a value, allowing the initiation of a nucleophilic attack on one of the sulfur atoms of the disulfide target. This results in the formation of a covalently bound mixed disulfide intermediate. In a second step, the thioredoxin free C-terminal active site thiol reduces the mixed disulfide, yielding the reduced substrate and oxidised thioredoxin.[193] Reduced thioredoxin is then regenerated *via* the thioredoxin reductase/NADPH system described above.[172]

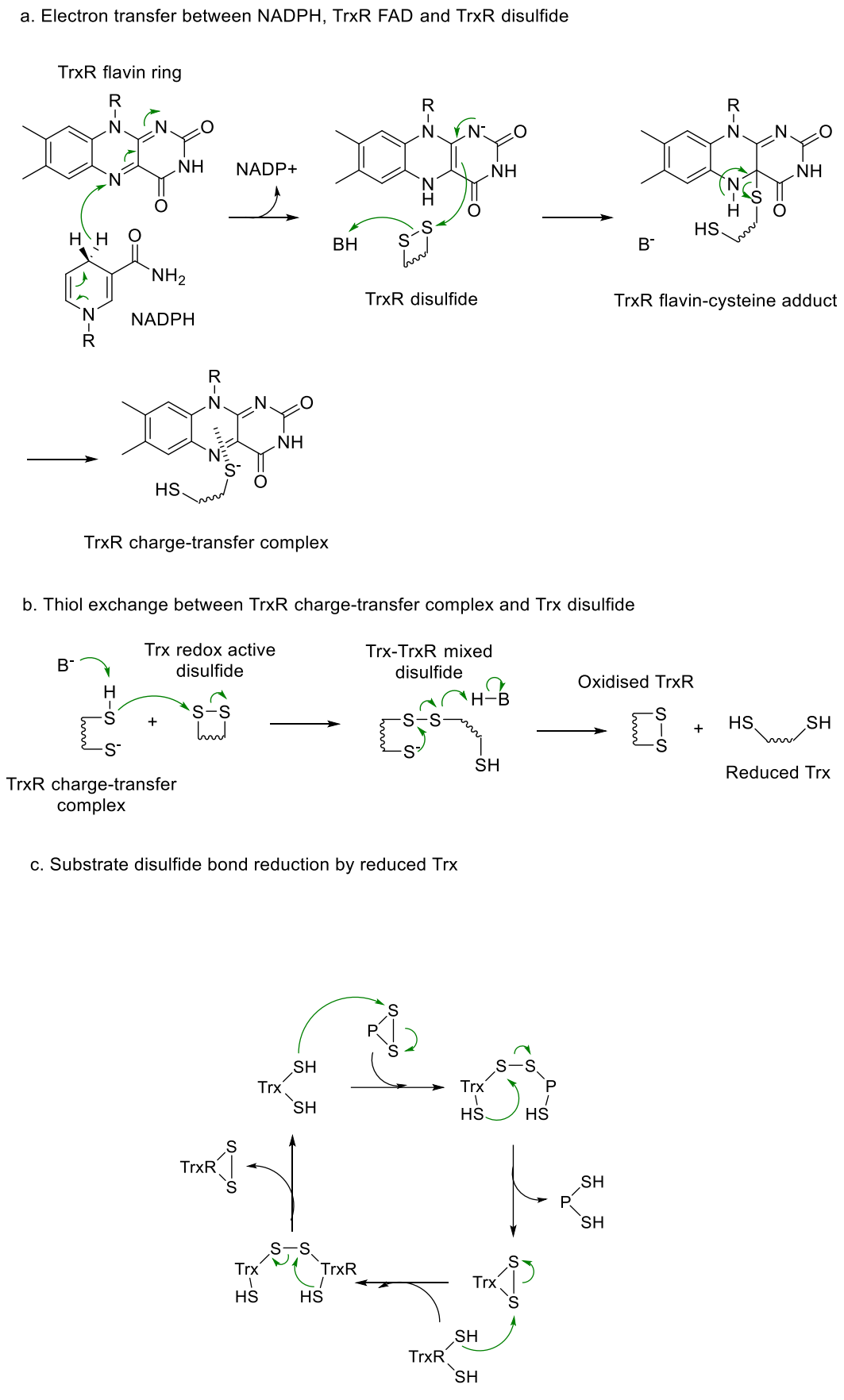

Figure 12. Electron transfers involved in disulfide bond reduction by the thioredoxin system, (B^-=basic amino acid, P=protein, TrxR=thioredoxin reductase & Trx= thioredoxin). a.

Formation of thioredoxin reductase charge-transfer complex *via* electron transfer between NADPH, and thioredoxin reductase flavin and disulfide. b. Reduction of thioredoxin disulfide *via* electron transfer from the TrxR charge-transfer complex. c. Substrate disulfide bond reduction *via* dithiol mechanism.

When reduced, flavins in solution are known to react with molecular oxygen by electron transfer from the reduced flavin to O_2.[202] This leads to the formation of a superoxide anion and semiquinone radical pair, which produce hydroperoxide and eventually decompose into hydrogen peroxide and oxidised flavin (Figure 13). This reaction takes place slowly due to spin inversion being required for the reaction of reduced flavin, a singlet, with molecular oxygen, a triplet, to form singlet products (H_2O_2 and FAD_{ox}).[202]

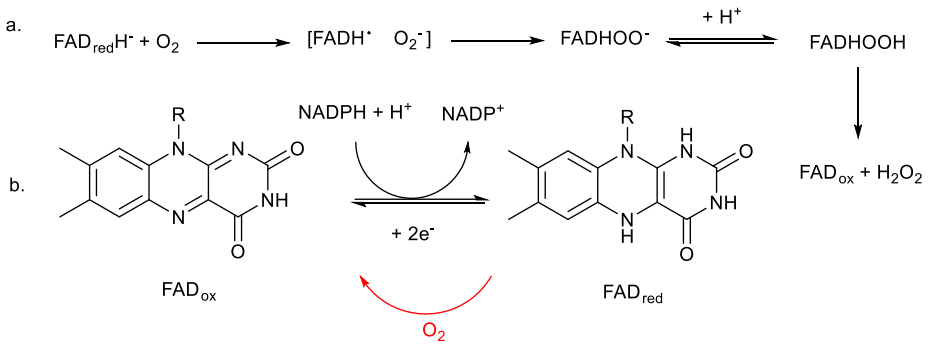

Figure 13. Reaction between FAD and O_2. a. Mechanism of reduced flavin reaction with molecular oxygen. b. Reduction of FAD by NADPH, with subsequent re-oxidation by molecular oxygen.

In this way, the presence of oxygen in air may re-oxidise the reduced FAD in thioredoxin reductase, leading to cyclic NADPH consumption with no corresponding substrate disulfide bond reduction.[174]

While the glutaredoxin system can be viewed as more sophisticated, being able to reduce both protein disulfides and GSH-mixed disulfides, the thioredoxin system functions as a broader-range disulfide reductant.[165,172,203] The absence of cross-reactivity between the two systems was demonstrated by Vlamis-Gardikas *et al*. (2002), where glutaredoxin 2 from *E. coli* did not appear as a substrate for the thioredoxin reductase enzyme of the same organism.[172] Interestingly, thioredoxin reductase 1 from yeast was unable to reduce human or *E. coli* thioredoxin.[174,178] Significant differences can indeed

be observed regarding enzymes from different organisms. For example, thioredoxin and thioredoxin reductase from *Bacillus subtilis* only share 47% and 38% identify with their counterparts from *E. coli*, respectively.

1.4.2. Other protein disulfide bond-reducing enzymes

1.4.2.1. The glutaredoxin system

The glutaredoxin system consists of glutaredoxin (Grx), glutathione (GSH), glutathione reductase (GrxR, EC 1.8.1.7.) and NADPH (Figure 14). It is present in organisms that contain glutathione and is therefore lacking in *Bacillus anthracis, Bacillus subtilis,* and *Mycobacterium tuberculosis*, amongst others.[98,171,204,205] The reduction of disulfide bonds by the glutaredoxin system has been described for a range of proteins, including insulin.[206] Glutaredoxins are central in the response against oxidative stress as the biological activity of many proteins is modified by the formation of glutathione (GSH)-mixed disulfides.[172,207]

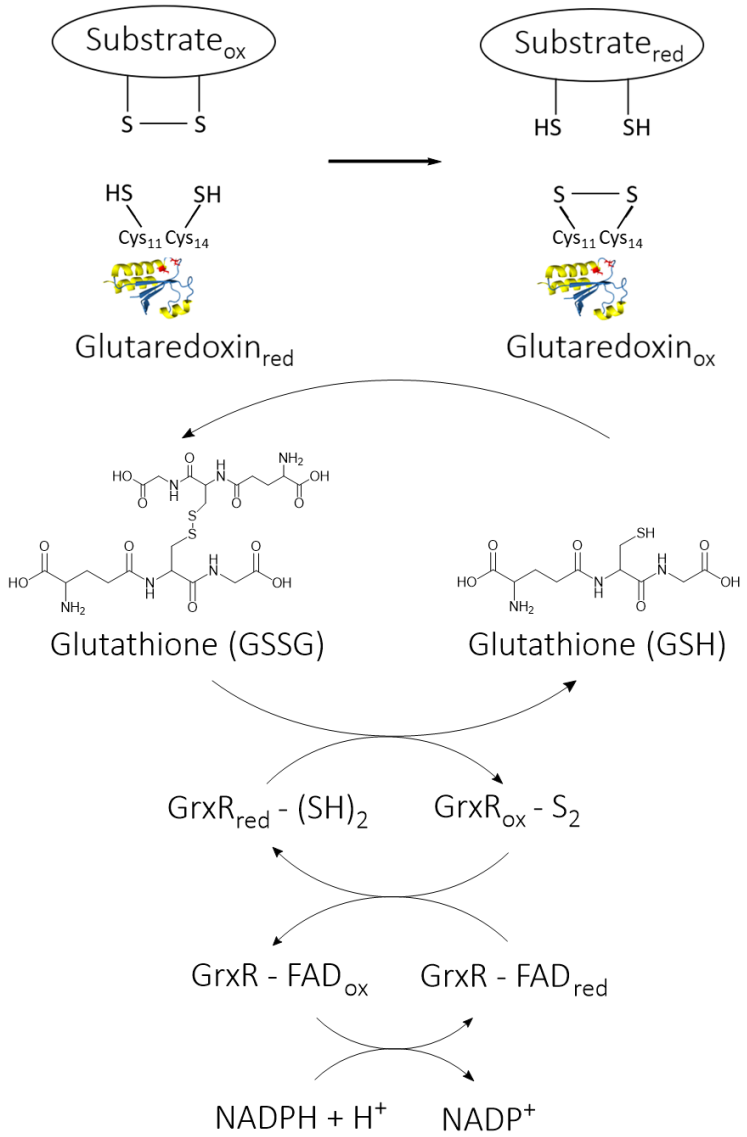

Figure 14. Schematic representation of *E. coli* glutaredoxin system electron transfer, from NADPH to glutathione reductase (GrxR), glutathione and glutaredoxin, resulting in substrate disulfide bond reduction.

Compared to thioredoxins, a serine residue sometimes replaces one of the two cysteine residues within the glutaredoxin active site, with corresponding enzymes referred to as monothiol glutaredoxins.[163,172] Glutathione reductases contain active cysteines, usually as a CXXXXC sequence motif, as well as a flavin domain, catalysing the reduction of glutathione disulfide (GSSG) to glutathione (GSH).[208,209]

Similarly to the thioredoxin system, an electron cascade occurs from NADPH to glutathione reductase FAD and then disulfide, which in turn reduces oxidised glutathione (GSSG).[200] Reduced glutathione, which is protonated by the glutathione reductase active site histidine neighbouring the flavin ring, then reduces glutaredoxin, which can finally reduce disulfides in target proteins *via* the dithiol mechanism (Figures 15a-c).[193,200,201,203,208] Oxidised glutaredoxin is then reduced nonenzymatically by reduced glutathione (GSH), which in turn is linked to the glutathione reductase/NADPH system (Figure 14).[171,185,210]

a. Thiol exchange between GrxR charge-transfer complex and GSSG

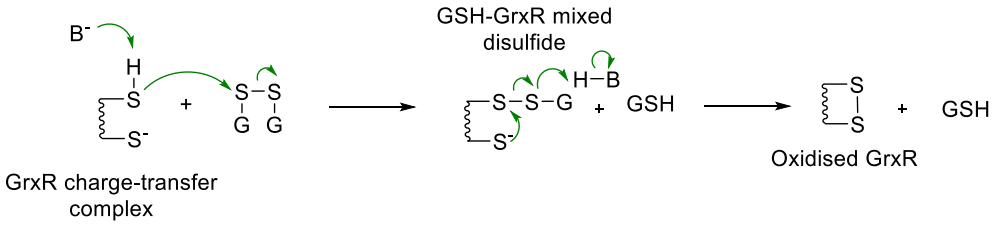

b. Thiol exchange between GSH and Grx

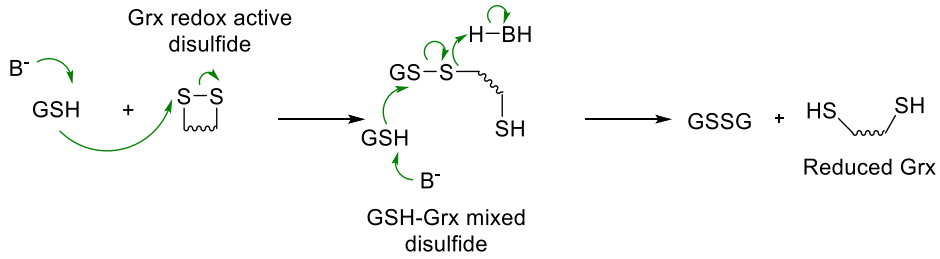

c. Substrate disulfide bond reduction by Grx *via* dithiol/monothiol mechanisms

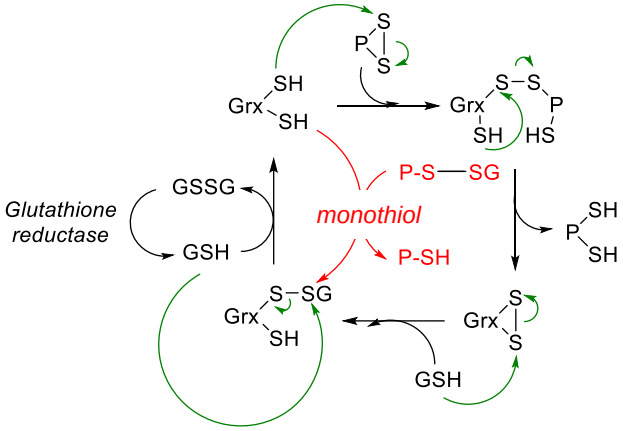

Figure 15. Electron transfers involved in disulfide bond reduction by the glutaredoxin system, (B^-=basic amino acid, P=protein, GrxR=glutathione reductase, GSSG=oxidised glutathione, GSH=reduced glutathione & Grx=Glutaredoxin). a. Reduction of oxidised glutathione by glutathione reductase charge-transfer complex. b. Reduction of glutaredoxin by reduced glutathione. c. Substrate disulfide bond reduction via dithiol or monothiol mechanisms.

Reduced glutaredoxin can also reduce glutathionylated proteins *via* the monothiol mechanism (Figure 15c), relying solely on the N-terminal active site Cys.[193] In this reaction, glutaredoxins specifically interact with the GSH moiety of the GSH-mixed disulfide target, and not the protein substrate, due to the glutaredoxin affinity for GSH. This results in the formation of a covalent GSH-mixed intermediate and the release of the non-GSH moiety in its reduced form. The mixed intermediate is then reduced by a second GSH molecule, generating glutathione disulfide (GSSG). Finally, glutathione reductase regenerates GSH by reducing the GSSG.[193]

1.4.2.2. Protein disulfide isomerase

Protein disulfide isomerases (PDI, EC 5.3.4.1) are involved with the formation or rearrangement of disulfide bridges in cysteine-containing proteins during oxidative protein folding in the endoplasmic reticulum (ER).[152,163,170,211] These 55 kDa enzymes catalyse disulfide formation (oxidation) as well as the rearrangement of incorrect disulfide pairings (isomerisation).[211] Protein disulfide isomerases are characterised by two catalytic domains, each containing the thioredoxin fold and CXXC catalytic

domain, separated by two non-catalytic domains and a highly acidic extension at the C-terminus, bearing the motif for the localisation of the ER. ERO1 is a flavoenzyme that recycles PDIs back to the oxidised state by transferring reducing equivalents to molecular oxygen with formation of hydrogen peroxide.[212,213] While PDI oxidase activity requires the reaction of an oxidised enzyme active site with a reduced substrate, the isomerase activity involves the attack of a reduced PDI active site on a substrate disulfide. Two mechanisms could then result in subsequent isomerisation. The first one involves the intermolecular reaction of the substrate cysteine with a different substrate disulfide, following which a substrate cysteine displaces PDI from the covalent complex and regenerates the enzyme. The second mechanism involves cycles of reducing substrate disulfides and re-oxidising them in different orientations.[211] The functional equivalent of PDI in prokaryote organisms is known as DsbA, a periplasmic, monomeric protein.[171]

PDI enzymes have been shown to successfully restore mechanical and thermal properties in wool as well as bleached hair by promoting the covalent attachment of keratin-based cysteine-containing peptides to the bleached hair.[91,152,214,215] Lundstrom *et al.* (1990) also demonstrated that calf liver PDI is a substrate for calf thymus thioredoxin reductase and catalyses NADPH-dependent insulin disulfide reduction, however, thioredoxin remains a better disulfide reductase.[216]

Overall, a wide range of protein disulfide reductases have to this day been expressed and characterised, with activities on a range of substrates, including insulin and oxidised glutathione. While disulfide bond-reducing enzymes have been identified in the context of microbial keratin degradation

with the potential to break disulfide bonds in feather keratin, these enzymes have not been characterised, and very little sequence information is available. The enzymatic disulfide bond reduction of keratin substrates, such as wool and human hair, has, however not been explored, to the best of our knowledge.

1.5. Protein crosslinking

The permanent setting of natural macromolecules for the modification of appearance and performance properties has been a topic of growing interest, especially in industries such as the textile (e.g. cotton, silk, wool etc.) and cosmetic (e.g. hair) industries.[217] In the case of non-highly crosslinked proteins, such as casein, morphological modifications can be achieved solely using water *via* hydrogen bond and ionic linkage interruptions. On the other hand, highly crosslinked proteins, such as hair keratin, contain disulfide bonds which remain intact in water. The cleavage of those bonds is therefore required to make new permanent morphologies.[59] The reformation of disulfide bonds or alternative crosslinking *via* amino acids beyond cysteines then allows for the permanent setting of new protein morphologies.[59]

In the context of permanent hair straightening, keratin disulfide bond reduction by chemical relaxers is followed by hair fibre crosslinking, using chemicals such as hydrogen peroxide, aimed at setting the new hair conformations in place.[218–220] With the aim of moving away from harsh chemicals, greener alternatives for hair crosslinking, such as citric acid, oxidised sucrose or cysteine-containing hair keratin peptides, have been described in the literature.[48,59,63,88,91,108] Despite inducing the formation of active agent-keratin crosslinks rather than hair keratin-keratin bonds, these methods constitute promising alternatives for the permanent setting of hair. Moreover, the rise of biotechnology and natural crosslinking activities of

enzymes offers a range of new possibilities. The value of enzymes as crosslinking agents for the setting of macromolecules such as keratin is founded on a large body of research exploring the biocatalytic formation of covalent bonds in a highly selective, atom-efficient and biocompatible manner.[34]

1.5.1. Protein crosslinking using enzymes

Enzymes have evolved over time to catalyse covalent modifications of proteins essential to pro- and eukaryotic cells.[35] Indeed, enzymes have natural crosslinking activities *in vivo*, involved in processes such as blood coagulation *via* fibrin crosslinking by Factor XIIIa, and skin-barrier formation, where keratin intermediate filaments, bound by filaggrin, are crosslinked by transglutaminases.[221–223] Enzymatic protein modifications occur at the functional groups of amino acid side chains and either involve the formation of molecule-(e.g. cofactors or lipids)-substrate crosslinks or substrate-substrate (intra- and intermolecular, e.g. disulfide bond formation) crosslinks.[35]

Heck *et al.* (2012) distinguished two different types of enzymatic protein crosslinking.[35] The first one involves the formation of a covalent substrate proteinyl-enzyme-thioester intermediate at the enzyme active site, followed by a nucleophilic attack by a substrate amine nucleophile releasing the bound substrate protein moiety from the enzyme (Figure 16). A range of enzymes are known to catalyse the formation of a new peptide bond between target molecules in this way, including sortases, peptidases and transglutaminases.[35]

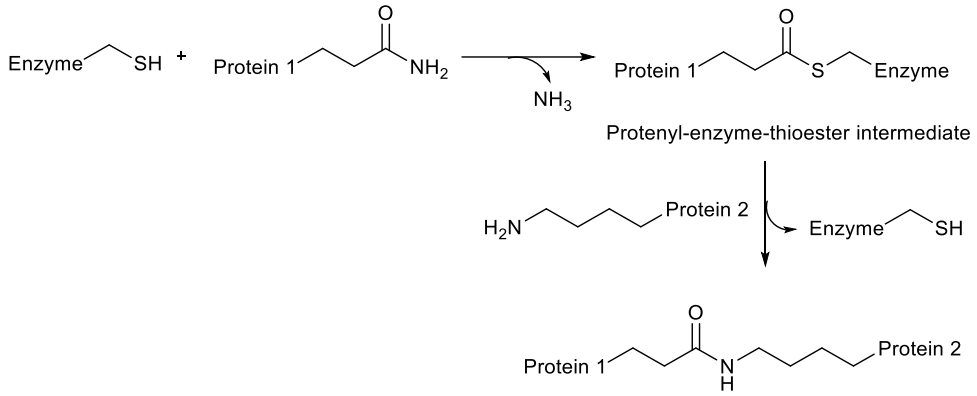

Figure 16. Enzymatic protein crosslinking *via* proteinyl-enzyme-thioester formation.

The second type of enzymatic crosslinking occurs *via* reactive species that are enzymatically generated. The resulting reactive species, such as quinones or radicals, may subsequently undergo chemical conversions to form protein crosslinks of various types. Only the first step of the mechanism, corresponding to the initial redox reaction with the primary substrate, is directly catalysed by the enzyme.[35] Enzymes operating *via* this mechanism include laccases, peroxidases, tyrosinases and lysyl oxidases.

1.5.2. Transglutaminases

Transglutaminases (EC 2.3.2.13) are a large family of enzymes known to catalyse the intermolecular crosslinking of glutamine and lysine side chains in peptide and protein substrates.[34,224] They are found in eukaryotes, archaea and bacteria and are responsible for a range of biological functions, including the formation of fibrin clots.[34] While eukaryotic transglutaminases have a four-domain structure and rely on Ca^{2+}, their prokaryotic counterparts exhibit a distinctive single-domain and are calcium-independent, allowing for more practicality of use.[34,35]

Transglutaminases first catalyse the formation of a proteinyl-glutamyl-thioester intermediate from the glutamine motif on a substrate side chain, facilitated by a cysteine, aspartate and histidine triad at the enzyme active

site.[34,37,225] The lysine motif from another chain then performs a nucleophilic attack on the thioester carbonyl, generating a covalently crosslinked product (Figure 17).[34] The number of proteins acting as glutamyl substrates for transglutaminases is, however, restricted, with both primary and three-dimensional protein structures determining substrate compatibility.[39,226] In this way, while transglutaminases have been shown to crosslink α-casein, an unstructured protein, no crosslinking occurred in the presence of structured proteins, such as β-lactoglobulin or BSA.[227] In the absence of free amine groups, transglutaminases also catalyse deamidation reactions, where water acts as an acyl acceptor.[37]

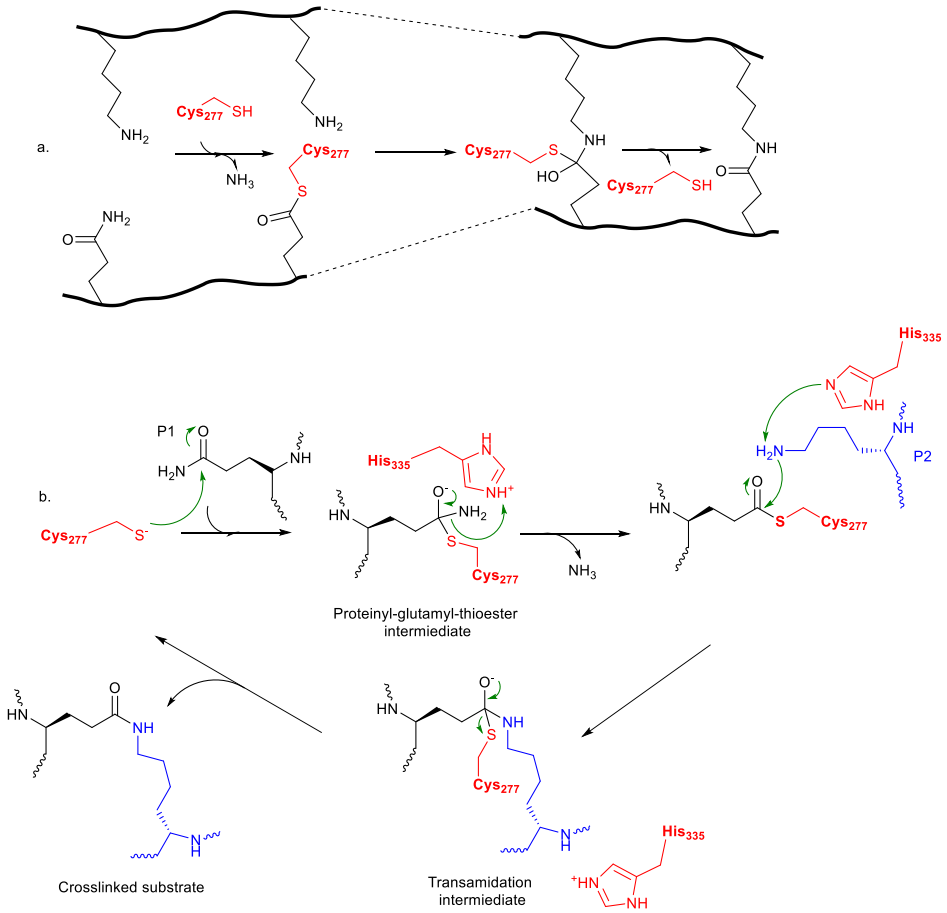

Figure 17. Transglutaminase-catalysed protein crosslinking *via* proteinyl-glutamyl-thioester intermediate. a. Crosslinking formation between protein glutamyl and lysine chains by transglutaminase active site cysteine. b. Mechanism behind transglutaminase catalysis of protein crosslinking.

Transglutaminases are currently being used at scale in a range of industries, such as the food and dairy industry towards processed meat, cheese and yoghurt manufacturing.[34,228–230] The use of microbial transglutaminases, which have optimum pH and temperature ranges of 6-7 and 40-50 °C and are approximately 38 kDa, has been reported towards wool manufacturing, where significant increases in wool strength and resistance to washes and bleaching were observed.[34,37,40,107,230–232] Chen *et al.* (2021) also related the successful crosslinking of wool-extracted keratin on fabrics through a microbial transglutaminase treatment, while Cui *et al.* (2013) detected keratin-keratin crosslinking in wool-extracted keratin gels by treatment with transglutaminase from *Streptoverticillium*.[107,233] Moreover, transglutaminases have been used to covalently graft amine-containing compounds to glutamine residues in keratins from skin, hair or nails.[152,234]

1.5.3. Laccases

Laccases (EC 1.10.3.2) are multicopper enzymes that have been discovered in fungi, plants and bacteria, with molecular weights ranging from 50 to 130 kDa depending on the organism.[235,236] These enzymes play key roles in the formation and degradation of lignin, with white-rot fungi (e.g. *Trametes versicolor*, optimum temperature and pH of 25 °C and 5) producing the most powerful laccases.[227,237–239] Laccase have been regarded as a “green tool”, requiring oxygen as the only co-substrate and releasing water as only by-product, and with many industrial application, such as juice stabilisation, bioactive coatings, bio-pulping in the paper industry or fibreboard preparation *via* wood fibre crosslinking to lignin.[34,235–237,240–243]

Laccases catalyse single-electron abstractions from a wide range of substrates, including ortho and para-diphenols, methoxy-substituted phenols, aromatic amines and thiols (Figure 18a).[235,236,244,245] The resulting

radicals may undergo subsequent coupling reactions, causing the formation of covalently linked products.[35] The oxidation of four substrate molecules goes along with the concomitant reduction of one equivalent of dioxygen to water, the only by-product of the reaction.[35,237,246] In proteins, exposed tyrosine side chains serve as the main substrate for oxidation by laccase, where the phenoxy radicals may spontaneously initiate non-enzymatic protein crosslinking mainly through the formation of iso-dityrosine bonds, as well as dityrosine and cysteine-tyrosine bonds (Figure 18b).[227,235,247–249] These bonds have been shown to be more prone to form in unstructured proteins, such as α-casein, than structured ones, potentially due to radical stabilisation taking place within globular proteins.[227] Protein folding indeed constitutes one of the main determining factors towards the extent of protein crosslinking.[235] Beyond tyrosine, tryptophan and cysteine, amongst others, have also been suggested as laccase substrates, however, laccase-catalysed reactions with proteins at the residue level remain poorly understood.[227,235,248–250]

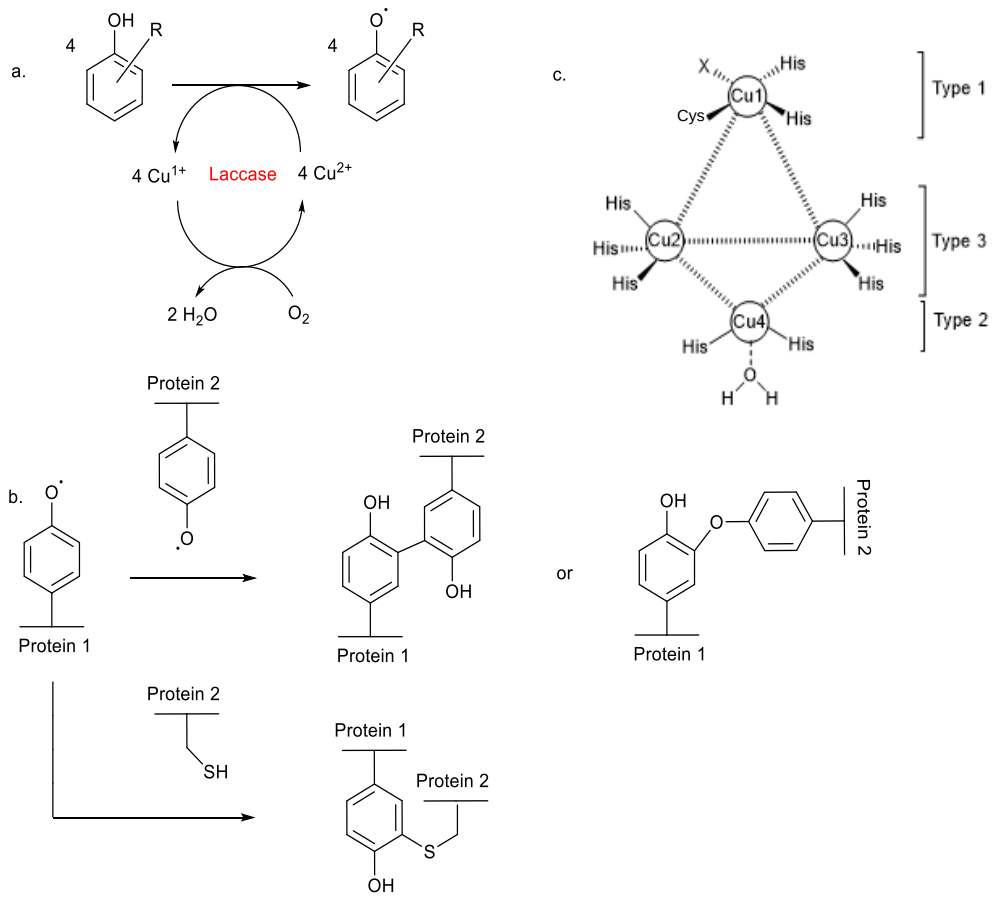

Figure 18. Laccase catalytic activity, with representation of multi-copper active site. a. General mechanism of laccase showing the oxidation of phenol substrates. b. Simplified formation of dityrosine and tyrosine-cysteine protein crosslinks from laccase-generated phenol radicals c. Laccase active site composed of three types of copper centres, where X=leucine, phenylalanine or methionine.

Laccase catalytic sites contain four copper atoms per protein unit, organised into three different types of structure (Figure 15c).[236,246,251] Due to its higher redox potential, type 1 copper is the substrate oxidation site. It is bound to two histidines and one cysteine residue, as well a fourth ligand, usually leucine or phenylalanine in fungal enzymes or methionine in bacteria, which influences the enzyme's redox potential (more hydrophobic ligands are usually associated with higher redox potentials).[252] Upon substrate oxidation, electrons are then transferred to Type 2 and 3 copper sites, which form the tri-nuclear cluster where molecular oxygen reduction occurs with subsequent release of water.[236,251] Halides have been shown to inhibit laccases at the Type 2/3 copper sites through binding, prohibiting the reduction of oxygen to

water and subsequently causing a break in terminal electron acceptance.[253,254] Moreover, positively charged amino acids, such as arginine, histidine and lysine, may induce favourable conformation changes in laccases *via* non-covalent interactions, leading to an enhancement in catalytic activity.[255]

Laccases possess relatively low redox potentials (<0.8 V), which restricts their activity to low-redox-potential substrates.[237,242] However, this limitation may be overcome by the inclusion of small-molecule compounds, known as mediators, which have the ability to enhance laccase activity by acting as "electron-shuttles" (Figure 19a-b).[237,242,243] In such laccase/mediator systems, the mediator is first oxidised by the laccase.[252] Resulting radicals are long-lived enough to then diffuse away from the enzymatic active site and can then, in turn, oxidise substrates that may not have otherwise entered the laccase active site due to large size, steric hindrance or high redox potential.[237,242,252] In this way, mediators may increase the accessibility of the reactive amino acids, thus improving crosslinking processes.[250] This may happen *via* different mechanisms, such as electron transfer (ET) and radical hydrogen atom transfer (HAT).[238] Moreover, Mattinen *et al.* (2005) reported that reactive mediator radicals were produced preferentially by laccases over tyrosine-containing peptide radicals.[256] While the use of mediators in industry has been limited by high cost and potential toxicity, the efficiency of laccase-mediator systems has been demonstrated towards the degradation of recalcitrant compounds.[237] One of the most commonly used laccase mediator is ABTS (2,2'-azino-bis(3-ethylbenzothioazoline-6-sulfonic acid)), which was the first synthetic compound to allow the oxidation of non-phenolic lignin structures.[237,243] ABTS gets oxidised by laccase into the cationic radical $ABTS^{\cdot+}$, stabilised by resonance (Figure 19c).[238] Interestingly, Hilgers *et al.*

(2018) observed the covalent coupling of ABTS with phenolic lignin subunit radicals, with ABTS grafting onto the substrate blocking further polymerisation.[238] Mediator-incorporation into the substrate protein structure has indeed been described in the literature, especially in structured proteins, such as β-lactoglobulin, often in trace amounts.[227,247]

A range of naturally-occurring phenols related to the lignin polymer (e.g. vanillin and acetosyringone) have also been investigated as potential mediators, which most likely are the true mediators in nature for laccase-catalysed lignin degradation.[237,241,242] Compared to synthetic mediators, the free radical activity of natural mediators is low, reducing risks of attack on laccase groups, as well as dimerisation or polymerisation, especially in the case of p-substituted phenolics combined with two methoxy groups (e.g. acetosyringone).[252,257] The efficiency of both vanillin and acetosyringone as laccase mediators has been reported in the literature.[252,258,259]

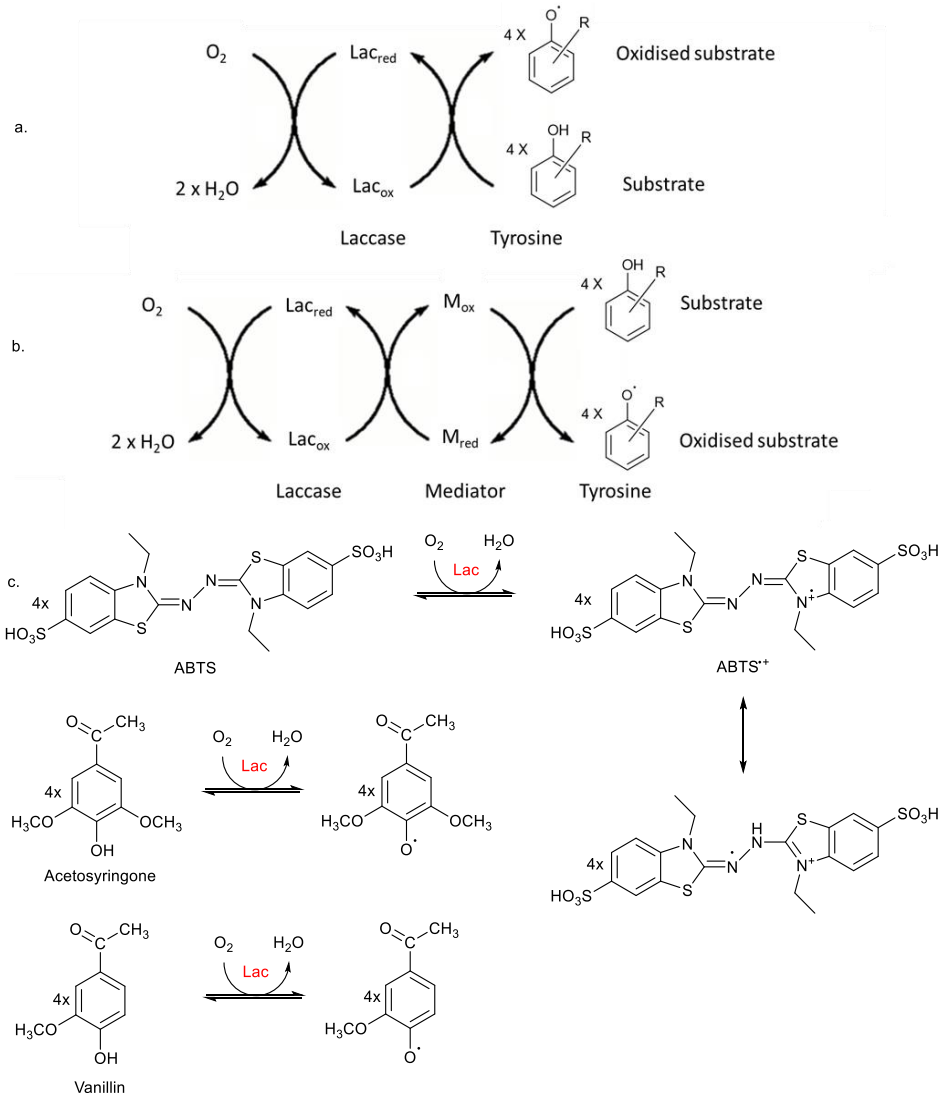

Figure 19. Role of mediators towards laccase catalysis. a. Laccase catalysis *via* direct oxidation. b. Laccase catalysis *via* mediator oxidation. c. Laccase oxidation of ABTS, acetosyringone and vanillin mediators into respective radicals.

Laccases have been investigated towards the improvement of wool performances. As an example, laccase from *Bacillus sp.* has been studied in the presence of TEMPO for the grafting of chitosan onto wool surface.[72,260] Moreover, Li *et al.* (2021) reported the grafting of tyrosine onto human hair using laccase from *Myceliophthora thermophila* towards the setting of a mechanically-induced shape, however, the effect was lost upon washing.[261,262]

1.5.4. Tyrosinases

Tyrosinases (EC 1.14.18.1) are di-copper enzymes found in both eukaryote and prokaryote organisms, with different physiological roles across organisms. These include the catalysis of the initial step of melanin formation from tyrosine in animals and fungi or the oxidation of phenolic groups in fruit involved in post-harvest browning.[34] Mushroom tyrosinases (approx. 120 kDa) are popular due to being commercially available and inexpensive, with optimum pH and temperature of 7 and 35 °C, respectively, and similar properties encountered across organisms.[263,264] Following activation through oxygen binding, tyrosinases catalyse two distinct reactions. The diphenolase cycle involves the conversion of diphenols to *o*-quinones, while the monophenolase cycle involves the catalysis of mono-phenolic compounds or surface-exposed tyrosine side chains of proteins to *ortho*-diphenol intermediates, which are subsequently oxidised to *ortho*-quinones with concomitant reduction of molecular oxygen to water. *Ortho*-quinones may then spontaneously react, mainly *via* Michael 1,4-additions, with the side chains of lysine, tyrosine, histidine or cysteine residues to form covalent bonds (Figure 20).[35] The reduced tyrosinase is then reactivated to its competent state *via* oxidation by molecular oxygen.[34]

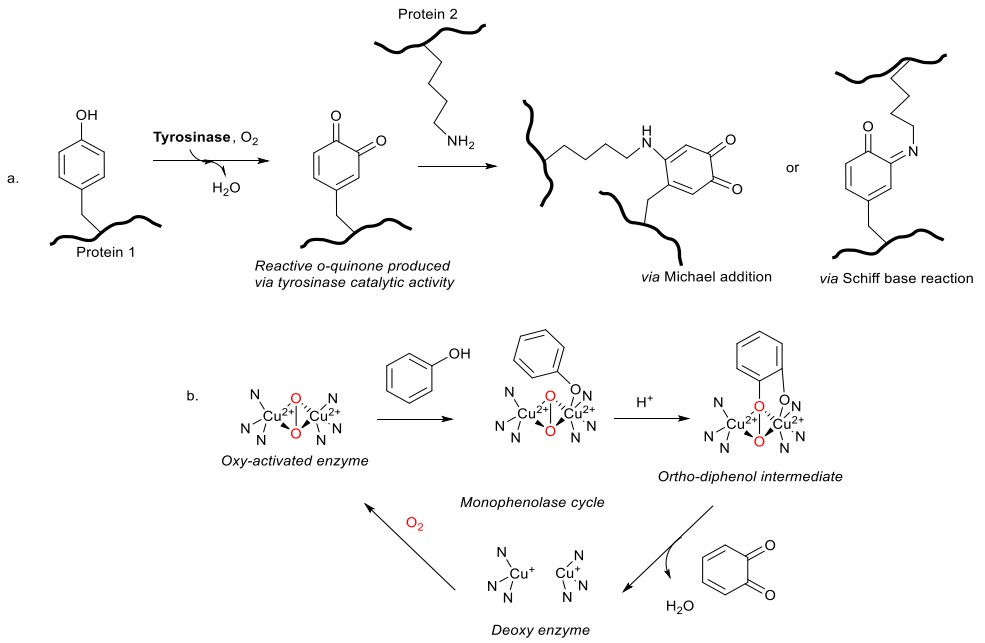

Figure 20. Tyrosinase-catalysed protein crosslinking *via* ortho-diphenol and ortho-quinone formation. a. Schematic representation of tyrosinase-catalysed protein crosslinking with two potential crosslinked products shown. b. Monophenolase phase of the tyrosinasecatalytic cycle via oxygen binding activation.

Tyrosinase activities have potential uses in a range of applications, such as the processing of casein waste from the dairy industry or the strengthening of wool and silk in the textile industry by crosslinking of biopolymers such as collagen and elastin to the polymer substrate.[34,265,266] Moreover, it has been shown that proteins with a high degree of complexity are not susceptible to crosslinking by tyrosinase.[39]

Overall, laccases, tyrosinases and transglutaminase have been investigated towards the crosslinking of wool keratin, specifically the binding of compounds to keratin, aimed at increased tensile strength and performance. The only evidence of enzymatic keratin-keratin crosslinking was shown for microbial transglutaminases on protease or reducing agent-pre-treated wool keratin.[107] The enzyme-catalysed formation of keratin-keratin crosslinks has, however, not been described in human hair.

1.5.5. Other protein crosslinking enzymes

A range of protein crosslinking enzymes, beyond transglutaminases, laccases and tyrosinases, have also been identified, including sulfhydryl oxidases, sortases, peroxidases and lysyl oxidases.

Sulfhydryl oxidases (EC 1.8.3.2.) catalyse the oxidation of free sulfhydryl groups in proteins to disulfides by using molecular oxygen as an electron acceptor and releasing hydrogen peroxide as a byproduct.[267] These enzymes carry a CXXC motif with an FAD cofactor. Buried thiols in folded proteins are, however, unreactive to this enzyme family, a protein must first be denatured to insert disulfides.[200,267,268]

Sortases (EC 3.4.22.70) are cysteine transpeptidases which catalyse the covalent attachment of surface proteins to the cell wall peptidoglycan. Sortase activity involves the cleavage of the peptide bond between threonine and glycine residues of the cell wall substrate, followed by a nucleophilic attack by the N-terminal glycine of the secondary substrate and the formation of an amide bond between the two substrates.[34] These enzymes are highly specific to substrate proteins with LPXTG, NPQTN, LPXTA or LAXTG motifs.[35,269]

Peroxidases (EC 1.11.1.7) catalyse the oxidation of tyrosine amongst other side chains in proteins, where the oxidation of two substrate molecules is accompanied by the reduction of hydrogen peroxide to water.[34,35,237]

Lysyl oxidases (EC 1.4.3.13) initiate the crosslinking of collagen and elastin chains in eukaryotic extracellular matrices. These enzymes, which rely on a covalently bound lysine tyrosinyl quinone cofactor, oxidise the primary amine on accessible lysyl substrate side chains into aldehyde, which may then undergo subsequent reactions (aldol condensation or Schiff base).[34,35]

Moreover, a range of highly specific enzymes catalysing covalent bond formation *in vivo* have been identified, including cystathione synthases and lanthionine synthetase.

Cystathione β-synthase (EC 4.2.1.22) and cystathione γ-synthase (EC 2.5.1.48) are pyridoxal phosphate (PLP)-dependent enzymes involved in cysteine biosynthesis *via* the transsulfuration pathway.[270] They catalyse the formation of cystathione from homocysteine and serine, or from cysteine and activated homoserine, respectively, with subsequent release of water.[268,271] These enzymes are also involved in hydrogen sulfide regeneration from cysteine.[272] In the absence of thiol, cystathione γ-synthase catalyses γ-elimination to form 2-oxobutanoate, succinate and ammonia.[273]

Lanthionine synthetases are catalysts that achieve macrocyclisations and form lanthionines *via* dehydration at serine/threonine residues followed by intermolecular crosslinking of cysteine thiols by Michael addition.[274]

Despite highly relevant activities in the context of permanent hair straightening, these enzymes may not appear as compatible active agents for a range of reasons, including the need for cofactor, the release of harsh by-products or the nature of substrates. Moreover, the potential for crosslink formation towards the permanent setting of natural macromolecules is not limited to thiol-thiol interactions.[48,59,88,91,108]

Permanent hair straightening treatments are very popular, with the constant emergence of novel technologies and ever-growing customer demand. However, chemicals involved in hair straightening techniques are usually toxic and environmentally hazardous, highlighting the need for safer biocompatible methods. In this way, enzyme-catalysed reactions offer an

inherently ‘greener’ and biocompatible approach to disulfide bond reduction and crosslinking.[34] This study explores the suitability of disulfide bond-reducing enzymes, as well as crosslinking enzymes as permanent hair-straightening active agents.

2. Aims and objectives

2.1. Overall aim

Current treatments associated with permanent hair straightening rely on the use of harsh chemicals, such as sodium hydroxide, ammonium thioglycolate and formaldehyde. These active agents carry severe health risks beyond hair damage and loss, highlighting the need for milder methods. To this end, bio-catalysis offers the potential of highly selective and environmentally friendly alternative processes. Considering that the chemistry involved in permanent hair straightening, i.e. disulfide bond reduction and crosslinking of folded proteins, is naturally prevalent in enzymes, their potential use as milder and biocompatible active agents is therefore of great interest.

Due to the importance of disulfide-thiol exchanges *in vivo*, a range of protein disulfide-reducing enzymes have been identified and characterised, including thioredoxin and glutaredoxin systems, as well as protein disulfide isomerases. These enzymes have been shown to reduce disulfide bonds in a range of protein substrates, such as oxidised glutathione and insulin. Knowledge is, however, lacking regarding enzymatic keratin disulfide bond reduction. Indeed, the large body of research looking at enzymes with keratin as a potential substrate has been directed towards keratin degradation and hydrolysis, mainly by keratinases. While the mechanism behind microbial keratin degradation remains uncertain, it is generally accepted that concomitant disulfide bond reduction plays a crucial role. In whole microorganisms, this may take the form of a cell-bound redox system, the secretion of a soluble reducing substance like sulfite, mechanical pressure brought about by mycelium growth or the concomitant action of a disulfide bond-reducing enzyme. In this way, two disulfide bond-reducing enzymes

have been isolated from *Bacillus* and *Stenotrophomonas* species with known activities on feather keratin, with only one N-terminal sequence available. However, disulfide bond-reducing enzymes have to this day not been assayed on wool or human hair keratin. The effect of keratinase on enzymatic disulfide bond reduction has also not yet been explored.

Moreover, enzymes are known to catalyse the formation of crosslinks *in* vivo in a range of substrates, such as casein and lignin. Many crosslinking enzymes have been identified and characterised, with some commonly used in industry towards a range of different applications such as yoghurt manufacturing or wool processing. The enzymatic formation of keratin-keratin crosslinks in hair has, however, not been investigated to date.

Therefore, identifying enzymes with potential disulfide bond-reducing and crosslinking activities that can accept keratin, and particularly human hair, as a substrate is of great interest and relevance. Their use as active agents for permanent hair straightening would offer a milder, biocompatible and highly selective alternative to harsh chemicals currently used on the market.

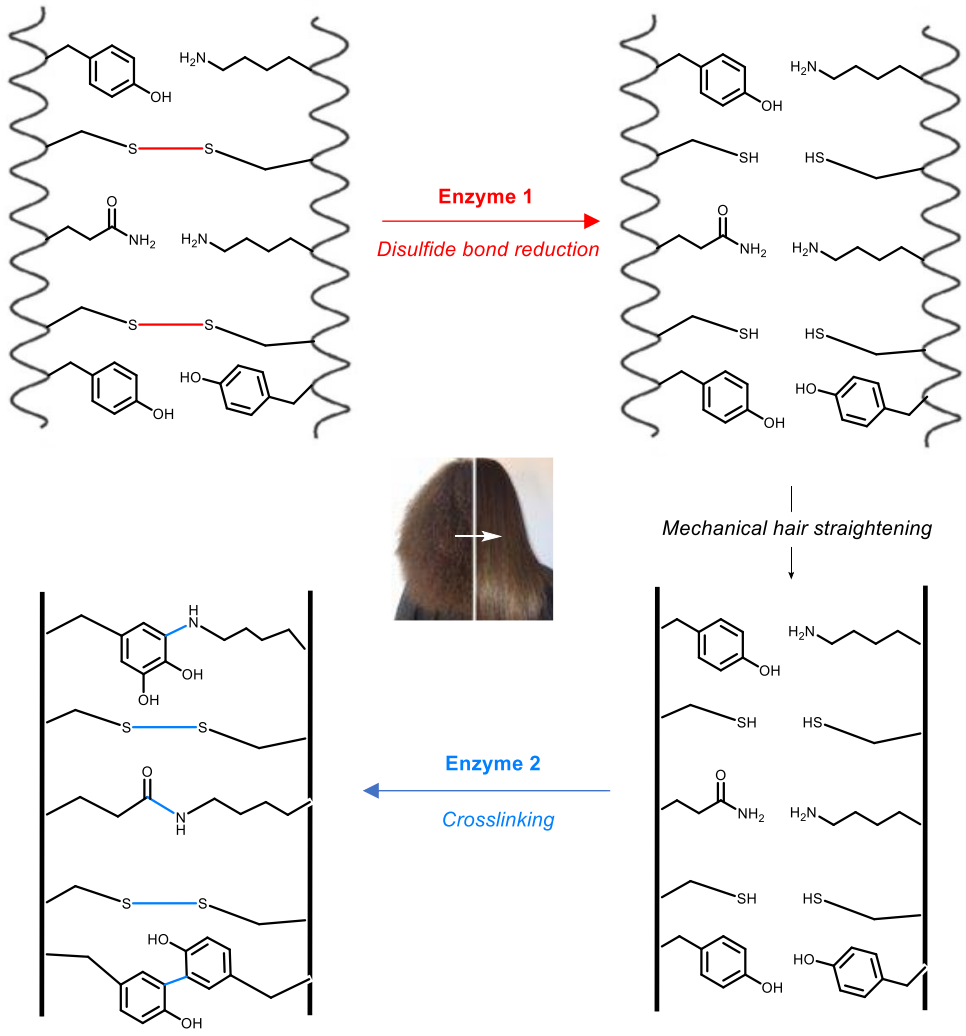

Figure 21. Hypothetical steps towards permanent enzymatic hair straightening *via* disulfide bond reduction and subsequent crosslinking.

This study investigates the potential use of enzymes in permanent hair straightening. Enzymatic catalytic steps for permanent hair straightening are predicted to involve the breaking of keratin disulfide bonds between keratin fibres by a first enzyme, followed by mechanical hair straightening and the formation of keratin-keratin crosslinks by a second enzyme to set the new morphology (Figure 21).

For the keratin disulfide bond reduction step, the thioredoxin system from *Bacillus subtills*, belonging to the family of disulfide bond reductases, will be investigated. Not only are *Bacillus* species popular bacterial workhorses among microbial enzyme producers, *Bacillus subtilis* is also known as a

keratin-degrading microorganism, where disulfide bond reduction is believed to play a crucial role. Moreover, *Bacillus subtilis* thioredoxin and thioredoxin reductase, which make up the thioredoxin system alongside an NADPH cofactor, have been expressed, purified and characterised with clear disulfide bond-reducing activities on folded proteins such as insulin. Keratinase from *Bacillus licheniformis*, an enzyme known to degrade chicken feather and hair keratin in the presence of reducing agents, will also be studied regarding its effect on the hair penetration and disulfide bond-reducing activity of the thioredoxin system. The impact enzymatic disulfide bond reduction may have on the keratinolytic activity of keratinase will also be considered.

A range of well-characterised protein crosslinking enzymes currently used in industry, including laccase from *Trametes versicolor*, tyrosinase from mushroom and microbial transglutaminase, will then be investigated towards the formation of intermolecular keratin-keratin crosslinks in hair.

The selected enzyme candidates will either be expressed and purified or commercially sourced before being assayed for respective disulfide bond-reducing and crosslinking activities on keratin. Solubilised wool will first be used as a soluble keratin substrate to avoid enzyme penetration issues associated with solid keratin substrates, before assaying enzymatic activities on solid hair.

2.2. Objectives

2.2.1. Enzymatic disulfide bond-reducing activities on keratin

This objective is to investigate the potential of enzymes for catalysing disulfide bond reduction in keratin substrates, specifically human hair, as a first step towards permanent hair straightening. First, both thioredoxin and

thioredoxin reductase from *Bacillus subtilis* will be expressed in *E. coli* and purified by Immobilised Metal-Affinity Chromatography (IMAC). The enzymes will then be assessed alongside an NADPH cofactor using a range of spectrophotometric assays involving the reaction of 5,5'-dithiobis(2-nitrobenzoic acid) (DTNB, Ellman's reagent) with free thiols as well as NADPH consumption upon substrate disulfide bond reduction. Solubilised wool substrates will initially be used to facilitate enzymatic keratin penetration before moving to solid human hair. Hair keratin structure opening will be investigated using a range of methods such as fibre swelling, delipidation and hair grinding and solubilisation. Moreover, the effect of keratinase from *Bacillus licheniformis* on enzymatic keratin disulfide bond reduction will be evaluated.

2.2.2. Formation of keratin-keratin crosslinks using enzymes

This objective involves the evaluation of well-characterised crosslinking enzymes as potential active agents for the durable setting of mechanically straightened human hair. The commercially available laccase from *Trametes versicolor*, tyrosinase from mushroom and microbial transglutaminase will be assayed for potential intermolecular crosslinking activity on keratin substrates. The crosslinking of soluble keratin from wool will first be investigated using a range of assays, including sodium dodecyl-sulfate polyacrylamide gel electrophoresis (SDS PAGE) and Size-Exclusion chromatography (SEC). Solid-hair crosslinking will then be assayed *via* tensile strength analyses.

Eventually, the suitability of selected disulfide bond-reducing and crosslinking enzymes as permanent hair-straightening active agents will be assessed.

3. Materials and methods

3.1. Materials

Media and buffers were prepared using deionised (dH_2O) and milliQ water (mQH_2O), respectively. distilled water. Chemicals were purchased from Merck, unless mentioned otherwise. Buffer pH was measured and adjusted using a pH electrode (HI1131, Hanna instruments). Cells and samples were incubated in New Brunswick Scientific Innova Incubator Shakers (Eppendorf). Plasmids were purified using the PureLink Quick Plasmid (Invitrogen) and QIAprep Spin (Qiagen) Miniprep Kits, according to the manufacturers' instructions. Sanger sequencing was performed by Source Bioscience and by the University of Nottingham Medical school using T7 promoter forward primer and T7 terminator reverse primer (Appendix Table 3.1).

SDS PAGE analyses. SDS PAGE analyses were performed using Pre-cast MiniProtean TGX 4-20% Sodium Dodecyl Sulphate Polyacrylamide Gel Electrophoresis (SDS PAGE) gels (BioRad) and run using a Mini-PROTEAN Tetra System (BioRad), and imaged using G:BOX Chmi XRQ gel doc system (Syngene). The following ladders were used: PageRuler™ Plus Unstained Protein Ladder 10-250 kDa (Thermofisher), 10-180 kDa PageRuler™ Prestained Protein Ladder (Thermofisher) and Precision Plus Prestained Protein Ladder 10-250 kDa (BioRad).

3.1.1. Protein expression

All biological experiments were conducted under aseptic conditions. All media and flasks were sanitised using a Prestige Classic 2100 benchtop autoclave (Medstore Medical), at operating temperatures and pressures of 126°C and 1.4 bar.

The *trxA* and *trxB* genes from *Bacillus subtilis* strain 168 (UniProt accession numbers P14949, 309 bp & P80880, 948 bp) were synthesised by GeneWiz. The *kerA* gene from *Bacillus licheniformis* PWD-1 (GenBank A78160.1, 1,457 bp) was synthesised by GeneArt (Invitrogen). *BamHI*, *NdeI*, *SacI* and *XhoI* restriction enzymes were purchased from ThermoFisher. Agarose gel analysis was conducted using 1Kb Plus DNA Ladder (Invitrogen) ladder.

E. coli DH5α, BL21, BL21(DE3), Rosetta(DE3) and BL21(DE3)RIPL competent cells were purchased from Merck. pET21a(+) and pMP89b plasmids were purchased from AddGene and Novagen, respectively. Details regarding plasmids, primers and bacterial strains used in this study can be found in the appendix (Tables 3.1-3). *Escherichia coli* strains were grown in Lysogeny Broth Miller (LB, 25 g/L, ThermoFisher). Where needed, growth media was supplemented with kanamycin or carbenicillin (100 µg/mL). LB agar was purchased from ThermoFisher and made up with dH_2O at LB and agar concentrations of 25 g/L and 12 g/L, respectively.

Cultures were grown in Erlenmeyer flasks in a shaker, and cells were harvested using an Avanti J-26 XP centrifuge (Beckman Coulter) or a 5810R centrifuge (Eppendorf), and then stored at -80°C in a DW-86L828J freezer (Haier Biomedical).

Sanger sequencing was performed by Source Bioscience and by the University of Nottingham Medical school, using T7 promoter forward primer and T7 terminator reverse primer.

3.1.2. Protein purification

Cells were lysed using a Model 120 Sonic Dismembrator (Fisher Scientific). Protein purification was performed with a HisTrap FF crude 1mL affinity column for protein purification (GE Healthcare) using an AKTA Fast Liquid

Protein Chromatography System purifier 10 (GE Healthcare). Purified enzyme fractions were dialysed using 14,000 Molecular Weight Cut-Off (MWCO) dialysis tubing cellulose membranes (Merck) and concentrated using Vivaspin® 50 (10,000 MWCO) centrifugal concentrators (Sartorius). Protein concentrations were measured both *via* the bicinchoninic acid (BCA) assay on a Fluostar OPTIMA plate reader (BMG Labtech) and *via* A280nm absorbance measurements acquired on a UV-2600 with a CPS-100 cell positioner (Shimadzu).

3.1.3. Enzymatic assays

Commercial keratinase (KerA) from *Bacillus licheniformis* (K4519, batches SLBT4138, SLCH6265 and SLCH6225), thioredoxin (Trx1) from *Escherichia coli* (T0910, batch #0000090758)), laccase (PoLac) from *Pleurotus ostreatus* (75117, batch #BCBH4411V), tyrosinase (Tyr) from mushroom (T3824 batch #SLCG8506) and microbial transglutaminase (Tg, SAE0159, batch #SLCH4794) were ordered from Merck. Laccases from *Trametes versicolor* (53739, Batch #1350185) was supplied by Honeywell. ABTS was purchased from VWR Life Science. Solid human hair and soluble wool keratin substrates Keratec™ IFP (batch #P13K2005) and Keratec™ ProSina (batch #21F19B111) were provided by Croda International. Azure-dyed sheep's wool (keratin azure) was purchased from Merck. Where mentioned, samples were centrifuged using the MiniSpin plus centrifuge (Eppendorf, for volumes < 1.5 mL) or centrifuge 5810 R (Eppendorf, for volumes > 2mL).

3.1.3.1. Enzymatic assays with soluble substrates

Soluble keratin purification was performed using SnakeSkin 3.5K Molecular Weight Cut-Off (MWCO) Dialysis Tubing (Thermo Scientific) and Vivaspin® 20 (3,000 MWCO) centrifugal concentrators (Sartorius Stedim Biotech).

Keratin concentrations were measured using BCA and Bradford assays on a Fluostar OPTIMA plate read (BMG Labtech).

Enzymatic activities were analysed *via* ultraviolet-visible (UV-Vis) spectrophotometric absorbance measurements acquired on a UV-2600 with a CPS-100 cell positioner (Shimadzu). Quartz QS High Precision Cell cuvettes (10 mM light path, Hellma analytics) were used for absorbance measurements, unless otherwise specified. SDS PAGE, viscosity measurements using a strain-controlled Modular Compact Rheometer MCR-301 (Anton Paar), Gel Permeation Chromatography (GPC) using an Agilent Infinity II stack equipped with a UV detector, RI detector, viscometer, light scatter detector and 2xOHGel Mixed M column and 5 µm OHGel guard column, and Size-Exclusion Chromatography (SEC) using a Superdex 200 Increase 10/300 GL column with an AKTA Fast Liquid Protein Chromatography System purifier 10 (GE Healthcare) were used to analyse activities of crosslinking enzymes.

3.1.3.2. Enzymatic assays with solid substrates

Solid hair samples were analysed *via* Scanning Electron Microscopy using a gold sputter coater machine (Turbo Carbon Coater) and a FEI XL30 Scanning Electron Microscope (Phillips). Tensile strength measurements were made using an Automated Crimper (AAs 1600, Dia-Stron) and a Miniature Tensile Tester (MTT680, Dia-Stron) Set Up complete with a Laser Micrometer (Mitutoyo LSM-6200) housed in a closed chamber with humidity control.

3.2. Gene cloning and protein expression

3.2.1. Thioredoxin (trxA) and thioredoxin reductase (trxB) from Bacillus subtilis

The *trxA* and *trxB* genes from *Bacillus subtilis* strain 168 (UniProt accession numbers P14949 & P80880) were codon-optimised for expression in *E. coli* and synthesised in a generic high copy plasmid (pUC-GW-Kan). The same plasmid was used for both genes, which were flanked by *NdeI* and *XhoI* restriction sites and were combined *via* a 9 bp base linker (Appendix Figure 3.1).

3.2.1.1. Preparation of pET21a::*trxA* & pET21a::*trxB* plasmids

pUC::trxA::trxB digestion. DNA fragments containing *trxA* and *trxB* genes from *Bacillus subtilis* were isolated by digestion of the pUC::*trxA*::*trxB* plasmid with *NdeI* and *XhoI* restriction enzymes. Samples (20 µL) were made-up on ice from 2 µL of FastDigest Green Buffer (ThermoFisher), 1 µL of *NdeI* and *XhoI* restriction enzymes, 3 µL of plasmid DNA and mQH_2O. The samples were incubated at 37 °C for 1 h, followed by denaturation at 65 °C for 20 min.

Agarose gel electrophoresis and extraction. trxA (309 bp) and *trxB* fragments (948 bp) were isolated and purified from the vector fragment (5.4 kbp) by agarose gel electrophoresis and gel extraction. DNA was loaded onto a 0.8% agarose (w/v) TAE (ThermoFisher) gel, containing 0.01% SYBERsafe (ThermoFisher): 5 µL of 1Kb Plus DNA Ladder (Invitrogen), and 12 µL of sample, made up of 2 µL of DNA, 2 µL of DNA Gel Loading Dye (6X, ThermoFisher) and 8 µL of dH_2O. The gel was run for 35 min at 210 V and imaged under a UV source. The gel was run for 90 min at 90 V. Resulting bands were then excised using a scalpel. DNA was purified using the

Purelink Quick Gel Extraction Kit (Invitrogen) according to the manufacturer's instructions and quantified by absorbance at 260 nm.

trxA and trxB ligation into pET21a. *trxA* and *trxB* fragments were individually ligated into *NdeI* and *XhoI* digested pET21a plasmids using T4 DNA Ligase Reaction Buffer (NEB) and T4 DNA Ligase (NEB). Samples (20 µL) were made-up on ice from 2 µL of T4 DNA Ligase Reaction Buffer, 1 µL of T4 DNA Ligase, 2.6 µL of double-digested pET21a vector, 4 µL of double-digested *trxA* or *trxB* insert and dH_2O. The ligation mix was then incubated at 16 °C overnight, followed by 10 minutes at 65 °C.

DH5α transformation with pET21a::trxA and pET21a::trxb. DH5α cells were transformed with the pET21a::*trxA* or pET21a::*trxB* ligation mix – a no-insert negative control was included. Plasmid DNA (5 µL, 500 ng) was added to a 20 µL aliquot of DH5α cells and the mixture was gently mixed. The *E. coli* mix was incubated on ice for 30 min prior to being heat-shocked for 60 s at 42 °C. After a further 15 min incubation on ice, cells were harvested by centrifugation at 4,000 g for 5 mins. Supernatants were removed and pellets resuspended in LB medium (100 µL). The transformed cells were then incubated at 37 °C for 1 h at 250 rpm, before cells (50 µL) were plated on LB agar supplemented with carbenicillin (100 µg/mL). The plates were incubated overnight at 37 °C.

pET21a::trxA and pET21a::trxb purification. Single colonies were used to inoculate LB medium (5 mL, supplemented with 100 µg/mL carbenicillin) overnight at 37 °C, 250 rpm. This was done for two colonies of each of *pET21a::trxA and pET21a::trxb*-transformed cells. pET21a::*trxA* & pET21a::*trxb* were then respectively isolated from culture by plasmid miniprep. Glycerol stocks were prepared from *E. coli* DH5α pET21a::*trxA* and pET21a::*trxB* colonies. Glycerol solution was made up from glycerol (50%

volume) and ddH_2O (50% volume) and autoclaved. Single colony-inoculated LB-carbenicillin overnight preculture (0.5 mL) was mixed with glycerol solution (0.5 mL) into cryovials and stored at -80 °C.

E. coli BL21(DE3) pET21a::trxA and E. coli BL21(DE3) pET21a::trxB construction. The pET21a::trxA and pET21a::trxB plasmids were transformed into E. coli BL21 (DE3) according to the manufacturer's instructions. Single colonies were used to inoculate LB medium (5 mL, supplemented with 100 µg/mL carbenicillin) overnight at 37 °C, 250 rpm. pET21a::*trxA* & pET21a::*trxB* were then respectively isolated from culture by plasmid miniprep. Plasmid DNA was quantified by absorbance at 260 *n*m. Cloning success was investigated *via* Polymerase Chain Reaction (PCR) using primers SEQ27 and SEQ 28 (Appendix Table 3.1).

Polymerase Chain Reaction. PCR samples were made-up on ice from pET21a::*trxA* and pET21a::*trxB* DNA (1 µL), 10 µM forward and reverse primers (2.5 µL), 5 x Q5 Reaction Buffer (10 µL), Q5 high-fidelity polymerase (0.5 µL), 10 mM dNTP (1 µL) and ddH_2O up to 50 µL. The mixture was then placed into a thermocycler. The PCR cycling condition comprised of an initial step of 30 s at 95 °C, a second step of 30 cycles including 10 s at 95 °C, 30 s at 60 °C and 95 s (extension time) at 65 °C, and a final extension step of 2 mins at 65 °C. The PCR product was assessed via agarose gel analysis and purified *by* gel extraction. DNA was quantified by absorbance at 260 nm and sequence verifications of the gene inserts (*trxA* and *trxB*, respectively) were performed by Sanger Sequencing using T7 promoter forward primer and T7 terminator reverse primer (Appendix Table 3.1) as the sequencing primers. For each PCR product (*trxA* and *trxB*), two 20 µL samples at 10 ng/µL concentrations were submitted, where each sample was used for both forward and reverse sequencing.

Glycerol stocks were prepared from E. coli BL21 (DE3) pET21a::trxA and pET21a::trxB colonies and stored at -80 °C.

3.2.1.2. Thioredoxin and thioredoxin reductase expression

Protein expressions were conducted as described by Parker et al. (2014).[175] pET21a::*trxA* and pET21a::*trxB E. coli* BL21 (DE3) transformed colonies were used to inoculate LB medium (15 mL, supplemented with100 µg/mL carbenicillin) overnight at 37 °C, 250 rpm. Starter cultures (500 µL) were then added to LB medium (50 mL, supplemented with 100 µg/mL carbenicillin, 250 mL Shake flask). The 50 mL cultures were grown at 37 °C, 250 rpm until the optical density at 600 nm (OD_{600}) reached 0.8. Samples (1 mL) were collected, centrifuged, and pelleted cells were stored at -20 °C as pre-induction controls. At that point, protein expressions were induced by the addition of IPTG (0.2 mM) to the cultures, which were then incubated for a further 2 hours at 37 °C, 250 rpm. Samples (1 mL) were collected, centrifuged and pelleted cells were stored at -20 °C. Cells were then harvested by centrifugation at 5,000 g for 15 minutes at 4 °C, supernatants were discarded and pellets were stored at -20 °C. Pelleted cells were resuspended in 10 mL of lysis buffer (1 protease inhibitor tablet, 10 mg of lysozyme, 1 µL DNAse and 10 mL of 50 mM Tris HCl buffer, pH 7.5) and incubated and stirred on ice for 1 h. The cells were then homogenised by ultrasonic treatment (5 min, 30 s on, 30 s off, 35% amplitude). Total protein (lysate) samples (1 mL) were collected and stored at -20 °C. Centrifugation at 15,000 g for 25 min at 4 °C allowed for the separation of cell debris (insoluble cell fraction) from the cell-free extract. Cell-free extract (supernatant, soluble protein) samples (1 mL) of the supernatant were collected, centrifuged, and pelleted cells were stored at -20 °C.

SDS-PAGE analyses. Protein expression samples (pre-induction control, lysate, cell-free extract & insoluble (dissolved in urea (3.5 mL, 6M)) were analysed by SDS PAGE. Samples (1 mL) were dissolved in 50 mM Tris HCl buffer (1 mL), pH 7.5. These dissolved samples (20 µ) were mixed with Laemmli sample buffer (20 µL, 4% SDS, 20% glycerol, 10% 2-mercaptoethanol, 0.004% bromophenol blue and 0.125 M Tris HCl (pH 6.8)) and denatured at 95 °C for 5 min. Protein ladder (5 µL) and samples (10 µL) were loaded onto pre-cast SDS PAGE gels and ran at 200 V, 400 mA for 35 min, with Tris-Glycine-SDS running buffer (14.4 g/L glycine, 3 g/L Tris, 1 g/L SDS). Gels were stained with Coomassie overnight and destained (40% methanol, 10% acetic acid in mQH_2O) overnight before being imaged.

Lower induction and incubation temperatures (30 °C), reduced IPTG concentrations (0.1 *m*M) and longer incubation periods (from 2 hours to overnight) were also trialled for *trxA* and *trxB* expression.

3.2.1.3. Thioredoxin and thioredoxin reductase purification

Protein purification was conducted as described by Parker et al. (2014).[175] Cell-free extract samples were loaded on a 5 mL His-Trap FF Crude column and purified by IMAC. The column was washed with 5 column volumes of water and equilibrated with 5 column volumes of binding buffer (50 mM sodium phosphate, 300 mM NaCl, 10 mM imidazole, 5% (w/v) glycerol, pH 7.6). The sample was injected using a 5 mL syringe, and the column was further washed with 3 column volumes of binding buffer (flow-through). Thioredoxin was eluted from the column on a 20-column volume 10-250 mM imidazole gradient, while thioredoxin reductase was eluted on a 20-column volume 10-1000 mM imidazole gradient.

Fractions containing the purified protein were identified by SDS PAGE. These were then combined into a dialysis bag and dialysed overnight against

1 L of 50 *m*M Tris HCl, pH 7.5 buffer to remove imidazole. The dialysed fractions (approximately 15 mL) were then concentrated using Vivaspin® ultrafiltration centrifugal concentrators. The column was rinsed with 5 mL of 50 mM Tris HCl buffer, pH 7.5 and centrifuged (4,000 g, 10 min at 10 °C). Sample (15 mL) was then loaded onto the column and centrifuged (4,000 g, 10 min at 10 °C) until a desired concentration was achieved. Thioredoxin and thioredoxin reductase protein concentrations and expression yields were determined using 280 nm absorbance measurements and BCA assay, respectively, as suggested by Parker et al. (2014).

A280 nm protein concentration determination. Thioredoxin (Ɛ_{280}=12,615 M^{-1} cm^{-1}, as estimated using Expasy Prot Param)[1] protein concentration was calculated from 280 nm absorbance as follows, using the Beer-Lambert law (A is the absorbance, Ɛ is the protein extinction coefficient ($M^{-1}cm^{-1}$), c is the concentration (M) and l is the pathlength (cm):

$$A_{280nm} = \varepsilon cl$$

Moreover, with a 1 cm path length cuvette, where M_w is in Daltons and protein concentration is in mg/mL:

$$Protein\ concentration\ = \frac{A_{280nm}}{\varepsilon} \times M_w$$

BCA assay. Protein concentrations were determined using a standard curve of bovine serum albumin (BSA), over a concentration range 0 to 2.0 mg mL^{-1}. Pierce Rapid Gold BCA Working Reagent (10.2 mL, Thermoscientific) was prepared by mixing Rapid Gold BCA Reagent A (10 mL, Thermoscientific) with Rapid Gold BCA Reagent B (0.2 mL, Thermoscientific). Standards and samples (20 µL) were pipetted into a 96-well plate, in triplicates, and Working Reagent (200 µL) was added to each well. The plate was then shaken for 30

seconds before being incubated at room temperature for 5 minutes. Absorbances were then measured at 480 nm, and the average blank (20 µL of deionised water in 200 µL of Working Reagent) 480 nm absorbance measurement was subtracted from the those of standard and sample replicates. Absorbances of BSA standards were then used to generate a standard curve (Figure 22), from which protein concentration was estimated.

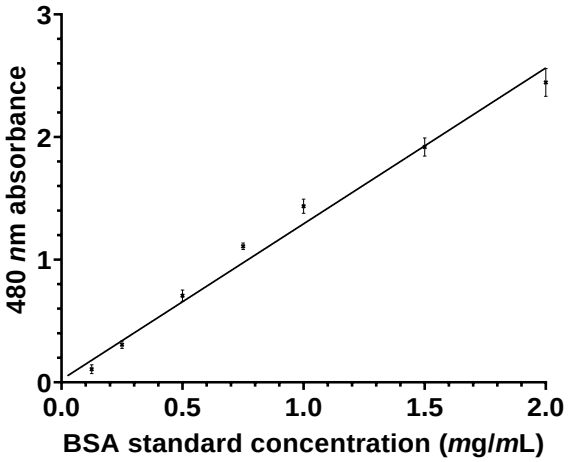

Figure 22. Example of BSA standard curve for BCA assay of purified thioredoxin reductase from *Bacillus subtilis*. 0-2.0 mg/mL BSA, triplicate measurements, line of best fit generated using GraphPad Pryzm, where y = 1.271x + 0.02125.

Purified thioredoxin and thioredoxin reductase were then analysed via SDS PAGE analysis and 200-800 nm absorbance spectra recording.

3.2.2. Keratinase from Bacillus licheniformis

The *kerA* gene from *Bacillus licheniformis* PWD-1 (UniProt accession number Q53521) used in this study was codon-optimised for expression in *E. coli* and received in a generic high copy plasmid (pUC::*kerA*). *BamHI* and *SacI* restriction sites were inserted manually using SnapGene.

3.2.2.1. Preparation of pMP89b::*kerA* plasmid

pUC::*kerA* a and pMP89b plasmids were digested with *BamHI* and *SacI* restriction enzymes. Digestion success was assessed via agarose gel electrophoresis, while *kerA* (1.1 kbp) and pMP89b (3 kbp) fragments were

isolated and purified by gel extraction. The *kerA* fragment was then ligated into the digested pMP89b plasmid. *E. coli* DH5α cells were transformed with the pMP89b::*kerA* ligation mix (2 µL, 200 ng) – *E. coli* DH5α cells were also transformed with digested pMP89b and *kerA* as negative controls. Single colonies were then screened by colony PCR.

Colony PCR. PCR samples (60 µL) were made-up on ice in from a ligation mix-transformed colony, 1.2 µL of 10 µM oligo-CF-F1 and oligo-CF-R1 primers (Appendix Table 3.1), 3 µL of 100% DMSO (Sigma-Aldrich), 1.2 µL of 10 mM of deoxynucleotide (dNTP) Solution Mix (NEB), 12 µL of 5 x Q5 Reaction Buffer (NEB), 0.2 µL of Taq DNA Polymerase (NEB) and 41.2 µL of dH_2O. The PCR cycling condition comprised an initial step of 30 s at 94 ºC, a second step of 35 cycles including 10 s at 94 ºC, 30 s at 54 ºC and 120 s (extension time) at 72 ºC, and a final extension step of 10 min at 72 ºC. PCR products were analysed via agarose gel analysis.

pMP89b::kerA purification and sequencing. A colony that was successfully transformed with pMP89b::*kerA* was used to inoculate LB medium (15 mL), supplemented with carbenicillin and cultured overnight at 37 °C, 180 rpm. pMP89b::*kerA* plasmid was then purified and sequenced. Plasmid DNA was quantified by absorbance at 260 nm.

3.2.2.2. Keratinase expression

E. coli BL21(DE3) pMP89b::kerA construction. pMP89b::*kerA* plasmid was transformed into *E. coli* BL21(DE3) cells according to the manufacturer's instructions. A single colony was used to inoculate LB medium (15 mL, supplemented with carbenicillin), and this was cultured for 7 h at 37 °C, 180 rpm before the cells were cryostocked (glycerol stocks). Transformation was verified *via* pMP89b::*kerA* purification, digestion followed by Sanger sequencing.

Keratinase expression. Protein expression was conducted as described by Hu *et a*l. (2013).[94] An *E. coli* BL21(DE3) pMP89b::*kerA* colony was used to inoculate LB medium (15 mL), supplemented with carbenicillin in a 50 mL sterile Falcon tube, and cultured for 16 h at 37 °C, 180 rpm. Starter culture (500 µL) was then added to LB medium (50 mL) supplemented with carbenicillin. The 50 mL culture was grown at 37 °C, 180 rpm until OD_{600} reached 0.6. *KerA* expression (pre-, pro- and mature protein) was then induced by the addition of IPTG (1 mM) to the culture after it had reached an OD_{600} of 0.6. After another 4.5 hours of incubation, cells were harvested at 8,000 g for 12 minutes at 4 °C. The pelleted cells were resuspended in 5 mL of lysis buffer ($1/8^{th}$ of a protease inhibitor tablet, 1.5 mg of lysozyme, 0.5 µL DNAse and 5 mL of 50 mM Tris HCl buffer, pH 7.5) and incubated on ice for 1 h, with stirring. The cells were then homogenised by ultrasonic treatment (5 min, 59 s on, 59 s off, 35% amplitude) and centrifuged at 8,000 g for 15 min at 4 ºC. Protein expression samples (pre-induction control, lysate, cell-free extract and insoluble (dissolved in urea (3.5 ml, 6M)) were then analysed via SDS PAGE. Post-IPTG induction incubation temperature as well as cell growth media and lysis buffer composition were varied throughout this study.

3.3. Enzymatic assays

3.3.1. Enzyme preparation and storage

Commercial keratinase (KerA, 32 kDa) from *Bacillus licheniformis* was received as a lyophilised powder and aliquoted as 76.9 units/mL[1] (0.22 mg/mL) in mQH_2O. Thioredoxin (TrxA, 11.4 kDa) and thioredoxin reductase (TrxB, 34.5 kDa) from *Bacillus subtilis* were aliquoted at 15.27 U/mL[2] (3.06 mg/mL) and 0.80 mg/mL concentrations, respectively. Commercial

[1] Based on enzymatic activities specified by supplier for specific batch
[2] Based on enzymatic activity calculations performed in this study

thioredoxin from *E.* coli (Trx1, 11.7 kDa) was received as a lyophilised powder and aliquoted as 2.35 U/mL^2 (0.5 mg/mL) in mQH$_2$O. Laccases from *Trametes versicolor* (TvLac, 63 *k*Da) and *Pleurotus oreatus* (PoLac, 64 kDa) were stored at -20 °C as 1 mg/mL (3.41 U/mL^2 and 2.94 U/mL^2, respectively) aliquots in mQH$_2$O for standard assays, and as 10 mg/mL (34.1 U/mL and 29.4 U/mL,) aliquots in mQH$_2$O for crosslinking treatments. Tyrosinase from mushroom (Tyr, 119.5 kDa) was received as lyophilised powder and aliquoted as 10.93 U/mL (1 mg/mL) in mQH$_2$O. Microbial transglutaminase (Tg, 38.3 kDa) was received as a lyophilised powder and aliquoted 0.74 U/mL^2 (52.6 µg/mL) in mQH$_2$O. All enzyme aliquots were stored at -20 °C. Unit definitions are given in Section 3.3.3. below.

3.3.2. Keratin substrate characterisation and pre-treatment

3.3.2.1. Soluble keratin substrate

3.3.2.1.1. Molecular weight distributions

Keratec™ IFP and Keratec™ ProSina molecular weight distributions were evaluated by SDS PAGE and SEC.

SDS PAGE analysis. Keratec™ IFP (20 µL of 6.5 mg/mL stock in deionised water) and Keratec™ ProSina (20 µL of 23.6 mg/mL stock in deionised water) were mixed with Laemmli sample buffer (20 µL) and incubated for 10 min at 100 °C. Protein ladder (5 µL) and samples (10 µL) were then loaded onto a pre-cast SDSPAGE gels and run at 200V, 400 mA for 35 minutes with running buffer. Gels were stained with Coomassie overnight, and destained before being imaged.

Size-Exclusion Chromatography. Keratec™ IFP (1 mL of 32.5 mg/mL stock in deionised water) was filtered through a 0.22 µm syringe filter (Starlab) and analysed by SEC using an AKTA Purifier liquid chromatography system. The chromatographic analyses were performed by injecting 500 µL of sample into

the Superdex 200 Increase 10/300 GL column. The chromatographic separations were performed in a refrigerated cabinet at 4.5 °C with 0.1 M Tris, and 150 mM NaCl (pH 8) as eluent, with a flow rate of 0.5 mL/min. The SEC profiles of the eluting proteins were determined with a UV-Vis detector linked to the SEC system and operating at 280 nm. Standard proteins of known molecular weights (Cytochrome c (12.4 kDa, 2 mg/mL), Carbonic Anhydrase (29 kDa, 3 mg/mL), Bovine Serum Albumin (66 kDa, 10 mg/mL), Alcohol dehydrogenase (150 kDa, 4 mg/mL), β-Amylase (200 kDa, 5 mg/mL) and Apoferritin (449 kDa, 10 mg/mL), stocks made in mQH_2O) were also analysed by SEC to enable retention volume comparisons and evaluation of crosslinked protein sizes. For each sample, 1.5 mL fractions were collected, and relevant ones were further analysed by SDS PAGE.

3.3.2.1.2. Peptide/protein contents

Peptide and protein contents of Keratec™ IFP and Keratec™ ProSina were investigated using the BCA and Bradford assays.

BCA assay. Keratec™ IFP (20 µL of 1 in 500-1000 dilutions of 6.5 mg/mL stock in deionised water) and BSA standards (20 µL) were pipetted into the plate alongside Working Reagent (200 µL). The plate was shaken, incubated at room temperature, and absorbances were then measured at 480 nm. Keratec™ IFP protein concentration was then estimated from the BSA standard curve.

Bradford assay. Protein concentrations were determined using a standard curve of bovine serum albumin (BSA), over a concentration range 0 to 1.0 mg/mL. Bradford reagent (300 µL, BioRad) was pipetted into a 96-well plate, followed by Keratec™ ProSina (10 µL of 1 in 2 dilution of 47.1 mg/mL stock in mQH_2O) or standard (10 µL), in triplicates. The plate was mixed and incubated in the dark at room temperature for 1 h. The control (Bradford

reagent only), standard and protein samples were analysed at a wavelength of 595 nm. The measurements were normalised by subtraction of a blank (300 µL of Bradford reagent with either 10 µL of mQH_2O (for standards) or 10 µL of 50 mM Tris-HCl, pH 7.5 (for protein samples)). Absorbances of BSA standards were then used to generate a standard curve, from which Keratec™ ProSina concentrations were estimated.

3.3.2.1.3. Keratec™ IFP thiol availability

Keratec™ IFP thiol availability was measured using the Ellman's assay.[275]

Ellman's assay. Keratec™ IFP (0.5 mL of 65 mg/mL stock, final conc. 3.25 mg/mL) was incubated with DTT (20.8 mg/mL, 0.13 M) in Ellman's buffer (100 mM Sodium Phosphate buffer with 1 mM EDTA buffer, pH 8) up to 10 mL for 1 hour at 37 °C, 250 rpm. Untreated Keratec™ IFP was also investigated as a negative control. Following incubation, DTT was removed by two dialyses operations using 3 kDa MWCO dialysis tubes, each against 1 L deionised water and performed overnight at room temperature. The number of dialysis cycles required to avoid DTT interference with the assay was evaluated by assaying the presence of DTT in the dialysis buffer for samples treated with a range of DTT concentrations (0-22.2 mg/mL in mQH_2O). To assay the presence of thiols in the sample and dialysis buffer, DTNB (20 µL of 4 mg/mL stock, final concentration of 0.08 mg/mL, 0.20 µM) was added to DTT-treated Keratec™ IFP (980 µL of 3.25 mg/mL stock, final conc. 3.19 mg/mL) or dialysis buffer (980 µL) and the samples were incubated at 37°C for 15 minutes. Thiol release was then measured *via* 412 nm absorbances. Samples were diluted where absorbances were too high (>2.5). The 412 nm absorbance of the final dialysis buffer was also measured to check for the successful removal of DTT. Thiol quantification was conducted using Beer Lambert's law as follows (A is the absorbance, Ɛ is the

TNB^{2-} extinction coefficient (13,6000 $M^{-1}cm^{-1}$ at pH 8), c is the concentration (mg/mmol) and l is the pathlength (cm).

$$A_{412nm} = \varepsilon cl$$

$$c = \frac{A_{412nm}}{\varepsilon l}$$

3.3.2.1.4. Keratec™ substrate dialysis

To remove any impurities or additives from the substrates, Keratec™ IFP and Keratec™ ProSina were dialysed at a 3 kDA MWCO at room temperature. Prior to dialysis, substrate viscosity was lowered by performing a 2x dilution in deionised water (7.5 mL substrate for a 15 mL total volume). Diluted substrates (15 mL) were then pipetted into respective pre-soaked dialysis bags, which were placed in deionised water (2 L) to stir overnight at room temperature, followed by two buffer exchanges with 4 h and overnight stirring, respectively. Substrate volumes pre- and post-dialysis were recorded to account for any dialysis-related dilutions.

Centrifugal buffer exchange by Vivaspin® 20 columns (3,000 MWCO) was also investigated for removal of impurities however, this method was hindered by the high viscosity associated with Keratec™ IFP and Keratec™ ProSina substrates.

The effects of dialysis on Keratec™ substrates were analysed *via* SDS PAGE and SEC.

3.3.2.2. Human hair substrate

3.3.2.2.1. Hair thiol availability

The thiol availability of human hair samples was measured using the Ellman's assay, similarly to what was described above for Keratec™ IFP (see section 3.3.2.1.3.). In brief, human hair (20 mg/mL) was incubated with DTT

(20.8 mg/mL, 0.13 M) in Ellman's buffer for 1 hour at 37 °C, 250 rpm. Untreated hair was also investigated. Following incubation, DTT was removed by five successive buffer rinsings (DTT-removal method assessed via Ellman's assay and ^{1}H-NMR) and substrates resuspended in buffer up to 1 mL. DTNB (0.20 µM) was then added before further incubation at 37°C for 15 minutes. Thiol release was then measured via 412 nm supernatant absorbances. 412 nm absorbances of final washes were also measured and subtracted from samples. Thiol quantification was then conducted using Beer Lambert's law.

3.3.2.2.2. Hair solubilisation

Human hair (100 mg) was incubated in NaOH (8.8 mL of 10 M stock in deionised water) in an oil bath at 90 °C for 15 minutes until complete dissolution, as suggested by Sarmani et al. (1997).[104] In the case of ionic liquid solubilisation, human hair (500 mg) was incubated in 1-Ethyl-3-methylimidazolium ethyl sulphate (EMIM[ESO_4]), 8 mL) in an oil bath at 120 °C overnight, inspired by work conducted by Zhang et al. (2017).[106] The compatibility of these solubilised hair substrates with enzymatic analyses were investigated *via* SDS PAGE and Ellman's assay.

3.3.2.2.3. Hair structure opening

Human hair (0.03 g) was incubated overnight at 37 °C, 250 rpm, according to a range of treatment conditions. When pre-delipidated, hair was washed with an SDS solution (100 mL of 15% w/v stock in deionised water), before being thorough rinsed and incubated in a 1:1 chloroform:methanol solution (3 mL). Delipidated or non-delipidated hair was then incubated in solutions of urea (3 mL, 8 M solution in deionised water), Tween 20 (3 mL, 0.16 µM solution in deionised water), sodium bicarbonate (3 mL, 1 M in deionised water), 1-Ethyl-3-methylimidazolium ethyl sulphate ([EMIM]ESO_4, 3 mL,

100% v/v), 1-Ethyl-3-methylimidazolium chloride ([EMIM]Cl, 3 mL, 10% v/v in deionised water), 1-Butyl-3-methylimidazolium chloride ([BMIM]Cl, 3 mL, 6% v/v in deionised water) or 1-Butyl-3-methylimidazolium bromide ([BMIM]Br, 3 mL, 6% v/v in deionised water), before thorough rinsing using deionised water, drying (60 °C, 72 h) and analysis *via* SEM. Non-delipidated hair was also incubated in Tris buffer, pH 7.5 overnight at 37 °C, 250 rpm as a control. A high-temperature hair sample, incubated overnight at 70 °C, 250 rpm was also included in this analysis.

Human hair (0.05 g) was also ground with a pestle and mortar into a powder using liquid nitrogen.

Scanning Electron Microscopy. A minimum of 6 strands per condition were fixed on a stud and coated with a gold sputter coater machine to improve the quality of sample images.[39] Sample images were then obtained under vacuum, using 10 kV accelerating voltage, 1,000-1,500x magnitude and a working distance of 13.5-23.5 mm.

3.3.3. Protein disulfide bond reduction assays

3.3.3.1. Insulin turbidity assay

The ability of the thioredoxin system from *E. coli* or *Bacillus subtilis* to reduce insulin disulfide bonds was explored similarly to what has been described by Holmgren *et al.* (1979), Du *et al.* (2012) and Che *et al.* (2020).[276–278]

Enzymatic disulfide bond reducing activity was initially assessed based on an insulin turbidity assay described by Holmgren *et al.*[278] A reaction cocktail was prepared from 100 mM sodium phosphate buffer (7.56 *m*L), 100 mM EDTA stock in deionised water (0.24 mL) and insulin (1.20 mL of 10 mg/mL stock in 50 mM Tris buffer). Thioredoxin stocks were made 0.47 U/ml (0.1 mg/mL) of Trx1 and 0.45 U/mL (0.09 mg/mL) of TrxA in mQH_2O, while DTT

was prepared as a 100 mM stock in deionised water. Test, blank and control samples were then prepared as follows (Table 2).

Table 2. Test, blank and control compositions for insulin turbidity assay of thioredoxins from *Bacillus subtilis* and *E.coli*.

	Test	Blank	Control
Reaction cocktail	0.75 mL	0.75 mL	0.75 mL
Thioredoxin (Trx1/TrxA)	0.08 mL	X	0.08 mL
Deionised water	0.16 mL	0.24 mL	0.17 mL
DTT	0.01 mL	0.01 mL	X

Final concentrations in Test samples were as follows: 1 mg/mL insulin, 0.038 U/ml (8 µg/mL) Trx1 or 0.040 U/mL (7 µg/mL) TrxA and 3 mM DTT.

Another version of this assay was investigated where DTT was replaced by thioredoxin reductase from *Bacillus subtilis* and NADPH. Briefly, Test samples were made up of reaction cocktail (0.75 mL), thioredoxin (0.12 mL of 2.35 U/ml (0.5 mg/mL) stock of Trx1 or 20 µL of 15.27 U/mL (3.1 mg/mL) stock TrxA, final conc. 0.3 U/mL or 0.06 mg/), TrxB (0.04 mL of 0.80 mg/mL, final conc. 32 µg/mL) and NADPH (78.6 µg/mL, 105.6 µM) in deionised water (up to 1 mL). All samples and controls were then mixed by swirling and incubated at 25 °C while the increase in ΔA_{650nm} was recorded every minute for up to 80 minutes.

Thioredoxin specific activity (U/mg) was then calculated as follows, where one unit causes a ΔA_{650nm} of 1.0 in 1 minute at 25 °C under conditions described in this assay:

$$U/mg = \frac{(\Delta A_{650nm}/\min \text{test} - \Delta A_{650nm}/\min \text{blank}) \times 1 \times \text{df}}{mg\ of\ thioredoxin}$$

where df = dilution factor, 1 = total volume (in mL) of assay and mg = mg of thioredoxin. ΔA_{650nm}/minute was calculated using the maximum linear rates for the test and blank samples.

3.3.3.2. NADPH-based assay

The reduction of substrate disulfide bonds was assayed by monitoring NADPH oxidation to $NADP^+$ *via* 340 nm absorbance decrease. NADPH degradation assays were conducted using a range of substrates.

Disulfide bond reduction with insulin. The ability of the thioredoxin system from *E. coli* or *Bacillus subtilis* to reduce insulin disulfide bonds was further explored similarly to what has been described by Du *et al.* (2012) and Che *et al.* (2020).[276,277] Insulin (91.8 *µ*L of 10 mg/mL stock, final conc. 1.22 mg/mL or 213 µM), Trx1 (59.0 µL of 2.35 U/mL (0.5 mg/mL) stock, final concentration of 39.3 µg/mL or 0.18 U/mL) or TrxA (10.8 µL of 15.27 U/mL (3.1 mg/mL) stock, final conc. 44.6 µg/mL or 0.22 U/mL) and TrxB (104.9 µL of 0.80 mg/mL stock, final conc. 111.9 µg/mL) were added to 0.50 mM Tris-HCl pH 7.5, 1 mM EDTA, up to 7.5 mL. Absorbance at 340 nm was then recorded to be subtracted from absorbance measurements taken after NADPH addition. The reaction was then initiated by addition of NADPH (0.178 mg/mL or 0.213 mM). The decrease in absorbance at 340 nm was then immediately monitored for up to one hour at 25 °C. Insulin only, no-insulin, no-enzyme, no-thioredoxin and no-NADPH controls were assessed, amongst others, where volume differences were adjusted using buffer. This experiment was also conducted with double the concentration of enzymes.

Disulfide bond reduction with Keratec™ IFP. Keratec™ IFP (50 µL of 65 mg/mL stock, final conc. 3.25 mg/mL) was incubated with TrxA (22.6-45.2 µL of 3.1 mg/mL stock, final conc. of 0.34-0.69 U/mL or 0.07-0.14 mg/mL) and TrxB (212.1-424.8 µL of 0.8 mg/mL stock, final conc. 0.17-0.34 mg/mL

for TrxB) were added to 0.50 mM Tris-HCl pH 7.5, 1 mM EDTA, up to 1 mL. The reaction was then initiated by addition of NADPH (10 µL of 16.7 mg/mL stock, final concentration of 0.167 mg/mL or 0.200 mM). This assay was also performed anaerobically, where the reaction cuvette containing Keratec™ IFP, thioredoxin and thioredoxin reductase was purged with argon before addition of NADPH and immediate 340 nm absorbance monitoring. The effect of Tween 20 (2-5% v/v), urea (5-10% w/v), [EMIM]ESO_4 (0.5-10% v/v), increased incubation temperature (50 °C) as well as KerA (10 µL of 76.9 units/mL (0.22 mg/mL) stock, final conc. of 0.77 U/mL or 2.2 µg/mL) addition was also evaluated on Bacillus subtilis thioredoxin system activity with Keratec™ IFP. Thiol release was calculated from final absorbances using Beer Lambert's law as follows (A is the absorbance, Ɛ is the NADPH extinction coefficient (6,220 $M^{-1}cm^{-1}$), c is the concentration (mg/mmol) and l is the pathlength (cm):

$$A_{340nm} = \varepsilon c l$$

$$c = \frac{A_{340nm}}{\varepsilon l}$$

Disulfide bond reduction with hair. NADPH degradation was also monitored in this way using hair as the substrate. Solid hair (0.02 g/mL), NaOH- or [EMIM]ESO_4-solubilised hair (0.02 g/mL eq.) or ground hair (0.02 mg/mL) was incubated with TrxA (45.2 µL of 15.27 U/mL (3.1 mg/mL) stock, final conc. 0.69 U/mL or 0.14 mg/mL) and TrxB (424.8 µL of 0.8 mg/mL stock, final conc. 0.34 mg/mL) in 0.50 mM Tris-HCl pH 7.5, 1 mM EDTA, up to 1 mL. The reaction was then initiated by addition of NADPH (0.18 mg/mL or 0.213 mM). The decrease in absorbance at 340 nm was then monitored by removing the hair from the cuvette prior to each measurement, for up to one hour at 25 °C. The effect of Tween 20 (0.5-5% v/v), urea (5-10% w/v),

[EMIM]ESO_4 (0.5-10%), increased incubation temperature (50 °C) as well as pre-treatment (5 mins or overnight, followed by thorough rinsing) with KerA (10 µL of 76.9 units/mL (0.22 mg/mL) stock, final conc. of 0.77 U/mL or 2.2 µg/mL) addition was also evaluated on *Bacillus subtilis* thioredoxin system activity on solid human hair.

Disulfide bond reduction in keratin azure. Keratin azure (0.02 g/mL) was incubated with TrxA (45.2 µL of 15.27 U/mL (3.1 mg/mL) stock, final conc. 0.69 U/mL or 0.14 mg/mL) and TrxB (424.8 µL of 0.8 mg/mL stock, final conc. 0.34 mg/mL) in 0.50 mM Tris-HCl pH 7.5, 1 mM EDTA, up to 1 mL. The reaction was then initiated by addition of NADPH (0.18 mg/mL or 0.213 mM). The decrease in absorbance at 340 nm was then monitored by removing the hair from the cuvette prior to each measurement, for up to one hour at 25 °C.

3.3.3.3. Ellman's assay

The enzymatic disulfide bond reduction of keratin substrates was also investigated *via* Ellman's assay (previously described in section 3.3.2.1.3.).

Reduction of Keratec™ IFP by the Bacillus subtilis thioredoxin system. Keratec™ IFP (50 µL of 65 mg/mL stock, final conc. 3.25 mg/mL) was incubated with TrxA (22.6-45.2 µL of 3.1 mg/mL stock, final conc. 0.34-0.69 U/mL or 0.07-0.14 mg/mL), TrxB (212.4-424.8 µL of 0.8 mg/mL stock, final conc. 0.17-0.34 mg/mL) and NADPH (0.167 mg/mL or 0.200 mM) in Ellman's buffer up to 1 mL for 1 hour at 37 °C, 250 rpm. A range of controls were included in this assay, where volume differences were accounted by adding buffer. Thiol release was then measured by incubation with DTNB (0.20 µM) and 412 nm absorbance recordings. Thiol quantification was conducted using Beer Lambert's law (TNB^{2-} extinction coefficient of 13,6000 $M^{-1}cm^{-1}$ at pH 8).

Reduction of human hair by the Bacillus subtilis thioredoxin system. Solid hair (8 mg/mL), ground hair (8 mg/mL, see section 3.3.2.2.3.), thoroughly rinsed pre-treated hair (10 mg/mL, see section 3.3.2.2.3.) or NaOH- and [EMIM]ESO_4 solubilised hair (5 mg/mL, see section 3.3.2.2.2.) was incubated with Trx1 (240 µL of 2.35 U/mL (0.5 mg/mL) stock, final conc. 0.56 U/mL or 0.12 mg/mL) or TrxA (45.2 µL of 15.27 U/mL (3.1 mg/mL stock), final conc. 0.69 U/mL or 0.14 mg/mL), TrxB (424.8 µL of 0.8 mg/mL stock, final conc. 0.34 mg/mL) and NADPH (0.18 mg/mL or 0.213 mM) in Ellman's buffer up to 1 mL for 1 hour (or overnight in the case of pre-treated hair) at 37 °C, 250 rpm. DTT was also investigated in this way for the regeneration of thioredoxin, based on the insulin turbidity assay (see section 3.3.3.1.).[31,275,278] Briefly, Trx1 (50 µL of 3.25 U/mL (0.5 mg/ml stock), final concentration of 0.047 U/mL or 0.01 mg/mL) was added to hair (8 mg/mL), in the presence or absence of DTT (3 mM) in Ellman's buffer up to 2.5 ml and incubated at 37°C, 250 rpm for 15 min. Following incubation, samples were rinsed with five successive buffer rinsings (dialysed or Buchner filtered in the case of ground hair). Thiol release was then measured (in samples and final washes) by incubation with DTNB (0.20 µM) followed by 412 nm absorbance and 400-500 nm spectra recordings. NaOH- and [EMIM]ESO_4 solubilised hair (5 mg/mL) were also investigated, however these substrates were not compatible with 412 nm absorbance measurements.

Further Ellman's assay investigations.

The release of thiols associated with hair (8 mg/mL) and Keratin azure (4-8 mg/mL) incubation with KerA (25-50 µL of 76.9 units/*m*L (0.22 *m*g/*m*L) stock, final conc. 0.77-1.54 units/*m*L or 2.2-4.4 *µ*g/*m*L), in the presence or absence of reducing agents (2% w/v DTT (20.8 *m*g/*m*L, 0.13 M) or 5% w/v (49.7 *m*g/*m*L) of sodium thioglycolate (0.44 M), glutathione (0.16 M), cysteine (0.41

M) or DTT (0.31 M)), was also investigated with Ellman's assays (2.5 mL assays, 1-24 hour incubation at 37 °C, 250 rpm, buffer rinsings)

The potential disulfide bond breaking activity of cysteinyl glycine, and therefore of γ-glutamyl-transpeptidase, on hair was also investigated. Briefly, hair (8 mg/mL) was incubated with DTT (0.385 mg/mL or 1 mM) or cysteinyl glycine (0.445 mg/mL or 1 mM) in Ellman's buffer up to 2.5 mL for 1 hour at 37 °C, 250 rpm, followed by buffer rinsings. Thiol release was then measured (in samples and final washes) by incubation with DTNB (0.20 µM) followed by 412 nm absorbance.

3.3.4. Keratinolytic assays

3.3.4.1. Casein assay

Merck's non-specific protease activity assay was used to evaluate keratinase's proteolytic activity.[279] Briefly, KerA (1 mL of 0.1-0.5 units/mL (0.29-1.43 µg/mL) stock in 10 mM sodium acetate buffer with 5 mM calcium acetate, pH 7.5 at 37 ºC, final conc. 0.01-0.05 units/mL or 0.03-0.14 µg/mL) was added to casein (5 mL of 6.5 mg/mL stock in 50 mM potassium phosphate buffer, pH 7.5, 37 ºC, final conc. 2.9 mg/mL) and incubated at 37 °C for 10 minutes, before addition of TCA (5 mL of a 18.0 mg/mL solution in deionised water, final conc. 8.2 mg/mL). A blank was also prepared, where enzyme was added after TCA. A range of controls (no casein, no TCA, no-enzyme etc.) were included, where deionised water was used to make up for volume differences. Samples and controls were then incubated for a further 30 minutes before the addition of Na_2CO_3 (5 mL of 62 mg/mL stock solution in deionised water) and Folin-Ciocalteau reagent (1 mL of 500 mM stock in deionised water). Samples were mixed by swirling and incubated at 37 °C for a further 30 minutes, before 0.45 µm filtration. 660 nm absorbances were then recorded. A standard curve was also prepared from 0.005-0.050

µmol/mL (0.9-9.0 mg/mL) L-tyrosine (Figure 23). A line of best fit with a corresponding slope equation was then generated, allowing for enzyme activity calculations.

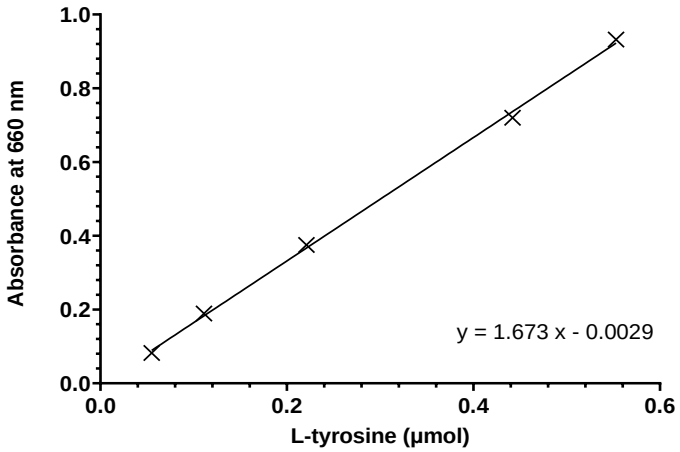

Figure 23. Casein assay standard curve. Plotted using 0.055-0.553 µmol L-tyrosine in ddH_2O, Na_2CO_3 and F&C reagent, up to 11 mL.

The enzymatic activity (units/mL) can then be calculated as follows, where the total volume of assay is 11 mL, the enzyme volume used is 1 mL, the time of assay is 10 min, and the cuvette (absorbance determination) volume is 1 mL:

$$\frac{Units}{mL} enzyme$$

$$= \frac{\mu mol\ tyrosine\ equivalents\ released\ \times total\ assay\ volume}{Enzyme\ volume\ \times time\ of\ assay\ \times Absorbance\ determination\ volume}$$

$$= \frac{\mu mol\ tyrosine\ equivalents\ released\ \times 11}{1\ \times 10 \times 1}$$

$$= \frac{\mu mol\ tyrosine\ equivalents\ released\ \times 11}{10}$$

One unit of protease activity will hydrolyse casein to produce colour equivalent to 1 µmole (181 µg) of tyrosine per minute at pH 7.5 at 37°C.

This assay was also attempted using Keratec™ IFP (5 mL of 13 mg/mL stock in 50 mM potassium phosphate buffer, pH 7.5, 37 ºC, final conc. 5.8 mg/mL) as the substrate instead of casein.

3.3.4.2. Keratin azure assay

The keratinolytic activity of keratinase was determined by the method of Navone et al. using keratin azure as the substrate.[30] KerA (50-200 µL of 76.9 units/mL (0.22 mg/mL) stock, final conc. 1.54-6.15 units/mL or 4.4-17.6 µg/mL) was added to keratin azure (4 mg/mL) in 100 mM Tris-HCl buffer, pH 8, up to 2.5 mL. Samples were incubated at 37 °C, 250 rpm for 1-72 h. After incubation, supernatant absorbances were measured at 595 nm, 400-800 nm spectra were also recorded. A negative control was made up of 0.01 g of keratin azure in 2.4 mL of 100 mM Tris-HCl buffer, pH 8. One unit of keratinolytic activity was defined as the amount of enzyme that resulted in an increase of 0.1 in absorbance at 595 nm after 30 min incubation. For keratinolytic activity determination in the presence of reducing agents, the keratin azure assay was performed as indicated with the addition of 2% w/v DTT (20.8 *m*g/*m*L, 0.13 M) or 5% w/v (49.7 *m*g/*m*L) of sodium thioglycolate (0.44 M), glutathione (0.16 M), cysteine (0.41 M) or DTT (0.31 M). The effect of pre-chopping the substrate prior to keratin azure analysis was also investigated. Attempts to swell the keratin fibre involved increasing reaction pH from 8 to 10.3 and adding urea (1 M) to the buffer. Temperature studies, with incubation temperatures ranging from 20 °C to 70 °C, were conducted.

Azure release associated with the incubation of keratin azure with the *Bacillus subtilis* thioredoxin system (TrxA (45.2 µL of 3.1 mg/mL stock, final conc. 0.69 U/mL or 0.14 mg/mL), TrxB (424.8 µL of 0.8 mg/mL stock, final conc. 0.34 mg/mL) and NADPH (0.18 mg/mL or 0.213 mM)) was also assessed using the keratin azure assay.

3.3.5. Crosslinking assays

3.3.5.1. Standard enzymatic assays

Laccase assay using ABTS. Laccase activity was determined by monitoring the oxidation of ABTS at 405 nm ($\mathcal{E}_{405}$=36,000 M^{-1} cm^{-1}).[280] TvLac (1-20 µL of 3.41 U/mL (1 mg/mL) stock, final conc. 0.003-0.068 U/mL or 1-20 µg/mL final concentration) or PoLac (1-20 µL of 2.94 U/mL (1 mg/mL stock), final conc. 0.003-0.059 or 1-20 µg/mL) was added to a solution of ABTS (10 µL of 100 mM stock in acetate buffer pH 5, final conc.1 mM) and oxygenated buffer (deionised water or 50 mM acetate buffer, pH5 - prepared by bubbling air into 10 mL of buffer for 30 minutes) up to 1 mL. A no-enzyme control was made from ABTS (1 mM) where the enzyme volume was replaced with the same volume of oxygenated buffer. 405 nm absorbance was immediately monitored at 25°C overtime for up to 10 minutes. Laccase activity was then determined as units per mg, where 1 U was defined as 1 µmol of ABTS oxidised per minute, using Beer-Lambert law:

$$\frac{\Delta A}{\Delta t} = \frac{\varepsilon l \Delta C}{\Delta t}$$

$$\frac{\Delta C}{\Delta t} = \frac{\Delta A}{\Delta t \varepsilon l}$$

$$\frac{\Delta n}{\Delta t} = \frac{\Delta A}{\Delta t \varepsilon l} \times v$$

where ΔA is the absorbance, Δt the assay duration (min), ε the substrate molar absorption coefficient of ABTS at 405 nm ($\mathcal{E}_{405}$=36,000 $M^{-1}.cm^{-1}$), l the optical path length (cm^{-1}), ΔC the molar concentration (mol/L) and v the assay volume (0.001 L).

The effects of solubilised keratin substrates, undialysed (Keratec™ IFP: 13 mg/mL & Keratec™ ProSina: 9.4 mg/mL) and dialysed (Keratec™ IFP: 5.5-

8.8 mg/mL & Keratec™ ProSina: 3.7 mg/mL), as well as 2-phenoxyethanol (80 mM), on laccase activity were investigated. For experiments with heat-deactivated enzyme, TvLac (0.5 mL of 3.41 U/mL (1.0 mg/mL) stock, final conc. 1.70 U/mL or 0.5 µg/mL) was pre-treated at 100°C for 15 minutes prior to incubation (repeated word) with ABTS in buffer as described above.

Tyrosinase assay using L-DOPA. Tyrosinase activity was determined by monitoring the oxidation of L-DOPA at 475 nm (ε_{475}=3,700 M^{-1} cm^{-1}).[281] Tyr (20 µL of 10.93 U/mL (1 mg/mL) stock, final conc. 0.22 U/mL or 1-20 µg/mL) was added to a solution of L-DOPA (10 µL of a 100 mM stock, final conc. 1 mM) and oxygenated 100 mM Tris buffer pH 7.5, or deionised water up to 1 mL. A no-enzyme control made from L-DOPA (1 mM) was included. 475 nm absorbance was immediately monitored at 25°C overtime for up to 10 minutes. Using Beer-Lambert law, tyrosinase activity was then determined as units per mg, where 1 U was defined as 1 µmol of L-DOPA oxidised per minute. Several factors, such as buffer composition, incubation temperature (25-37°C) and effect of undialysed (6.5 mg/mL) and dialysed (11.0 mg/mL) Keratec™ IFP were investigated to understand their consequences on tyrosinase activity.

Transglutaminase assay using Cbz-Gln-Gly. Transglutaminase activity was determined as described by Folk *et al.* (1966) where the transglutaminase-catalysed formation of Cbz-Gln-Gly-hydroxamate from Cbz-Gln-Gly and hydroxylamine can be monitored at 525 nm.[282] A reaction cocktail (10 mL) was made in deionised water from Cbz-Gln-Gly (120 mg or 35.6 mM), in 5 mL of a 100 mM hydroxylamine and 10 mM reduced glutathione solution made in deionised water, with 50 µL of a 1 M calcium chloride stock in deionised water and 2 mL of 1 M Tris buffer at pH 6, 37 °C. The reaction cocktail pH was adjusted to 6 at 37 °C using a 100 mM NaOH solution made in in deionised water). Tg (30 *µ*L of 0.74 U/*m*L (52.6 *µ*g/*m*L) stock, final conc.

0.097 U/*m*L or 6.86 *µ*g/*m*L) was incubated for 10 minutes at 37 °C in 200 *µ*L of this reaction cocktail. A standard was made from L-Glutamic Acid γ-monohydroxamate (100 *µ*L from a 10 *m*M in deionised water). Test and standard blanks were made from reaction cocktail (200 *µ*L) or deionised water (100 *µ*L), respectively. Trichloroacetic acid (TCA, 500 *µ*L of 12% v/v stock) and ferric chloride (500 *µ*L of 5% w/v stock) solutions were then added to standards, test and blanks (transglutaminase (0.097 U/*m*L or 6.86 *µ*g/*m*L) was added to test blank). Precipitates were removed by centrifugation and sample absorbances recorded at 525 nm using quartz cuvettes. Transglutaminase activity was determined against the L-Glutamic Acid γ-monohydroxamate standard, as follows:

$$\frac{Units}{mg}\ (enzyme)$$

$$= \frac{(A_{525nm-test} - A_{525nm-test\ blank}) \times final\ test\ volume}{(A_{525nm-std} - A_{525nm-std\ blank}) \times final\ standard\ volume \times \frac{mg(enzyme)}{Reaction\ volume} \times Reaction\ time}$$

$$\frac{(A_{525nm-test} - A_{525nm-test\ blank}) \times 1.23}{(A_{525nm-std} - A_{525nm-std\ blank}) \times 1.1 \times \frac{mg(enzyme)}{0.23} \times 10}$$

Final test, final standard and reaction volumes corresponded to 1.23, 1.1 and 0.23 *m*L, respectively, while the reaction time was 10 minutes. One unit catalyses the formation of 1 *µ*mol of hydroxamate per minute. The effects of undialysed (1.9 *m*g/*m*L) and dialysed (3.2 *m*g/*m*L) Keratec™ IFP on transglutaminase activity were also investigated.

3.3.5.2. Enzymatic crosslinking of soluble keratin substrates

3.3.5.2.1. Enzymatic crosslinking reactions with soluble keratin substrates

Keratec™ IFP or Keratec™ ProSina were used either as dialysed or undialysed preparations. Crosslinking enzymes (TvLac (50 *µ*L of a 34.1 U/mL (10 *m*g/*m*L) stock, final conc.1.70 U/mL or 0.50 mg/mL), PoLac (50 µL of a 29.4 U/mL (10 mg/mL) stock, final conc. 1.47 U/mL or 0.50 mg/mL), Tyr (500 µL of a 10.93 U/mL (1 mg/mL) stock, final conc. 5.47 U/mL or 0.5

mg/mL) or Tg (250 µL of a 0.74 U/mL (52.6 µg/mL) stock, final conc. 0.19 U/mL or 13.15 µg/mL) were incubated with Keratec™ substrates (0.6-32.5 mg/mL) in buffer up to 1 mL overnight at 37°C and 250 rpm. The buffers used were as follows: deionised water for laccases and Tris buffer, pH 7.5 and pH 6 for tyrosinase and transglutaminase, respectively. The addition of mediators (ABTS, vanillin or acetosyringone), added as stock solutions at a final concentration of 1 mM in the reaction, was also investigated. Negative controls without enzyme and without substrate were tested by replacing the volumes of enzyme or substrate stock with the same volume of respective buffer. 1-ethyl-3-(3-dimethylaminopropyl)carbodiimide (EDC, 56 mM) was investigated as a potential crosslinking positive control. Following overnight incubation, samples were immediately analysed using a range of techniques. Relevant crosslinking conditions were replicated as necessary to provide robustness to the assays.

The addition of an overnight dialysis step at room temperature against 2 L deionised water was trialled post-substrate enzymatic treatment to avoid potential interferences in later analyses.

3.3.5.2.2. Analyses of enzymatic crosslinking with soluble keratin substrates

Turbidity assay. Turbidity was investigated as a potential indicator of casein crosslinking, based on work conducted by Puri *et al.* (2021) on transglutaminase and casein powder.[18] Casein from bovine milk (6 mg/mL final concentration) was dissolved in potassium phosphate buffer, pH 7.5 with gradual heating up to 85 °C and stirring. Casein solution was incubated with TvLac (20 µL of 3.41 U/mL (1 mg/mL) stock, final conc. 0.068 U/mL or 20 µg/mL), Tyr (20 µL of 10.93 U/mL (1 mg/mL) stock, final conc. 0.22 U/mL or 20 µg/mL) or Tg (20 µL of 0.74 U/mL (52.6 µg/mL) stock, final conc. 0.015 U/mL or 1.05 µg/mL) up to 1 mL, at 5, 25 and 55 °C for 30 minutes. No-

enzyme controls were investigated, where the volume of the enzyme was replaced by the same volume of potassium phosphate buffer, pH 7.5. Turbidity was then assessed *via* 600 nm absorbance measurements.

Viscosity assay. Viscosity was also investigated as potential indication of keratin crosslinking, based off work conducted by Elbalasy *et al.*, 2022.[283] A potential increase in sample viscosity upon incubation of Tyr with Keratec ™ IFP compared to untreated substrate was observed by eye. New samples were then prepared, where TvLac (60 µL of 3.41 U/mL (1 mg/mL) stock, final conc. 0.204 U/mL or 60 µg/mL), Tyr (60 µL of 10.93 U/mL (1 mg/mL) stock, final conc. 0.66 U/mL or 60 µg/mL) or Tg (60 µL of 0.74 U/mL (52.6 µg/mL) stock, final conc. 0.045 U/mL or 3.15 µg/mL) were incubated with undialysed Keratec™ IFP (32 mg/mL) in acetate pH 5 (TvLac), Tris pH 7.5 (Tyr) and Tris pH 6 (Tg) buffers. Rheology measurements were then conducted at 25°C in controlled shear rate mode. The sheer rate was logarithmically increased from 0.01 to 100 s^{-1}. Non-enzymatic controls were also investigated, where volume differences were adjusted using buffer.

Size-Exclusion Chromatography. Crosslinked samples (1 *m*L, see 3.3.5.2.1. section) were filtered through a 0.22 µm syringe filter (Starlab) and analysed by SEC (see section 3.3.2.1.1.), injecting 500 *µ*L of sample into the Superdex 200 Increase 10/300 GL column. For each sample, 1.5 ml fractions were collected, and relevant ones were further analysed by SDS PAGE and Bradford assay.

SDS-PAGE. Crosslinking samples (20 *µ*L, see 3.3.5.2.1. section) were mixed with Laemmli sample buffer and incubated for 10 min at 100 °C. Protein ladder (5 *µ*L) and samples (10 *µ*L) were then loaded onto an SDS PAGE gel and run at 200V, 400 mA for 35 minutes using running buffer. Gels were stained with Coomassie overnight, and destained before being imaged.

3.3.5.3. Enzymatic crosslinking reactions and analyses of solid human hair

Three human hair tresses, each composed of 2 g of hair, were washed with Sodium Dodecyl Sulfate (SDS, 10% solution) before thorough rinsing under cold water. Each tress was then incubated for 20 minutes with DTT (77 mg/mL or 0.5 M) in deionised water (20 mL) at room temperature, before being thoroughly rinsed under cold then warm (80 °C) water. Each hair tress was then incubated overnight at 37 °C, 120 rpm, under various conditions. Hair tress 1 was incubated with deionised water (40 mL) as a negative control, while hair tresses 2 and 3 were both incubated with TvLac (20 mL of a 6.82 U/mL (2 mg/mL) stock in deionised water, final conc. 3.41 U/mL or 1 mg/mL), either in deionised water (20 mL) or in the presence of vanillin (20 mL of a 0.3 mg/mL stock in deionised water, final concentration of 1mM). All three tresses were finally rinsed under both cold and warm (80 °C) water before being placed at 80 °C for 20 minutes to deactivate any remaining enzyme. The hair was then dried at 60 °C for 72 hours before being analysed by tensile strength.

Tensile strength analysis (performed in Croda International labs). Following hair treatment and thorough drying, 100 hair fibres per condition were crimped in 30 mm length between brass taps using an automated crimper. Each hair crimp was then loaded into a Tensile Test carrousel and samples were left to equilibrate at 50% Relative Humidity (RH) for 3 hours. The cross-sectional area of hair fibres was then measured using a laser micrometre, with 5 measurements made along the length of the fibre. The tensile tester was finally used to break each hair fibre and measure the break strength in gram force (gmf). The following parameters were used:

Table 3. Dia-stron MTT680 Tensile Tester Parameters.

Setting	Value
Extension (%)	100
Rate	20 mm/min
Gauge Force	2
Maximum Force	200
Break Threshold	10

Data was then analysed using the UvWin software (available at Croda international).

4. Reduction of keratin disulfide bonds by the thioredoxin system from *Bacillus subtilis*

4.1. Background

Keratin is a waste-product from a range of industries (e.g. poultry, leather etc.), and its degradation has been extensively studied.[21,22] With the aim of moving away from harsh chemical treatments necessary to degrade this highly crosslinked polymer, a range of microorganisms with keratinolytic activity have been identified, including *Bacillus subtilis*, *Streptomyces* spp. and *Bacillus licheniformis*.[23–26] While the mechanism behind microbial keratin degradation remains unclear, the secretion of extracellular enzymes, keratinases, with concurrent keratin structure opening *via* disulfide bond reduction is generally accepted.[21,23,24,26,30,98,123–126] In whole microorganisms, disulfide bond reduction may take the form of a cell-bound redox system, the secretion of a soluble reducing substance like sulfite, mechanical pressure brought about by mycelium growth or the concomitant action of a secreted disulfide bond reducing enzyme.[98]

While keratin degradation using whole microorganisms is slow, the identification and characterisation of enzymes with relevant activity on keratin allows the engineering of enzymes with higher activity and stability.[121,122] The use of isolated enzymes also presents many advantages for commercial applications, such as faster scale-up, more reaction specificity and easier storage.[27–30] In this way, a range of enzymes have been isolated from keratin-degrading microorganisms, mainly keratinases.[25,31,32] Very few disulfide bond-reducing enzymes associated with keratin degradation have indeed been identified.[26,97]

This chapter investigates the use of isolated enzymes with potential keratin disulfide bond-reducing activity as mild and biocompatible active agents in

the context of permanent hair straightening. A disulfide bond-reducing enzyme from *Bacillus halodurans* involved in feather keratin degradation was isolated by Prakash *et al.* (2010), and constitutes the only (N-terminal) sequence available regarding an enzyme with disulfide bond-reducing activity on keratin.[24] The N-terminal sequence was therefore used as the starting point for a sequence search aimed at identifying potential enzyme candidates. While a range of protein disulfide bond-reducing enzymes have been characterised, a focus was placed on enzymes isolated from keratin-degrading organisms, with high disulfide bond-reducing activity on both intra- and intermolecular bonds and a broad range of substrates, including folded proteins. In this way, the thioredoxin system from *Bacillus subtilis*, formed of thioredoxin, thioredoxin reductase and NADPH, was selected for further investigations.[84,98,183,184,175–182] Despite the need for a cofactor, the small size of thioredoxins appeared as a potential advantage towards the penetration of solid substrates, such as keratin.[284] Moreover, thioredoxin and thioredoxin reductase from *Bacillus subtilis* have been readily expressed and purified.[175] These enzymes have also shown high activity on a range of substrates, such as the globular protein insulin, and are able to reduce intermolecular disulfide bonds in oxidised glutathione.[185–187] The potential disulfide bond-reducing activity on keratin of the thioredoxin system from *Bacillus subtilis*, despite being isolated from a keratin-degrading organism, has, however not been assessed.

The focus is therefore placed on the expression, purification and characterisation of thioredoxin and thioredoxin reductase from *Bacillus subtilis* for potential reduction of disulfide bonds in keratin. The system is here assessed using solid human hair *via* different methods, such as Ellman's and NADPH-consumption assays. Solubilised wool is also

investigated as potential substrate to avoid enzymatic penetration barriers encountered with insoluble proteins such as hair. Indeed, hair is composed of highly crosslinked and tightly packed keratin chains forming the cortex, which are protected from environmental damage and penetration by surrounding cuticle layers.[6,9,41,46] The opening of keratin structure is also investigated in an attempt to facilitate enzyme penetration into the hair. This is done *via* a range of treatments, including hair grinding and solubilisation, delipidation, as well as treatment with swelling agents such as urea.[58–62] Commercially available *E. coli* thioredoxin is also assayed for comparison.

The mechanism behind microbial keratin degradation, including the importance of concomitant disulfide bond reduction, is also investigated using KerA from *Bacillus licheniformis*, a very well-characterised and commercially-available keratinase.[25,31,32] The keratinolytic activity of KerA is assayed using keratin azure, a chromogenic substrate developed for the accurate assessment of keratinolysis.[21,30,125,285] The effect of disulfide bond reduction *via* incubation with reducing agents such as DTT or with the thioredoxin system from *Bacillus subtilis* is evaluated on keratinase activity.[26,286] DTT, amongst other reducing agents, was selected for its repeatedly reported efficiency at yielding high keratinolytic activity.[21,26,98,105,287] Moreover, the impact of keratinase on keratin disulfide bond reduction and whether it allows better reducing agent or enzyme penetration into the keratin fibres is also investigated.

4.2. Keratin substrates

In this thesis, two solubilised wool keratin substrates are evaluated: Keratec™ IFP and Keratec™ ProSina. Both were provided by Croda

International and are believed to contain 2-phenoxyethanol as a preservative.

4.2.1. Keratec™ IFP

Keratec™ IFP is a purified protein fraction isolated from New Zealand wool, made up of multicomponent soluble forms of Intermediate Filament Protein (IFP). It is patented and commercialised by Croda International as a keratin-derived active that helps protect the hair from environmental strain by both penetrating the cortex and creating a shield on the surface of the hair. Keratec™ is composed of intact keratin proteins with molecular weights ranging from 40,000 to 60,000 Daltons, as well as keratin peptides of around 3,000-4,000 Daltons.[288] The amino acid composition of Keratec™ IFP can be seen in Table 4.

Patents have been published regarding the preparation of intact soluble wool keratin intermediate filament proteins *via* oxidative sulfitolysis, followed by extraction, resulting in a highly S-sulfonated keratin derivative.[288–290] This reaction relies on a sulfonating agent, such as sodium sulfite, which cleaves cystine to cysteine and S-sulfocysteine (Figure 24). An oxidant then forms disulfide bonds from resulting cysteines, to be subjected to another round of sulfitolysis until total conversion is obtained. Moreover, the literature around keratin solubilisation seems to suggest that disulfide bonds are affected during the process.[99,106]

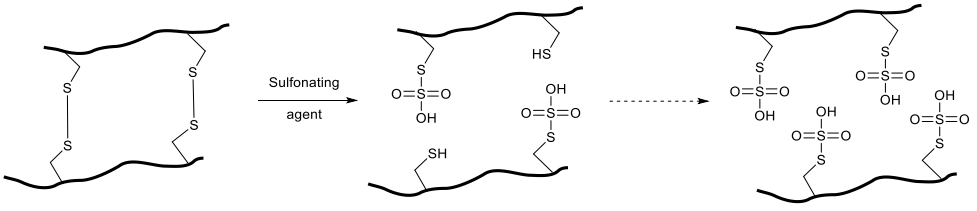

Figure 24. Mechanism of wool solubilisation *via* oxidative sulfitolysis, yielding a highly S-sulfonated soluble derivative.

In this way, while the exact composition and solubilisation process behind Keratec™ IFP was not disclosed, it is considered that at least a portion of keratin disulfide bonds was affected by wool solubilisation. In this way, Keratec™ IFP is investigated in this chapter as a substrate containing a mixture of disulfide bonds and S-sulfocysteine bonds, referred to as "sulfur-sulfur" bonds.

A protein content of 65.0 mg/mL and pH of 7.9 was measured for the specific Keratec™ IFP batch used in this assay (personal exchange with Croda International QC team).

Table 4. Amino acid composition of Keratec™ IFP and Keratec™ ProSina substrates, provided by Croda International, with human hair amino acid composition for comparison.[21]

Amino Acid	**Keratec™ IFP** % w/w	**Keratec™ ProSina** *% w/w*	**Human hair** *% w/w*
Aspartic acid	7.9	8.0	7.6
Threonine	6.5	6.4	6.9
Serine	11.0	9.7	11.7
Glutamic acid	15.3	16.5	11.6
Proline	5.5	6.4	9.6
Glycine	8.2	4.5	6.6
Alanine	7.5	4.6	5.2
Cysteine	4.3	5.4	10.0
Valine	6.5	5.5	6.2
Methionine	0.2	0.6	2.5
Isoleucine	3.6	3.3	3.1
Leucine	8.7	9.0	7.1
Tyrosine	1.1	3.4	1.2
Phenylalanine	2.4	2.9	1.9

Histidine	0.9	1.6	1.1
Lysine	2.1	3.1	3.0
Arginine	7.1	9.3	4.9

4.2.2. Keratec™ ProSina

Keratec™ ProSina also corresponds to a purified protein fraction isolated from pure New Zealand wool. It is patented and commercialised by Croda International as a novel keratin peptide for the treatment and protection of hands, nails and hair. Keratec™ ProSina is made *via* a non-disclosed mild proprietary process leaving the natural cysteine content of the keratin in an active S-sulphonated form, which is then able to crosslink with the keratin in nails or hair (personal exchanges with Croda international).[291] It is composed of peptides with molecular weights between 2500 and 3000 Daltons. The amino acid composition of Keratec™ ProSina can be seen on Table 4.

A peptide content of 47.1 mg/mL and pH of 5.8 was measured for the specific Keratec™ ProSina batch used in this assay (personal exchange with Croda International QC team).

4.2.3. Keratin azure

A range of chromogenic keratin substrates have been developed for the accurate assessment of keratinase activity, such as azokeratin and keratin azure.[21,30,125,285] The former is prepared by coupling keratin with a diazotised arylamine while the latter is commercially available, made from sheep's wool and therefore well-suited for α-keratin degradation analyses.[21,285] Keratin azure corresponds to azure dye-impregnated sheep's wool, where Remazol Brilliant Blue R (RBBR), an anthraquinone dye widely used in the textile industry, is covalently bound to keratin.[292,293] RBBR dye carries a precursor

to a vinyl sulfone group, which mainly forms covalent bonds with hydroxy and other amino groups in the wool by the successive release of sodium hydrogen sulfate ($NaHSO_4$) and Michael addition (Figure 25). When hydrolysed, for example, by keratinases, keratin azure releases soluble dye bound-small peptides and amino acids, which can be monitored *via* 595 nm absorbance measurements (Figure 26).[292,293]

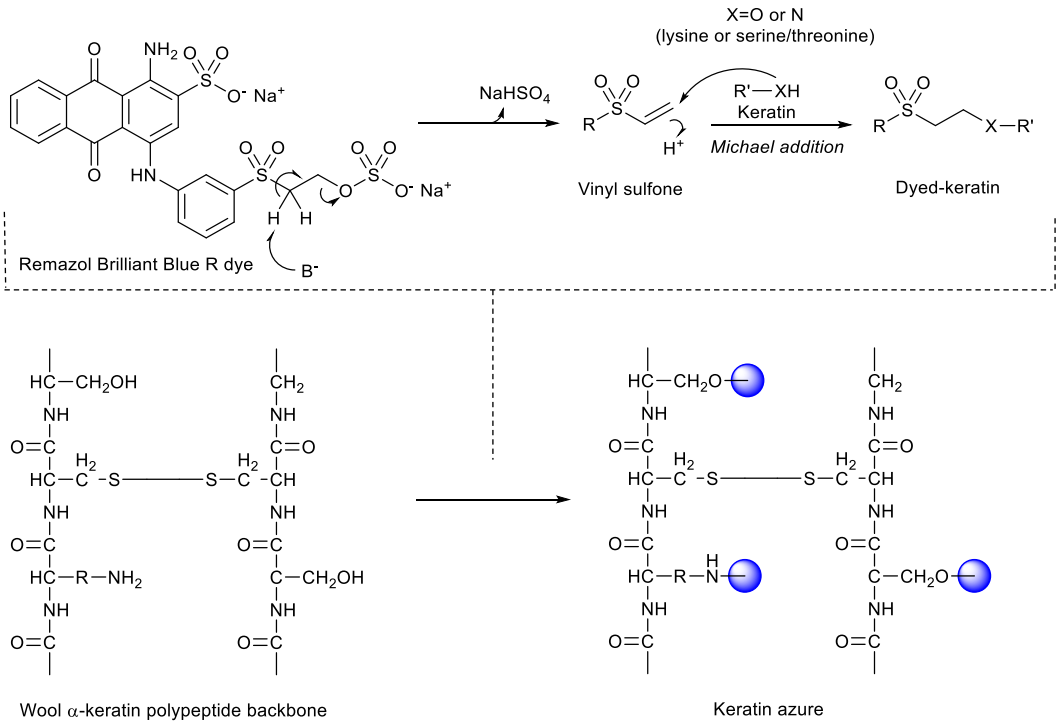

Figure 25. Formation of keratin azure through Remazol Brilliant Blue R dyeing of wool keratin, via successive sodium hydrogen sulfate release and Michael addition.

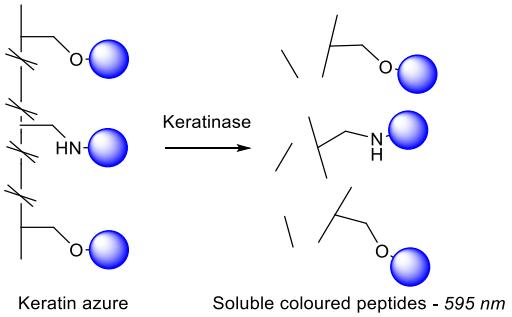

Figure 26. Keratin azure hydrolysis by keratinase with subsequent release of soluble coloured peptides, which can be detected at 595 nm.

4.3. Sequence search

Prakash *et al.* (2010) analysed the mechanisms of chicken feather keratin degradation by *Bacillus halodurans*, and identified an enzyme with disulfide bond reducing activity on keratin (enzyme 1).[29] The *N*-terminal amino acid sequence of enzyme 1 was determined and had significant homology with disulfide reductases, according to the authors (Appendix Table 4.1).[29] This represents the only sequence information disclosed for a keratin disulfide bond-reducing enzyme to date.

These findings were used as the starting point of a thorough sequence search aimed at finding suitable enzyme candidates for the reduction of keratin disulfide bonds. The N-terminal sequence disclosed by Prakash *et al.* (2010) was first analysed using the protein BLAST function from the NCBI database.[294] This yielded no results for *Bacillus* organisms altogether, and no proteins from different organisms possessed the fragment of interest at the N-terminal. Protein disulfide reductases from *Bradyrhizobium* sp. BTAi1 (A), *Rhodobacter sphaeroides* (B) and *Francisella tularensis* subsp. *mediasiatica* (C), all disulfide bond-reducing enzymes, were identified by the authors as having the closest N-terminal sequence compared to Enzyme 1 (Table 5).[294]

Table 5. Homology analysis of N-terminal amino acid sequences of Enzyme 1 from *Bacillus halodurans*, by Prakash *et al.* (2010).[294] NCBI Reference Sequence numbers included.

Name	Origin	N-terminal amino acid sequence	Identity with Enzyme 1 (%)
Enzyme 1 (query)	*Bacillus halodurans*	QPNDPADDWN	100%
Protein-disulfide reductase (A)	*Bradyrhizobium* sp. BTAi1	QPNDQAQIDAW (WP-012043775.1)	64%

Glutathione-disulfide reductase (B)	*Rhodobacter sphaeroides*	PVDDW (ESW61626.1)	80%
Glutathione reductase (C)	*Francisella tularensis* subsp. *mediasiatica*	PANEW (WP 216374122.1)	60%

The full protein sequences of enzymes (A)-(C) were accessed and revealed a singular CXXC motif for enzyme (A), characteristic of thioredoxins and glutaredoxins, while enzymes (B) and (C) possessed a CXXXXC motif, distinctive of dithiol glutathione reductase (Appendix Table 4.1).[208,209194] The active site cysteine amino acid thiols in these disulfide bond-reducing enzymes are known to undergo reversible oxidation-reduction by shuttling between a dithiol and a disulfide form in the catalytic process.[170] Enzymes (A)-(C) were however disregarded due to a lack of characterisation in the literature.

With the aim of identifying well-characterised enzymes with disulfide bond-reducing activities, the focus of this sequence search was placed on enzymes with two catalytic cysteines at their active sites, characteristic of disulfide bond reductases.[295] Blasting was conducted based on the protein sequences of enzymes (A), (B) and (C) against specific organisms such as *E. coli* and *Bacillus*, known for their keratin-degrading activities (Appendix Table 4.2).[27,296–299] A range of enzymes were in this way identified, mainly from the thioredoxin and glutaredoxin families, associated with CXXC or CXXXXC active site motifs.[295] Enzyme characteristics (mechanism, expression, characterisation, substrate, crystal structure etc.) were investigated.[27,296–299] A range of enzymes were in this way selected, according to expression and characterisation records available in the

literature, as well as known activity on protein substrates such as insulin (Appendix Table 4.3).

Thioredoxin and thioredoxin reductase from *Bacillus subtilis*, as part of the thioredoxin system alongside NADPH, were eventually selected as promising candidates.[175,300] This choice was based on a range of factors, such as the small size of thioredoxins, appearing as a potential advantage towards keratin penetration, the high identity between the *Bacillus subtilis* thioredoxin and the commercially available one from *E. coli*, as well as the fact that the organism *Bacillus subtilis* is established as a keratin-degrading organism.[132,284] Moreover, the thioredoxin system from *Bacillus subtilis* has been expressed and characterised with known activity on proteins such as insulin and oxidised glutathione, while its disulfide bond-reducing potential is yet to be determined on keratin substrates.[98,175]

To this end, thioredoxin and thioredoxin reductase from *Bacillus subtilis* were expressed in *E. coli* according to the method of Parker *et al.* (2014).[175]

4.4. Expression and purification of thioredoxin and thioredoxin reductase from *Bacillus subtilis*

4.4.1. Preparation of pET21a::trxA and pET21a::trxB plasmids

The codon-optimised thioredoxin (*trxA*) and thioredoxin reductase (*trxB*) genes were synthesised by Genewiz and cloned into pET21a vectors, between the *NdeI* and *XhoI* restriction sites. Successful cloning was confirmed by PCR (Figure 27), and pET21a::*trxA* and pET21a::*trxB* plasmids were transformed into BL21(DE3) *E. coli* strains.

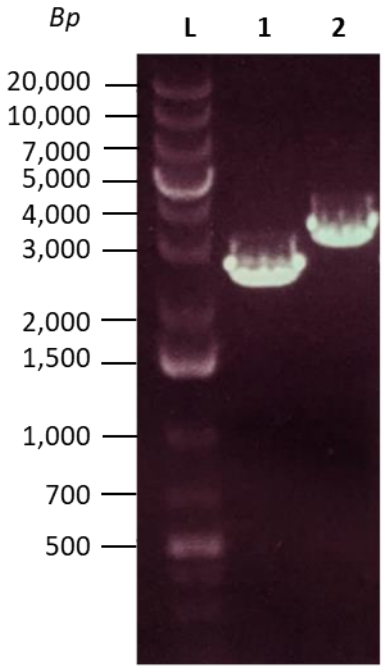

Figure 27. Agarose gel analysis of *trxA* and *trxB* PCR products, corresponding to amplified *trxA* and *trxB* genes within identical DNA template (2457 bp and 3096 bp respectively). L=ladder, 1=*trxA* gene and 2=*trxB* gene.

The clear bands observed at around 2500 bp and 3100 bp correspond to amplified *trxA* (309 bp) and *trxB* (948 bp), respectively. Indeed, as a result of the primers used (Appendix Table 3.1), the genes were amplified alongside a 2,148 bp portion of the pET21a plasmid (Appendix plasmid maps 1b and 2b), therefore expected to yield bands at 2,457 bp and 3096 bp, respectively, as observed here (Figure 27).The successful ligation of *trxA* and *trxB* into pET21a was further confirmed by Sanger sequencing (Appendix Figure 4.1).

4.4.2. Thioredoxin (TrxA) and thioredoxin reductase (TrxB) expression

Protein expression was initially attempted at low scale (50 mL), where cell cultures were incubated at 37 °C, 250 rpm, until an OD_{600} of 0.8 was reached (Appendix Figure 4.2).[175] Cells were induced using IPTG after 5 hours for *trxA* and 4.5 hours for *trxB* before a further 2-hour incubation. Successful expression was confirmed by SDS PAGE (Figure 28).

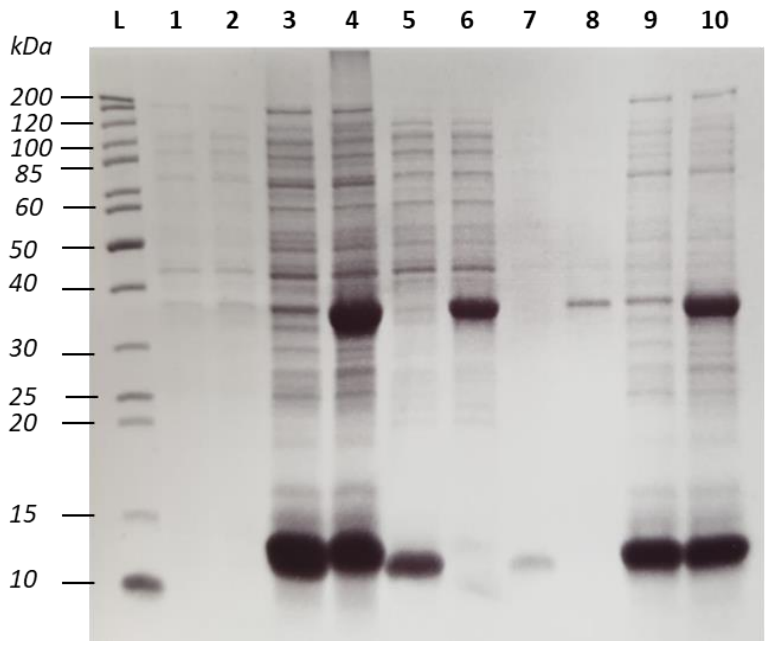

Figure 28. SDS PAGE analysis of initial expression of thioredoxin and thioredoxin reductase from *Bacillus subtilis*, 50 mL, 37°C, 250 rpm. L=protein ladder, lanes 1-2:= trxA and trxB pre-induction controls, lanes 3-4= trxA and trxB lysates, lanes 5-6= trxA and trxB cell-free extracts, lanes 7-8= 10x diluted trxA and trxB cell-free extracts, lanes 9-10= trxA and trxB insoluble fractions.

Strong bands were observed in the lysate, cell-free extracts and insoluble fractions at around 11.5 *k*Da for thioredoxin and 35 kDa thioredoxin reductase, indicating the successful expression of both *Bacillus subtilis* enzymes. The strong bands observed at around 11-14 kDa in both TrxA and TrxB insoluble fractions were also observed by Parker *et al.* (2014), and may correspond to lysozyme.[175,301,302]

Due to seemingly high proportions of protein remaining in the insoluble fractions, expression temperatures and IPTG concentrations were reduced to 30 °C and 0.1 mM, respectively, in an attempt to slow protein production down and limit the presence of aggregation and insoluble proteins.[303,304] No TrxA or TrxB over-expression was achieved under these conditions, and insoluble proteins could still be observed (Appendix Figure 4.3). Initial expression conditions, as described by Parker *et al.* (2014), were therefore kept for the expression of *trxA* and *trxB* from *Bacillus subtilis*.

4.4.3. Thioredoxin (TrxA) and thioredoxin reductase (TrxB) purification

Following protein expression, thioredoxin and thioredoxin reductase from *Bacillus subtilis* were purified *via* Ni^{2+} metal-affinity chromatography. In the case of thioredoxin (TrxA), a peak was observed at an imidazole concentration of approximately 150 *m*M, in accordance with the literature for this specific enzyme.[175] Purified fractions around this 150 mM peak were analysed *via* SDS PAGE (Figure 29), then combined, dialysed to remove imidazole, and concentrated. A thioredoxin protein concentration of 4.05 mg/mL was estimated from the absorbance measured at 280 nm (Appendix Figure 4.4).[175]

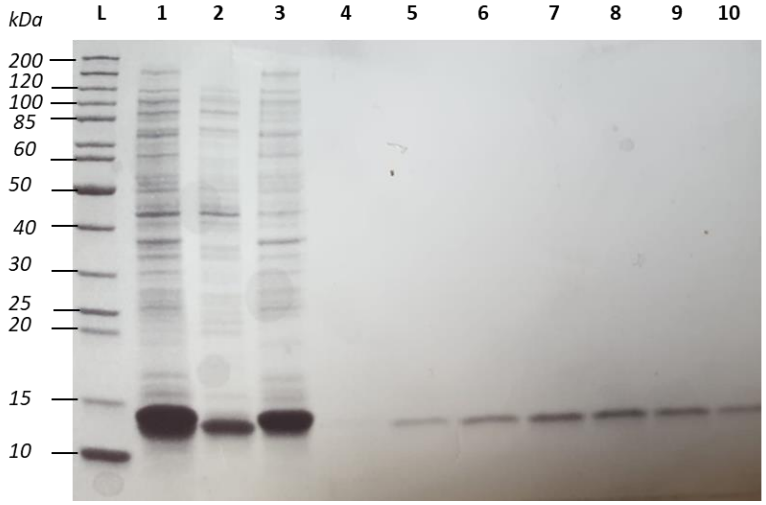

Figure 29. SDS PAGE analysis of the HisTag IMAC purification of thioredoxin from *Bacillus subtilis*. L= protein ladder, lane 1= lysate, lane 2= cell-free extract, lane 3= insoluble fraction, lane 4= A9 fraction, lane 5= A11 fraction, lane 6= A12 fraction, lane 7= B12 fraction, lane 8= B11 fraction, lane 9= B10 fraction, lane 10= B9 fraction.

Similarly, thioredoxin reductase (TrxB) purification fractions were analysed *via* SDS PAGE (Appendix Figure 4.5), combined, dialysed and concentrated. A protein concentration of 0.8 *m*g/*m*L was then estimated for purified thioredoxin reductase using the BCA assay with BSA standards (Appendix Figure 4.6 and Table 4.4).[175]

Purified, dialysed and concentrated thioredoxin and thioredoxin reductase from *Bacillus subtilis* were then analysed by SDS PAGE (Figure 30). Clear bands were observed at 11 and 37 kDa for thioredoxin and thioredoxin reductase, respectively, confirming successful expression and purification.

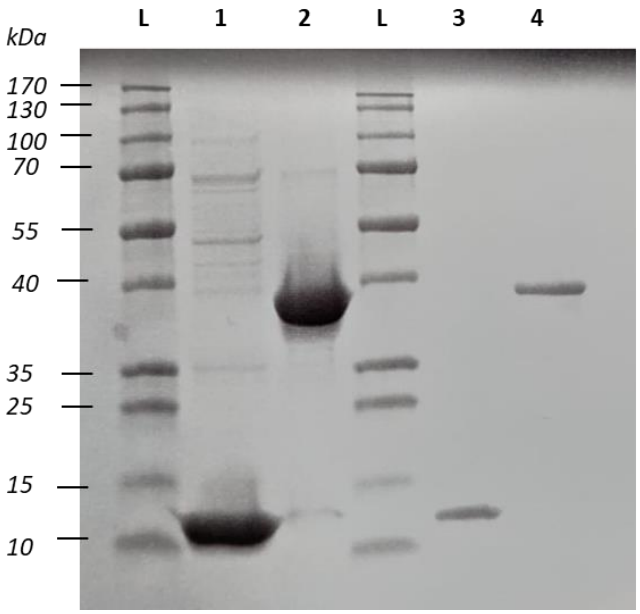

Figure 30. SDS PAGE analysis of purified, dialysed and concentrated thioredoxin and thioredoxin reductase from *Bacillus subtilis*. L= protein ladder, lane 1= thioredoxin, lane 2= thioredoxin reductase, lane 3= 10-times diluted thioredoxin and lane 4= 10x diluted thioredoxin reductase.

The absorbance spectra for purified thioredoxin and thioredoxin reductase are shown in Figure 31. The latter is a flavoprotein, which exhibited a light yellow colour in solution; the spectrum indeed displayed the characteristic absorbances of the FAD ring, with peaks at around 380 and 455 nm corresponding to π_1 to π_3 and π_2 to π_3 transitions, respectively.[184,305–307]

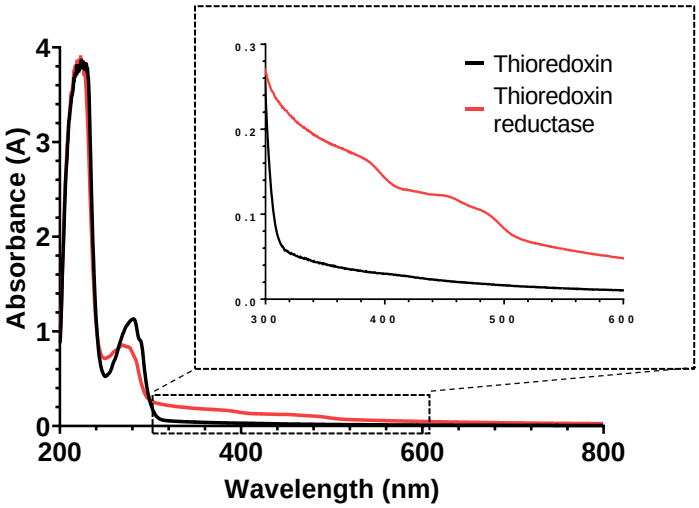

Figure 31. Absorbance spectra recorded for purified thioredoxin and thioredoxin reductase from *Bacillus subtilis*, TrxA (0.78 mg/mL) and TrxB (0.20 mg/mL) in deionised water.

The absorbance values were relatively low due to low FAD concentrations in the sample, in accordance with the literature. Indeed, 0.2 mg/mL of thioredoxin reductase was loaded into the cuvette, corresponding to 5.75 µM, compared to 10 µM of thioredoxin reductase from *Bacillus anthracis* loaded by Gustafsson *et al.* (2012), which yielded absorbance maxima of around 0.1, compared to 0.2 observed in this study.[184]

4.5. Reduction of disulfide bonds in insulin by the thioredoxin system

4.5.1. Insulin turbidity assay

Holmgren's insulin disulfide bond-reducing activity assay was used to evaluate thioredoxin's ability to break disulfide bonds in insulin, in the presence of DTT or thioredoxin reductase and NADPH for the regeneration of its reduced form.[278] Such activity has been commonly described in the literature for thioredoxins from a range of organisms, including *E. coli*, *Bacillus anthracis* and *Bacillus subtilis*.[184,308] This assay relies on the principle that the reduction of insulin disulfide bonds promotes the aggregation of

insulin chain B, associated with an increase in turbidity measurable *via* 650 nm absorbance measurements.[278]

Commercial thioredoxin from *E. coli* (Trx1) and thioredoxin from *Bacillus subtilis* (TrxA) were first incubated with DTT and insulin in sodium phosphate buffer, and 650 nm absorbances were recorded over time (Figure 32). The use of DTT in excess allowed for the measurement of disulfide bond-reducing activity of thioredoxin without thioredoxin reductase and NADPH. According to Arner *et al*. (1999), the regeneration of active thioredoxin by DTT is much faster than the direct reduction of insulin by DTT, suggesting that this assay measured the insulin disulfide bond reducing activity of thioredoxin, while DTT was regenerating reduced thioredoxin, as thioredoxin reductase and NADPH would usually do.[309]

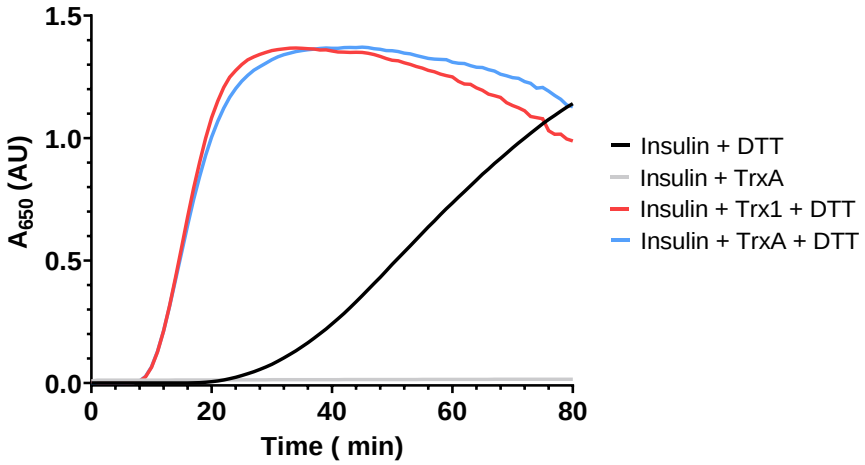

Figure 32. Turbidity assay measuring the reduction of disulfide bonds in insulin by thioredoxins from *Bacillus subtilis* and *E. coli* in the presence of DTT. Trx1 (0.038 U/mL, 8 µg/mL) or TrxA (0.035 U/mL, 7 µg/mL) incubated with insulin (1 mg/mL) and DTT (3 mM) in 0.1 M sodium phosphate buffer pH 7 at 25 °C, no-DTT control included.

An increase in 650 nm absorbance can be observed for the sample containing insulin and DTT (no enzyme), in alignment with expected insulin disulfide bond reduction by DTT. The rate difference observed for insulin disulfide bond reduction by thioredoxins compared to DTT (in the absence of thioredoxins) has been described in the literature, specifically for thioredoxin

from *E. coli*.[278] In this way, the disulfide bond-reducing activities of thioredoxins from *Bacillus subtilis* and *E. coli* were confirmed with insulin as the substrate. In the absence of DTT, no increase in 650 nm absorbance was observed for thioredoxin and insulin due to the absence of a regeneration mechanism.

The specific activities for thioredoxins from *E. coli* and *Bacillus subtilis* were determined, where Δ_{650nm} values were calculated for the first 25 minutes until absorbances reached a plateau. The rate of insulin reduction by DTT was also calculated, using Δ_{650nm} across the full 80 minutes. A lag in turbidity formation was observed both in the presence and absence of thioredoxin, which has been noted in the literature, suggesting that the process of insulin chain precipitation is not immediate following disulfide bond reduction.[278] Respective activities of 4.69 U/mg and 4.99 U/mg were obtained for thioredoxins from *E.coli* and *Bacillus subtilis*, where one unit causes an ΔA_{650nm} of 1.0 in 1 minute at 25 °C under conditions described in this assay.

Next, thioredoxin reductase from *Bacillus subtilis* was investigated as the thioredoxin reducing power, instead of DTT, with the reducing equivalents supplied by NADPH.[310] As a control, the addition of thioredoxin reductase from *Bacillus subtilis* to DTT and insulin was investigated, where the absence of turbidity observed confirmed that thioredoxin reductases are selective for thioredoxins (Appendix Figure 4.7).[311] Both *E. coli* and *Bacillus subtilis* thioredoxins were independently incubated with thioredoxin reductase from *Bacillus subtilis* and NADPH, in excess, and 650 nm absorbances were recorded over time (Figure 33). This assay was attempted using identical thioredoxin concentrations described above in the presence of DTT (Figure 32), with no success. This may have been linked to the lower thioredoxin reductase concentrations included in the assay relative to the amounts of

DTT previously added. It could also be that thioredoxin reductase may not have been fully reconstituted with flavin.[312] Higher enzymatic concentrations were therefore investigated.

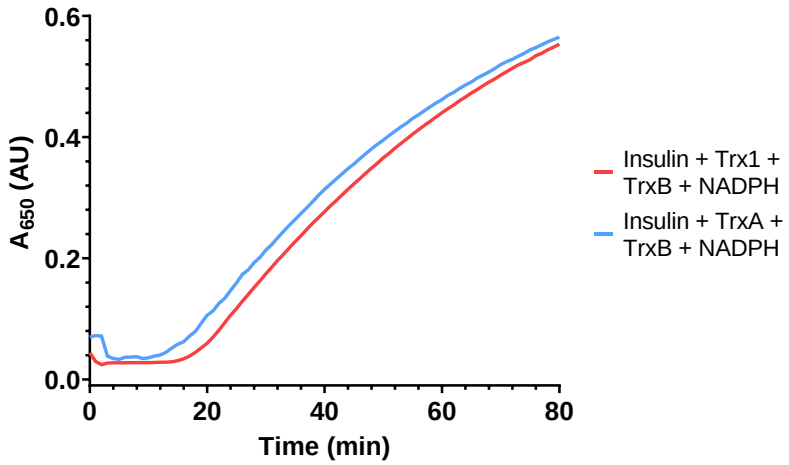

Figure 33. Turbidity assay measuring the reduction of insulin disulfide bonds by *Bacillus subtilis* thioredoxin, thioredoxin reductase and NADPH. Trx1 (0.28 U/mL, 0.06 mg/mL) or TrxA (0.30 U/mL, 0.06 mg/mL) incubated with insulin (1 mg/mL), TrxB (32 µg/mL) and NADPH (105.6 µM) in 0.1 M sodium phosphate buffer pH 7 at 25 °C.

Increases in 650 nm absorbance can be observed for thioredoxin from both *E. coli* and *Bacillus subtilis*, in the presence of *Bacillus subtilis* thioredoxin reductase and NADPH. This suggests that the thioredoxin system from *Bacillus subtilis* has disulfide bond-reducing activity for insulin as the substrate. The comparable absorbance increase obtained for thioredoxin from *E. coli* is unexpected, as thioredoxin reductases have been described as selective for thioredoxins from the same organism.[172,174,178]

4.5.2. NADPH-based assay with insulin as the substrate

Du *et al.* (2012) and Che *et al.* (2020)'s NADPH consumption assay was then used to further confirm the insulin disulfide bond-reducing activity of the thioredoxin system from *Bacillus subtilis*. This assay relies on electron transfer taking place across the thioredoxin system, from NADPH to thioredoxin reductase, thioredoxin and finally to the substrate. While NADPH in its reduced form absorbs light at 340 nm, the oxidised form ($NADP^+$) does

not.[313] In this way, substrate disulfide bond reduction can be monitored *via* NADPH oxidation through 340 nm absorbance measurements over time. This assay has commonly been used to evaluate the activities of a range of protein disulfide reductase enzymes by monitoring the consumption of NADPH spectrophotometrically at 340 nm.[177,182,314–317]

Thioredoxins from *Bacillus subtilis* or *E. coli* were incubated with thioredoxin reductase from *Bacillus subtilis* and insulin at 25 °C and 340 nm absorbance was monitored over time upon NADPH addition (Figure 34).

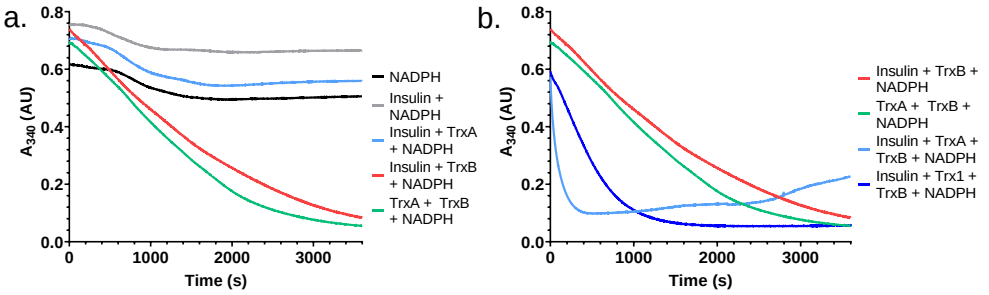

Figure 34. NADPH consumption monitoring of insulin disulfide bond reduction by the thioredoxin system from *Bacillus subtilis*, a. controls and b. samples. Insulin (1.22 mg/mL), Trx1 (0.18 U/mL, 39.3 µg/mL) or TrxA (0.22 U/mL, 44.6 µg/mL) and TrxB (0.11 mg/mL) were added to 0.50 mM Tris-HCl pH 7.5, 1 mM EDTA. The reaction (0.75 mL) was then initiated by addition of NADPH (0.213 mM) at 25 °C.

A range of controls were included in this assay (Figure 31a, see Appendix Figure 4.8 for further controls). The absence of thioredoxin reductase was associated with stable 340 nm absorbances over time. However, the presence of thioredoxin reductase and NADPH led to a steady 340 nm absorbance decrease over time, also observed by Che *et al.* (2020).[277] This phenomenon may be associated with electron transfers occurring between the thioredoxin reductase FAD ring and oxygen, and was later investigated using solubilised keratin as the substrate (see section 4.6.2.1).[202]

Despite the slow and steady absorbance decrease observed in the presence of TrxB and NADPH, a much faster absorbance decrease was seen upon addition of TrxA to TrxB and NADPH. This confirmed previous observations

(section 4.5.1.) that insulin disulfide bonds are indeed being reduced *via* the thioredoxin system. The difference in activity between Trx1 and TrxA was due to thioredoxin concentrations of 3.33 and 3.92 μM, respectively.

Unexpectedly, once the 340 nm absorbance reached around 0.1, an increase in absorbance was observed in the sample containing both insulin and the *Bacillus subtilis* thioredoxin system. This phenomenon was observed to a larger extent at higher enzymatic concentrations (Figure 35).

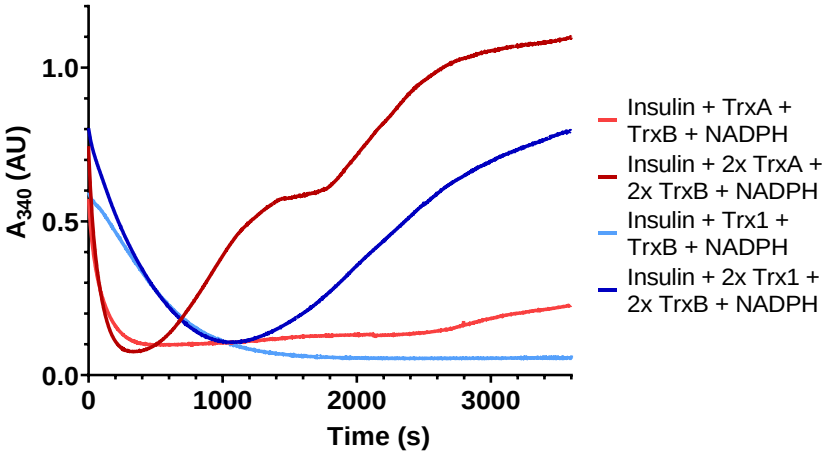

Figure 35 - NADPH consumption monitoring of insulin disulfide bond reduction by the thioredoxin system from *Bacillus subtilis* with increased enzymatic concentrations. Insulin (1.22 mg/mL) was incubated with Trx1 (0.18-0.36 U/mL, 39.3-78.6 µg/mL) or TrxA (0.22-0.44 U/mL, 44.6-89.2 mg/mL), TrxB (0.11-0.22 mg/mL) and NADPH (0.213 mM) at 25 °C.

This subsequent increase in 340 nm absorbance was further investigated by recording absorbance spectra at a range of incubation times (Appendix Figure 4.9). While NADPH consumption could initially be monitored *via* a specific decrease in 340 nm absorbance, high absorbances were then noted across wavelengths, indicating the development of turbidity upon insulin disulfide bond reduction by the thioredoxin system, as previously discussed (see section 4.5.1.). A lag between disulfide bond reduction and insulin precipitation was here again observed.

The NADPH-based assay was successfully used to monitor intramolecular disulfide bond-reducing activity of the thioredoxin system from *Bacillus subtilis* using insulin as soluble protein substrate. Oxidised glutathione was briefly investigated as a substrate for enzymatic intermolecular disulfide bond reduction. While the thioredoxin system from *Saccharomyces cerevisiae* has been shown to be able to reduce oxidised glutathione *in vivo*, low 340 nm absorbance decreases were observed upon incubation of the thioredoxin system from *Bacillus subtilis* with oxidised glutathione (Appendix Figure 4.10).[187] Oxidised glutathione is normally reduced as part of the glutathione system, composed of glutaredoxin, glutathione reductase and NADPH, where glutathione reductase specifically recycles oxidised glutathione back to its reduced form.[318] Therefore, the thioredoxin system may not specifically reduce GSSG.

4.6. Reduction of disulfide bonds in keratin by the thioredoxin system

Once the disulfide bond-reducing activity of the thioredoxin system from *Bacillus subtilis* had been confirmed using insulin as a substrate, further investigations were conducted on keratin, more specifically, solubilised wool and solid human hair. Soluble keratin, in the form of Keratec™ IFP, was explored as a substrate in a way to overcome penetration barriers associated with solid keratin, such as human hair. However, the exact composition of this solubilised wool product was not disclosed; it was therefore considered to contain a mixture of disulfide bonds and S-sulfocysteine bonds, referred to as “sulfur-sulfur” bonds.

Keratec™ IFP and human hair were both characterised before use in *Bacillus subtilis* thioredoxin system activity investigations.

4.6.1. Keratin substrate characterisation

4.6.1.1. Protein content evaluation of Keratec™ IFP

The protein content of Keratec™ IFP was initially investigated using the Bradford assay, which is based on the binding of Coomassie Brilliant Blue G-250 to proteins, resulting in a colour change in the visible spectrum. However, keratin precipitation was repeatedly observed upon contact with Bradford reagent which hindered analyses.

The BCA assay, a copper-based assay involving a protein-induced Biuret reaction followed by the chelation of bicinchoninic acid with the resulting cuprous ions, was instead used to determine Keratec™ IFP protein concentrations.[319] Protein concentrations ranging between 83 and 108 mg/mL were calculated from a BSA standard curve (Appendix Figure 4.11 and Table 4.5). These values, which should be interpreted with caution due to the use of BSA as the standard, were slightly higher than the 65 mg/mL protein concentration suggested by Croda International for Keratec™ IFP.

4.6.1.2. Keratec™ IFP thiol content

The thiol content in Keratec™ was determined using Ellman's assay, following substrate incubation with DTT. DTT is commonly used for disulfide bond reduction, particularly in the context of keratin degradation, synergically with keratinase.[21,26,105,120] Moreover, DTT has also been shown to reduce S-sulfocysteine bonds and can therefore be used towards thiol availability quantifications despite the lack of clarity towards the nature of sulfur-sulfur bonds in Keratec™ IFP (see section 4.2.1.).[320] Ellman's assay relies on the reaction of 5,5'-Dithiobis-(2-nitrobenzoic acid), or DTNB, with thiolate anions (at pH>7), yielding a mixed disulfide as well as TNB^{2-}, a yellow-coloured product which can be monitored by an increase in absorbance at 412 nm (Figure 36).[321] This assay has been commonly used to assess the disulfide

bond-reducing activities of thioredoxin and glutaredoxin systems.[98,180,322,323] In this way, upon incubation with DTT, each reduced substrate disulfide bond is expected to yield two thiols, associated with the release of two TNB^{2-} equivalents upon DTNB addition.

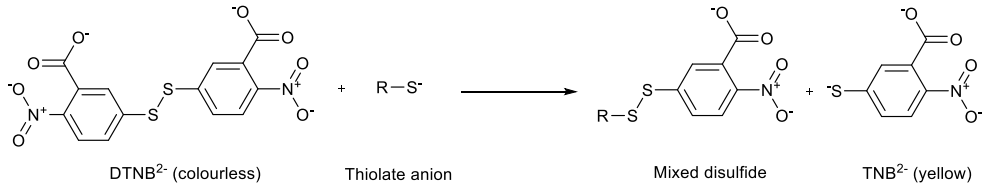

Figure 36. Reaction mechanism of DTNB with thiolate anion yielding a mixed disulfide and TNB^{2-}, a yellow-coloured compound which can be detected at 412 nm.

In the case of S-sulfocysteine, one thiol would be released per bond broken, alongside sulfite. However, cystine sulfonation in keratin is associated with the release of S-sulfocysteine and cysteine, where the latter may then be reoxidised to cystine. Therefore, for each disulfide bond equivalent in Keratec™ IFP, there may be two S-sulfocysteines. In this way, thiol release observed upon substrate incubation with an excess of DTT should be comparable, regardless of the nature of the sulfur-sulfur bonds, under the premise of an end-point assay. However, the reaction of DTNB with sulfite ions has been reported in the literature and may be associated with the release of TNB^{2-}, which may interfere with the reasoning described here.[324,325]

Keratec™ IFP was incubated with DTT, which was then dialysed out before incubation with DTNB, to avoid interference. Absorbances at 412 nm were then recorded (Figure 37). A DTT concentration of <0.44 mg/mL in solution, achieved by two successive 1-litre dialyses, was deemed compatible with Ellman's assays (Appendix Figure 4.12).

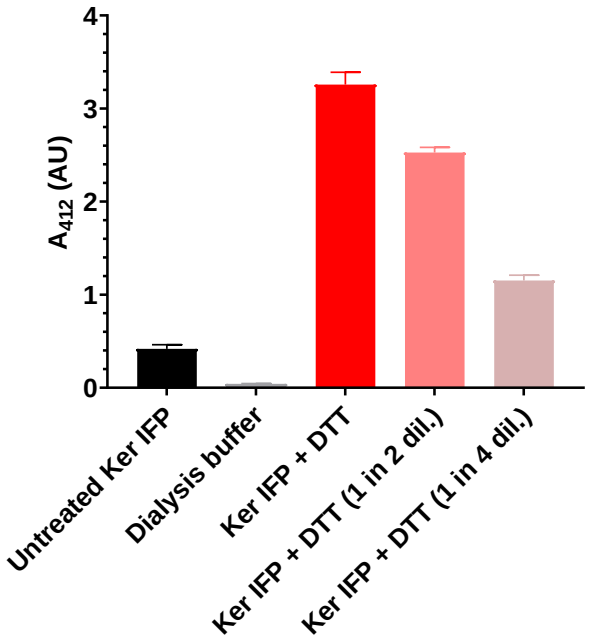

Figure 37. Ellman's assay to determine maximum thiol availability in Keratec™ IFP following DTT treatment. Keratec™ IFP (Ker IFP, 3.25 mg/mL) was incubated with DTT (0.13 M) in Ellman's buffer for 1 hour at 37 °C, 250 rpm, followed by 2 cycles of dialysis in Ellman's buffer, 30 min incubation with DTNB (0.20 µM) and 412 nm absorbance measurements - data given as average values of triplicate reactions and shown ± the standard deviation.

Thiols were clearly detected following Keratec™ IFP incubation with DTT as can be seen by the increase in 412 nm absorbance, and were quantified using Beer Lambert's law. The absorbance of the dialysis buffer and untreated Keratec™ IFP were both subtracted from the Keratec™ IFP + DTT sample absorbance. A thiol concentration of 0.31 µmol/mL was calculated in the sample containing 3.25 mg/mL Keratec™ IFP per 1 mL assay. This resulted in a thiol concentration of 95.4 µmol/g protein in Keratec™ IFP. This value must be taken with a pinch of salt as a gram of protein may not exactly relate to a gram of solubilised wool. Popescu *et al.* (2007) reported a cystine concentration of 460 µmol/g of wool in merino wool, corresponding to a maximum thiol content of 920 µmol/g of wool.[49] While there is a 10-fold difference between the thiol concentration calculated here compared to what is reported in the literature, Weigmann *et al*. (1968) noted that not all disulfide bonds in solvent-extracted wool were accessible to DTT.[287]

4.6.1.3. Human hair thiol content

Similarly to Keratec™ IFP (section 4.6.1.2.), Ellman's assays were conducted to investigate the thiol availability in human hair using DTT as the reducing agent. Hair was incubated with DTT, which was thoroughly rinsed, before DTNB addition and 412 nm absorbance measurements (Figure 38). Five successive buffer rinsings were deemed most efficient for DTT removal from hair (Appendix Figures 4.13 and 4.14).

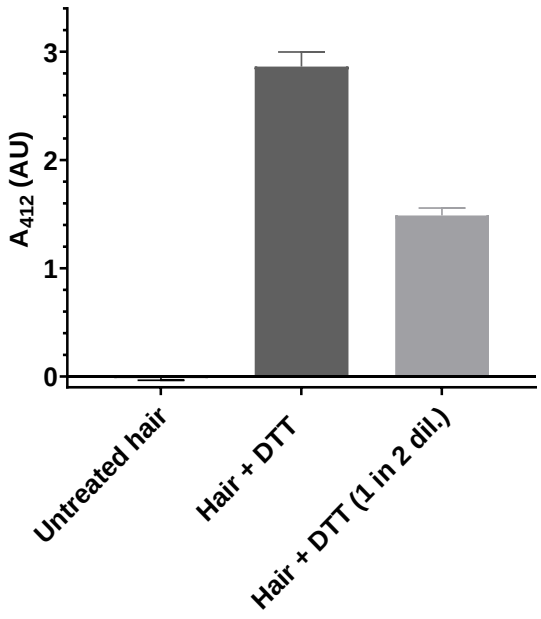

Figure 38. Ellman's assay to determine maximum thiol availability in hair following DTT treatment. Hair (20 mg/mL) was incubated with DTT (0.13 M) in Ellman's buffer for 1 hour at 37 °C, 250 rpm, followed by 5 buffer rinsings, 30 min incubation with DTNB (0.20 µM) and 412 nm absorbance measurements - data given as average values of triplicate reactions (final wash subtracted from sample absorbance) and shown ± the standard deviation.

A thiol concentration of 0.22 µmol/mL was calculated, using Beer Lambert's law, in the sample containing 0.02 g of hair per 1 mL assay. This resulted in a thiol concentration of 10.95 µmol/g of human hair. Popescu *et al.* (2017) reported a cysteine concentration of 1435 µmol per gram of hair.[49,326] This 100-fold difference with calculations conducted here may be explained in two ways. First of all, as mentioned previously, not all disulfide bonds may be accessible to DTT, as reported by Weigmann *et al.* (1968) on solvent-extracted wool.[287] This effect would be expected to be more pronounced in

the case of a solid substrate, such as human hair, due to higher barriers to penetration. Moreover, the Ellman's assay was developed for the determination of thiols in solution and might not be suitable for solid materials.[321] Indeed, in the case of reductively processed protein fibres, such as DTT-reduced hair, part of TNB^{2-} may remain adsorbed to the solid protein structure, preventing precise spectrophotometric thiol quantification.[321] Buchacher *et al.* (2022) therefore reported a new method, using reverse titration and involving $K_3[Fe(CN)_6]$ and K_2CrO_4 as reagents, based on the oxidation of thiols formed by wool-cystine reduction.[321] The authors reported thiol concentrations between 6.83 and 26.17 µmol/g for $NaBH_4$-reduced solid wool keratin fibres, which according to them, constitutes a minor share of the disulfide groups present in wool keratin, explained by the limited accessibility and penetration depth of solutions into the fibres. For these reasons, the relatively low thiol concentrations observed here for DTT-treated hair is unsurprising.

Nonetheless, the penetration of DTT, a 154 Da compound, into the hair cortex was here confirmed, in line with work conducted by Cruz *et al.* (2017) and Malinauskyte *et al.* (2020), where the authors observed the penetration of low and mid-molecular weight peptides, up to 2,577 Da, into the hair cortex, while high molecular weight peptides (> 75,000 Da) were seen to adsorb onto the hair surface.[48,57]

4.6.2. Reduction of sulfur-sulfur bonds in Keratec™ IFP by the thioredoxin system

The activity of the thioredoxin system from *Bacillus subtilis* on Keratec™ IFP was assessed both using the Ellman's and NADPH-based assays. This was aimed at identifying potential enzymatic activities on a keratin substrate while avoiding barriers to penetration encountered with solid keratin.

The uncertainty regarding whether cysteine amino acids are present as cystines or S-sulfocysteines in Keratec™ IFP was considered here. While the main catalytic activity of thioredoxin systems corresponds to the reduction of protein disulfide bonds, their ability to reduce S-sulfocysteine to L-cysteine has been noted in the literature.[189–191] In this way, thioredoxin system activity could here be tested, regardless of whether cystines or S-sulfocysteines were being reduced.[191]

4.6.2.1. NADPH-based assay

A range of substrate, enzyme and NADPH concentrations and ratios were investigated for NADPH-based assay optimisation purposes (Appendix Figure 4.15). Keratec™ IFP was incubated in the presence of the *Bacillus subtilis* thioredoxin system and NADPH consumption was monitored at 340 nm (Figure 39). A significant decrease in 340 nm absorbance was observed over time, and detected across replications, indicating thioredoxin system activity on Keratec™ (Appendix Figure 4.16). NADPH consumption *via* substrate reduction was clearly distinguishable from the flavin/O_2 pathway, as indicated by the no-thioredoxin controls. As expected, reduced enzyme concentrations were associated with lower activity, and therefore slower decrease in 340 nm absorbance, yet the absorbance decrease was still much greater than the negative controls.

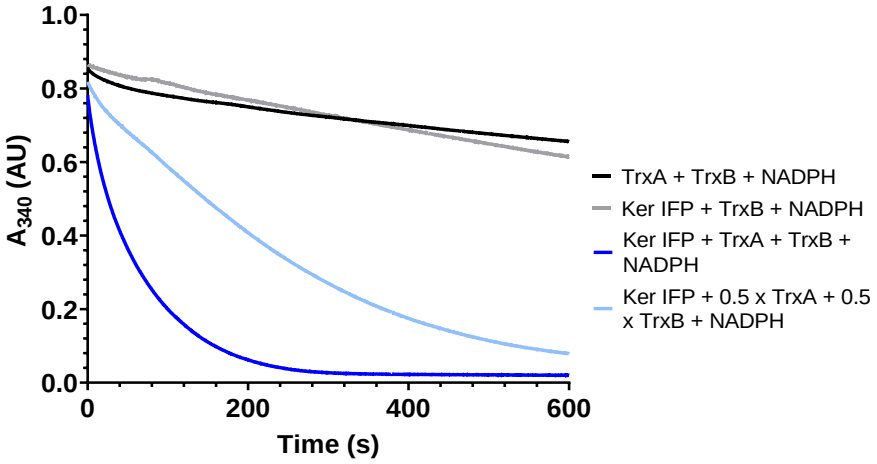

Figure 39 - NADPH consumption monitoring of Keratec™ IFP disulfide bond reduction by the *Bacillus subtilis* thioredoxin system. Keratec™ IFP (Ker IFP, 3.25 mg/mL) was incubated with TrxA (0.35-0.70 U/mL, 0.070-0.14 mg/mL), TrxB (0.17-0.34 mg/mL) and NADPH (0.200 mM) in 0.50 mM Tris-HCl pH 7.5, 1 mM EDTA at 25 °C, up to 1 mL. Absorbances taken prior to NADPH addition were subtracted. The decrease of enzymatic concentrations by half was also investigated.

4.6.2.2. Ellman's assay

Ellman's assay was used to further investigate the potential activity of the thioredoxin system from *Bacillus subtilis* on Keratec™ IFP. The solubilised wool substrate was incubated with TrxA, TrxB and NADPH, followed by DTNB addition and 412 nm absorbance measurements (Figure 40). Samples were incubated for one hour in order to ensure reaction completion (reaction terminated within 6 minutes as seen in Figure 39). Controls were included in this assay to account for potential interferences from Keratec™ IFP with 412 nm absorbances due to its yellow tint, and the thioredoxin system with DTNB, although DTNB has been shown as a substrate mainly for mammalian thioredoxin reductases.[327–330] Dialysis prior to DTNB addition was also explored for DTT and thioredoxin system removal, however, this step was disregarded due to loss of substrate and lack of control over sample dilution.

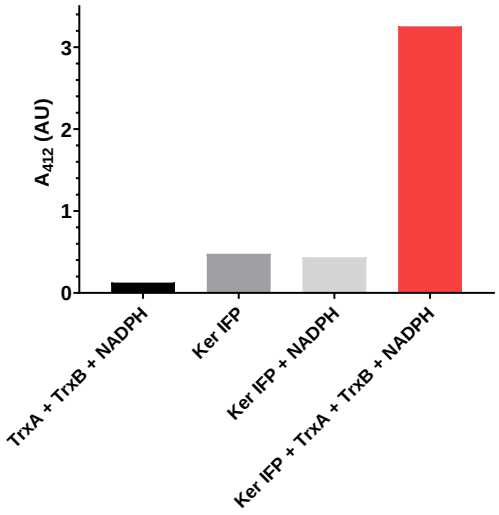

Figure 40. Ellman's assay of the *Bacillus subtilis* thioredoxin system activity on Keratec™ IFP. Keratec™ IFP (Ker IFP, 3.25 mg/mL) was incubated with TrxA (0.70 U/mL, 0.14 mg/mL), TrxB (0.34 mg/mL) and NADPH (200 µM) in 100 mM Sodium Phosphate buffer with 1 mM EDTA, pH 8 up to 1 mL, at 37 °C for 1 hour. A range of controls were included and volumes were adjusted using buffer. DTNB (0.2 mM) was then added, followed by 15 minute-incubation at room temperature and 412 nm absorbance measurements.

Keratec™ IFP showed some absorbance interference at 412 nm due to its pale-yellow colour; however, the addition of thioredoxin was associated with a great increase in 412 nm absorbance, confirming the activity of the *Bacillus subtilis* thioredoxin system for Keratec™ IFP observed with the NADPH assay. Such activity was further indicated by the presence of a clear 412 nm peak in the absorbance spectrum taken of the thioredoxin system and Keratec™ IFP sample (Appendix Figure 4.17).

4.6.2.3. Disulfide vs. S-sulfocysteine bond reduction in Keratec™ IFP

Both assays described above (Figures 39 and 40) were then used for quantitative investigations of the *Bacillus subtilis* thioredoxin system activity on Keratec™ IFP.

Regarding the NADPH-consumption assay (Figure 39), total NADPH consumption was quantified *via* Beer Lambert's law by measuring the decrease in 340 nm absorbance upon reaction completion (t300s). It was hypothesised that in the presence of thioredoxin, thioredoxin reductase

selectively reduces thioredoxin over oxygen in air, which requires spin inversion.[202] This was justified by the clear differences in rate between the two NADPH consumption pathways, substrate reduction or O_2/flavin electron transfer. In this way, it was assumed that the absorbance decrease observed within the first 300 seconds of incubation of the thioredoxin system from *Bacillus subtilis* with Keratec™ IFP corresponded to substrate reduction. The decrease in 340 nm absorbance associated with NADPH consumption *via* the O_2/flavin pathway was therefore not considered (see section 4.6.2.1). An NADPH consumption of 0.121 µmol/mL was calculated, compared to the 0.200 µmol/mL of NADPH added in this assay. This discrepancy may have been relative to the use of a slightly degraded NADPH stock, or potential delays in starting absorbance recordings following manual NADPH injection, however, the latter seemed unlikely due to similar starting absorbances observed across samples.

Thiol release associated with the incubation of the thioredoxin system with Keratec™ IFP was then quantified *via* Beer-Lambert's law based on 412 nm absorbances obtained with Ellman's assay (Figure 40). The absorbance associated with Keratec™ IFP's yellow tint was subtracted. A thiol release of 0.204 µmol/mL (62.8 µmol/g of wool) was calculated, compared to a substrate thiol availability of 0.31 µmol/mL (95.4 µmol/g of wool) previously measured using DTT (see section 4.6.1.2.). Comparable thiol release associated with *Bacillus subtilis* thioredoxin system activity on Keratec™ IFP was observed across replications (Appendix Figure 4.18). While the thioredoxin system has been shown to have much higher disulfide bond-reducing activity on insulin than DTT, the incubation of solubilised wool with DTT was associated with greater thiol release than the thioredoxin system.[278]

Overall, the higher thiol release corresponding to Keratec™ IFP reduction observed for DTT may be linked to the size of the compound (154 Da) compared to thioredoxin (11.4 kDa), allowing for better disulfide bond access within the solubilised keratin substrate.

Looking more specifically at the hypothesised mix between disulfide and S-sulfocysteine bonds in Keratec™ IFP, the reduction of a disulfide bond by the thioredoxin system is associated with the release of two thiols, while the reduction of S-sulfocysteine yields one thiol (and sulfite). Moreover, Ellman's assay measures the release of thiols, while the NADPH-based assay measures the consumption of NADPH, where one equivalent of NADPH consumed corresponds to one reduced sulfur-sulfur bond (Figure 41).

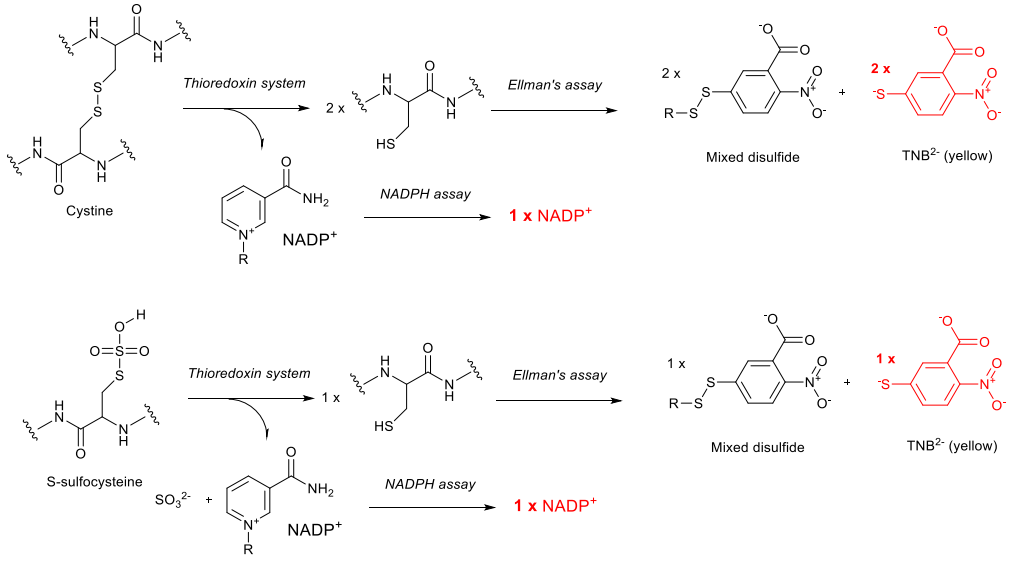

Figure 41. Stoichiometric evaluation of the quantitative analyses of cystine/S-sulfocysteine reduction by the *Bacillus subtilis* thioredoxin system *via* Ellman's assay and NADPH monitoring.

In this way, if all cysteine amino acids in solubilised wool substrate were conserved as disulfide bonds, where n = mols consumed in each assay, then:

$$\frac{n(Ellman's\ assay)}{n(NADPH\ assay)} = 2$$

On the other side, the reduction of an S-sulfocysteine bond is associated with the release of one thiol and sulfite.[190] Therefore, if all cysteine amino acids in Keratec™ IFP existed as S-sulfocysteine, then:

$$\frac{n(Ellman's\ assay)}{n(NADPH\ assay)} = 1$$

Therefore, the comparison of NADPH consumption quantification and thiol release quantification (Ellman's assay) may be used as an indication of whether the thioredoxin system from *Bacillus subtilis* is reducing disulfide bonds or S-sulfocysteines in solution.

The NADPH consumption of 0.121 µmol/mL calculated above may therefore correspond to a thiol release between 0.121 µmol/mL (30.8 µmol/g of wool, in the case of all cysteines present as S-sulfocysteines) and 0.242 µmol/mL (61.7 µmol/g of wool, in the case of all cysteines as cysteines), compared to 0.204 µmol/mL (62.8 µmol/g of wool) calculated using Ellman's assay. This 1 to 1.7 molar equivalence calculated between NADPH consumption (NADPH-based assay) and total thiol release (Ellman's) may further confirm that a mix of S-sulfocysteines and disulfides are found in Keratec™ IFP. However, the reaction of DTNB with sulfite ions has been reported in the literature and may be associated with the release of TNB^{2-}, which would interfere with the reasoning described above.[324,325] Moreover, the fact that for each disulfide bond equivalent in Keratec™ IFP, there may be two S-sulfocysteines was also not considered here. Outcomes must also be taken with a pinch of a salt due to potential NADPH consumption interferences in the presence of oxygen.

4.6.2.4. Further investigations

4.6.2.4.1. Anaerobic conditions

The reaction of reduced flavins in solution with molecular oxygen has been described in the literature, occurring *via* electron transfer from the reduced flavin to O_2.[202] This reaction takes place slowly due to spin inversion being required for the reaction of reduced flavin, a singlet, with molecular oxygen, a triplet. Once oxidised, the flavin can then be reduced over and over again *via* electron transfer from NADPH, until it is not available anymore. This phenomenon was therefore considered as a potential explanation towards the slow and steady decrease in 340 nm absorbance observed in the presence of thioredoxin reductase and NADPH, without thioredoxin, both for insulin (Figure 34) and Keratec™ IFP (Figure 39) as substrates.

In this way, the NADPH-based assay was attempted anaerobically, where the reaction cuvette containing Keratec™ IFP, thioredoxin and thioredoxin reductase was purged with argon before the addition of NADPH and immediate 340 nm absorbance monitoring (Appendix Figure 4.19). The decrease in 340 nm absorbance observed in the presence of thioredoxin reductase and NADPH (no thioredoxin) was minimised as a result, confirming the O_2-flavin hypothesis described above. However, as this slow and steady O_2-flavin NADPH consumption could be accounted for using negative controls, aerobic reaction conditions were kept in use due to impracticalities associated with working anaerobically.

4.6.2.4.2. Effect of additives

Hair structure opening was later investigated for improved enzymatic penetration using a range of additives (see section 4.6.3.3.). The inhibitive effects of such additives on *Bacillus subtilis* thioredoxin system activity were therefore briefly explored, using Keratec™ IFP as the substrate (Appendix

Figure 4.20), and are summarised in Table 7 below. The baseline enzymatic activity was calculated under standard assay conditions as follows, where t is the timeframe in which absorbance decrease was monitored and v is the volume of the assay (1 mL):

$$Baseline\ activity\ (U.mL^{-1}s^{-1}) = \frac{\Delta_{340}(Ker\ IFP + Trx\ system)}{t \times v} - \frac{\Delta_{340}(Ker\ IFP + TrxB + NADPH)}{t \times v}$$

NADPH consumption *via* O_2/flavin was in this way taken into consideration by subtracting the absorbance decrease associated with a no-thioredoxin control, although it remains unclear whether, in the presence of thioredoxin, NADPH solely gets consumed *via* the substrate reduction pathway. Relative enzymatic activities for each condition were calculated as percentages of the baseline activity.

Table 6. Evaluation of the effect of Tween 20, urea, [EMIM]ESO_4 and high incubation temperature on thioredoxin system from *Bacillus subtilis* activity on Keratec™ IFP *via* NADPH consumption monitoring.

Conditions investigated	Enzymatic activities relative to baseline
Keratec™ IFP + Trx system in 2% Tween 20	94.5 %
Keratec™ IFP + Trx system in 5% Tween 20	0 %
Keratec™ IFP + Trx system in 5% urea	112 %
Keratec™ IFP + Trx system in 10% urea	35.9 %
Keratec™ IFP + Trx system in 1% EMIM	85.9 %
Keratec™ IFP + Trx system in 5% EMIM	54 %
Keratec™ IFP + Trx system in 10% EMIM	39 %
Keratec™ IFP + Trx system at 70 °C	197 %

The addition of urea was associated with a slight increase in thioredoxin system activity on Keratec™ IFP, in line with its ability to break non-covalent bonds and loosen up the keratin fibre.[331] Moreover, a significant increase in thioredoxin system activity was noted at higher temperature (25 °C to 70 °C), in line with what has been described in the literature for thioredoxin systems from a range of organisms.[332,333] Overall, Tween 20, urea and [EMIM]ESO_4 did not inhibit the thioredoxin system from *Bacillus subtilis* up to 5% v/v, 5% w/v and 0.1% v/v concentrations, respectively, which was taken into consideration during later hair structure opening investigations.

4.6.3. Human hair disulfide bond reduction by the thioredoxin system

While it remained unclear whether the significant activity detected for the thioredoxin system from *Bacillus subtilis* on Keratec™ IFP corresponded to the reduction of disulfide bonds, S-sulfocysteine bonds, or both, the potential disulfide bond-reducing activity on human hair keratin was then investigated. In an attempt to facilitate enzymatic penetration into the hair cortex, a range of substrate treatments were investigated, including the grinding and solubilisation of hair, as well as potential fibre swelling using additives such as urea.[331] Both Ellman's and NADPH-based assays were used to this end.

4.6.3.1. Untreated solid human hair

Initially, the ability of commercial thioredoxin from *E. coli* to reduce disulfide bonds was assessed on untreated solid human hair, with DTT as the reducing power. The insulin turbidity assay indeed confirmed the suitability of DTT as reducing agent for thioredoxin (see section 4.5.1.) in the presence of insulin.[309] However, this is not known for keratin as a substrate. Therefore, DTT was incubated with human hair, in the presence and absence of *E. coli* thioredoxin (Figure 42). The hair was thoroughly rinsed before DTNB addition

and 412 nm absorbance measurements to avoid DTT interference. Higher thiol release was observed in the presence of thioredoxin, over three replications, however, the absorbance difference with the no-thioredoxin control was not statistically significant (P(T<=t) one-tail of 0.106 obtained *via* a two-sample assuming unequal variances t-Test).

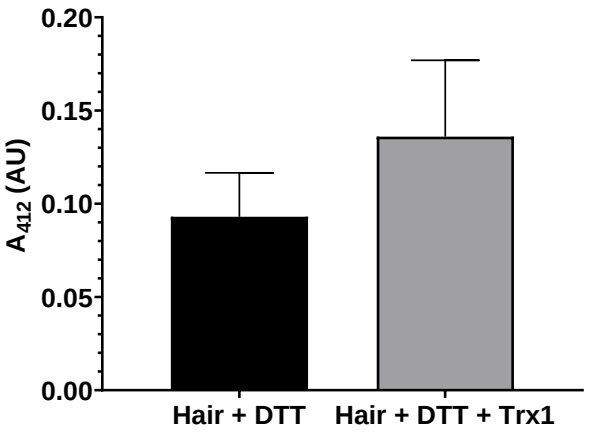

Figure 42. Ellman's assay of solid human hair disulfide bond reduction by *E. coli* thioredoxin and DTT. Hair (0.08 g/mL) was incubated with Trx1 (0.047 U/mL, 0.010 mg/mL) and DTT (3 mM) in 100 mM Sodium Phosphate buffer with 1 mM EDTA, pH 8 up to 2.5 mL, for 15 minutes at 37 °C, followed by thorough buffer rinsing. Substrates were resuspended in buffer (2.5 mL) and DTNB (0.20 μM) was added and incubated for 15 minutes at room temperature. 412 nm absorbances were then recorded - data given as average values of triplicate absorbance measurements (final buffer rinsing absorbance subtracted from sample absorbances) and shown ± the standard deviation.

Further replications were conducted with increased thioredoxin concentrations, with no significant difference in thiol release observed in the presence or absence of thioredoxin, suggesting a lack of activity for hair. DTT and hair concentrations and ratios were also varied, without success. These observations may suggest that DTT was not suitable as a reducing agent for thioredoxin in the presence of human hair. However, this is unlikely, considering barriers to DTT reaction with human hair are expected to be much higher than in the case of soluble substrates, such as insulin. This potential lack of disulfide bond reducing activity of thioredoxin from *E.coli* in solid human hair was further explored.

The potential activities of *E. coli* and *Bacillus subtilis* thioredoxins on solid human hair were then investigated *via* thioredoxin reductase and NADPH regeneration, instead of DTT (Figure 43). Very low 412 nm absorbances were recorded compared to the positive control containing DTT, again suggesting a lack of activity of the thioredoxin system for solid hair as a substrate.

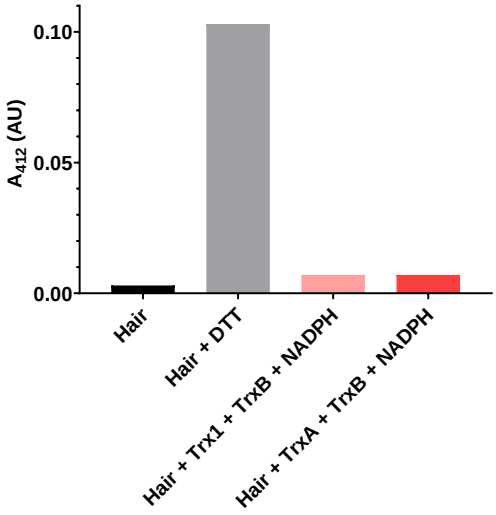

Figure 43. Ellman's assay of solid human hair disulfide bond reduction by the *Bacillus subtilis* thioredoxin system. Hair (0.08 g/mL) was incubated with DTT (3 mM), Trx1 (0.56 U/mL, 0.12 mg/mL) or TrxA (0.70 U/mL, 0.14 mg/mL), TrxB (0.34 mg/mL) and NADPH (213 µM) in 100 mM Sodium Phosphate buffer with 1 mM EDTA, pH 8 up to 1 mL, for 1 hour at 37 °C. Following thorough buffer rinsing, substrates were resuspended in buffer (1 mL), DTNB (0.20 µM) was added and incubated for 15 minutes at room temperature. 412 nm absorbances were then recorded (final buffer rinsing absorbance subtracted from sample absorbances).

This lack of clear disulfide bond reducing activity of the *Bacillus subtilis* thioredoxin system on solid hair was further observed *via* the NADPH degradation assay. The assay was adapted for a solid substrate. Typically, the reaction was performed as a heterogeneous hair-buffer mixture, and sample supernatants were measured (A340nm and full spectra) at regular time intervals (Figure 44 and Appendix Figure 4.21).

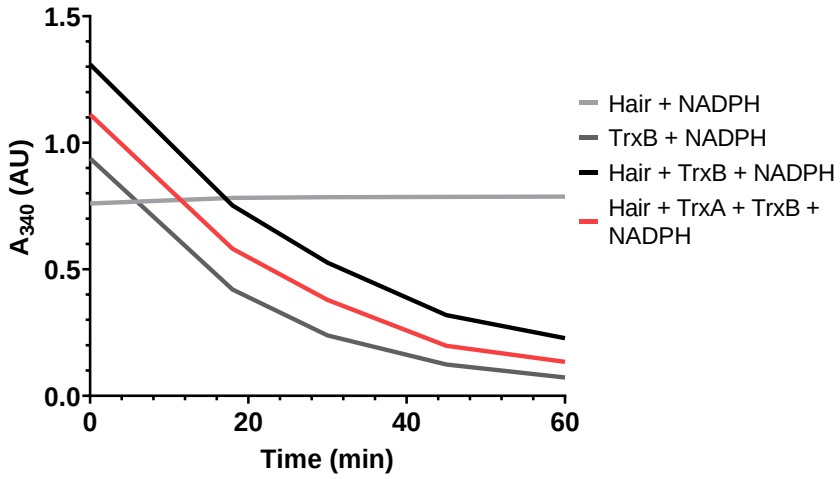

Figure 44. NADPH consumption monitoring of solid human hair disulfide bond reduction by the *Bacillus subtilis* thioredoxin system. Hair (0.02 g/mL) was incubated with TrxA (0.70 U/mL, 0.14 mg/mL), TrxB (0.34 mg/mL) and NADPH (0.213 mM) were added to 0.50 mM Tris-HCl pH 7.5, 1 mM EDTA, up to 1 mL. The decrease in absorbance at 340 nm was then monitored at regular intervals for up to one hour at 25 °C, by pipetting the sample supernatant into the quartz cuvette prior to every measurement.

Similar rates of 340 nm absorbance decreases were observed for samples both in the presence or absence of thioredoxin, suggesting that NADPH was being converted to $NADP^+$ *via* the flavin/O_2 pathway and, therefore, that disulfide bonds in hair were not being reduced by the thioredoxin system.

While clear thioredoxin system activity was observed on Keratec™ IFP, the lack of activity noted for solid hair was put down to the nature of the substrate. Indeed, thioredoxins from various organisms, including *Salmonella typhimurium* and *E. coli,* have been shown to reduce S-sulfocysteine bonds to cysteine.[189–191] It was therefore assumed that the thioredoxin system from *Bacillus subtilis* is equally able to reduce disulfide bonds and S-sulfocysteine bonds in substrates, as suggested in the literature.[191] In this way, considering that the system was able to reduce bonds in solubilised wool (disulfide or S-sulfocysteine), the potential of the thioredoxin system to reduce disulfide bonds in soluble keratin had therefore been demonstrated. Therefore, it was assumed that the lack of enzymatic disulfide bond reduction observed in solid hair was related to the highly crosslinked and tightly packed substrate

structure, preventing enzymes (≥11.4 kDa) from reaching the hair cortex.[6,9,41,46]

In an attempt to facilitate the penetration of thioredoxin from *Bacillus subtilis* into the hair, a range of treatments were investigated, including hair grinding, and solubilisation.

4.6.3.2. Ground hair

The grinding of keratin substrates prior to spectrophotometric analyses has been described in the literature, most likely to improve measurement accuracy by increasing reaction homogeneity.[27,334,335] Solid human hair was ground using liquid nitrogen and a pestle and mortar prior to treatment with the thioredoxin system from *Bacillus subtilis*, in an attempt to increase homogeneity within assays and facilitate enzymatic penetration (Appendix Figure 4.22). The supernatant was pipetted into a quartz cuvette prior to absorbance measurements to avoid any interference from the suspended powder. However, no enzymatic disulfide bond reducing activity was detected for the ground substrate. This was not unsurprising, as grinding allows the substrate to be broken down into smaller fragments, rather than opening up the keratin structure. Ground hair was also investigated as a substrate for an Ellman's assay, where enzymes and NADPH were rinsed using either dialysis or Buchner filtration prior to DTNB addition to avoid interference (Appendix Figure 4.23). Both these rinsing methods led to significant substrate losses, and as a result, 412 nm absorbances were very low. No conclusions could be drawn.

4.6.3.3. Treated solid human hair

In an attempt to facilitate enzyme penetration into the hair cortex, a range of pre-treatments were investigated. Hair delipidation was attempted using 15% w/v sodium lauryl ether sulphate followed by incubation with 1:1

methanol/chloroform, based on a range of methods described in the literature.[57,66,67] Hair was also treated with a range of additives, such as urea, Tween20 and ionic liquids.[58–62] Scanning Electron Microscopy (SEM) was then used to investigate the effect of these treatments on hair structure, with fibre swelling, lifted cuticles and exposed cortex all indicative of fibre structure opening.

A minimum of six strands per condition were analysed by SEM, and overall observations across all six strands are reported here (Figure 45). Untreated hair exhibited cuticles in very good condition (Figure 45a), while high-temperature incubation (Figure 45b) and delipidation (Figure 45c) were associated with very slight cuticle damage. Cuticle damage was also observed upon treatment with Tween 20 (Figure 45d), a non-ionic surfactant commonly used as a detergent. Incubation of both delipidated and non-delipidated hair with urea, which absorbs moisture from the environment and draws it to the hair, inducing swelling, led to cuticle damage and lifting, as well as fibre swelling (Figure 45e).[87,336] Finally, incubation of non-delipidated and delipidated hair with low concentrations of ionic liquids led to the apparition of fibre swelling, defects and cracks (Figures 45f-i).

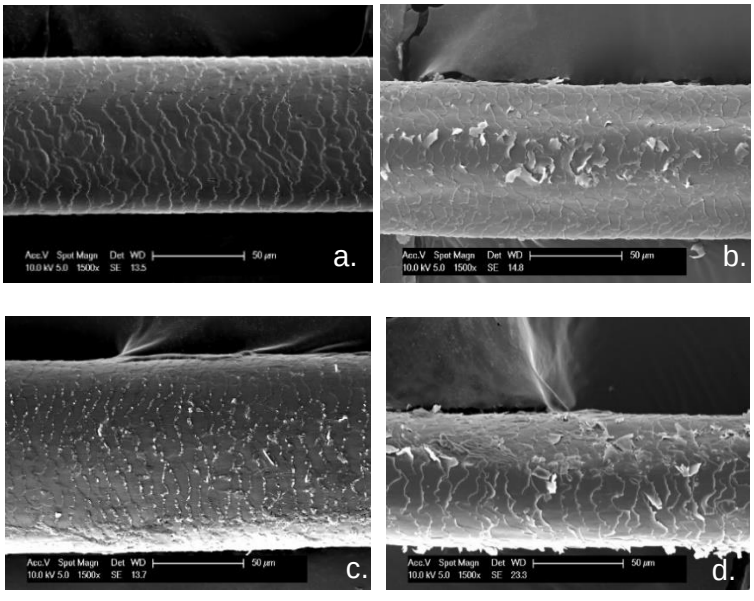

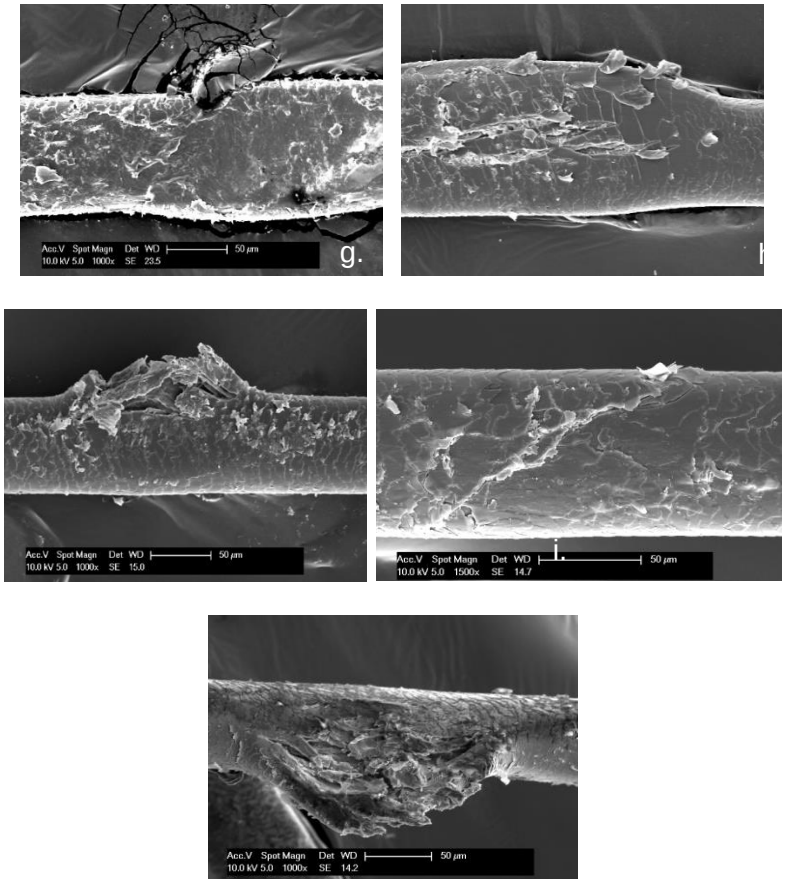

Figure 45. Scanning Electron Microscopy analysis of pre-treated human hair. Hair (0.03 g) was exposed to a range of pre-treatments (3 mL). (a) Untreated hair, (b) hair incubated at high temperature (70 °C instead of 30 °C), (c) Delipidated hair (d) hair incubated with Tween 20 (2% w/v), (e) hair incubated with urea (8 M), (f) hair incubated with [EMIM]ESO_4 (100%), (g) hair incubated with [EMIM]Cl (0.03 mg/mL), (h) hair incubated with [BMIM]Cl (0.03 mg/mL) and (i) hair incubated with [BMIM]Br (0.5 mg/mL).

In this way, the effects of various pre-treatments on hair integrity were investigated using SEM. Significant hair damage was observed in the presence of Tween 20, urea and ionic liquid treatments.

Pre-treated solid hair samples were then investigated by Ellman's assay to evaluate potential penetration of the thioredoxin system from *Bacillus subtilis* into the hair cortex as a result of hair structure opening. Following pre-incubation of intact hair with the various additives, hair was thoroughly rinsed before further overnight incubation with the thioredoxin system. Hair samples were rinsed again prior to DTNB addition and 412 nm absorbance measurements (Figure 46). Absorbances remained low across all samples, suggesting a lack of enzymatic disulfide bond reducing activity on solid hair.

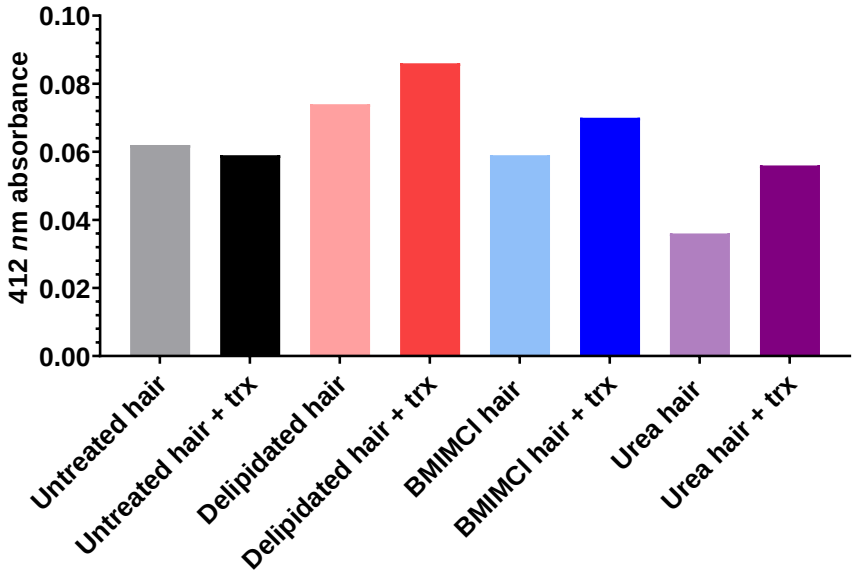

Figure 46. Ellman's assay of disulfide bond reduction of pre-treated human hair by the *Bacillus subtilis* thioredoxin system. Hair (10 mg/mL) was pre-incubated overnight at 37 °C, 250 rpm, with 1:1 chloroform:methanol following a wash with 15% w/v SDS (delipidated hair), [BMIM]Cl (0.03 mg/mL) or urea (8M) in 100 mM sodium phosphate buffer with 1 mM EDTA, pH8, up to 3 mL. Hair samples were then thoroughly rinsed, then further incubated overnight at 37 °C, 250 rpm, with TrxA (0.70 U/mL, 0.14 mg/mL), TrxB (0.34 mg/mL) and NADPH (213 µM) in 1 mL of 100 mM sodium phosphate buffer, 1 mM EDTA, pH 8, before being finally rinsed prior to addition of DTNB (0.20 µM) in sodium phosphate buffer with 1 mM EDTA, pH 8, up to 1 ml, 15 min incubation at room temperature and 412 nm absorbances recording.

Despite the hair structure opening observed *via* SEM as a result of various pre-treatments (delipidation, incubation with urea, ionic liquids etc.), the thioredoxin system from *Bacillus subtilis* was not able to penetrate into the hair cortex and reduce disulfide bonds. Similar observations were made using the NADPH consumption assay (Figure 47), where hair was incubated with the thioredoxin system in the presence of promising additives at concentrations known not to inhibit enzymatic activity (see section 4.6.2.4.2.). Indeed, no NADPH consumption beyond the rate of the O_2/flavin pathway was observed under any condition assayed.

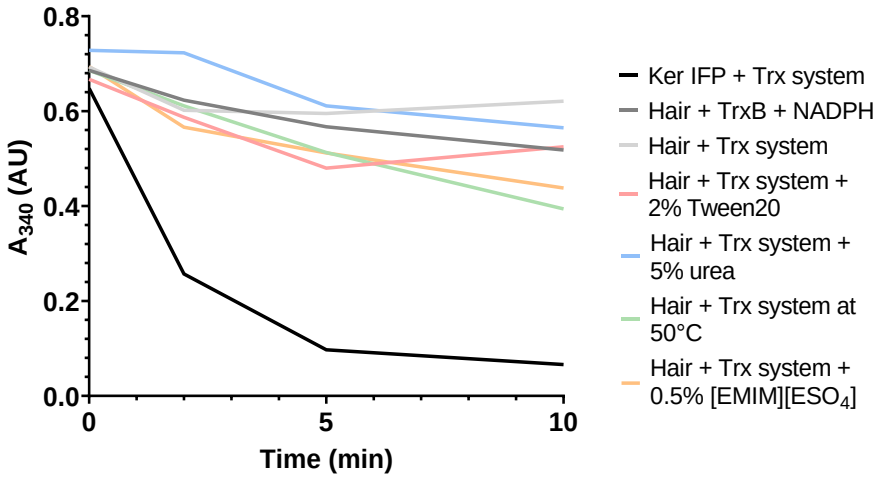

Figure 47. NADPH degradation assay of solid human hair disulfide bond reduction by the *Bacillus subtilis* thioredoxin system in the presence of a range of additives. Hair (0.02 g/mL) was incubated with TrxA (0.70 U/mL, 0.14 mg/mL), TrxB (0.34 mg/mL) and NADPH (0.213 mM) in 0.50 mM Tris-HCl pH 7.5, 1 mM EDTA, up to 1 mL, in the presence of Tween20 (2% v/v), urea (5% w/v) or [EMIM]ESO_4 (0.5% v/v). The decrease in absorbance at 340 nm was then monitored at regular intervals for up to one hour at 25 or 50 °C, by pipetting the sample supernatant into the quartz cuvette prior to every measurement.

4.6.3.4. Solubilised hair

Hair solubilisation was then attempted to facilitate enzymatic access to hair keratin, similarly to Keratec™ IFP. A range of methods have been described in the literature regarding keratin solubilisation, mainly from wool but also feathers and hair.[72,91,99,100,106–109] Two approaches for hair keratin solubilisation were investigated, using NaOH (10 M in water) at 90 °C for 15 minutes as suggested by Sarmani *et al.* (1997) or [EMIM]ESO_4 (100%) at 120 °C overnight, inspired by work conducted by Zhang *et al.* (2017)[104,106]. While sodium hydroxide is known to break disulfide bonds, amongst other bonds, in hair keratin, NaOH-solubilisation was attempted with the idea that some disulfide bonds may remain intact.[5,73] Moreover, the use of ionic liquids as tunable green solvents (low flammability, lack of vaporisation) has been described in the literature towards hair solubilisation, where the combined effects of anions and cations allow for the breaking of covalent and non-covalent interactions in keratin.[100,101,106,112–117] While a minimum of 65% disulfide bond breakage was reported as a requirement for complete

solubilisation by ionic liquids according to Zhang *et al.* (2017), the possibility of intact disulfide bonds in solubilised hair was in this way investigated.[106]

Both methods led to successful hair solubilisation, however, ionic-liquid solubilised hair turned into a very dark and viscous liquid. The [EMIM]ESO_4-solubilisation of bleached hair was then attempted to avoid the dark colour potentially associated with melanin.[337] However, a dark heterogenous viscous liquid was again obtained. A range of dilutions were performed to lower the [EMIM]ESO_4-solubilised substrate viscosity and opacity. SDS PAGE analysis revealed severe smearing for undiluted solubilised hair, while dilutions beyond 1 in 2 were not concentrated enough to exhibit bands (Appendix Figure 4.24).

The solubilised hair substrates were then investigated using NADPH-based and Ellman's assays (Appendix Figure 4.25, Figure 48). The opacity and viscosity of ionic liquid-solubilised hair interfered with absorbance measurements, and no thioredoxin system reducing activity was observed on the centrifuged substrate either (Appendix Figure 4.26). In the case of NaOH-solubilised hair, a clear lack of disulfide bond reducing activity was also observed. This overall lack of disulfide bond reducing activity detected for the thioredoxin system from *Bacillus subtilis* was unsurprising due to significant disulfide bond reduction occurring upon NaOH and [EMIM]ESO_4 solubilisation of human hair.[106,338]

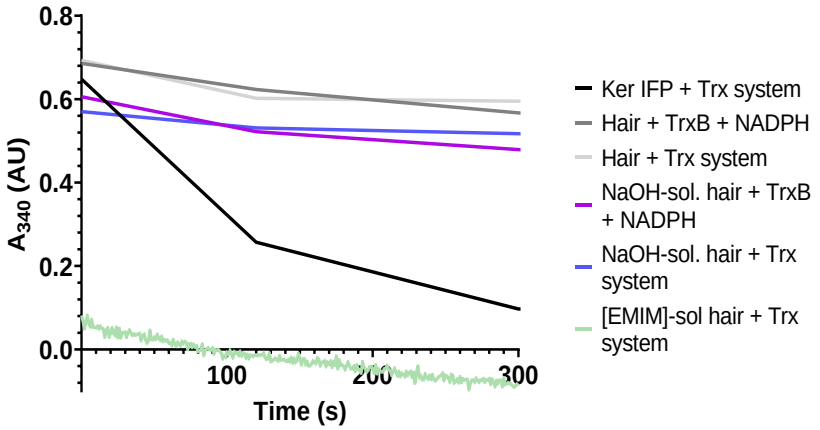

Figure 48. Disulfide bond reduction analysis by the *Bacillus subtilis* thioredoxin system in solubilised hair *via* NADPH consumption monitoring. NaOH and [EMIM]ESO_4 solubilised human hair (0.02 g/mL eq.) was incubated with TrxA (0.70 U/mL, 0.14 mg/mL), TrxB (0.34 mg/mL) and NADPH (0.213 mM) in 0.50 mM Tris-HCl pH 7.5, 1 mM EDTA, up to 1 mL). The decrease in absorbance at 340 nm was then monitored over time for up to one hour at 25 °C.

4.7. Effect of keratinase from *Bacillus licheniformis* on disulfide bond reduction

In an attempt to facilitate the penetration of the thioredoxin system from *Bacillus subtilis* inside the hair cortex as a result of a lack of disulfide bond reducing activity detected on hair as the substrate, keratinase from *Bacillus licheniformis* was investigated for potential hair structure opening *via* keratin peptide bond cleavage (Figure 49).

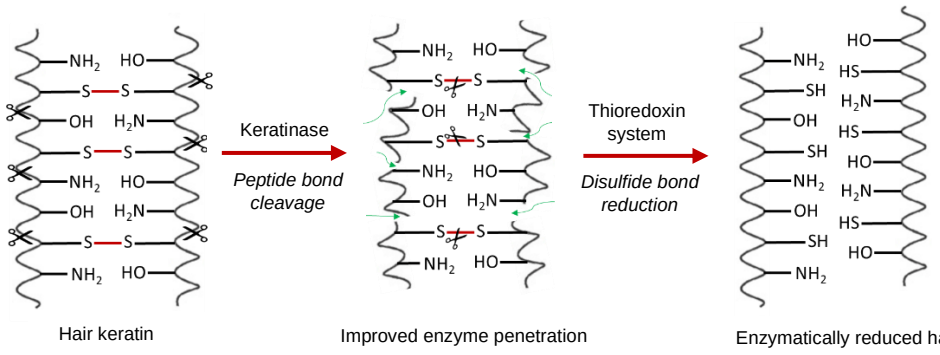

Figure 49. Hypothetical hair structure opening by keratinase for easier thioredoxin system penetration.

4.7.1. Expression attempts of keratinase (KerA) from Bacillus licheniformis

The expression of KerA from *Bacillus licheniformis* was initially attempted in *E. coli*. The codon-optimised *kerA* gene was synthesised by GeneArt and cloned into pMP89b, between *BamHI* and *SacI* restriction sites (Appendix Figure 6 and Appendix Table 3.2). Cloning success was confirmed by agarose gel analysis, PCR and Sanger sequencing (Appendix Figures 4.27-28), following which pMP89b::*kerA* plasmid was transformed into BL21(DE3) *E. coli* strains. Protein expressions were then attempted at a low scale (50 mL, 37 °C, 180 rpm, 4.5-hour incubation), however, no bands were seen on SDS PAGE at around 32 kDa where keratinase would be expected (Appendix Figure 4.29).[31] Several modifications to the expression conditions were investigated in an attempt to express KerA, including lower expression temperatures (30 °C) and varied lysis buffer compositions, with no success (Appendix Figure 4.30).

The *kerA* gene used in this study was synthesised based on the sequence described by Lin *et al.* (1995) comprising the signal peptide, while expression conditions were inspired by work on *kerA* conducted by Hu *et al.* (2013) in the absence of signal peptide (Appendix Figure 4.31).[25,32] In this way, the presence of a signal peptide may have been hindering expression, which has been described in the literature for protein expression in *E. coli*.[134,339,340] It was therefore decided to investigate the activity of the commercial keratinase (KerA) from *Bacillus licheniformis*, supplied by Merck, before any further expression attempts.

4.7.2. Effect of disulfide bond reducing agents on keratinolytic activity

The importance of disulfide bond reduction towards enzymatic keratin degradation has been extensively described in the literature. [22,26,344,345,28,33,128,156,162,341–343] In this way, commercial keratinase from *Bacillus licheniformis* was investigated for keratinolytic activity, both in the presence and absence of DTT, a reducing agent with reported efficiency at yielding high keratinolytic activity.[21,26,98,105,287] The keratin azure assay, involving the monitoring of soluble dye-bound peptides and amino acids released upon peptide bond cleavage (see section 4.2.3.), was used to this end. [292,293]

4.7.2.1. Keratinolytic activity of keratinase

The keratinolytic activity of keratinase from *Bacillus licheniformis* was first investigated over time in the absence of a reducing agent. The enzyme was incubated with keratin azure for up to 72 hours at 37°C, and 595 nm absorbances were recorded throughout (Figure 50). A no-substrate control was investigated, and absorbances at 595 nm remained at 0 over time.

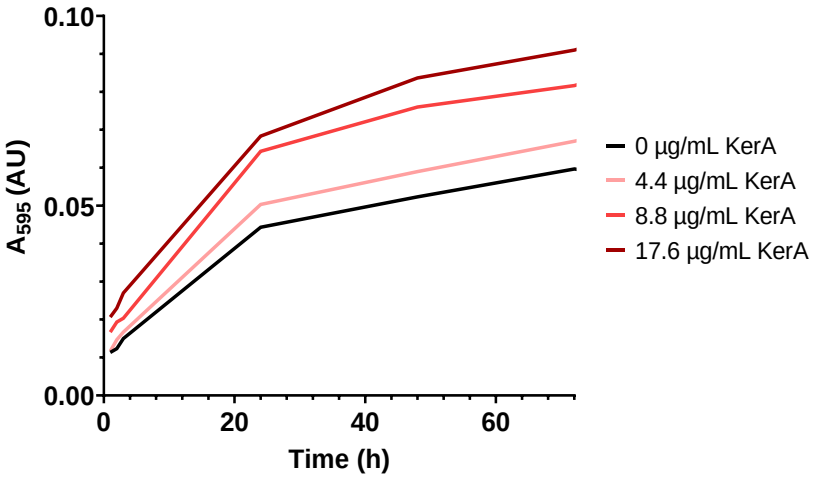

Figure 50. Keratin azure assay of keratinase from *Bacillus licheniformis* over a range of concentrations. Keratin azure (4 mg/mL) was incubated for 72 hours at 37 °C,250 rpm with KerA (1.5-6.2 U/mL, 4.4-17.6 µg/mL) in Tris buffer, pH 8, after which 595 nm absorbances were recorded.

While a slight increase in 595 nm absorbance was observed over time across samples, absorbances remained very low (below 0.10 after 72 hours) compared to what had been reported in the literature.[30,285,346] For example, Navone *et al.* (2018) measured a keratinolytic activity for keratinase from *Bacillus licheniformis* of around 16,000 KU/g of protein, where 1 KU is defined as the amount of keratinase needed to yield an increase of 0.1 in absorbance at 595 nm after 1 hour incubation at 37 °C.[30] This is over 20 times higher than the 780 KU/g of protein calculated from the 0.08 mg/mL keratinase and keratin azure sample from the assay described above (Figure 47) after 1 hour incubation at 37 °C, 250 rpm. However, the authors used *Bacillus licheniformis* fermentation solubles containing KerA rather than the isolated enzyme, which may have led to increased keratinolytic activities.[30]

Replications of this assay yielded comparably low 595 *n*m absorbances with high error bars (Appendix Figure 4.32). As a result, the proteolytic activity of the commercial enzyme was investigated using the supplier's non-specific protease activity assay on casein.[279,347] When proteases digest casein, tyrosine is liberated and reacts with Folin-Ciocalteau reagent, a mixture of phosphomolybdate and phosphotungstate, to produce a blue-coloured chromophore, quantifiable *via* 660 nm absorbance measurements.[279] A standard curve was generated using 0.005-0.050 µmol/mL (0.9-9.0 mg/mL) L-tyrosine to determine the number of micromoles of tyrosine liberated during the reaction and, in this way, calculate keratinase activity (Appendix Figure 4.33). However, very low A_{650nm} values (<0.03) were recorded across all keratinase concentrations assayed, even following enzyme concentration increases and the use of a new enzyme batch, suggesting a lack of casein proteolytic activity (Appendix Figure 4.34.).

A series of controls were then assessed to investigate the constantly low 660 nm absorbances observed using the casein assay (Figure 51). The presence of L-tyrosine in casein was confirmed by 660 nm absorbance values of around 0.2 for samples (a) and (d). TCA successfully precipitated casein (eliminated by filtration), as can be seen with sample (b). The baseline treatment (f) again gave a very low 660 nm absorbance, however, the introduction of keratinase after TCA addition (e) seemed to be associated with higher absorbance. This was repeatedly observed despite keratinase alone not absorbing at 660 nm (c). Since TCA was shown to precipitate casein successfully, it remains unclear what the absorbance observed for sample (e) corresponds to. The supplier was unable to provide further support, and this assay was therefore deemed inconclusive.

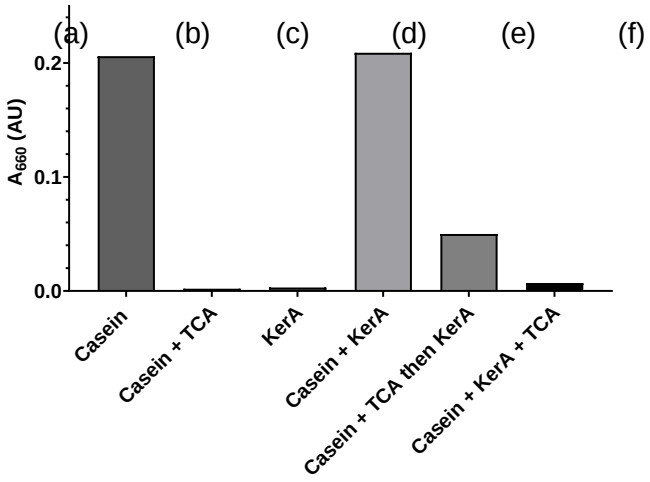

Figure 51. Keratinolytic activity assay of keratinase from *Bacillus licheniformis* on casein. Baseline treatment (f) corresponds to KerA (0.05 U/mL or 0.15 µg/mL) incubated with casein (2.9 mg/mL) for 10 minutes at 37 °C before TCA (8.2 mg/mL) addition. Casein digestion was monitored at 660 nm absorbance. A range of controls (a-e) were included, where volumes were made up using a buffer.

Keratec™ IFP was also attempted as a substrate to detect tyrosine release upon keratinase activity, however, the soluble keratin substrate has a significant proportion of L-tyrosine (see section 4.2.1.) and was therefore

associated with high 660 nm absorbances when untreated (Appendix Figure 4.35).

4.7.2.2. Effect of reducing agents on keratinase activity

The keratinolytic activity of keratinase from *Bacillus licheniformis* was further investigated using the keratin azure assay in the presence of DTT as a reducing agent, which has been associated with increased 595 nm absorbances in the literature.[30,346] The enzyme was therefore incubated with keratin azure and DTT, and 595 nm absorbances were monitored over time (Figure 52). A significant rise in keratinase activity was observed in the presence of DTT, with a six-fold increase in 595 nm absorbance detected. The release of Remazol Brilliant Blue dye was confirmed by the full absorbance spectrum (Appendix Figure 4.36). This was observed over a range of replications (Appendix Figure 4.37). Keratinase samples incubated with DTT were therefore used as a positive control for later experiments.

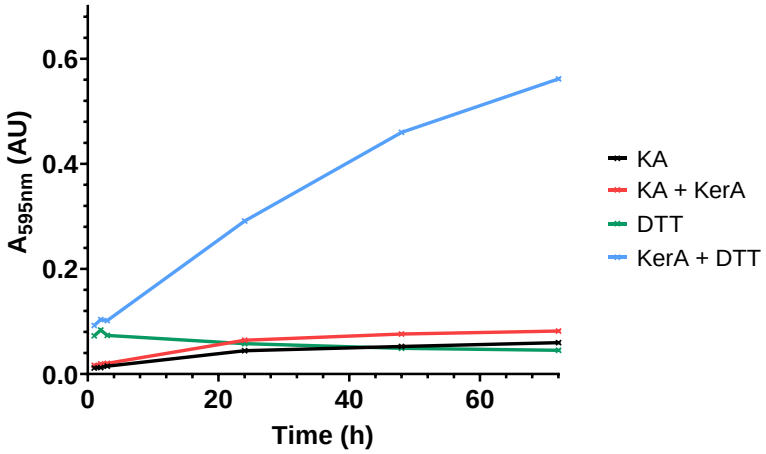

Figure 52. Keratin azure assay of keratinase from *Bacillus licheniformis* in the presence of DTT. Keratin azure (KA, 4 mg/mL) was incubated with KerA (3.1 U/mL, 8.8 µg/mL) and/or DTT (0.13 M) in Tris buffer pH 8 for up to 96 hours at 37 °C, 250 rpm.

The considerable increase in keratinolytic activity observed here upon incubation with a reducing agent is due to DTT's ability to penetrate solid keratin substrates, potentially due to its small size (154 Da), and reduce

disulfide bonds between keratin chains (see section 4.6.1.3). Indeed, the penetration of peptides of up to 2,577 Da in the hair cortex has been reported in the literature.[30,57] Keratin disulfide bond reduction then results in improved keratinase access to proteolytic cleavage sites in the keratin backbone, which the enzyme (32 kDa) may otherwise be too big to access.[346]

In an attempt to move away from DTT, a harmful reducing agent with acute oral toxicity, milder alternatives with known keratin disulfide bond reducing abilities, such as glutathione and cysteine, were explored (Figure 53).[48,59,348–350] Cysteine precipitation was observed in samples, potentially due to its low solubility, preventing any spectrophotometric analyses.

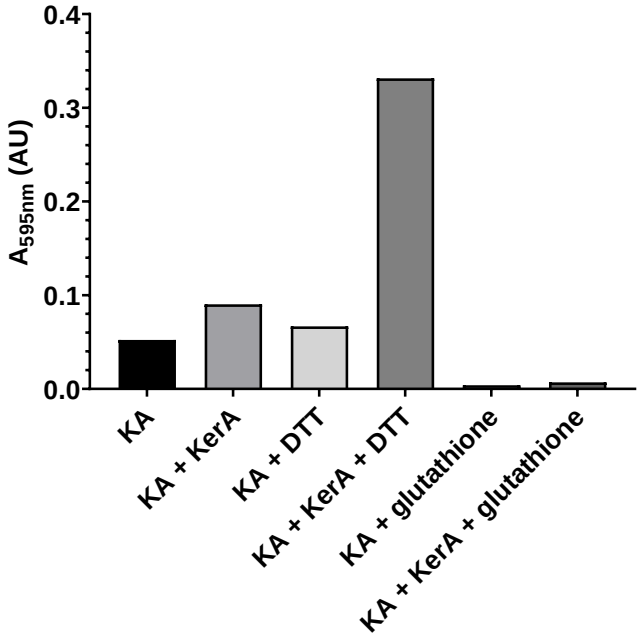

Figure 53. Keratin azure assay of keratinase from *Bacillus licheniformis* exploring DTT, glutathione and cysteine as reducing agents. Keratin azure (KA, 4 mg/mL) incubated with KerA (3.1 U/mL 8.8 µg/mL) and reducing agents (DTT: 0.31 M, glutathione: 0.16 M & cysteine: 0.41 M) in Tris buffer pH 8 for 20 h at 37 °C, 250 rpm - cysteine samples incompatible with absorbance measurements.

Moreover, samples containing glutathione and keratin azure, in the presence and absence of keratinase, showed lower absorbances than the untreated keratin azure control, with a notable decrease in absorbance over time. This phenomenon was observed across replications (Appendix Figure 4.38),

suggesting that glutathione may react with Remazol Brilliant Blue R dye released during incubation. Another dye, methylene blue, is known for turning colourless when reduced to leukomethylene blue, for example, by ascorbic acid.[351] Glutathione may therefore react with RBBR in such a way that the dye turns colourless and cannot be detected at 595 nm anymore. For these reasons, DTT was therefore kept as the reducing agent of choice.

4.7.2.3. Further keratinase activity investigations

The effect of further keratin structure opening, in the form of substrate chopping and fibre swelling, was investigated on *Bacillus licheniformis* keratinase using the keratin azure assay in an attempt to facilitate enzyme penetration for a potential increase in keratinolytic activity. The use of chopped (ground) keratin azure, which has been described in the literature, was investigated as a potential substrate, however, no difference was observed compared to the intact substrate (Appendix Figure 4.39).[285,334,346,352] This could be explained by the fact that, while chopping substrates may facilitate absorbance measurements as a result of increased homogeneity, this process may not lift cuticles or open-up keratin structure.

Keratin azure fibre swelling was also investigated *via* buffer pH increase and urea addition, which was associated with higher 595 nm absorbances across samples and controls alike (Appendix Figure 4.40).[58–62] This may be due to a higher susceptibility of dye-release from keratin azure as a result of fibre swelling.

The effect of increasing incubation temperature from 37 °C to 70 °C was also investigated in an attempt to increase keratinolytic activities observed across keratin azure assays. Abdel-Fattah *et al.* (2018) showed optimal activity for keratinase from *Bacillus licheniformis* at pH 8 and 65 °C.[353] Keratin azure was in this way incubated with keratinase at 37 or 70 °C, and 595 nm

absorbances were recorded over time (Figure 54). Significant amounts of dye release were, however, observed for the 70 °C-incubated samples, even in the absence of keratinase. Comparably high amounts of keratin azure auto-degradation were observed at 70°C across replications (Appendix Figure 4.41), suggesting the incompatibility of this assay at such high temperatures. While the keratin azure assay is usually performed at temperatures of 37 °C and below, it may be that when exposed to significantly higher temperatures, Remazol Brilliant Blue R slowly leaches out of the keratin structure.[30,285,346]

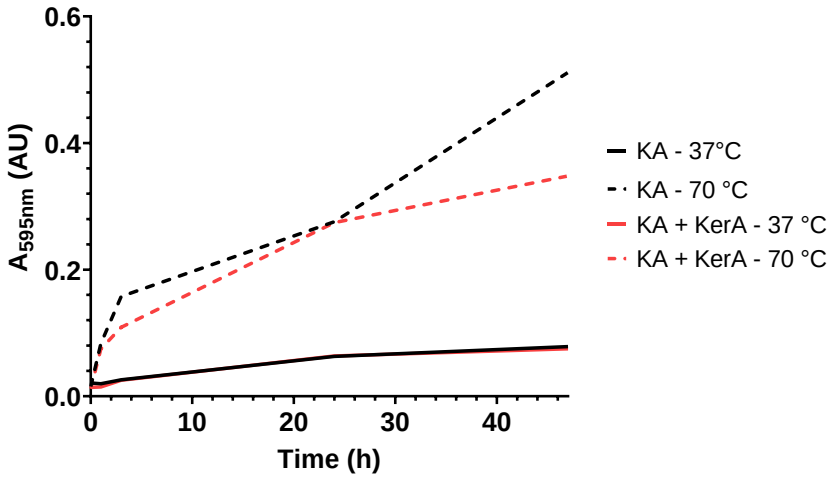

Figure 54. Keratin azure assay exploring the effect of incubation temperature on activity of keratinase from *Bacillus licheniformis*. Keratin azure (KA, 4 mg/mL) was incubated with KerA (3.1 U/mL, 8.8 µg/mL) and DTT (0.31 M) in Tris buffer pH 8 for 47 h at 37-70 °C, 250 rpm.

Further temperature studies were conducted in triplicates, investigating incubation temperatures between 20 and 70 °C (Appendix Figure 4.42). These investigations confirmed keratin azure auto-degradation at 70 °C, and significant variations were observed overall between replications. In this way, the reliability of the keratin azure was questioned due to the leaching of dye observed as well as reproducibility issues associated with the nature of the substrate. A lack of sensitivity and standardisation was indeed reported by

Gupta *et al.* (2006) and Gonzalo *et al.* (2020), who noted limited comparability and reproducibility between studies.[285,354]

4.7.3. Effect of keratinase on keratin disulfide bond reduction

While the effect of disulfide bond reduction by enzymes or other reducing agents on keratinase activity has been extensively reported in the literature, the impact of keratinase on keratin disulfide bond reduction, especially for insoluble keratin (e.g. hair), has not been explored.[22,26,344,345,28,33,128,156,162,341–343] Keratinase from *Bacillus licheniformis* appears to rely on the reduction of keratin disulfide bonds to cleave peptides bonds (Figure 52). It was therefore hypothesised that the cleavage of peptide bonds may, in turn, expose further disulfide bonds for reduction by DTT. This was investigated here using Ellman's assay, where keratinase was incubated with both keratin azure (Figure 55) and hair (Figure 56) in the presence and absence of DTT. The lack of disulfide bond-reducing activity of keratinase from *Bacillus licheniformis*, as suggested by Lin *et al.* (1995), investigated as a control, was confirmed using both keratin azure and hair as substrates (Appendix Figure 4.43).[31]

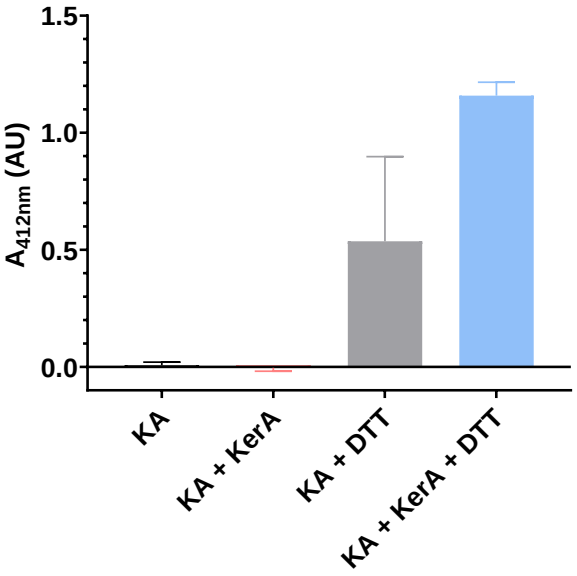

Figure 55. Ellman's assay of keratinase activity on keratin azure in the presence of DTT. Keratin azure (KA, 4 mg/mL) was incubated with KerA (1.5 U/mL, 4.4 µg/mL) and DTT (49.7 mg/mL, 0.31 M) in Ellman's buffer for 24 hours at 37 °C, 250 rpm, followed by 5 buffer rinsings and 30 min incubation with DTNB (0.08 mg/mL or 0.20 µM) and 412 nm absorbance measurements -- data given as average values of triplicate reactions (sample-final was final wash subtracted from sample absorbance h) and shown ± the standard deviation.

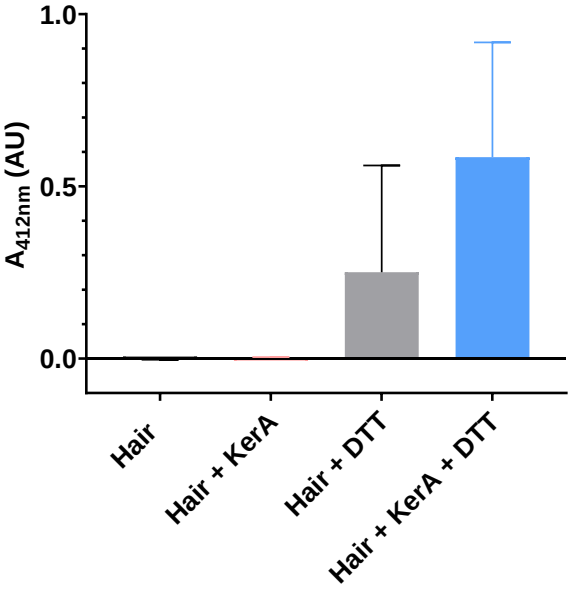

Figure 56. Ellman's assay of keratinase activity on human hair in the presence of DTT. Hair (8 mg/mL) was incubated with KerA (1.5 U/mL, 4.4 µg/mL) and DTT (49.7 mg/mL, 0.31 M) in Ellman's buffer for 1 hour at 37 °C, 250 rpm, followed by five buffer rinsings and 30 min incubation with DTNB (0.08 mg/mL or 0.20 µM) and 412 nm absorbance measurements - data given as average values of triplicate reactions (final wash subtracted from sample absorbance) and shown ± the standard deviation.

In the case of both solid keratin substrates, the presence of keratinase, and therefore the potential concomitant peptide bond cleavage, was associated

with higher disulfide bond reduction than when DTT alone was incubated with substrates. Absorbance spectra were taken following incubation with DTNB and confirmed the formation of a 412 nm peak for the sample containing keratin azure, DTT and keratinase (Appendix Figure 4.44). While these observations suggest that the keratinase-catalysed cleavage of peptide bonds may reveal more disulfide bonds for DTT to reduce, significant variations can be seen across replications. The potential adsorption of TNB^{2-} to solid keratin fibres during Ellman's assay, which was developed for the determination of thiol release in solution, may be preventing precise spectrophotometric thiol quantification.[321]

The impact of keratin azure fibre swelling through increased buffer pH and urea addition, which was investigated with the aim of facilitating keratinase penetration of keratin fibres and, as a result, potentially increasing levels of disulfide bond reduction, showed no effect. The impact of keratinase on solid keratin disulfide bond reduction by reducing agents beyond DTT were also explored, including cysteine, thioglycolic acid, glutathione and TCEP. As previously observed, cysteine was associated with the formation of insoluble particles hindering absorbance measurements, while thioglycolic acid was not rinsed from the substrate easily and therefore interfered with Ellman's assay. In the case of both hair and keratin azure as substrates, the highest keratinase impact on reducing agent disulfide bond reducing activity was observed using DTT, similar to what was reported in the literature (Figure 57a-b).[21,26,98,105,287] Relatively high absorbance variations were again observed across replications.

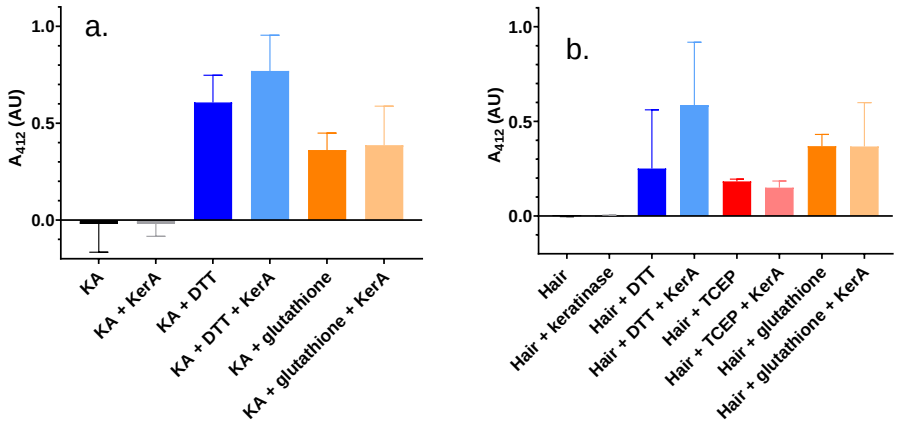

Figure 57 - Ellman's assay on keratin azure (a) or hair (b) with keratinase and reducing agents. Incubation of keratin azure (KA, 8 mg/mL) or hair (8 mg/mL) with KerA (1.5 U/mL, 4.4 µg/mL) and reducing agents (DTT: 0.31 M, glutathione: 0.16 M, cysteine: 0.41 and TGA: 0.54 M) for 1 hour at 37 °C, 250 rpm, followed by five buffer rinsings and 30 min incubation with DTNB (0.20 µM) and 412 nm absorbance measurements - data given as average values of triplicate reactions (final wash subtracted from sample absorbance) and shown ± the standard

Overall, while the addition of *Bacillus licheniformis* keratinase seemed to be associated with slightly increased keratin disulfide bond reduction by DTT, these observations were not statistically significant due to high absorbance variations across replications.

4.7.4. Effects of combining Bacillus subtilis thioredoxin system and Bacillus licheniformis keratinase

Following investigations of the effect of keratinase-catalysed peptide bond hydrolysis on solid keratin disulfide bond reduction by DTT, the impact of keratinase on the *Bacillus* subtilis thioredoxin system was explored here. In the absence of enzymatic disulfide bond reduction observed using solid keratin substrates (see section 4.6.3.), despite attempts to open up keratin structure, it was hypothesised that peptide bond cleavage might allow the penetration of thioredoxin into the solid keratin substrate, making disulfide bonds more accessible to the enzyme. However, the penetration of small reducing agents like DTT into the hair cortex and subsequent disulfide bond reduction has been shown in this study to be necessary for keratinase activity (see section 4.7.2.2.). Due to the sizes of both thioredoxin from *Bacillus*

subtilis (11.4 kDa) and keratinase from *Bacillus licheniformis*, a lack of penetration into the hair cortex and, altogether, an absence of solid keratin disulfide bond reduction was expected.

NADPH consumption was, in this way, monitored towards the potential disulfide bond reduction of solid hair by thioredoxin from *Bacillus subtilis*, where the substrate was pre-incubated with keratinase from *Bacillus licheniformis* (Figure 58). A clear lack of enzymatic disulfide bond-reducing activity was observed, suggesting that the thioredoxin system was not able to reach the hair cortex. The lack of effect of keratinase-catalysed peptide bond hydrolysis may, however, be associated with the inability of keratinase as well to penetrate the substrate, as keratinolytic activity was previously detected only in the presence of DTT. The pre-incubation of human hair with keratinase in the presence of DTT (followed by substrate rinsing), as well as the simultaneous incubations of the thioredoxin system and keratinase with solid keratin substrates may be explored, however, a lack of enzymatic activity as a result of substrate penetration issues is expected.

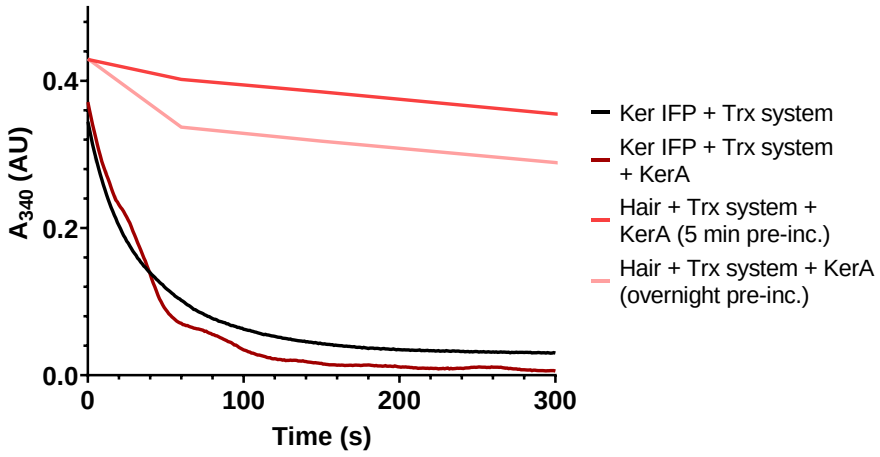

Figure 58. Analysis of the effect of *Bacillus licheniformis* keratinase on disulfide bond reducing activity of the *Bacillus subtilis* thioredoxin system on solid human hair. Hair (0.02 g/mL) was pre-incubated with KerA (0.75 U/mL 2.2 µg/mL) for 5 minutes or overnight at 37 °C, 250 rpm. Pre-treated hair was then rinsed and incubated with TrxA (0.70 U/mL, 0.14 mg/mL), TrxB (0.34 mg/m) and NADPH (0.100 mM) were added to 0.50 mM Tris-HCl pH 7.5, 1 mM EDTA, up to 1 mL. The decrease in absorbance at 340 nm was then monitored at

regular intervals for up to one hour at 25 °C, by pipette the sample supernatant into the quartz cuvette prior to every measurements.

4.8. Alternative enzymatic keratin disulfide bond reduction

Cysteinyl glycine, a strong reducing agent able to reduce disulfide bonds in feather keratin, was also investigated in the context of evaluating the potential of γ-glutamyl transpeptidases for enzymatic keratin disulfide bond reduction.[22,156,162] Indeed, γ-glutamyl transpeptidase from *Bacillus subtilis* has been shown to provide reducing activities for keratin decomposition by the relative protease.[162] However, cysteinyl glycine exhibited very low levels of disulfide bond reduction in hair (Appendix Figure 4.45). Increased concentrations were investigated but were seen to interfere with Ellman's assay due to incomplete removal before DTNB addition. The potential exploration of γ-glutamyl transpeptidases for disulfide bond reduction in human hair was therefore not investigated any further.

5. Enzymatic crosslinking of keratin

5.1. Background

The permanent setting of natural macromolecules for the modification of appearance and performance properties has been a topic of growing interest, for example, in the textile (e.g. cotton, silk, wool etc.) and cosmetic (e.g. hair) industries.[217] While preliminary disulfide bond reduction may be necessary in highly-crosslinked proteins, the formation of crosslinks allows for the permanent setting of any mechanically-induced morphology.[59] In the context of hair straightening, the reformation of disulfide bonds (e.g. hydrogen peroxide) or alternative crosslinking (e.g. formaldehyde) between keratin chains allows for the permanent setting of straightened hair while restoring mechanical robustness of the hair fibres.[59,218–220] With the aim of moving away from harsh chemicals typically used, greener alternatives towards hair keratin crosslinking have been developed, relying on milder active agents such as oxidised sugar, citric acid and cysteine-containing keratin peptides.[48,63,355] These methods involve the formation of crosslinks between the active agent and the hair keratin, rather than substrate keratin-keratin bonds, and are associated with inferior hair setting effects compared to current available treatments. The development of biotechnologically-derived active agents in cosmetic formulations thus offers a range of new possibilities towards milder crosslinking methods.[93]

This chapter explores the potential of isolated enzymes as mild and biocompatible crosslinking agents in the context of permanent hair straightening.[30,94] Enzymes have evolved over time to catalyse covalent modifications in proteins, involved in essential processes such as fibrin crosslinking towards blood coagulation. [35,221–223] In this way, a range of protein crosslinking enzymes have been identified and characterised, and

are currently used in numerous industries (e.g. dairy and textile industries).[35–37] The focus was here placed on well-characterised enzymes with relatively low substrate specificity, known activity on folded proteins with the ability to catalyse the formation of intermolecular bonds in the absence of toxic by-products. While the reformation of disulfide bonds, following their reduction in the first step of permanent hair straightening, appeared like a logical pathway, enzymes operating *via* a thiol-related mechanism such as lanthionine synthetase and cystathione-β-synthase were rapidly disregarded due to their highly site-specific mechanisms, potential need for cofactors as well as lack of activity on folded proteins and concurrent release of hydrogen peroxide.[268,270–274] Sulfhydryl oxidases, which catalyse the oxidation of free sulfhydryl groups to disulfides in proteins were also not considered due to a lack of activity reported for folded proteins as well as associated hydrogen peroxide release as by-product.[200,267,268] The potential for protein crosslinking in the context of permanent hair straightening is, however, not limited to thiol-thiol interactions, and the formation of crosslinks beyond disulfides may actually result in improved fibre strength.[48,59,88,91,108]

In this way, commercially available-transglutaminases, laccases and tyrosinases were selected as candidates for keratin-keratin crosslinking investigations. Transglutaminases catalyse the crosslinking of glutamine and lysine protein side chains *via* a proteinyl-enzyme-thioester intermediate, while laccases and tyrosinases react with tyrosine side chains, amongst others, in proteins to generate radical and diphenol reactive species, respectively, which may then undergo successive protein crosslinking.[34,35,224,235,236,244,245] Improved substrate compatibility has been described for laccases through the use of mediators, small compounds acting as “electron-shuttles”, which can help overcome redox or steric

barriers.[237,242,243] Transglutaminases, laccases and tyrosinases are currently being used in a range of industries (e.g. food, wool, dairy etc.) and have exhibited activities for a range of proteins, including β-casein, gelatine, as well as keratin (specifically wool).[35–40] Indeed, laccases and tyrosinases have been shown to crosslink low-molecular weight keratins, polysaccharides, as well as elastin and collagen to wool fibres, associated with increased tensile strength and performance, as well as human hair.[72,260,265,266] Laccases were also shown to successfully graft tyrosine amino acids to human hair.[261,262] The formation of substrate keratin-keratin crosslinks has, however, not been described for laccases or tyrosinases, while transglutaminases were shown to form crosslinks within protease/reducing agent-pre-treated wool keratin (soluble and solid).[40,107,231] To the best of our knowledge, the formation of keratin-keratin crosslinks in human hair has, to this day, not been investigated enzymatically.

Commercial enzymes, including laccase form *Trametes versicolor*, tyrosinase from mushroom and microbial transglutaminase, are investigated here. Solubilised wool is used as a substrate aimed at overcoming potential enzyme penetration barriers associated with insoluble hair keratin. Enzymatic crosslinking activity on soluble keratin is investigated using a range of assays, including SDS PAGE and SEC. Promising enzymatic treatments are then assessed using solid hair as the substrate, *via* tensile strength measurements.[39,108,356–360] The potential need for preliminary keratin treatment prior to enzymatic crosslinking, as suggested in the literature, is considered.[40,107,231]

5.2. Enzyme activities with standard substrates

The standard activities of laccase from *Trametes versicolor*, tyrosinase from mushroom and microbial transglutaminase on ABTS, L-DOPA and Cbz-gln-gly, respectively, were independently investigated.[244,282,361] The impact of Keratec™ IFP and Keratec™ ProSina (solubilised wool) on crosslinking enzymes was also investigated, aimed at detecting any potential inhibiting effects associated with their use as substrates.

5.2.1. Laccase ABTS assay

The activity of laccase from *Trametes versicolor* was determined spectrophometrically based on its capacity to oxidise ABTS, as previously reported in the literature.[244,280] ABTS oxidation results in the formation of a dark green cationic radical $ABTS^{\cdot+}$ (Figure 19), which can be detected *via* absorbance measurements at 405 nm. Following the oxidation of four ABTS molecules, the fully reduced laccase copper cluster then binds molecular oxygen, resulting in the release of two water molecules and an oxidised enzyme.[236,241,280]

Laccase was incubated in acetate buffer pH 5 at 25 °C and 405 nm absorbance was monitored over time upon ABTS addition (Figure 59). No ABTS oxidation was detected in the absence of laccase, as expected. Using the Beer-Lambert law, the increase in 405 nm absorbance observed in the presence of the enzyme was converted to specific activity in units per mg, where one unit was defined as 1 µmol of ABTS oxidised per minute. The specific activity was calculated as 3.11 U/mg in acetate buffer at pH 5 at 25 °C.

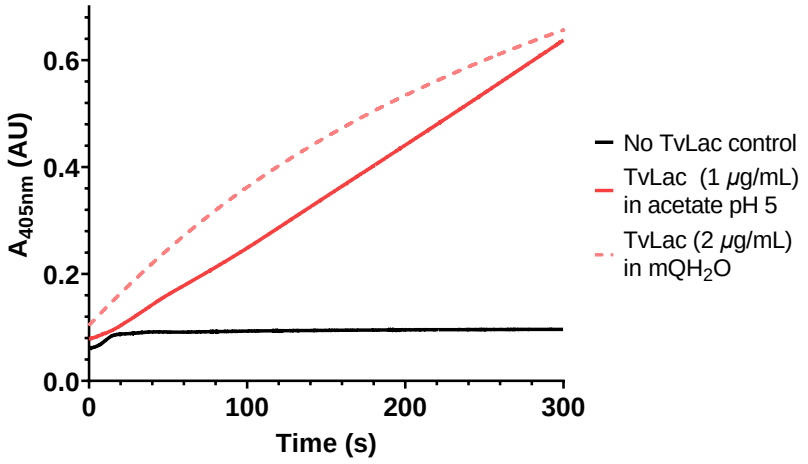

Figure 59. Activity analysis of laccase from *Trametes versicolor via* ABTS oxidation monitoring. TvLac (3.41-68.2 mU/mL, 1-20 µg/mL) was incubated with ABTS (1 mM) in acetate buffer pH 5 or deionised water at 25 °C and 405 nm absorbance monitored over time.

Keratec™ IFP precipitation was detected in acetate buffer at pH 5. Deionised water was therefore evaluated as a suitable medium for laccase-keratin crosslinking experiments to follow. A 2-fold decrease in laccase activity was observed in deionised water compared to acetate buffer pH 5 (similar absorbances detected for 2x enzyme concentration), with a slight decrease in rate observed after 2-minute-reaction time. This was expected, due to a change in pH away from the enzyme's optimal pH (5) towards neutral pH, resulting in shifts in the enzyme's ionic interactions and shape, associated with reduced activity.[318]

5.2.1.1. Effects of solubilised keratin substrates on laccase activity

The effects of soluble wool keratin substrates on laccase activity were then investigated to check compatibility with laccase keratin crosslinking assays (Figure 60). Indeed, the presence of 2-phenoxyethanol, salts or differences in pH associated with Keratec™ substrates may have an impact on enzymatic activities. The addition of Keratec™ IFP led to a complete loss in laccase-catalysed ABTS oxidation. Following a 10-fold increase in enzyme concentration, some ABTS oxidation was observed over-time, but activity

remained low. Similar patterns were observed in the presence of Keratec™ ProSina, to a slightly lesser extent.

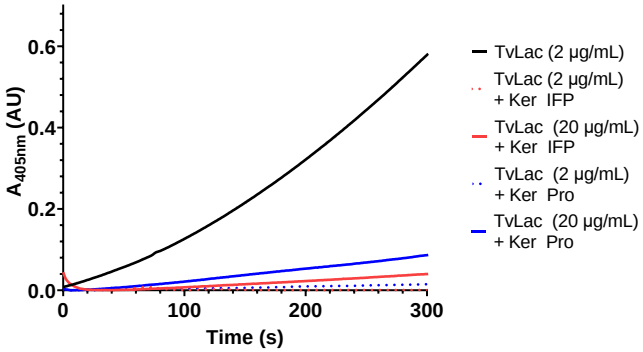

Figure 60. Effect of Keratec™ substrates on laccase-catalysed ABTS oxidation. TvLac (6.82-68.2 mU/mL, 2-20 µg/mL) was incubated with ABTS (1 mM) and Keratec™ IFP (Ker IFP, 13 mg/mL) or Keratec™ ProSina (Ker Pro, 9.4 mg/mL) in dH_2O at 25 °C and 405 nm absorbance monitored over time (t=0 405 nm absorbances associated with Keratec™ substrates subtracted).

Overall, the presence of Keratec™ IFP and Keratec™ ProSina clearly interfered with the monitoring of laccase-catalysed $ABTS^{\cdot+}$ release. At this point, a few hypotheses were formulated, including the potential enzyme inhibition by 2-phenoxyethanol or the possibility of ABTS acting as mediator and getting reduced by the keratin substrate (see section 1.5.3., Figure 19), thus inhibiting the colorimetric detection of $ABTS^{\cdot+}$.[244] The high salt-content in both Keratec™ IFP and Keratec™ ProSina may also have impacted laccase activity, by inhibiting the reduction of oxygen to water at the Type 2/3 copper sites, causing a break in electron acceptance, as suggested in the literature.[253,254]

Information is limited regarding the exact composition of Keratec™ substrates, yet it is known that 2-phenoxyethanol is used as a preservative (as indicated by Croda International). 2-phenoxyethanol was therefore investigated *via* the ABTS assay and did not hinder laccase activity (Appendix Figure 5.1).

5.2.1.2. Effects of dialysed Keratec™ substrates on laccase activity

Aimed at lowering potential enzyme inhibition by Keratec™ substrates during crosslinking, additives and salts were removed by dialysis in deionised water using a 3 kDa MWCO membrane. During the dialysis step, substrates were diluted, as shown in Table 7, measured as volume changes. Across this study, the concentrations indicated for both dialysed and undialysed Keratec™ substrates are based on concentrations indicated here (Table 7).

Table 7. Effect of dialysis on Keratec™ substrate concentrations (calculated as a result of volume changes pre- and post-dilution).

	Keratec™ IFP	**Keratec™ ProSina**
Protein/peptide content (Croda Int.) – undialysed substrate	65.0 mg/mL	47.1 mg/mL
Protein/peptide content (Croda Int.) – dialysed substrate	22.1 mg/mL	14.6 mg/mL

The effect of dialysed Keratec™ substrates on laccase from *Trametes versicolor* activity was then investigated *via* ABTS oxidation monitoring (Figure 61). The impact of Keratec™ substrates on laccase activity was lowered with dialysis beyond what would be expected accounting for substrate dilution. This suggests that the presence of salts in Keratec™ substrates, which were removed, at least partly with dialysis, may have been hindering laccase activity. Indeed, the high viscosity of these Keratec™ substrates may have prevented complete salt removal by dialysis.

While marginally lower dialysed Keratec™ ProSina concentrations were used in the assay, the slightly higher levels of ABTS oxidation observed compared to dialysed Keratec™ IFP may have been associated with pH differences between the two substrates (7.9 and 5.5 for undialysed Keratec™ IFP and ProSina, respectively), which may not have been fully equilibrated upon dialysis due to high viscosity. Nonetheless, dialysed Keratec™ IFP and

Keratec™ ProSina were deemed compatible with laccase keratin crosslinking assays.

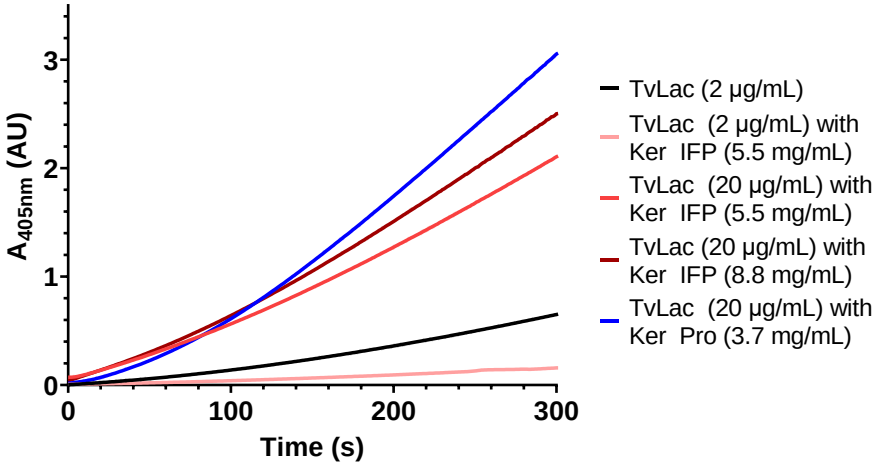

Figure 61. Effect of dialysed Keratec™ substrates on laccase-catalysed ABTS oxidation. TvLac (6.82-68.2 mU/mL, 2-20 µg/mL) was incubated with ABTS (1 mM) and Keratec™ IFP (Ker IFP, 5.5-8.8 mg/mL) or Keratec™ ProSina (Ker Pro, 3.7 mg/mL) in dH_2O at 25 °C and 405 nm absorbance monitored over time (t=0 405 nm absorbances associated with Keratec™ substrates subtracted).

5.2.1.3. Further ABTS laccase activity work

The thermal inactivation of laccase was investigated for potential use of the heat-inactivated enzyme as a negative control in later assays (Figure 62). Laccase incubation at 100 °C for 15 minutes led to a complete loss of activity in the absence of $ABTS^{\cdot+}$ detection.[362]

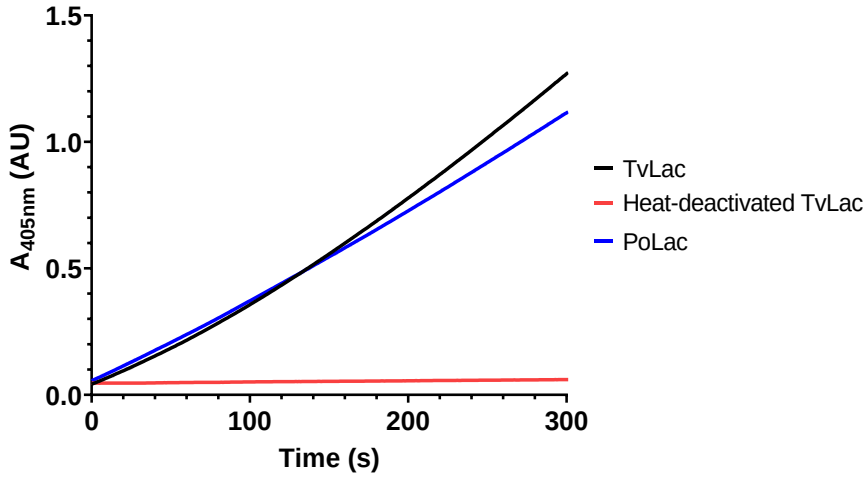

Figure 62. f. TvLac (6.82 mU/mL, 2 µg/mL, pre-incubated at 100 °C for 15 min or not) or PoLac (5.88 mU/mL, 2 µg/mL) was incubated with ABTS (1 mM) in dH_2O at 25 °C and 405 nm absorbance monitored over time.

Laccase from another white-rot fungus, *Pleurotus ostreatus*, was also investigated for comparison, due to the enzyme's potentially higher enzymatic activity reported in the literature compared to laccase from *Trametes versicolor*.[363–365] Both *Trametes versicolor* and *Pleurotus ostreatus* laccases exhibited similar ABTS oxidation rates, with a marginally lower activity for the latter (Figure 62). Using the Beer-Lambert law, a specific activity of 2.94 U/mg in deionised water at 25 °C was calculated for laccase from *Pleurotus ostreatus*, compared to 3.11 U/mg for laccase from *Trametes versicolor*. Work was therefore pursued focusing on laccase from *Trametes versicolor*.

5.2.2. Tyrosinase L-DOPA assay

The activity of tyrosinase from mushroom was evaluated as previously reported, by monitoring the formation of dopachrome over time *via* 475 nm absorbance.[281] Tyrosinase catalyses the oxidation of tyrosine to L-DOPA and that of L-DOPA into dopaquinone. This assay focuses on the latter oxidation, where dopaquinone rapidly autoxidises into dopachrome, which can be detected at 475 nm (Figure 63). The presence of molecular oxygen allows for the regeneration of the oxidised enzyme.[366]

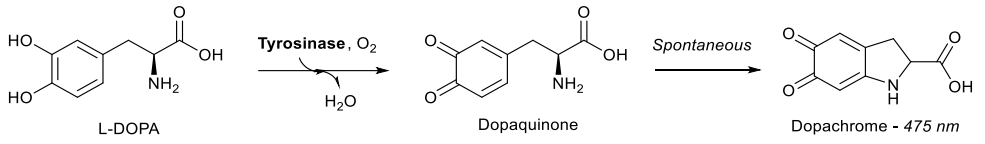

Figure 63. Tyrosinase-catalysed conversion of L-DOPA to dopaquinone and dopachrome, which can be detected *via* 475 nm absorbance measurements.

Tyrosinase was incubated in Tris buffer pH 7 at 25 °C and 475 nm absorbance was monitored over time upon L-DOPA addition (Figure 64a). No dopachrome formation was detected in the absence of tyrosinase, as expected. Using the Beer-Lambert law, the increase in 475 nm absorbance recorded in the presence of the enzyme was converted to specific activity in

units per mg, where one unit was defined as 1 µmol of L-DOPA oxidised per minute. A specific activity of 10.93 U/mg was calculated for tyrosinase from mushroom, in Tris buffer pH 7 at 25 °C.

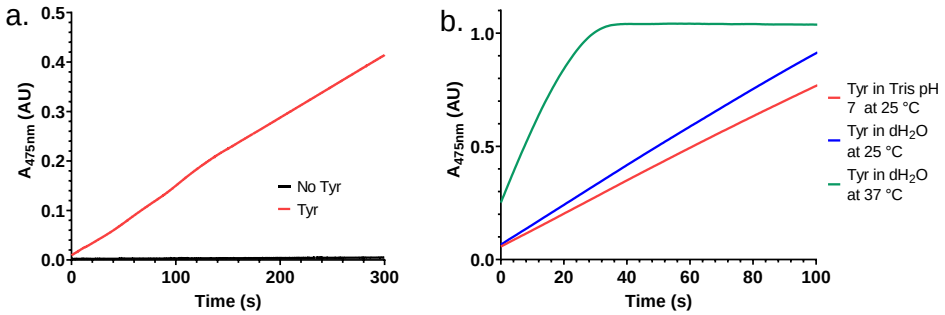

Figure 64. Activity analysis of tyrosinase from mushroom *via* dopachrome formation monitoring. a. Tyrosinase-catalysed L-DOPA oxidation monitoring, Incubation of Tyr (21.86 mU/mL, 2 µg/mL) with L-DOPA (1 mM) in 100 mM Tris buffer, pH 7 at 25°C. b. Investigation of the effect of temperature and buffer on tyrosinase activity, incubation of tyrosinase (0.22 U/mL, 20 µg/mL) with L-DOPA (1 mM) in 100 mM Tris buffer, pH 7 or dH_2O at 25 °C or 37 °C. 475 nm absorbances were monitored over time.

Comparable rates of tyrosinase-catalysed L-DOPA oxidation and subsequent dopachrome released were observed in deionised water compared to Tris buffer pH 7 (Figure 64b). An increase in tyrosinase activity was observed upon raising the incubation temperature from 25 °C to 37 °C, in accordance with what has been noted in the literature (Figure 64b).[264,367] The effect of Keratec™ IFP on tyrosinase activity was also investigated to check compatibility with tyrosinase keratin crosslinking assays. Tyrosinase was incubated with L-DOPA in the presence of both undialysed and dialysed substrates (Figure 65). The addition of undialysed Keratec™ IFP led to a significant reduction in dopachrome release, similar to observations made with laccase. The high-salt content in Keratec™ IFP may again be inhibiting the reduction of oxygen to water at the tyrosinase active site.[368,369] In this way, the presence of Keratec™ IFP upon dialysis had minimal impact on tyrosinase-catalysed L-DOPA oxidation into dopachrome, once again confirming the earlier hypothesis of high salt contents in Keratec™ IFP hindering enzymatic activities.

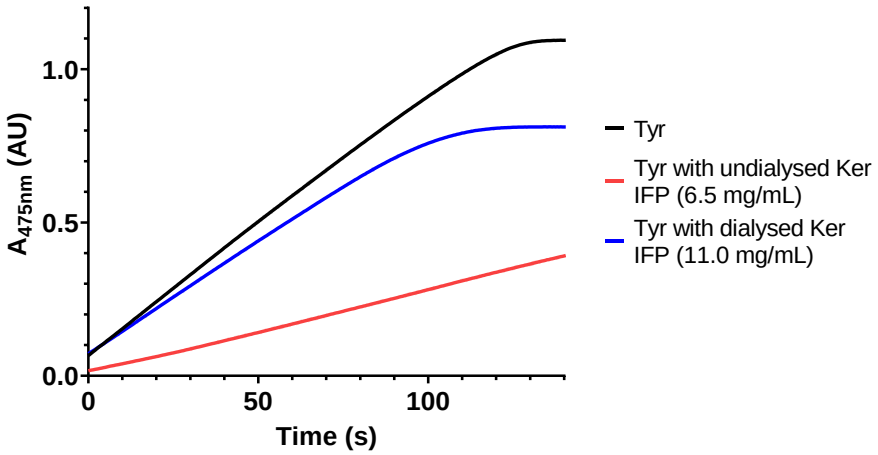

Figure 65. Effect of undialysed and dialysed Keratec™ IFP on tyrosinase activity on L-DOPA. Tyr (0.22 U/mL, 20 µg/mL)) was incubated with L-DOPA (1 mM) and undialysed Keratec™ IFP (Ker IFP, 6.5 mg/mL) or dialysed Keratec™ IFP (Ker IFP, 11.0 mg/mL) in dH_2O at 25 °C and 475 nm absorbance were monitored over time (t=0 475 nm absorbances associated with Keratec™ substrates subtracted).

In this way, dialysed Keratec™ IFP was deemed compatible with tyrosinase keratin crosslinking assays.

5.2.3. Transglutaminase Cbz-Gln-Gly assay

The activity of microbial transglutaminase was monitored *via* the Cbz-Gln-Gly assay, previously reported in the literature.[282] This assay allows for the monitoring of Cbz-Gln-Gly-hydroxamate formation *via* absorbance measurements at 525 nm. Indeed, transglutaminase catalyses the formation of an isopeptide bond between Cbz-Gln-Gly and hydroxylamine, resulting in the release of Cbz-Gln-Gly-hydroxamate (Figure 66).[360]

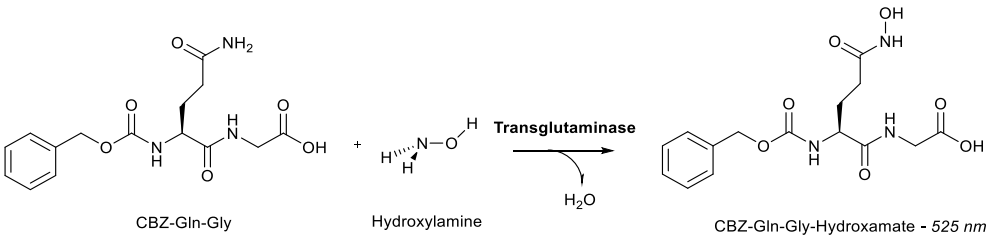

Figure 66. Transglutaminase-catalysed formation of Cbz-Gln-Gly-hydroxamate from Cbz-Gln-Gly and hydroxylamine.

Transglutaminase was incubated with CBZ-gln-gly, hydroxylamine, reduced glutathione and calcium chloride in Tris buffer pH 6 at 37 °C and formation of Cbz-Gln-Gly-hydroxamate was measured at 525 nm (Figure 67). No Cbz-Gln-Gly-hydroxamate formation was detected in the absence of

transglutaminase, as expected. The specific activity observed for transglutaminase was then calculated in units per mg from a standard curve, where one unit was defined as catalysing the formation of 1 µmol of hydroxamate per minute at pH 6 at 37 °C. A specific activity of 14.11 U/mg was obtained in Tris buffer at pH 6 at 37 °C.

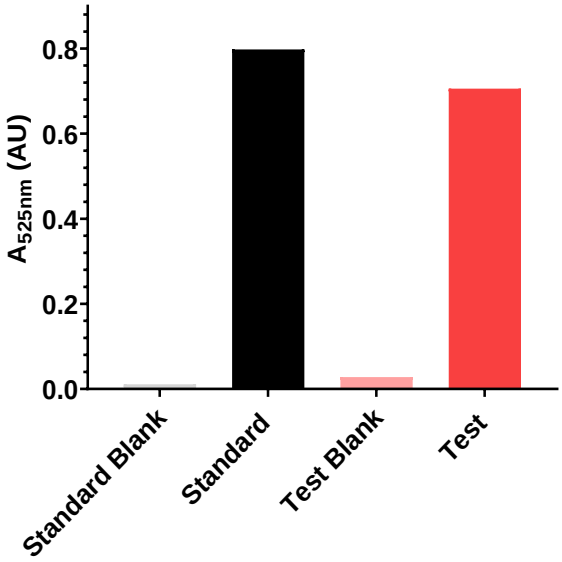

Figure 67. Activity analysis of microbial transglutaminase *via* Cbz-Gln-Gly assay. Test was composed of Tg (0.097 U/mL, 6.86 µg/mL), Cbz-Gln-Gly (31 mM), hydroxylamine (87 mM), reduced glutathione (8.7 mM) and calcium chloride (4 mM) in Tris buffer pH6 and deionised water, at pH 6, 37 °C (test blank without transglutaminase). Standard was made from L-Glutamic Acid γ-monohydroxamate (1mM) in deionised water (standard blank without L-Glutamic Acid γ-monohydroxamate). Absorbances were recorded at 525 nm.

The effect of dialysed Keratec™ IFP on transglutaminase activity was also investigated, with no hindrance observed towards Cbz-Gln-Gly-hydroxamate formation (Appendix Figure 5.2). This confirms the compatibility of the dialysed substrate with transglutaminase keratin crosslinking assays.

5.3. Crosslinking of soluble keratin substrates by laccase, tyrosinase and transglutaminase

Standard activities were confirmed for laccases from *Trametes versicolor* and *Pleurotus ostreatus*, mushroom tyrosinase and microbial transglutaminase. These enzymes were then further investigated using a range of protein substrates, including casein, Keratec™ IFP and Keratec™

ProSina, across different protein crosslinking assays. This was done in order to identify adequate methods for the potential detection of enzymatic keratin crosslinking.

5.3.1. Preliminary protein crosslinking assays

5.3.1.1. Turbidity assay for enzymatic crosslinking of casein

Turbidity was initially investigated as a potential marker for protein crosslinking by laccase, tyrosinase and transglutaminase based on a method suggested by Puri *et al.* (2021).[356] β-casein generally exists in its monomeric form but the formation of micelle-type structures has been observed at increased temperatures (>25 °C), resulting in high turbidity.[370,371] Puri *et al.* (2021) investigated the crosslinking of β-casein by microbial transglutaminase (mTG). The authors observed a loss of β-casein monomers' ability to form micelles upon crosslinking with mTG, due to a decreased lysine residue availability.[356] Crosslinked β-casein monomers, therefore, exhibited modified secondary structure and molecular mobility, preventing reassociation with casein micellar phase or self-association into micelles. In this way, crosslinked β-casein lost its ability to form aggregates and therefore was not associated with turbidity development upon temperature increase. Turbidity development, or lack thereof, was therefore investigated *via* 600 nm absorbance as a measure for casein crosslinking in the presence of laccase, tyrosinase or transglutaminase. Of particular relevance to the crosslinking activities of laccase, tyrosinase and transglutaminase, β-casein is composed of 1.9% tyrosine, 0.5% tryptophan, 0% cysteine, 9.1% glutamine and 5.3% lysine.[372] Laccases and tyrosinases, which are known to oxidise tyrosine (and in some cases tryptophan and cysteine), side chains in proteins were therefore expected to be associated

with lower β-casein crosslinking activity compared to transglutaminase, known to crosslink glutamine and lysine side chains.[34,35,224,227,235]

A casein solution was incubated at a range of temperatures for 30 minutes and showed the highest turbidity increase at 55 °C (Appendix Table 5.1). In this way, laccase, tyrosinase and transglutaminase were respectively incubated in casein solution for 2 hours at 55°C. No decrease in casein turbidity was observed in the presence of tyrosinase, laccase and transglutaminase (Table 8), suggesting a lack of β-casein crosslinking. This lack of enzymatic crosslinking observed may be a result of a mix of α_{s1}casein, α_{s2}casein, β-casein and κ-casein, which have different aggregation behaviours, used as the substrate instead of solely β-casein.[356] This turbidity assay for crosslinking analysis was not investigated further.

Table 8. Enzymatic β-casein crosslinking monitoring *via* 660 nm absorbance. TvLac (68.2 mU/mL, 20 µg/mL), Tyr (21.86 mU/mL, 20 µg/mL) or Tg (0.015 U/mL, 1.05 µg/mL) was incubated with casein (6 mg/mL) in potassium phosphate buffer pH 7.5 at 55 °C for 2 hours, before 600 nm absorbance measurements.

Sample	*600 nm absorbance*
Casein-only control	2.326
Laccase + casein	2.260
Tyrosinase + casein	2.368
Transglutaminase + casein	2.228

5.3.1.2. SDS PAGE assay for enzymatic crosslinking of gelatine

SDS PAGE analysis has been commonly used in the literature for crosslinking analysis.[38,39,107,356–358] Laccase, tyrosinase and transglutaminase were loaded on an SDS PAGE gel as no-substrate controls for later crosslinking analyses (Appendix Figure 5.3). All bands were faint compared to Keratec™ substrates, hence would not interfere with the analysis.

Gelatine was first assessed as a substrate for enzymatic crosslinking in an attempt to replicate work conducted by Jus *et al.* (2012) with a range of enzymes, including laccase from *Trametes versicolor*.[39] The authors reported <50 kDa band disappearance upon gelatine crosslinking using SDS PAGE, associated with an increased molecular weight of the crosslinked substrate. Laccase from *Trametes versicolor* was, in this way, incubated with gelatine before SDS PAGE analysis (Appendix Figure 5.4). The disappearance of >150 kDa bands, instead of low molecular weight ones, was observed. Although SDS PAGE band disappearance has been described in the literature as an indication of possible crosslinking, the lack of bands stuck in the gel wells refuted the hypothesis that crosslinked products may have been too large to migrate through the gel.[38,39,107,357,358] It may be that gelatine precipitation occurred before gel loading, although this was not observed by eye. Gelatine was, therefore, not investigated further as a substrate.

5.3.1.3. Viscosity assay for enzymatic crosslinking of soluble keratin

An increase in viscosity was then investigated as another potential marker for protein crosslinking, inspired by work performed by Elbalasy *et al.* (2020) on keratin networks crosslinked *via* electron irradiation, amongst others.[81,283,356] The viscosity of tyrosinase-incubated Keratec™ IFP was initially observed by eye and appeared slightly higher than the no-enzyme control. Keratec™ IFP was then incubated overnight with laccase, tyrosinase or transglutaminase before analysis using a Modular Compact Rheometer (Appendix Figure 5.5). Viscosity values obtained were of the same order of magnitude as solubilised keratin samples similarly analysed in the literature. However, no significant viscosity increase was observed upon enzymatic treatment.[81] While enzymatic activities may have been hindered in the

presence of undialysed Keratec™ IFP (see section 5.2.), viscosity measurements were not further investigated for crosslinking analysis.

5.3.1.4. Keratec™ substrate characterisation and pre-treatment

5.3.1.4.1. Molecular weight distributions

Prior to further crosslinking investigations, Keratec™ IFP and Keratec™ ProSina were analysed by SDS PAGE to understand molecular weight distributions within these substrates. Significant smearing was seen for both substrates, in alignment with soluble keratin substrate analyses reported in the literature.[81,359,373] Keratec™ IFP exhibited protein molecular weights ranging from 10 kDa to over 250 kDa. A thick band was observed at around 40 kDa, in accordance with the 40-60 kDa range described by Kelly *et al.* (2005), while some protein appeared stuck in the gel well (Figure 68a), potentially due to protein aggregation as a result of denaturation.[288,374] On the other hand, Keratec™ ProSina displayed a thick smear up to 15 kDa, with a lot of peptides below 10 kDa, compared to the 2,500–3,000 kDa range mentioned by Croda International (Figure 68b).[375] SDS PAGE analysis nonetheless confirmed the lower molecular weight keratin composition of Keratec™ ProSina compared to Keratec™ IFP, as suggested by Croda International.[375]

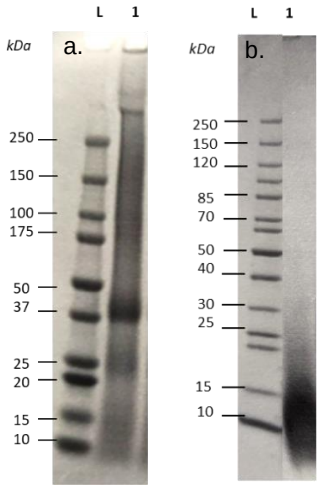

Figure 68. SDS PAGE analyses of undialysed Keratec™ IFP (a) and Keratec™ ProSina (b). Ladder (5 µL) and undialysed Keratec™ IFP (6.5 mg/mL, a.) or undialysed Keratec™ ProSina (23.6 mg/mL) samples (10 µL) were loaded on the gel and ran at 200V, 400 mA for 35 mins, L= BioRad (a.) or Thermofisher (b.) protein ladders, 1=substrate sample.

Keratec™ IFP was also analysed using size-exclusion chromatography (SEC) as a control for further enzymatic crosslinking assays.[39] Size-exclusion chromatography separates clusters according to their hydrodynamic volume, where smaller clusters diffuse further into the column pores while larger clusters elute faster.[376–378] It is important to note that SEC, unlike SDS PAGE, measures the native, rather than subunit molecular weights of proteins.[379] Proteins of known molecular weights were first injected in the SEC column for calibration purposes (Figure 69a), and a calibration curve was then constructed by plotting the logarithm of molecular weight against retention volume with a simple linear regression (Figure 69b).

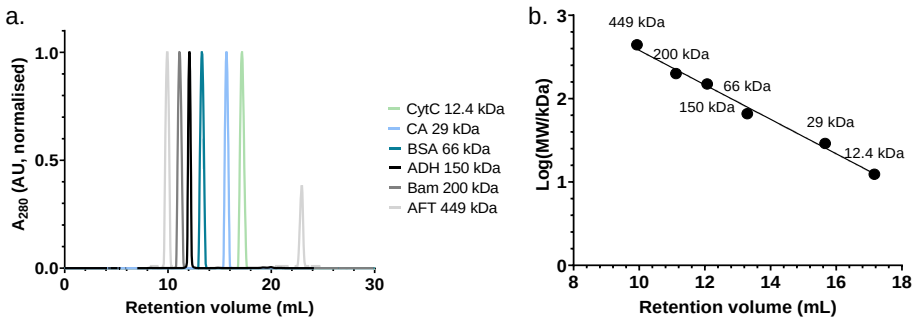

Figure 69. SEC calibration with proteins of known molecular weights (a) with associated calibration curve (b), where R^2=0.99. CytC = Cytochrome c (2 mg/mL), CA = Carbonic anhydrase (3 mg/mL), BSA = Bovine Serum Albumin (10 mg/mL), ADH = Alcohol dehydrogenase (4 mg/mL), BAM = β-Amylase (5 mg/mL) and AFT = Apoferritin (10 mg/mL).

Keratec™ IFP was then injected into the SEC column and elution was monitored *via* 280 nm absorbance measurements (Figure 70a). SEC elution peaks associated with Keratec™ IFP were observed at retention volumes 7-9, 19 and 29 mL. In an attempt to relate SEC elutions to substrate molecular weights, a range of SEC fractions (1-5, as indicated on Figure 70a) were collected and ran on SDS PAGE (Figure 70b). Fractions 1-3 corresponded to a wide range of molecular weights, with a strong protein concentration at around 40 kDa, as well as a shift towards lower molecular weights (less bands > 250 kDa) for Fraction 3 compared to Fraction 1. Fractions 4 and 5 were associated with molecular weights of approximately 15 kDa and below. The peak observed at 30 mL did not show a protein band on SDS PAGE gel, and most likely corresponded to an additive present in Keratec™ IFP. In this way, SEC and SDS PAGE appeared to be somewhat in accordance with each other, with a high proportion of proteins at around 40 kDa, as well as 10-15 kDa, observed with both methods.

The molecular weights associated with elution peaks obtained *via* SEC were then compared to the literature using the calibration curve (Figure 69b).[288] In this way, the 7-9 and 19 mL peaks corresponded to molecular weights of approximately > 610.7 and 5.2 kDa, respectively, compared to 40-60 kDa and 10-15 kDa ranges observed *via* SDS PAGE analysis (Figure 70b) and the 1-250 kDa range suggested by Kelly *et al.* (2005) (Table 9).[288]

These discrepancies between SEC and SDS PAGE analyses may have been linked to oligomeric states of Keratec™ IFP proteins. For example, it is possible that the fraction eluted at 7 ml contained associations of 10-12 peptide fragments, which would have dissociated under the denaturing conditions used in SDS PAGE (Table 9). It is also important to note that the SEC elution peaks associated with Keratec™ IFP were outside the calibration range and that hydrodynamic differences would be expected

between globular proteins, such as BSA and apoferritin, and keratin, a fibrous protein. Indeed, linear-chain proteins like keratin may be associated with higher hydrodynamic volumes and therefore elute faster than globular proteins, which would diffuse further into the column pores.[376] Protein aggregation has also been noted as an SEC limitation, although SEC samples were filtered.[380] Moreover, the difficulty in obtaining accurate molecular weight information for proteins, which vary in shape and hydrodynamic volume, based on calibration curves has been reported in the literature.[381–384]

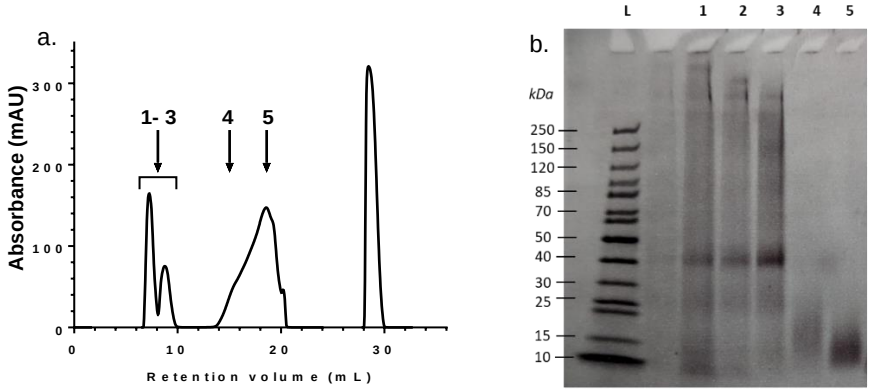

Figure 70. SEC analysis of undialysed Keratec™ IFP (a) and SDS PAGE analysis of Keratec™ IFP SEC fractions (b). Undialysed Keratec™ IFP (32.5 mg/mL) in deionised water was loaded onto the SEC column (a), while 5 µL ladder and SEC fractions 1-5 (10 µL) were loaded on the gel and ran at 200V, 400 mA for 35 mins, where lanes 1-3 correspond to retention volumes of 7-10 mL (SEC fractions 1-3), while lanes 4 and 5 (SEC fractions 4-5) relate to retention volumes around 15 and 18 mL, respectively (b).

Table 9. Keratec™ IFP molecular weights based on SEC and SDS PAGE analyses.

Retention volume / mL	Molecular weights from SDS PAGE analysis / kDa	Molecular weights from calibration curve / kDa
7-9	40-60	1582.7-610.7
15	10-25	35.1
19	10-15	5.2

5.3.1.4.2. SEC analysis on dialysed Keratec™ substrates

Due to enzymatic inhibitions associated with the use of undialysed Keratec™ IFP and Keratec™ ProSina, dialysed Keratec™ substrates were then

investigated by SEC (Figure 71a). Dialysed Keratec™ ProSina exhibited a peak at a retention volume of around 18 mL (Figure 71a), in alignment with the 10-15 kDa thick band obtained *via* SDS PAGE (Figure 68b) according to previous SEC fraction SDS PAGE analyses (Figure 70). Moreover, the analysis of dialysed Keratec™ IFP *via* SEC revealed the loss of a low molecular weight peak observed at around 29 mL for the undialysed substrate (Figure 71b), suggesting that lower molecular weight proteins, additives or contaminants were successfully removed *via* dialysis.

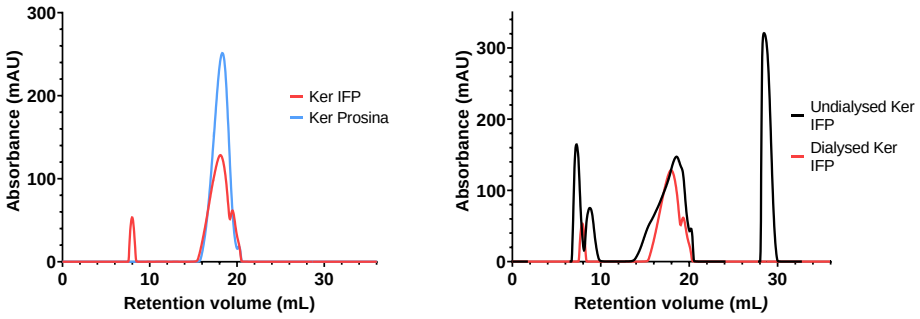

Figure 71. SEC analysis of dialysed Keratec™ IFP and Keratec™ ProSina (a) and undialysed vs. dialysed Keratec™ IFP (b). Keratec™ IFP (Ker IFP, 19.9 mg/mL) and Keratec™ ProSina (Ker Pro, 7.3 mg/mL) in deionised water (a) and dialysed (19.9 mg/mL) and undialysed (32.5 mg/mL) Keratec™ IFP in deionised water (b) were loaded onto the SEC column.

Despite identical sample volumes loaded onto the SEC column across samples, variations in absorbance intensities were observed, which was also reported in the literature.[385] Moreover, differences in the peaks eluting between 8 and 10 mL were seen across samples, which may have been linked to the difficulty of separating polydisperse macromolecules like gelatine or keratin *via* SEC, resulting in unresolved areas between peaks as reported in the literature.[386] Following these observations, SEC was considered as a qualitative assay towards enzymatic crosslinking of keratin.[384–386]

5.3.1.4.3. EDC as positive control for keratin crosslinking

N-(3-Dimethylaminopropyl)-*N′*-ethylcarbodiimide (EDC) is a known crosslinker which has been shown to react with carboxyl groups in aspartic and glutamic residues in proteins such as a collagen and gelatine.[386,387] Nucleophilic attack by a primary amine then results in the formation of an amide bond with the original carboxyl group.[386,388] EDC was also shown to crosslink human hair keratin with alginate aimed at improved mechanical properties, but the formation of keratin-keratin crosslinks has not been described for EDC in the literature. The crosslinker was briefly investigated *via* SEC for the crosslinking of Keratec™ substrates for potential use as a positive control in later experiments (Appendix Figure 5.6), however, no crosslinking was observed across replications (Appendix Figure 5.7).[39]

5.3.2. Enzymatic crosslinking of Keratec™ substrates

The enzymatic crosslinking of keratin was then investigated using both SDS PAGE and SEC, two methods described in the literature for crosslinking analysis.[38,39,107,356–358]

5.3.2.1. Laccase crosslinking of Keratec™ substrates

5.3.2.1.1. Laccase crosslinking of Keratec™ IFP

Laccase from *Trametes versicolor* was incubated overnight with Keratec™ IFP and analysed by SEC for the qualitative monitoring of protein molecular weights in an attempt to identify substrate crosslinking (Figure 72a-c).[39] The effect of overnight incubation on laccase was checked by addition of ABTS, and the strong green colour observed as a result confirmed that the enzyme was still active. Moreover, an enzyme-only control was analysed by SEC to check for potential interference with substrate elution, and no peaks were observed at such low laccase concentrations.

The incubation of Keratec^{TM} IFP with laccase was associated with a shift of the main 18 mL peak towards higher molecular weights, observed across replications (Figure 72a-c), which has been described in the literature as evidence for successful crosslinking.[39] The apparition of small peaks in the 10-15 mL region was also noted, corresponding to proteins with increased molecular weights.[389] While the laccase-catalysed formation of keratin-keratin bonds has not been described in the literature, Keratec^{TM} IFP was here successfully crosslinked by laccase from *Trametes versicolor*.[39,389] The ability of the enzyme to catalyse the single-electron abstraction from tyrosine, tryptophane or cysteine side chains in soluble keratin, and the subsequent crosslinking with other keratin side chains was indeed demonstrated.[35,227,235,236,244,245]

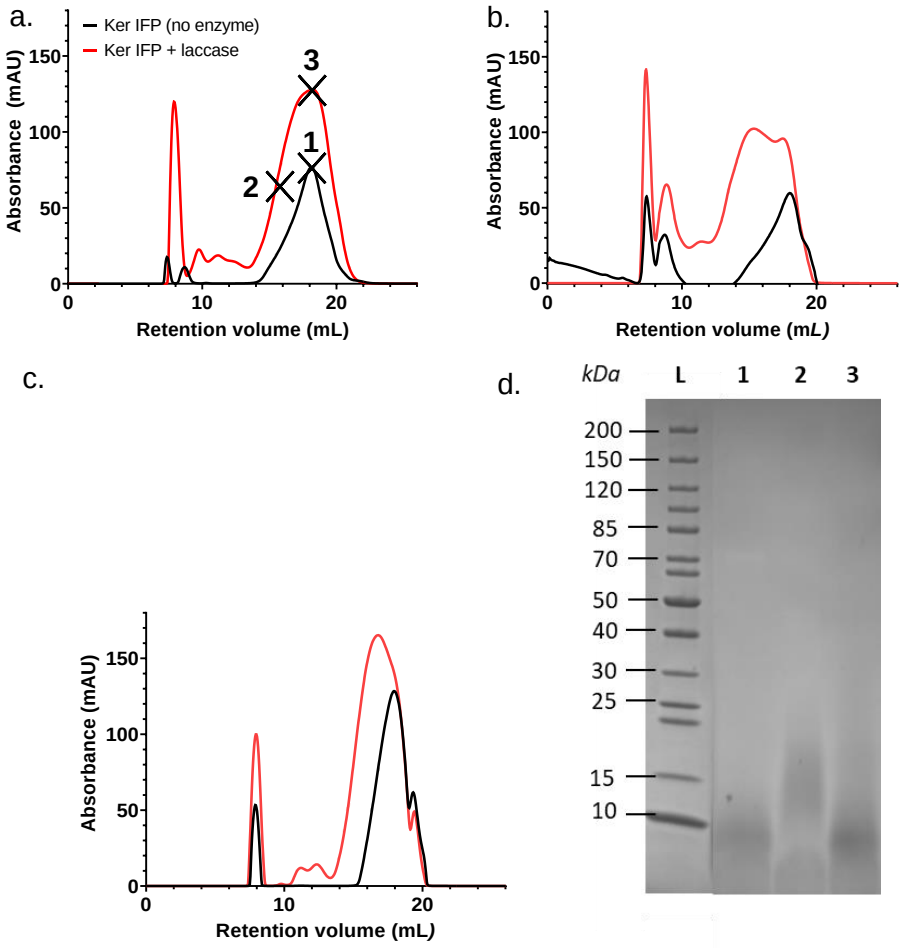

Figure 72. SEC analysis of Keratec™ IFP crosslinking by laccase from *Trametes versicolor* (a.-c.) with SDS PAGE analysis of SEC fractions (d.). (a.-c.) TvLac (1.71 U/mL, 0.5 mg/mL) incubated with dialysed Keratec™ IFP (Ker IFP, 11.1 mg/mL (a.-b.) and 19.9 mg/mL (c.)) in dH_2O at 37°C, 250 rpm, overnight. (d.) L=protein ladder, 1=Dialysed Keratec™ IFP, 18 mL fraction, 2=Dialysed Keratec™ IFP + laccase, 15 mL fraction & 3=Dialysed Keratec™ IFP + laccase, 18 mL fraction.

Selected SEC fractions (corresponding to retention volumes indicated by crosses on Figure 72a chromatogram) were then further analysed using SDS PAGE (Figure 72d) and Bradford assays. Absorbances of peaks between 10 and 15 mL retention volumes were too low for further analysis. SDS PAGE analysis confirmed previous observations where peaks in the 15-20 mL elution region were associated with bands between 10 and 20 kDa on the gel. Fraction 2 exhibited higher molecular weight proteins (15-20 kDa) than fractions 1 and 3 (10-15 kDa), as expected (Figure 72d). Moreover, comparable retention volumes on SEC across different samples (fractions 1 and 3) were associated with bands of similar molecular weights on SDS

PAGE, conferring some robustness to the SEC-SDS PAGE assay system. The detection of proteins, in opposition to additives, for example, by SEC was further confirmed by Bradford analysis of fractions, which yielded protein concentrations of between 0.87 and 1.52 mg/mL (Appendix Figure 5.8).

5.3.2.1.2. Effect of undialysed Keratec™ IFP on laccase activity

Laccase was also incubated with undialysed Keratec™ IFP and analysed *via* SEC (Figure 73) to evaluate hindrance caused by undialysed substrate as suggested by previous ABTS laccase assays (see Section 5.2.1.1.). No clear peak shift or formation was observed on the chromatogram in the presence of laccase compared to the no-enzyme control. These observations suggest a lack of clear enzymatic crosslinking activity in the presence of undialysed substrate, in line with previous observations. In this way, any further SEC analyses were conducted on dialysed Keratec™ substrates.

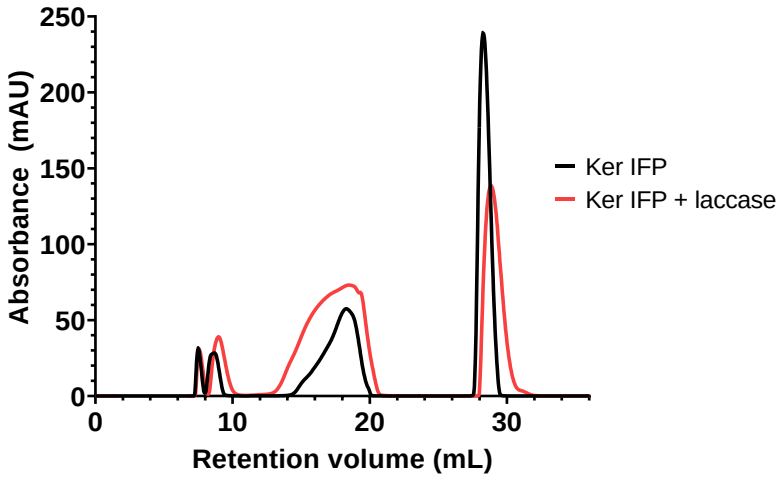

Figure 73. SEC analysis of undialysed Keratec™ IFP crosslinking by *Trametes versicolor* laccase. TvLac (1.71 U/mL, 0.5 mg/mL) was incubated with undialysed Keratec™ IFP (Ker IFP, 6.5 mg/ml) in deionised water overnight at 37°C, 250 rpm.

5.3.2.1.3. Effect of heat-inactivated laccase on SEC analysis

The effect of laccase heat-inactivation on Keratec™ IFP crosslinking was then investigated to confirm that any laccase activity detected *via* SEC

corresponded to laccase activity rather than the mere presence of the enzyme. In this way, heat-inactivated laccase was incubated with Keratec™ IFP and analysed *via* SEC (Figure 74). SEC elution patterns of the heat-inactivated laccase sample and the no-enzyme control were comparable, with no peak formation or shift, suggesting that changes in elution observed for active laccase in the presence of Keratec™ IFP were indeed related to crosslinking.

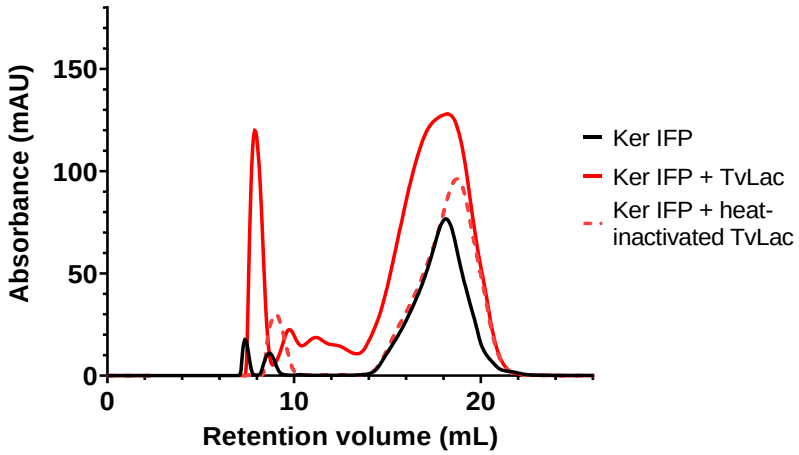

Figure 74. Effect of heat-inactivated laccase from *Trametes versicolor* on SEC analysis. TvLac (1.71 U/mL, 0.5 mg/mL) was heat-inactivated (15 mins at 100°C) and incubated with dialysed Keratec™ IFP (Ker IFP, 11.1 mg/mL) in dH_2O, overnight at 37°C, 250 rpm.

5.3.2.1.4. *Pleurotus ostreatus* laccase crosslinking of Keratec™ IFP

While comparable activities were measured for laccase from *Pleurotus ostreatus* and *Trametes versicolor via* ABTS oxidation (see section 5.2.1.3.), keratin crosslinking activities of the two enzymes were compared using SEC (Figure 75).[363] Similar shifts of the 18 mL retention volume peak towards higher molecular weights were observed for both enzymes, as well as the apparition of small peaks at retention volumes of around 10-15 mL, further confirming the keratin crosslinking activity of both white-rot fungi laccases.

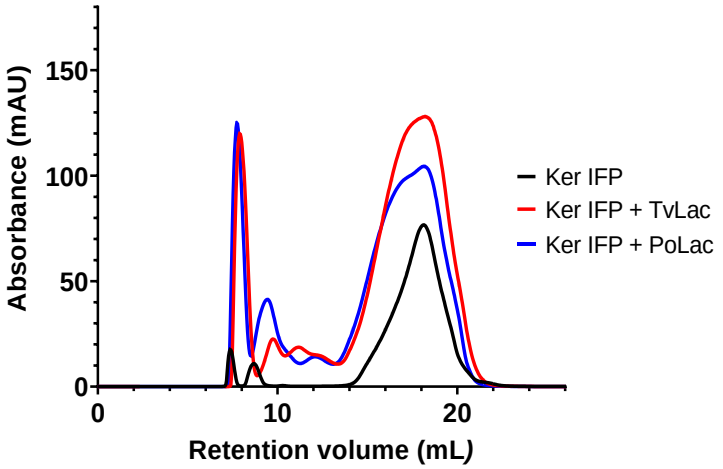

Figure 75. SEC analysis of dialysed Keratec™ IFP crosslinking by laccases from *Trametes versicolor* and *Pleurotus ostreatus*. TvLac (1.71 U/mL, 0.5 mg/mL) or PoLac (1.47 U/mL, 0.5 mg/mL) was incubated with dialysed Keratec™ IFP (Ker IFP, 11.1 mg/mL) in dH_2O, overnight at 37°C, 250 rpm.

5.3.2.1.5. Effect of mediators on Keratec™ IFP crosslinking by laccase

The effect of naturally occurring vanillin and acetosyringone mediators was then investigated on Keratec™ IFP crosslinking by laccase from *Trametes versicolor*.[242] Mediators are low molecular weight compounds, which are oxidised by the enzyme to stable radicals, which in turn oxidise substrates that would otherwise not get oxidised by laccases.[242] In this way, laccases may be too large to penetrate human hair, or their redox potential may be too low, and the use of a mediator may then allow keratin crosslinking.[237,242] Mediators indeed increase the accessibility of reactive amino acids, such as tyrosine or tryptophane, leading to enhanced crosslinking.[250] While ABTS was the first synthetic laccase-mediator to allow the oxidation of non-phenolic lignin structures, vanillin and acetosyringone are naturally-occurring phenols with reduced free radical activity compared to synthetic mediators, associated with lower risks of attack on laccase groups.[252,257,363–365]

Laccase from *Trametes versicolor* was here incubated with Keratec™ IFP in the presence or absence of vanillin and acetosyringone (Figure 76a-b). As previously noted, Keratec™ IFP crosslinking by laccase was observed *via* a slight shift of the 18 mL peak towards larger molecular weights combined

with the apparition of small peaks in the 10-15 mL region. In the presence of mediators, both acetosyringone and vanillin, more significant peak shifts as well as the apparition of peaks at 10-15 mL at higher intensities were observed on respective chromatograms. Indeed, ratios of 10-15 mL to 8 mL peaks were higher in the presence of mediators, suggesting an increased fraction of crosslinked proteins. This seemingly enhanced laccase keratin crosslinking activity may be explained by the increased accessibility of reactive amino acids associated with the presence of mediators.[250]

Laccases are known to preferentially react with mediators over protein amino acids, therefore, the formation of keratin-keratin crosslinks in solubilised wool has here been demonstrated *via* both laccase-only and laccase-mediator pathways.[247] The latter is of particular interest as it may help overcome the penetration issues encountered for enzymatic activities on solid substrates, such as hair.

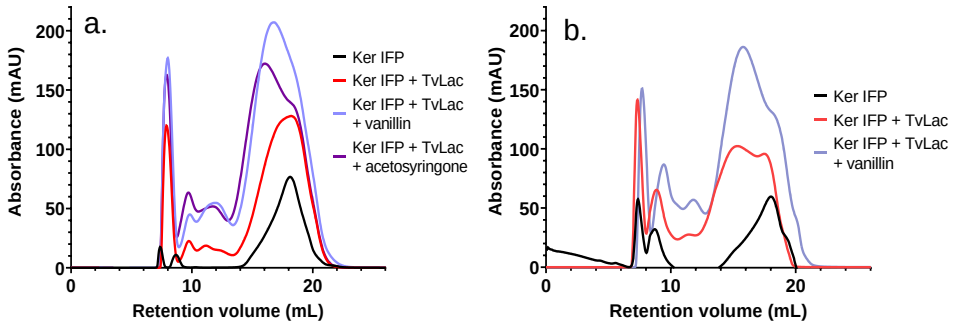

Figure 76. Effect of mediators on dialysed Keratec™ IFP crosslinking by *Trametes versicolor* laccase *via* SEC. TvLac (1.71 mg/mL, 0.5 mg/mL) was incubated with dialysed Keratec™ IFP (Ker IFP, 11.1 mg/mL) in the presence or absence of mediators (vanillin and acetosyringone, 1mM) in dH_2O, overnight at 37°C, 250 rpm – (b) is a replication of (a).

ABTS was also investigated as a mediator, and while its incubation with laccase and Keratec™ IFP led to the formation of peaks in the 11-14 mL region, peak ratios were similar to the no-mediator sample (Appendix Figure 5.9).

5.3.2.1.6. SDS PAGE analysis of laccase crosslinking activity on Keratec^{TM} IFP

The potential of laccases to form keratin-keratin crosslinks in solubilised wool observed by SEC was further investigated using SDS PAGE analysis. Laccases from *Trametes versicolor* and *Pleurotus ostreatus* were incubated overnight with dialysed Keratec^{TM} IFP and loaded onto an SDS PAGE gel (Figure 77). The effects of vanillin and acetosyringone mediators as well as enzyme thermal inactivation were also investigated on keratin-keratin crosslinking by laccase from *Trametes versicolor*.

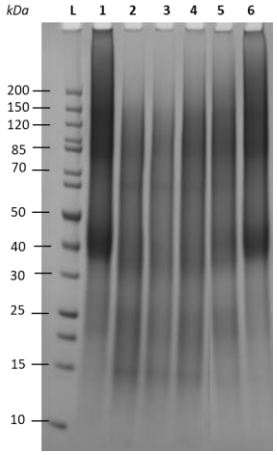

Figure 77. SDS PAGE analysis of dialysed Keratec^{TM} IFP crosslinking by laccases from *Trametes versicolor and Pleurotus ostreatus*. TvLac (1.71 U/mL, 0.5 mg/mL – heat inactivation: 15 min at 100 °C) or PoLac (1.47 U/mL, 0.5 mg/mL) was incubated with dialysed Keratec^{TM} IFP (11.1 mg/mL) in dH_2O overnight at 37°C, 250 rpm, in the presence or absence of mediators (vanillin and acetosyringone, 1mM) – L=protein ladder, 1=Keratec^{TM} IFP, 2= Keratec^{TM} IFP + Tv-laccase, 3=Keratec^{TM} IFP + Tv-laccase + vanillin, 4=Keratec^{TM} IFP + Tv-laccase + acetosyringone, 5=Keratec^{TM} IFP + Po-laccase, 6=Keratec^{TM} IFP + heat-deactivated Tv-laccase.

Smearing was observed in all lanes, which has been commonly described in the literature for soluble keratin substrates, associated with sample complexity.[81,359,373]. Moreover, significant band disappearance, especially towards higher molecular weights, was noted in lanes 2 to 4, corresponding to Keratec^{TM} IFP treatment with laccase from *Trametes versicolor*, in the presence or absence of mediators. Similar band disappearance was noted upon Keratec^{TM} IFP incubation with laccase from *Pleurotus ostreatus*. While band disappearance has been described in the literature as an indication of

substrate crosslinking in association with the accumulation of high molecular weight proteins in wells, the apparent loss of proteins over 200 kDa observed here, combined with the absence of proteins stuck in the wells remains confusing.[38,39,107,357,358] It is possible that crosslinking occurred and was associated with substrate precipitation, which was not loaded onto the gel.[107] In this way, these observations may further confirm indications *via* SEC that Keratec™ IFP is indeed being crosslinked by laccase, both in the presence and absence of mediators. This is especially plausible in the absence of band disappearance observed when laccase was inactivated prior to incubation with the substrate.

Laccase activity on undialysed Keratec™ IFP was also investigated *via* SDS PAGE analysis (Appendix Figure 5.10), and a lack of keratin crosslinking was observed in the absence of band disappearance, in line with Keratec™ IFP-laccase inhibition reported above (Section 5.2.1.1).

5.3.2.1.7. Laccase crosslinking of Keratec™ ProSina

The crosslinking activity of laccase from *Trametes versicolor* was then explored using dialysed Keratec™ ProSina, as an alternative soluble keratin substrate with a narrow range of molecular weights as seen *via* SDS PAGE analysis (Figure 68b). In this way, laccase was incubated with dialysed Keratec™ ProSina overnight before injection into the SEC column (Figure 78). Keratec™ ProSina exhibited one main peak at a retention volume of around 18 mL, in line with previous SDS-SEC concordance observations (see section 5.3.1.4.1.). No shift in the elution peak was observed upon treatment with laccase, suggesting a lack of crosslinking activity for dialysed Keratec™ ProSina. Considering Keratec™ ProSina has higher proportions of tyrosines and cysteines (Table 4), the crosslinking activity of laccase towards this substrate would therefore be expected to be higher than

Keratec™ IFP. One explanation could be that, considering the molecular weight differences between the two substrates, dimers or polymers formed by small peptides in Keratec™ ProSina may be harder to detect by SEC compared to the larger dimers or polymers formed in Keratec™ IFP.

The use of ABTS as a mediator was also investigated using SEC, but no crosslinking was detected either (Appendix Figure 5.11). The substrate-grafting of ABTS *via* covalent coupling, which blocks polymerisation, has been described in the literature and could potentially explain this lack of activity observed in the presence of ABTS.[238]

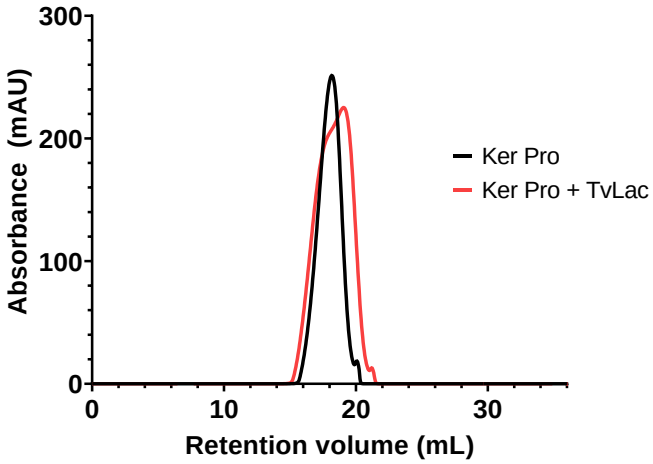

Figure 78. SEC analysis of laccase from *Trametes versicolor* on dialysed Keratec™ ProSina. TvLac (1.71 U/mL, 0.5 mg/mL) was incubated with dialysed Keratec™ ProSina (Ker Pro, 7.3 mg/mL) in dH_2O, overnight at 37°C, 250 rpm.

Laccase crosslinking activity on Keratec™ ProSina was further assessed *via* SDS PAGE analysis (Figure 79). No band disappearances or shifts towards higher molecular weights were observed under any of the crosslinking treatments conducted, including in the presence of vanillin and acetosyringone, in line with what was observed using SEC.

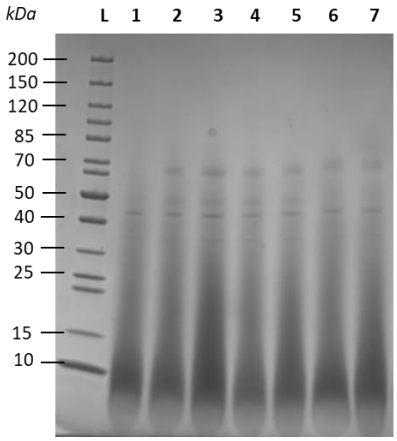

Figure 79. SDS PAGE analysis of laccase from *Trametes versicolor* or *Pleurotus ostreatus* on dialysed Keratec^{TM} ProSina. TvLac (1.71 mg/mL, 0.5 mg/mL) or PoLac (1.47 mg/mL, 0.5 mg/mL) was incubated with dialysed Keratec^{TM} ProSina (7.3 mg/mL) in dH_2O in the presence or absence of mediators (vanillin and acetosyringone, 1mM), overnight at 37°C, 250 rpm - L=protein ladder, A=Dialysed Keratec^{TM} ProSina, B&C=Dialysed Keratec^{TM} ProSina + Tv-laccase, D&E=Dialysed Keratec^{TM} ProSina + Tv-laccase + vanillin, F=Dialysed Keratec^{TM} ProSina + Po-laccase, G=Dialysed Keratec^{TM} ProSina + Po-laccase + vanillin.

Overall, the formation of keratin-keratin crosslinks in Keratec^{TM} IFP by laccases from *Trametes versicolor* and *Pleurotus ostreatus* was demonstrated, both *via* the laccase-only and laccase-mediator pathways, using SEC and SDS PAGE. On the other hand, no crosslinking activity was detected for laccase from *Trametes versicolor* on Keratec^{TM} ProSina as the substrate, which may have been linked to the more challenging detection of smaller crosslinked peptides, associated with lower molecular weight differences between monomers, dimers and polymers, compared to larger crosslinked proteins.

Tyrosinase and transglutaminase were then investigated towards the formation of keratin-keratin crosslinks in solubilised wool substrates.

5.3.2.2. Tyrosinase crosslinking of Keratec^{TM} IFP

Tyrosinase from mushroom was then investigated for potential crosslinking of Keratec^{TM} IFP, using both SEC and SDS PAGE analyses. In this way, tyrosinase was incubated overnight with dialysed Keratec^{TM} IFP before injection in an SEC column (Figure 80). An enzyme-only control was also

analysed by SEC to check for potential interference with substrate peak elution, and no peaks were observed at such low tyrosinase concentrations.

Unlike what was observed using laccases, the treatment of Keratec™ IFP with mushroom tyrosinase was not associated with the apparition of new peaks or peak shifts towards higher molecular weights.

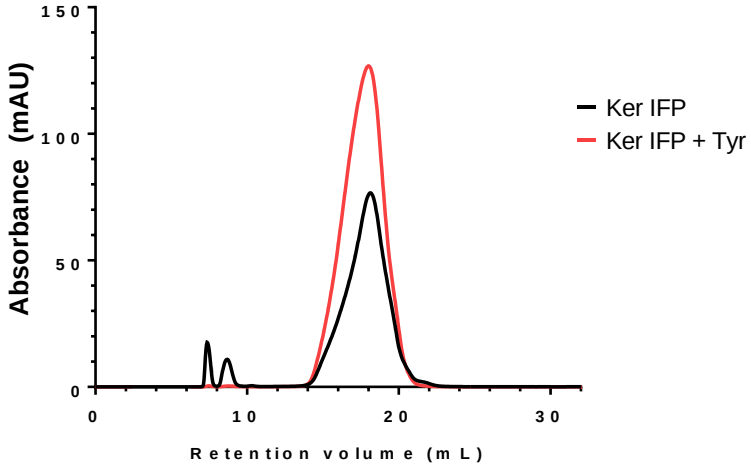

Figure 80. SEC analysis of mushroom tyrosinase activity on dialysed Keratec™ IFP. Tyr (5.46 U/mL, 0.5 mg/mL) was incubated with dialysed Keratec™ IFP (Ker IFP,11.1 mg/mL) in dH_2O overnight at 37°C, 250 rpm in the presence or absence of mediators (vanillin or acetosyringone, 1mM).

Mushroom tyrosinase activity on dialysed Keratec™ IFP was also assessed using SDS PAGE (Figure 81). No significant band disappearance was detected upon substrate treatment with tyrosinase, however, a slight increase in proteins aggregated in the gel well was noted, described in the literature as a potential indication for crosslinking. This was observed across replications (Appendix Figure 5.12).[38,357,358] It may therefore be that crosslinking indeed took place, resulting in keratin aggregation. However, because SEC samples were filtered prior to injection into the column, it may be that the aggregates observed by SDS PAGE were removed prior to SEC analysis, which could also explain the disappearance of 8-10 mL elution peaks seen upon treatment of Keratec™ IFP with tyrosinase.

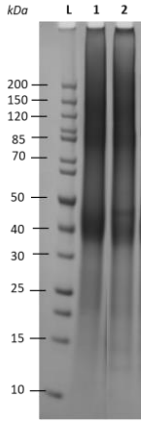

Figure 81. SDS PAGE analysis of dialysed Keratec^{TM} IFP crosslinking by tyrosinase from mushroom. Tyr (5.46 U/mL, 0.5 mg/mL) was incubated with dialysed Keratec^{TM} IFP (11.1 mg/mL) in dH_2O at 37°C, 250 rpm - L=protein ladder, 1=Dialysed Keratec^{TM} IFP, 2=Dialysed Keratec^{TM} IFP + tyrosinase, 3=Dialysed Keratec^{TM} IFP + tyrosinase + acetosyringone, 4=Dialysed Keratec^{TM} IFP + tyrosinase + vanillin.

Overall, the results observed *via* SDS PAGE and SEC upon incubation of tyrosinase from mushroom with Keratec^{TM} IFP did not constitute unambiguous evidence that keratin-keratin crosslinking occurred. A range of reasons could explain a potential lack of tyrosinase activity on soluble keratin, including the high degree of complexity of the substrate, which has been shown to hinder crosslinking by tyrosinases, as well as tyrosine being the sole target of tyrosinase catalysed-protein crosslinking.[35,39]

5.3.2.3. Transglutaminase crosslinking of Keratec^{TM} IFP

Microbial transglutaminase was then investigated for the potential crosslinking of Keratec^{TM} IFP, using both SEC and SDS PAGE analyses. In this way, transglutaminase was incubated overnight with dialysed Keratec^{TM} IFP before injection in an SEC column (Figure 82). A transglutaminase-only control was also analysed by SEC and yielded no peaks on the chromatogram. The treatment of dialysed Keratec^{TM} IFP with transglutaminase was not associated with the formation of new peaks or peak shifts towards higher molecular weights compared to the untreated substrate. This was observed across replications (Appendix Figure 5.13-14).

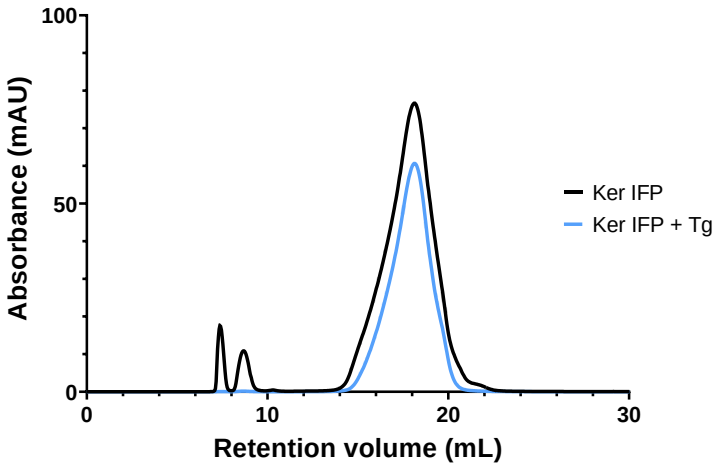

Figure 82. SEC analysis of microbial transglutaminase activity on dialysed Keratec™ IFP. Tg (0. 19 U/mL, 13.15 µg/mL) was incubated with dialysed Keratec™ IFP (Ker IFP, 11.1 mg/mL) in Tris buffer pH 6 overnight at 37°C, 250 rpm in the presence or absence of reduced glutathione (65.1 µM).

Microbial transglutaminase activity on dialysed Keratec™ IFP was also assessed using SDS PAGE (Figure 83). Similarly to what was observed for tyrosinase, no band disappearance was seen for transglutaminase-treated Keratec™ IFP. A significant increase in well-stuck proteins was, however visible for treated Keratec™ IFP compared to the untreated substrate, observed across replications (Appendix Figure 5.15). Coupled with the disappearance of the 8-10 mL elution peaks upon enzymatic treatment, it may again be that Keratec™ IFP crosslinking did occur in the presence of transglutaminase, but that sample filtration prevented the detection of crosslinked proteins *via* SEC.

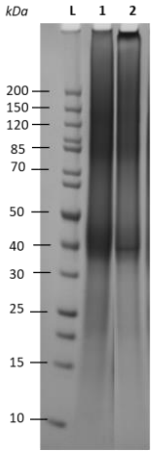

Figure 83. SDS PAGE analysis of dialysed Keratec™ IFP crosslinking by microbial transglutaminase. Tg (0. 19 U/mL or 13.15 µg/m) was incubated overnight with Keratec™ IFP (11.1 mg/mL) in Tris buffer, pH6 at 37°C, 250 rpm – L=ladder, 1=Dialysed Keratec™ IFP, 2=Dialysed Keratec™ IFP + transglutaminase.

Again, those results do not constitute unambiguous evidence that keratin-keratin crosslinks were formed upon solubilised keratin treatment with microbial transglutaminase. The steric restrictions associated with structured proteins may have limited keratin from acting as a glutamyl substrate for transglutaminase.[39,226]

It was then decided to investigate whether the promising laccase keratin-keratin crosslinking results obtained for dialysed Keratec™ IFP *via* SEC and SDS PAGE analyses could be replicated onto solid human hair keratin as the substrate.

5.4. Crosslinking of human hair by laccase

Tensile strength is a measure of a material's ability to resist deformation under tension or stretching force, and has commonly been used as a measure of hair integrity, for example, following cosmetic treatments.[390–394] It has been demonstrated that the tensile properties of hair are mostly provided by the cortex, dominated by α-keratins.

In this way, chemically-damaged cuticles were shown to be associated with no impact on tensile properties.[391,395] Tensile strength properties have also

been reported as a potential marker for crosslinking, in a range of materials such as epoxy resin, keratin films, as well as solid human hair.[59,63,108,396]

In this way, tensile strength analyses were performed in this study to investigate potential hair crosslinking by laccase following promising results obtained on solubilised wool *via* SEM and SDS PAGE analyses. Solid human hair was first washed and treated with DTT, aimed at reducing substrate disulfide bonds and opening up hair structure for better enzyme penetration.[107,108,389] The reduced hair was then thoroughly rinsed before overnight incubation with laccase from *Trametes versicolor*, in the presence or absence of vanillin mediator. Tensile strength analyses were then performed on each of the 100 strands per condition, and parameters including fibre diameter, elasticity, break load and toughness were measured. Untreated hair (washed and DTT-treated) was used as a negative control.

Tensile strength analyses are usually plotted as stress-strain curves, which are obtained by gradually applying load to a sample and measuring subsequent deformation. A range of parameters can, as a result, be evaluated, such as elastic deformation, stiffness, break stress, elongation at break, as well as toughness. While data was collected for 100 strands per condition in this study, a stress-strain curve corresponding to a single hair assessment is included for illustrative purposes only, as it does not account for substantial variations between strands (Figure 84).

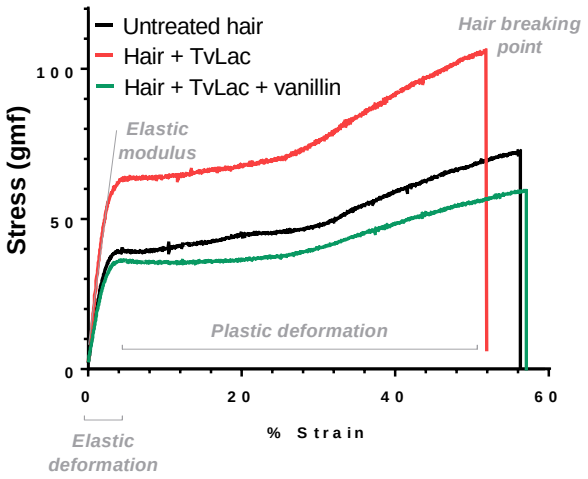

Figure 84. Singular hair strand stress-strain curve upon treatment with *Trametes versicolor* laccase. Hair strands (100) were washed with SDS (10% solution) and rinsed under cold water, before a pre-incubation with DTT (0.5 M), thorough rinsing under warm water and overnight incubation with TvLac (3.41 U/mL, 1 mg/mL), in the presence or absence of vanillin (1 mM), at 37 °C, 120 rpm. Following a final rinsing, the hair was dried at 60 °C for 72 hours before tensile strength analysis.

A simulated stress-strain curve was also generated as an average of all 100 strands per condition evaluated (Figure 85). However, no significant differences between untreated-reduced hair and laccase-treated reduced hair, both in the presence and absence of vanillin.

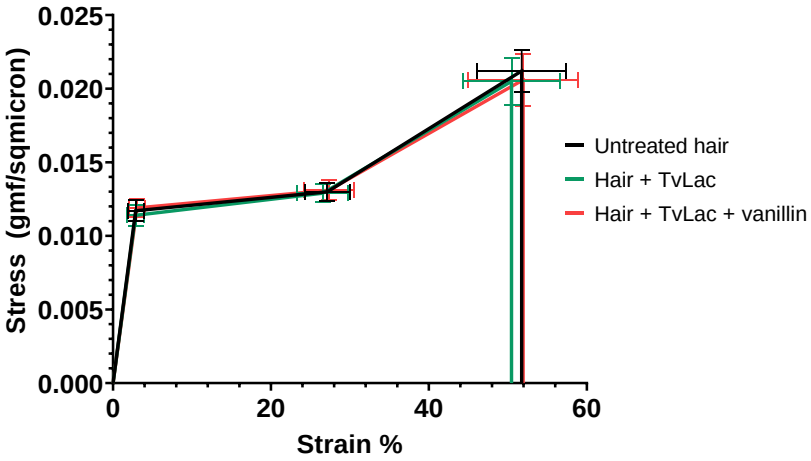

Figure 85. Simulated average hair stress-strain curve for the evaluation of potential *Trametes versicolor* laccase crosslinking. Hair strands (100) were washed with SDS (10% solution) and rinsed under cold water, before a pre-incubation with DTT (0.5 M), thorough rinsing under warm water and overnight incubation with TvLac (3.41 U/mL or 1 mg/mL), in the presence or absence of vanillin (1 mM), at 37 °C, 120 rpm. Following a final rinsing, the hair was dried at 60 °C for 72 hours before tensile strength analysis - data given as average values of measurements obtained for 100 hair strands and shown ± the standard deviation.

A series of parameters, including break strength, strain and elastic modulus, were then further investigated across samples, where natural variations in fibre diameter were accounted for. Break strength, or tensile strength, refers to the stress needed to break the hair fibre. It was therefore investigated as a potential indication of fibre crosslinking, as suggested by Mi *et al.* (2019), where crosslinked hair would be expected to require more stress to break (Figure 86).[108] However, no significant change in break strength was observed across the conditions evaluated in this study. A break stress-strain curve was also plotted to evaluate the strain sustained by fibres before fracture. While an increase in break extension may have been indicative of a more resilient fibre, no significant differences were observed across conditions (Figure 87).[108,396]

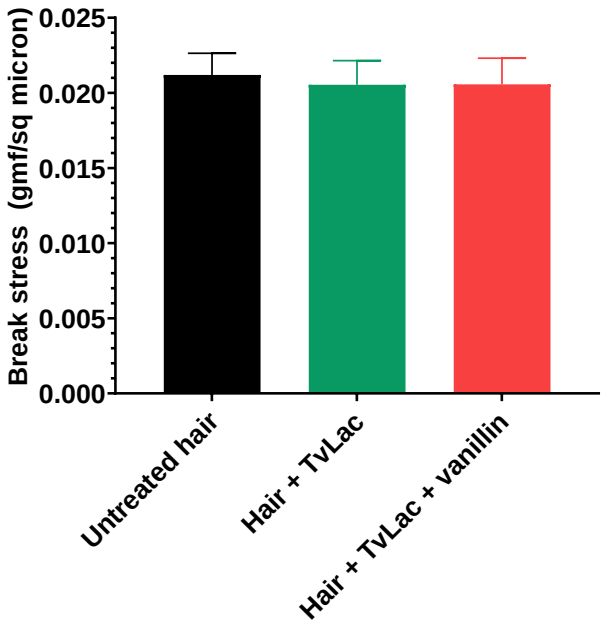

Figure 86. Hair break stress analysis upon treatment with *Trametes versicolor* laccase. Hair strands (100) were washed with SDS (10% solution) and rinsed under cold water, before a pre-incubation with DTT (0.5 M), thorough rinsing under warm water and overnight incubation with TvLac (3.41 U/mL,1 mg/mL), in the presence or absence of vanillin (1 mM), at 37 °C, 120 rpm. Following a final rinsing, the hair was dried at 60 °C for 72 hours before tensile strength analysis - data given as average values of measurements obtained for 100 hair strands and shown ± the standard deviation.

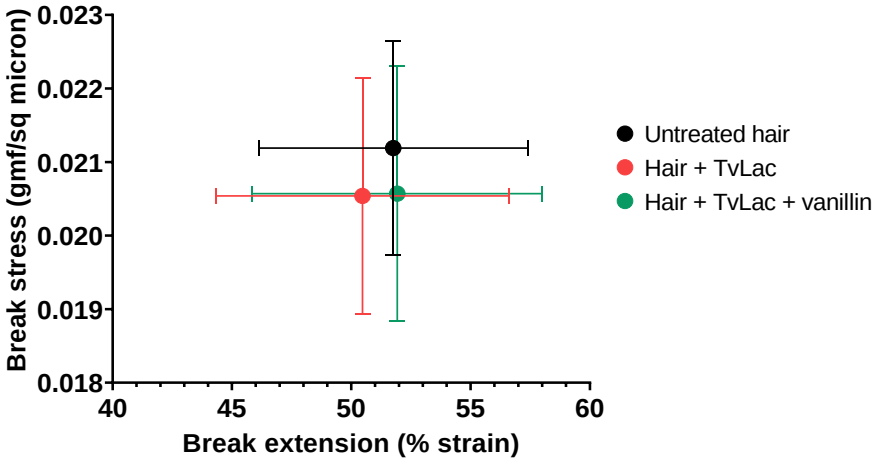

Figure 87. Hair stress-strain upon treatment with *Trametes versicolor* laccase. Hair strands (100) were washed with SDS (10% solution) and rinsed under cold water, before a pre-incubation with DTT (0.5 M), thorough rinsing under warm water and overnight incubation with TvLac (3.41 U/mL or 1 mg/mL), in the presence or absence of vanillin (1 mM), at 37 °C, 120 rpm. Following a final rinsing, the hair was dried at 60 °C for 72 hours before tensile strength analysis - data given as average values of measurements obtained for 100 hair strands and shown ± the standard deviation.

Moreover, the elastic modulus, which is calculated as the ratio of stress to strain when the deformation is solely elastic (recovered upon release of applied force), may be used as a measure of hair fibre stiffness. While the elastic modulus is closely related to fibre water tension, it was investigated as a potential indication of crosslinking, where higher stiffness was expected upon crosslinking. However, no significant differences were observed between enzyme-treated and untreated reduced hair (Figure 88).

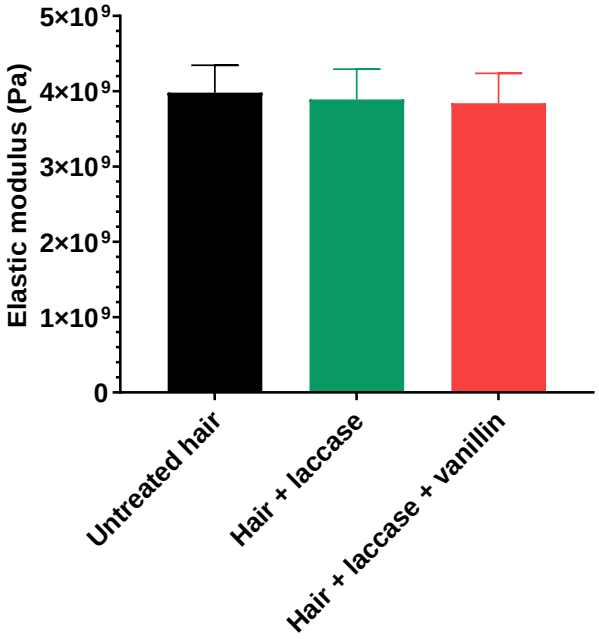

Figure 88. Hair elastic modulus upon treatment with *Trametes versicolor* laccase. Hair strands (100) were washed with SDS (10% solution) and rinsed under cold water, before a pre-incubation with DTT (0.5 M), thorough rinsing under warm water and overnight incubation with TvLac (3.41 U/mL or 1 mg/mL), in the presence or absence of vanillin (1 mM), at 37 °C, 120 rpm. Following a final rinsing, the hair was dried at 60 °C for 72 hours before tensile strength analysis - data given as average values of measurements obtained for 100 hair strands and shown ± the standard deviation.

Overall, no fibre crosslinking was observed upon treatment of reduced hair with laccase from *Trametes versicolor*, in the presence or absence of vanillin mediator. While it is possible that tensile strength analyses were not suitable for the detection of crosslinking, it appears that laccase was not able to penetrate into the hair cortex. The fibres were pre-treated with DTT in an attempt to open up the hair structure and facilitate enzyme penetration, as has been seen for keratinase enzymes.[107,108,389] However, following discussions with Croda, the relatively high tensile strengths observed for DTT- reduced fibres may indicate that the hair had been reoxidised in air. Further work would be needed in order to evaluate this hypothesis. Under the assumption that the hair structure was not opened as a result of DTT-treatment, crosslinking would still have been expected to occur *via* the laccase-mediator route. Indeed, laccase from *Trametes versicolor* was shown to successfully form keratin-keratin bonds *via* vanillin-mediation in

solubilised keratin. Moreover, DTT has been shown to successfully penetrate the hair fibre and reduce disulfide bonds (see section 4.6.1.3.). Considering that DTT and vanillin are almost identical in size, vanillin should have been able to reach the hair cortex. This was, however, not observed, as indicated by an absence of improved tensile strength properties upon hair treatment with laccase. It may have been that laccase-oxidised vanillin, a highly reactive molecule with unpaired electrons, was unable to penetrate the hair as a result of strongly negative surface charge (higher in the case of damaged hair).[397,398] In addition, “over-crosslinking” has been described in the literature, where the sliding of keratin fibres becomes restricted as a result of increased intra- and intermolecular interactions, leading to decreases in elongation and, therefore, tensile strength.[59,108] It may therefore be of interest to evaluate hair crosslinking with varying enzyme concentrations and treatment durations.

6. Discussion, conclusions and future works

The potential of enzymes as milder and biocompatible alternatives to harsh chemicals currently used in permanent hair straightening treatments was investigated. The use of isolated enzymes indeed presents many advantages, such as low toxicity, high selectivity, atom-efficiency and mild reaction conditions.[27–30,34] Enzymatic catalytic steps for permanent hair straightening were predicted to involve the breaking of keratin disulfide bonds between keratin fibres by a first enzyme, followed by mechanical hair straightening and the formation of keratin-keratin crosslinks by a second enzyme to set the new morphology.

6.1. Thioredoxin system reducing activity on soluble keratin and solid human hair

Due to the importance of disulfide-thiol exchanges *in vivo*, a range of protein disulfide bond-reducing enzymes have been characterised.[163–167] Knowledge is, however, lacking towards the enzymatic reduction of disulfide bonds in keratin. While keratin is abundantly available as a waste product from a range of industries (e.g. poultry, leather), the large body of research looking at enzymes with keratin as a potential substrate has been directed towards its degradation or valorisation into a range of products, such as animal feed.[60,72,97–102] A range of keratin-degrading microorganisms have been identified over the years, including *Bacillus subtilis*, *Bacillus licheniformis* and *Streptomyces* spp.[25,26,29–31,97,98,120] The exact mechanism *via* which microbial degradation of keratin occurs remains unclear, but the combined action of keratinase enzymes and disulfide bond reduction is generally accepted.[21,30,98,123–126] Different hypotheses have emerged regarding how keratin disulfide bonds are broken in *vivo*, one being the concurrent secretion

of disulfide bond-reducing enzymes.[21,98] In this way, several keratin disulfide bond-reducing enzymes have been identified from keratin-degrading microorganisms.[25–27,98,120] The only sequence information available in the literature is the N-terminal sequence of "Enzyme 1" form *Bacillus halodurans*, which was shown to reduce disulfide bonds in keratin and oxidised glutathione.[24] It was therefore used as the starting point for a sequence search which identified potential enzyme candidates for the reduction of disulfide bonds in the context of permanent hair straightening. The well-characterised thioredoxin system from *Bacillus subtilis* was eventually selected for further investigations according to a range of factors, including its ability to reduce disulfide bonds in a range of protein substrates such as insulin, the small size of thioredoxin (11.4 kDa), as well as the keratin-degradation activity of *Bacillus subtilis*.[98,132,175,284,300]

The thioredoxin system from *Bacillus subtilis* was successfully expressed in *E. coli* and purified using IMAC, according to the method of Parker *et al.* (2014).[175] The disulfide bond-reducing activity of thioredoxin on folded protein substrates was successfully demonstrated on insulin (4.99 U/mg), based on DTT regeneration. This was done by monitoring the development of turbidity, based on the aggregation of insulin chain B upon disulfide bond reduction.[278] Interestingly, a lag was observed between disulfide bond reduction in insulin and the development of turbidity in solution, also noted in the literature.[278] While thioredoxins are regenerated to their reduced state *via* electron transfer from NADPH/thioredoxin reductase *in vivo*, the compatibility of DTT to selectively reduce thioredoxins in the presence of disulfide substrates was here confirmed.[278] As expected, a significantly higher rate of disulfide bond reduction by thioredoxin compared to DTT was observed.[278] Insulin disulfide bond reduction by the thioredoxin system from *Bacillus*

subtilis, based on NADPH/thioredoxin reductase regeneration, was then confirmed *via* the monitoring of NADPH consumption over the course of the reaction. A slow and steady NADPH consumption was noted in the absence of thioredoxin or substate, which was established as electron transfer occurring between molecular oxygen in air and the flavin ring system of thioredoxin reductase.[202] This slow and steady decrease was indeed corrected under anaerobic assay conditions. While this alternative NADPH consumption pathway had to be taken into consideration, the faster NADPH consumption rate associated with substrate disulfide bond reduction was easily distinguished. Aerobic assay conditions were therefore maintained, for ease. Commercial thioredoxin from *E. coli* was also investigated using the NADPH-consumption assay, for comparison, and yielded similar activities than its *Bacillus subtilis* counterpart. Interestingly, *E. coli* thioredoxin was successfully regenerated by thioredoxin reductase from *Bacillus subtilis, via* electron transfer from NADPH, despite the lack of cross-reactivity between organisms described in the literature.[172,174,178] The cleavage of intermolecular bonds by the thioredoxin system from *Bacillus subtilis*, attempted using oxidised glutathione as the substrate, was, however, not demonstrated. This was unsurprising considering that oxidised glutathione is usually reduced as part of the glutathione system, where glutathione reductase specifically recycles oxidised glutathione back to its reduced form.[318]

The thioredoxin system from *Bacillus subtilis* was then assayed on keratin substrates. Solubilised keratin, mainly Keratec™ IFP, was initially investigated aimed at avoiding any potential barriers to enzyme penetration associated with the use of solid keratin.[9,49,55,56,321] Indeed, hair is composed of highly crosslinked and tightly packed keratin chains forming the cortex, which are protected from environmental damage and penetration by

surrounding cuticle layers.[6,9,41,46] While the exact composition of Keratec™ IFP was not disclosed by Croda International, the solubilised wool substrate may have been prepared *via* oxidative sulfitolysis, a process during which cystines are converted to S-sulfocysteines.[288–290] It was therefore hypothesised that at least a portion of keratin disulfide bonds were converted to S-sulfocysteines over the course of wool solubilisation. Thiol availabilities in both Keratec™ IFP and solid human hair were confirmed *via* Ellman's assays following substrate incubation with an excess of DTT, a highly reactive reducing agent able to reduce disulfide bonds in keratin.[21,26,98,105,287] DTT was also shown to reduce S-sulfocysteine bonds.[320] Regarding Keratec™ IFP, a thiol content of 95.4 µmol/g of wool was calculated, compared to 920 µmol/g of cysteine described in the literature for Merino wool.[49] This discrepancy may have been due to not all disulfide bonds being available to DTT, as shown in solvent-extracted wool in the literature.[287,399] Regarding solid human hair, a thiol content of 10.95 µmol/g of hair was calculated compared to a cysteine content of 1435 µmol/g in hair described in the literature.[49,326] A few reasons were stipulated behind such a disparity. Firstly, the lack of DTT accessibility towards disulfide bonds described in the literature for soluble keratin would be expected to be more significant in solid substrates, especially in the heavily crosslinked and tightly-packed hair keratin.[287] Moreover, Ellman's assay is aimed at thiol quantification in solution. The potential adsorption of TNB^{2-} to reduced solid protein structures may therefore have prevented precise spectrophotometric measurements.[321] Nonetheless, the penetration of DTT, a 154 Da compound, into the hair cortex was here observed, in line with work conducted by Cruz *et al.* (2017) and Malinauskyte *et al.* (2020).[48,57] The authors indeed observed the penetration of low and mid-molecular weight peptides, up to 2,577 Da, into

the hair cortex, while high molecular weight peptides (> 75,000 Da) were seen to adsorb onto the hair surface.

The ability of the thioredoxin system from *Bacillus subtilis* to reduce sulfur-sulfur bonds in soluble keratin was then demonstrated, both *via* NADPH consumption and Ellman's assays. While thioredoxins are known to catalyse disulfide bond reductions in protein substrates, these enzymes have also been shown to reduce S-sulfocysteine bonds to cysteine.[189–191] In this way, the significant reducing activity observed for the *Bacillus subtilis* thioredoxin system on Keratec™ IFP may have been associated with the reduction of disulfide bonds, S-sulfocysteine bonds, or a mixture of both. This was further explored *via* the quantification of thiol release, resulting from thioredoxin system incubation with Keratec™ IFP, using Beer-Lambert law in the context of both NADPH consumption and Ellman's assays. While Ellman's assays are associated with the direct detection of thiol release, NADPH-based assays monitor NADPH consumption associated with disulfide (or S-sulfocysteine) reduction. The correspondence between NADPH consumption and thiol release, therefore, depends on the nature of the bonds being broken. Indeed, while the reduction of disulfide bonds would correspond to the release of two thiols per NADPH equivalent, the reduction of S-sulfocysteine would be associated with the release of one thiol, alongside sulfite. In this way, the 1 to 1.7 molar equivalence calculated between NADPH consumption (NADPH-based assay) and total thiol release (Ellman's assay) may further indicate a mixture of both disulfide and S-sulfocysteine bonds in Keratec™ IFP. However, sulfite ions may have been interfering with Ellman's assay by reacting with DTNB.[324,325] Moreover, the fact that for each disulfide bond equivalent in Keratec™ IFP, there may be two S-sulfocysteines was also not considered here.

The disulfide bond-reducing activity of the thioredoxin system from *Bacillus subtilis* was then explored on hair, using NADPH-based and Ellman's assays. Considering the ability of the thioredoxin system to reduce both disulfide and S-sulfocysteine bonds, coupled with the clear reducing activity detected in this study on soluble keratin, the apparent lack of enzymatic disulfide bond reduction observed in hair was attributed to the highly crosslinked and tightly packed structure of the substrate, preventing enzymes from reaching the hair cortex.[6,9,41,46,321] In this way, a range of methods were investigated towards the potential opening of the hair structure for easier enzyme penetration. These included hair grinding, delipidation, swelling, and solubilisation.[27,57,106,334,335,58–62,66,67,104] The absence of enzymatic disulfide bond reduction observed with ground hair as the substrate was put down to the lack of keratin structure opening associated with the grinding process. Hair was solubilised according to two methods, using either NaOH or [EMIM]ESO_4, however, hair disulfide bonds were believed to have been broken during both solubilisation processes, the latter also yielding a highly dark and viscous liquid which was not compatible with spectrophotometric measurements.[104,106] While some level of keratin structure opening was detected *via* SEM following hair treatment with urea, Tween 20 and various ionic liquids, the thioredoxin system was not able to penetrate the hair cortex, as indicated by the absence of disulfide bond reduction observed.[30]

In a further attempt to allow *Bacillus subtilis* thioredoxin penetration into the hair cortex to reduce disulfide bonds, the cleavage of peptide bonds by keratinase (KerA) from *Bacillus licheniformis* was then investigated. Commercial keratinase from *Bacillus licheniformis* was used following failed attempts at expressing the enzyme in *E. coli*, which were potentially

associated with the presence of the signal peptide in the gene sequence.[134,339,340] The well-characterised KerA belongs to the family of keratinases, which catalyse the hydrolysis of peptide bonds in recalcitrant keratin substrates.[25,31,32] Improved keratinase activities in the presence of reducing agents have been readily reported in the literature, though the exact mechanism remains unclear.[21,22,342–345,26,28,30,33,128,156,162,341] It was here hypothesised that reducing agents, by their small sizes, may penetrate into hair keratin, and allow the opening of the keratin structure by reducing disulfide bonds, thus facilitating enzymatic penetration and providing better access to the proteolytic cleavage sites in the keratin backbone.[346] This was confirmed *via* keratin azure assays, which revealed enzymatic keratinolytic activity only in the presence of DTT. DTT, which was selected for its reported efficiency at yielding high keratinolytic activity, allowed keratinase penetration into solid keratin, which would otherwise not be possible due to its size (32 kDa).[21,26,98,105,287] Despite attempts to shift towards milder reducing agents such as cysteine and glutathione, DTT activity remained unmatched.[48,59,348–350] Various attempts were made at further improving keratinase activity on solid keratin substrates in the form of substrate chopping, swelling (increased pH, urea), and increased incubation temperature, but no increase in enzymatic activity was detected.[58–62,285,334,346,352] Interestingly, higher absorbances were observed across all samples, including substrate-only controls in the presence of urea or alkaline pH. This may have been due to higher susceptibility of dye-release from keratin azure as a result of fibre swelling.[400] Overall, significant variations were observed across keratin azure assay replications, where Remazol Brilliant Blue was seen to slowly leach out of the keratin structure at higher incubation temperatures. Therefore, the keratin azure assay's reliability was

questioned, in line with a lack of sensitivity and standardisation reported in the literature.[285,354]

While the effect of disulfide bond reduction on keratinase activity has been vastly reported in the literature, the potential impact of keratinolysis on disulfide bond reduction has not been assessed.[22,26,344,345,28,33,128,156,162,341–343] As keratinase from *Bacillus licheniformis* appeared to rely on the reduction of solid keratin disulfide bonds to cleave peptides bonds, it was hypothesised that the cleavage of peptide bonds may, in turn, expose further disulfide bonds for reduction by DTT. The addition of keratinase to both keratin azure and hair was associated with slightly increased disulfide bond reduction levels in the presence of DTT, however, variations were again observed across replications. This was put down to the potential adsorption of TNB^{2-} to solid keratin structure during Ellman's assay, preventing precise spectrophotometric thiol quantifications.[321] The potential increase in disulfide bond reduction in the presence of keratinase was further explored using the thioredoxin system from *Bacillus subtilis*. More specifically, the ability of keratinase to render disulfide bonds in solid keratin substrates available for enzymatic reduction was investigated. However, an absence of disulfide bond-reducing activity of the thioredoxin system on hair was observed, despite substrate pre-incubation with keratinase. This was not entirely surprising as keratinase had been shown to rely on disulfide bond reduction by DTT to cleave peptide bonds in solid substrates. It was therefore concluded that the sizes of both thioredoxin and keratinase enzymes prevented their penetration of highly-crosslinked and densely packed hair.

Future work may be conducted towards identifying the exact mechanism behind the reduction of sulfur-sulfur bonds in Keratec™ IFP, *via* sulfite detection, for example.[401] This may provide confirmation towards whether

keratin intermolecular disulfide bonds are being reduced by the thioredoxin system from *Bacillus subtilis*. The hypothesis suggesting that enzyme penetration is the main barrier to enzymatic disulfide bond reduction in hair may, in this way, be confirmed. Additional investigations may explore ways to improve enzymatic penetration in hair, as well as alternative enzyme candidates (Appendix Table 4.2-3). Moving away from enzymes relying on cofactors, such as NADPH, would present a cost advantage towards potential reaction scale-up. Protein disulfide isomerases (PDI), which catalyse the formation and breakage of disulfide bonds, may be considered as potential candidates.[211,402] The development of robust assays towards the detection of disulfide bond reduction and peptide bond breaking in solid hair may further facilitate the evaluation of enzymes as active agents for permanent hair straightening. Further research towards a better understanding of keratin degradation in *vivo* may also be relevant, providing better insights towards the mechanism by which an extracellular keratinase and intracellular protein disulfide reductase can work jointly. The potential secretion of an intracellularly-generated reducing power has been described in the literature.[98]

6.2. Enzymatic crosslinking of soluble keratin and solid human hair

The permanent setting of natural macromolecules, for the modification of appearance and performance properties, has been a topic of growing interest in various industries (e.g. textile, cosmetic). In this way, a wide range of protein crosslinking enzymes have been identified and characterised, with relevance to many potential applications such as improving meat structure and increasing wool strength.[35–40] While the reduction of disulfide bonds in highly-crosslinked substrates may be a prerequisite, the potential for

crosslinking formation is not limited to thiol-thiol interactions.[48,59,88,91,108] Three enzymes were here investigated towards keratin crosslinking in the context of permanent hair straightening: laccase from *Trametes versicolor*, tyrosinase from mushroom, and microbial transglutaminase. These enzymes were selected for a range of reasons, including high activity, relatively large substrate range, known activity on folded proteins, current uses in industry and absence of toxic by-product generation.[35–40] Transglutaminases are known to catalyse the crosslinking of glutamine and lysine protein side chains *via* a proteinyl-enzyme-thioester intermediate, while laccases and tyrosinases react with tyrosine side chains, amongst others, in proteins to generate radical and diphenol reactive species, respectively, which may then undergo successive protein crosslinking.[34,35,224,235,236,244,245] Of particular relevance in the context of difficulties encountered towards enzymatic hair penetration, the use of small molecules (mediators) as electron-shuttles for laccases may help overcome redox or steric barriers to activity.[237,242,243] While laccases, tyrosinases and transglutaminase have been investigated towards the crosslinking of wool keratin to increase tensile strength and performance, the focus has been placed on binding compounds to keratin rather than on the formation of keratin-keratin crosslinks.[40,72,107,231,260,265,266] The only evidence of enzymatic keratin-keratin crosslinking was shown for microbial transglutaminases on protease or reducing agent-pre-treated wool keratin.[40,107,231] In this way, the enzymatic formation of keratin-keratin crosslinks in human hair has not been explored.

The standard activities of laccase (3.11 U/mg), tyrosinase (10.83 U/mg) and transglutaminase (14.11 U/mg) were successfully demonstrated spectrophotometrically on known substrates (ABTS, L-DOPA and Cbz-Gln-Gly, respectively).[244,282,361] All three enzymes retained significant activity in

deionised water despite laccase's optimal pH of 5. This was particularly useful for investigations on Keratec™ IFP to avoid substrate precipitation encountered at lower pHs, as well as towards the development of mild processes. Solubilised wool substrates, Keratec™ IFP and Keratec™ ProSina, were first investigated as soluble keratin substrates in an attempt to reduce barriers to enzymatic penetration associated with solid keratin substrates.[321] However, significant activity inhibition was observed across enzymes in the presence of those soluble substrates. Several hypotheses were formulated to justify these observations, such as the potential interference of solubilised wool with the assays, of particular relevance to the spectrophotometric monitoring of ABTS oxidation by laccase. As a laccase mediator, oxidised ABTS may have been reacting with tyrosine side chains in keratin, thus interfering with laccase activity analyses.[244] It was, however, deemed unlikely that solubilised wool would be interfering with all three standard assays. In this way, the effect of removing potentially disruptive additives from Keratec™ IFP and Keratec™ ProSina, of which the exact composition is not known, was investigated *via* dialysis. While the viscous nature of both substrates may have led to partial additive removal, dialysed Keratec™ IFP and Keratec™ ProSina were associated with much lower levels of enzyme inhibition than undialysed substrates. These observations were put down to the relatively high salt contents in both Keratec™ IFP and Keratec™ ProSina. Indeed, salts have been shown to inhibit the reduction of oxygen to water at the Type 2/3 copper sites in laccase, causing a break in electron acceptance and, therefore, in enzymatic activity.[253,254] Keratin crosslinking investigations were thus conducted using dialysed Keratec™ substrates, before moving onto solid human hair.

While a range of potential crosslinking assays were trialled towards the detection of enzymatic protein crosslinking in soluble substrates, SDS PAGE and SEC appeared as the most compatible methods.[38,39,81,107,283,356–358] Untreated Keratec™ substrates were initially assessed as controls for further crosslinking analyses. Significant smearing was observed for both Keratec™ IFP and Keratec™ ProSina on SDS PAGE gels, in alignment with soluble keratin analyses reported in the literature.[81,359,373] Despite the wide range of molecular weights detected for these solubilised wool substrates, thicker bands were obtained at 40-50 kDa for Keratec™ IFP and 5-20 kDa for Keratec™ ProSina. Regarding SEC, a calibration curve was plotted using globular standard proteins, such as carbonic anhydrase and BSA, which revealed discrepancies between SEC and SDS PAGE Keratec™ IFP molecular weight analyses. This may have been linked to the oligomeric states of Keratec™ IFP proteins, as SEC and SDS PAGE respectively measure the native and subunit molecular weights of proteins. Moreover, the globular proteins used as standards may diffuse further into the column pores than fibrous proteins, such as keratin, and, as a result, exhibit comparatively lower molecular weights (later elution).[376] Similar difficulties in obtaining accurate molecular weight information with SEC for proteins based on calibration curves have been reported in the literature.[381–384] SEC was thus mainly used for the qualitative analysis of potential molecular weight increases associated with protein crosslinking based on comparisons between untreated and treated keratin substrates. Notably, the presence of elution peaks in SEC chromatograms was seen to correlate with thicker bands observed on SDS PAGE gels. Indeed, Keratec™ IFP SEC analysis was associated with peaks in two main retention volume regions (8-10 mL & 15-20 mL, with a large peak at around 30 mL removed with dialysis), corresponding to molecular weights of 40-50 kDa and 10-15 kDa,

respectively, as indicated by SDS PAGE analysis. One main elution peak in the 15-20 mL region was observed for Keratec™ ProSina, in accordance with the 5-20 kDa molecular weights revealed by SDS PAGE.

Upon the treatment and SEC analysis of Keratec™ IFP with laccase from *Trametes versicolor*, shifts in the 8-10 mL elution peaks were detected towards higher molecular weights, across replications. The apparition of small peaks in the 10-15 mL region was also noted compared to the untreated substrate. These observations, described in the literature as potential evidence for crosslinking, indicated an increase in protein molecular weight.[39] In this way, while the laccase-catalysed formation of keratin-keratin bonds had not been described in the literature, Keratec™ IFP was successfully crosslinked by laccase from *Trametes versicolor* in this study.[39,389] The ability of laccase to catalyse the single-electron abstraction from tyrosine, tryptophane or cysteine side chains in soluble keratin, and the subsequent crosslinking with other keratin side chains was indeed demonstrated.[35,227,235,236,244,245] The potential of another highly active white-rot fungi laccase from *Pleurotus ostreatus* to catalyse the formation of keratin-keratin crosslinks in Keratec™ IFP was also investigated and confirmed *via* SEC.[363–365] While laccase activity on solubilised keratin was confirmed, the addition of naturally-occurring vanillin and acetosyringone mediators was also explored, due to their ability to enhance crosslinking by increasing the accessibility of reactive amino acids.[250,252,257,363–365] The incubation of Keratec™ IFP with laccase and vanillin or acetosyringone was associated with more significant peak shifts towards higher molecular weights and the apparition of higher intensity-peaks in the 10-15 mL region on SEC chromatograms, compared to in the absence of mediators. These observations may have indicated enhanced keratin-keratin crosslinking in

the presence of mediators, in line with the expected increased accessibility of keratin amino acids to mediators compared to laccase.[250] Moreover, laccases have been reported to preferentially react with mediators over protein amino acids.[256] Therefore, the formation of keratin-keratin crosslinks in solubilised wool was demonstrated here, both *via* the laccase-only and laccase-mediator pathways.[247] The latter was of particular interest towards the investigation of enzymatic crosslinking in solid human hair, as a way to potentially overcome barriers to enzyme penetration.

SDS PAGE analyses were also conducted towards the potential laccase-catalysed crosslinking of Keratec™ IFP. Significant band disappearances were observed both in the presence and absence of mediators, described in the literature as an indication of substrate crosslinking.[38,39,107,357,358] Despite a lack of high molecular weight proteins aggregated in gel wells usually observed upon crosslinking, the combination of SEC and SDS PAGE results suggested that soluble keratin was successfully crosslinked by laccase, both in the presence and absence of mediators. Keratec™ ProSina was then investigated as a lower molecular weight-solubilised wool substrate. However, no indications of crosslinking were observed upon SDS PAGE and SEC analyses. This may have been linked to the more challenging detection of smaller crosslinked peptides, associated with lower molecular weight differences between monomers, dimers and polymers, compared to larger crosslinked proteins.

Tyrosinase from mushroom and microbial transglutaminase were then investigated towards keratin-keratin crosslinking in Keratec™ IFP. SEC analyses revealed a lack of peak formation or shift towards higher molecular weights upon treatment with either enzyme, suggesting an absence of crosslinking activity.[39] Although no band disappearance was detected with

SDS PAGE, significant increases in proteins aggregated were observed in wells for tyrosinase and transglutaminase-treated Keratec™ IFP, compared to the untreated substrate. It was thus hypothesised that keratin-keratin crosslinking may have indeed taken place and led to substrate aggregation. However, these crosslinked-protein aggregates would have been removed by the filtration step prior to sample injection into the SEC column, which would explain the lack of crosslinking observed, in line with the disappearance of peaks at 8-10 mL retention volumes observed upon substrate treatment with either tyrosinase or transglutaminase. However, these results obtained *via* SEC and SDS PAGE analyses did not constitute unambiguous evidence that keratin-keratin crosslinking had occurred. The high degree of complexity of the substrate was suggested as a potential barrier to tyrosinase and transglutaminase crosslinking, as reported in the literature.[35,39,226]

The promising keratin-keratin crosslinking ability of laccase from *Trametes versicolor* for soluble keratin, both in the presence and absence of mediators, was then further investigated on solid hair *via* tensile strength analyses. Improvements in tensile properties have been described in the literature following hair crosslinking, with a limit above which keratin fibres become restricted as a result of increased intra- and intermolecular interactions, resulting in decreased fibre tensile strength and elongation.[59,108] Hair samples were pre-treated with DTT in an attempt to open up the hair structure and facilitate enzyme penetration, as observed with keratinase.[107,108,389] However, reduced fibres exhibited surprisingly high tensile strength, suggesting that the hair may have been reoxidised in air, prior to enzymatic treatment. The treatment of reduced hair with laccase from *Trametes versicolor*, in the presence and absence of vanillin, had no

significant effect on fibre tensile strength. Under the assumption that laccase (63 kDa) was not able to penetrate into the hair cortex, crosslinking *via* the laccase-mediator route would still have been expected. Indeed, both vanillin and DTT are very similar in size, and the latter has been shown to successfully penetrate the hair fibre. Moreover, human hair was shown to contain higher proportions of tyrosine and cysteine amino acids, of particular relevance to laccase catalysis, than Keratec™ IFP, which was successfully crosslinked by laccase both in the presence and absence of vanillin.[49] It was thus hypothesised that the penetration of laccase-oxidised vanillin, a highly reactive molecule with unpaired electrons, maybe have been affected by negative charges at the hair surface, which are higher in the case of damaged hair.[397,398]

Additional work may involve the exploration of a wider range of assays for the robust detection of keratin crosslinking. While crosslinking analyses *via* mass spectrometry may be hindered by substrate complexity, SEC fractionation-mass spectrometry may be of interest.[384,403,404] Regarding SEC, mass transfer analyses may be carried out to evaluate whether crosslinked-keratin aggregates are being removed by filtration prior to analysis. While laccases from white-rot fungi appeared as promising crosslinking candidates for solubilised keratin, with high activity at physiological pH and water as only by-product, it may be relevant to explore laccases from a larger selection of organisms. The laccase-mediator pathway may provide a solution to penetration issues associated with the large sizes of enzymes; therefore, a wider range of mediators may be explored. Additional investigations towards the exact mechanism of laccase-catalysed crosslinking may also help gain an understanding of specific side chains being targeted by the enzyme. Further work towards the detection of enzymatic crosslinking in solid hair

may involve both wet and dry tensile strength analyses, looking into the effect of varying enzymatic concentration and incubation duration, as well as investigating the need and success of a pre-treatment reduction step. While some highly efficient permanent hair straightening treatments have shown to rely solely on keratin fibre crosslinking (e.g. formaldehyde), it may be that successful enzymatic crosslinking of hair would be sufficient for permanent hair straightening, with no necessary preliminary disulfide bond reduction and, therefore, less potential damage.[5,18,45,63,76–79]

This project explored the potential use of enzymes as biocompatible active agents in the context of permanent hair straightening. Current treatments available on the market rely on harsh chemicals and have been associated with severe risks to both consumers and hair-dressing professionals alike. Therefore, the development of milder and greener alternatives represents an exciting research opportunity. Enzymatic permanent hair straightening was envisaged as a two-step process. A first enzyme would break disulfide bonds in hair, allowing for the opening of the hair structure, which would then be mechanically straightened. A second enzyme would then allow the permanent setting of the new morphology *via* the formation of crosslinks in hair. While enzymes naturally catalyse disulfide bond reduction and crosslink formation reactions *in vivo*, there is a clear lack of knowledge regarding the potential of keratin as a substrate. To address this critical gap in the literature, the enzymatic disulfide bond reduction and crosslinking of soluble and solid keratin was investigated in this project. In this way, the thioredoxin system from *Bacillus subtilis* was shown to break sulfur-sulfur bonds, in the form of S-sulfocysteine or disulfide bonds, in solubilised wool, an observation novel to this project. However, this promising activity on soluble keratin did not

translate onto solid keratin substrates such as human hair. Human hair is known for its highly crosslinked and tightly packed structure, where a cuticle layer prevents penetration into the hair cortex. Despite multiple attempts at opening the hair structure to facilitate enzymatic penetration, no disulfide bond reduction was detected. Barriers to penetration were also encountered in the context of enzymatic crosslinking of hair. While the formation of keratin-keratin crosslinks was demonstrated in solubilised wool by laccase from white-rot fungi, this novel activity could not, however, be replicated in human hair. Despite the promising enzymatic activities on soluble keratin unveiled in this study, challenges remain towards the delivery mechanism of those enzymes into the hair cortex to allow for the catalysis of relevant modifications in the context of permanent hair straightening.

The research presented in this thesis sets the foundation for future investigations towards the suitability of enzymes as efficient biocompatible active agents, within the cosmetic sector and beyond. The successful development and formulation of an enzymatic permanent hair straightening treatment holds great promise to enhance the quality of life of customers globally, as a milder and greener alternative to current methods,

7. References

1 Statistica, Size of the global hair care market from 2012 to 2024, https://www.statista.com/statistics/254608/global-hair-care-market-size/, (accessed 20 November 2018).

2 R. Potter, Biotech in Cosmetics, https://theeconreview.com/2017/11/12/biotech-in-cosmetics/, (accessed 10 January 2019).

3 S. Asbeck, C. Riley-Prescott, E. Glaser and A. Tosti, *Cosmetics*, 2022, **9**, 17.

4 V. N. B. Sishi, J. C. Van Wyk and N. P. Khumalo, *South African Med. J.*, 2019, **109**, 941–946.

5 A. L. Miranda-Vilela, A. J. Botelho and L. A. Muehlmann, *Int. J. Cosmet. Sci.*, 2014, **36**, 2–11.

6 R. J. Patinvoh, O. A. Osadolor, K. Chandolias, I. Sárvári Horváth and M. J. Taherzadeh, *Bioresour. Technol.*, 2017, **224**, 13–24.

7 L. J. Wolfram, *J. Am. Acad. Dermatol.*, 2003, **48**, 106–14.

8 Z. D. Draelos, *Hair care : an illustrated dermatologic handbook*, CRC Press, 2004.

9 M. F. D. Gavazzoni Dias, *Int. J. Trichology*, 2015, **7**, 2–15.

10 B. Bhushan, in *Biophysics of Human Hair*, Springer, Berlin, 2010, pp. 1–19.

11 O. A. Olasode, *J. Pakistan Assoc. Dermatologists*, 2009, **19**, 203–207.

12 A. J. McMichael, *J. Investig. Dermatology Symp. Proc.*, 2007, **12**, 6–9.

13 B. J. Kaur, H. Singh and A. Lin-Greenberg, *J. Natl. Med. Assoc.*, 2002, **94**, 121–123.

14 R. D. Sinclair, *J. Investig. Dermatology Symp. Proc.*, 2007, **12**, 2–5.

15 A. J. McMichael, *J. Am. Acad. Dermatol.*, 2003, **48**, 127–133.

16 D. Rucker Wright, R. Gathers, A. Kapke, D. Johnson and C. L. Joseph, *J. Am. Acad. Dermatol.*, 2011, **64**, 253–262.

17 European Patent Office, EP0809481B1, 1996.

18 J. N. Hatsbach de Paula, F. M. A. Basílio and F. A. Mulinari-Brenner, *An. Bras. Dermatol.*, 2022, **97**, 193–203.

19 S. Pitman, How biotechnology has impacted the cosmetics business in 2016, https://www.cosmeticsdesign.com/ARTICLE/2016/12/12/HOW-BIOTECHNOLOGY-HAS-IMPACTED-THE-COSMETICS-BUSINESS-IN-2016, (accessed 10 January 2019).

20 K. V. Sajna, R. K. Sukumaran and L. D. Gottumukkala, in *Industrial*

Biorefineries & White Biotechnology, Elsevier, 2015, pp. 607–652.

21 J. Qiu, C. Wilkens, K. Barrett and A. S. Meyer, *Biotechnol. Adv.*, 2020, **44**, 107607.

22 Z. W. Li, S. Liang, Y. Ke, J. J. Deng, M. S. Zhang, D. L. Lu, J. Z. Li and X. C. Luo, *Commun. Biol.*, 2020, **3**, 1–13.

23 C. G. Cai, B. G. Lou and X. D. Zheng, *J. Zhejiang Univ. Sci. B*, 2008, **9**, 60–67.

24 P. Prakash, S. K. Jayalakshmi and K. Sreeramulu, *Appl. Microbiol. Biotechnol.*, 2010, **87**, 625–633.

25 X. Lin, D. W. Kelemen, E. S. Miller and J. C. H. Shih, *Appl. Environ. Microbiol.*, 1995, **61**, 1469–1474.

26 S. Yamamura, Y. Morita, Q. Hasan, K. Yokoyama and E. Tamiya, *Biochem. Biophys. Res. Commun.*, 2002, **294**, 1138–1143.

27 S. Rahayu, D. Syah and M. Thenawidjaja Suhartono, *Biocatal. Agric. Biotechnol.*, 2012, **1**, 152–158.

28 S. Gupta and R. Singh, *Indian J. Microbiol.*, 2014, **54**, 466–470.

29 P. Prakash, S. K. Jayalakshmi and K. Sreeramulu, *Appl. Microbiol. Biotechnol.*, 2010, **87**, 625–633.

30 L. Navone and R. Speight, *PLoS One*, 2018, **13**, 1–21.

31 X. Lin, C. G. Lee, E. S. Casale and J. C. H. Shih, *Appl. Environ. Microbiol.*, 1992, **58**, 3271–5.

32 H. Hu, J. He, B. Yu, P. Zheng, Z. Huang, X. Mao, J. Yu, G. Han and D. Chen, *Biotechnol. Lett.*, 2013, **35**, 239–244.

33 P. Ramnani, R. Singh and R. Gupta, *Can. J. Microbiol.*, 2005, **51**, 191–196.

34 R. M. A. Maddock, G. J. Pollard, N. G. Moreau, J. J. Perry and P. R. Race, *Biopolymers*, 2020, **111**, 1–17.

35 T. Heck, G. Faccio, M. Richter and L. Thöny-Meyer, *Appl. Microbiol. Biotechnol.*, 2013, **97**, 461–475.

36 B. Caballero, L. Trugo and P. Finglas, in *Encyclopedia of food sciences and nutrition: Volumes 1-10*, 2003, pp. 1436–48.

37 M. Kieliszek and A. Misiewicz, *Folia Microbiol. (Praha).*, 2014, **59**, 241–250.

38 G. H. a. De Jong and S. J. Koppelman, *J. Food Sci.*, 2002, **67**, 2798–2806.

39 S. Jus, I. Stachel, M. Fairhead, M. Meyer, L. Thöny-Meyer and G. M. Guebitz, *Biocatal. Biotransformation*, 2012, **30**, 86–95.

40 G. Du, L. Cui, Y. Zhu and J. Chen, *Enzyme Microb. Technol.*, 2007, **40**, 1753–1757.

41 H. Lee, K. Noh, S. C. Lee, I. K. Kwon, D. W. Han, I. S. Lee and Y. S. Hwang, *Tissue Eng. Regen. Med.*, 2014, **11**, 255–265.

42 A. L. Horvath, *ScientificWorldJournal.*, 2009, **9**, 255–271.

43 B. Wang, W. Yang, J. McKittrick and M. A. Meyers, *Prog. Mater. Sci.*, 2016, **76**, 229–318.

44 H. H. Bragulla and D. G. Homberger, *J. Anat.*, 2009, **214**, 516–559.

45 C. Cruz, C. Costa, A. Gomes, T. Matamá and A. Cavaco-Paulo, *Cosmetics*, 2016, **3**, 26.

46 R. Araújo, M. Fernandes and A. Cavaco-paulo, Artur, Gomes, *Adv. Biochem. Eng. Biotechnol.*, 2010, **11**, 121–143.

47 C. Bolduc and J. Shapiro, *Clin. Dermatol.*, 2001, **19**, 431–436.

48 C. F. Cruz, M. Martins, J. Egipto, H. Osório, A. Ribeiro and A. Cavaco-Paulo, *RSC Adv.*, 2017, **7**, 51581–51592.

49 C. Popescu and H. Höcker, *Chem. Soc. Rev.*, 2007, **36**, 1282–91.

50 B. Wang, W. Yang, J. McKittrick and M. A. Meyers, *Prog. Mater. Sci.*, 2016.

51 I. Guryanov, E. Naumenko and R. Fakhrullin, *Appl. Surf. Sci. Adv.*, 2022, **7**, 1–11.

52 P. Strnad, V. Usachov, C. Debes, F. Grä, D. A. D. Parry and M. Omary Bishr, *J. Cell Sci.*, 2011, **124**, 4221–32.

53 J. Yu, D. wen Yu, D. M. Checkla, I. M. Freedberg and A. P. Bertolino, *J. Invest. Dermatol.*, 1993, **101**, 56–59.

54 J. Chao, A. E. Newsom, I. M. Wainwright and R. A. Mathews, *j. Soc. Cosmet. Chem*, 1979, **30**, 401–413.

55 B. Bhushan, *Prog. Mater. Sci.*, 2008, **53**, 585–710.

56 B. Bhushan and C. Latorre, in *Nanotribology and Nanomechanics (Second Edition): An Introduction*, 2008, pp. 1325–1485.

57 E. Malinauskyte, R. Shrestha, P. A. Cornwell, S. Gourion-Arsiquaud and M. Hindley, *Int. J. Cosmet. Sci.*, 2021, **43**, 26–37.

58 A. Tinoco, A. F. Costa, S. Luís, M. Martins, A. Cavaco-Paulo and A. Ribeiro, *Appl. Sci.*, 2021, **11**, 1–15.

59 H. Xu, K. Song, B. Mu and Y. Yang, *ACS Omega*, 2017, **2**, 1760–1768.

60 P. M. M. Schrooyen, P. J. Dijkstra, R. G. Oberthü, A. Bantjes and J. Feijen, *J. Agric. Food Chem.*, 2000, **48**, 4326–4334.

61 R. S. Asquith and A. K. Booth, *Text. Res. J.*, 1970, **40**, 1–10.

62 M. F. Bories, M. C. Martini, M. F. Bobin Et and J. Cotte, *Int. J. Cosmet. Sci.*, 1984, **6**, 213–229.

63 N. V. Patil and A. N. Netravali, *Fibers*, 2022, **10**, 1–14.

64 C. Davis, P. N. A. Khofar, U. K. A. Karim, R. A. Rashid, M. M. Mahat and M. I. A. Halim, *Mater. Today Proc.*, 2019, **29**, 244–249.

65 B. Singh and S. Umapathy, *J. Biophotonics*, 2011, **4**, 315–323.

66 A. L. V. Villa, M. R. S. Aragão, E. P. dos Santos, A. M. Mazotto, R. B. Zingali, E. P. de Souza and A. B. Vermelho, *BMC Biotechnol.*, 2013, **13**, 1–11.

67 M. Essendoubi, M. Meunier, A. Scandolera, C. Gobinet, M. Manfait, C. Lambert, D. Auriol, R. Reynaud and O. Piot, *Int. J. Cosmet. Sci.*, 2019, **41**, 203–212.

68 D. Mondragon De La Cruz, Bangor University, 2020.

69 N. H. Federation, Hair and Beauty Industry Statistics, https://www.nhf.info/advice-and-resources/hair-and-beauty-industry-statistics/, (accessed 2 December 2018).

70 A. N. Syed and A. R. Naqvi, *Cosmet. Toilet.*, 2000, **115**, 47–52.

71 N. M. George and A. Potlapati, *Int. J. Res. Dermatology*, 2021, **7**, 748–752.

72 J. M. Cardamone, *J. Mol. Struct.*, 2010, **969**, 97–105.

73 L. S. Abraham, A. M. Moreira, L. H. De Moura, M. F. R. Gavazzoni Dias and F. A. S. A. Addor, *Surg. Cosmet. Dermatology*, 2009, **1**, 178–185.

74 US20020159962A1, 2002.

75 J. McKittrick, P. Y. Chen, S. G. Bodde, W. Yang, E. E. Novitskaya and M. A. Meyers, *JOM*, 2012, **64**, 449–468.

76 C. L. Galli, F. Bettin, P. Metra, P. Fidente, E. De Dominicis and M. Marinovich, *Regul. Toxicol. Pharmacol.*, 2015, **72**, 562–568.

77 M. H. Maneli, P. Smith and N. P. Khumalo, *J. Am. Acad. Dermatol.*, 2014, **70**, 276–280.

78 J. L. Mazzei, É. V. Figueiredo, L. J. Da Veiga, C. A. F. Aiub, P. I. C. Guimarães and I. Felzenszwalb, *J. Appl. Toxicol.*, 2010, **30**, 8–14.

79 M. P. Galiotte, P. Kohler, G. Mussi and G. J. Figaro Gattás, *Ann. Occup. Hyg.*, 2008, **52**, 645–651.

80 W. S. Simpson and G. Crawshaw, *Wool: Science and technology*, 2002.

81 C. Tonin, A. Aluigi, A. Varesano and C. Vineis, *Nanofibers*, 2010, **86**, 139–158.

82 M. V. R. Velasco, *Int. J. Trichology*, 2022, **14**, 197–203.

83 T. Barreto, F. Weffort, S. Frattini, G. Pinto, P. Damasco and D. Melo, *Ski. Appendage Disord.*, 2021, **7**, 265–271.

84 A. Miranda-Vizuete, A. E. Damdimopoulos, J. Å. Gustafsson and G. Spyrou, *J. Biol. Chem.*, 1997, **272**, 30841–30847.

85 S. E. Anderson, K. K. Brown, L. F. Butterworth, A. Fedorowicz, L. G. Jackson, H. F. Frasch, D. Beezhold, A. E. Munson and B. J. Meade, *J. Immunotoxicol.*, 2009, **6**, 19–29.

86 B. Ma, X. Qiao, X. Hou and Y. Yang, *Int. J. Biol. Macromol.*, 2016, **89**, 614–621.

87 A. Kuzuhara and T. Hori, *Biopolymers*, 2005, **79**, 324–334.

88 S. Y. Kim, J. H. Kim, Y. Kang, J. W. Yoo, J. Choi and H. J. Lee, *J. Clean. Prod.*, 2022, **363**, 132535.

89 A. Rinaldi, Healing beauty?, http://embor.embopress.org/content/9/11/1073.full, (accessed 11 January 2019).

90 S. Fagien, *Plast. Reconstr. Surg.*, 1999, **103**, 701–713.

91 C. Leichner, C. Steinbring, R. A. Baus, D. Baecker, R. Gust and A. Bernkop-Schnürch, *J. Colloid Interface Sci.*, 2019, **534**, 533–541.

92 M. Pereira-Silva, A. M. Martins, I. Sousa-Oliveira, H. M. Ribeiro, F. Veiga, J. Marto and A. C. Paiva-Santos, *Acta Biomater.*, 2022, **142**, 14–35.

93 Croda International, Microbial biotechnology in cosmetics, https://www.crodapersonalcare.com/en-gb/our-brands/sederma/microbial-biotechnology-in-cosmetics, (accessed 15 March 2022).

94 W. Liu and P. Wang, *Biotechnol. Adv.*, 2007, **25**, 369–84.

95 S. Li, X. Yang, S. Yang, M. Zhu and X. Wang, *Comput. Struct. Biotechnol. J.*, 2012, **2**, 1–11.

96 P. L. Gupta, M. Rajput, T. Oza, U. Trivedi and G. Sanghvi, *Nat. Products Bioprospect.*, 2019, **9**, 267–278.

97 P. Prakash, S. K. Jayalakshmi and K. Sreeramulu, *Appl. Biochem. Biotechnol.*, 2010, **160**, 1909–1920.

98 Z. Peng, J. Zhang, G. Du and J. Chen, *ACS Sustain. Chem. Eng.*, 2019, **7**, 9727–9736.

99 M. Dąbrowska, A. Sommer, I. Sinkiewicz, A. Taraszkiewicz and H. Staroszczyk, *Environ. Sci. Pollut. Res.*, 2022, **29**, 24145–24154.

100 Y. Zhang, W. Zhao and R. Yang, *ACS Sustain. Chem. Eng.*, 2015, **3**, 2036–2042.

101 X. Liu, Y. Nie, Y. Liu, S. Zhang and A. L. Skov, *ACS Sustain. Chem. Eng.*, 2018, **6**, 17314–17322.

102 J. C. H. Shih, *Poult. Sci.*, 1993, **72**, 1617–1620.

103 S. Y. Wong, C. C. Lee, A. Ashrafzadeh, S. M. Junit, N. Abrahim and O. H. Hashim, *PLoS One*, 2016, **11**, 1–15.

104 S. B. Sarmani, R. B. Hassan, M. P. Abdullah and A. Hamzah, *J. Radioanal. Nucl. Chem.*, 1997, **216**, 25–27.

105 S. Deb-Choudhury, J. E. Plowman and D. P. Harland, *Methods Enzymol.*, 2016, **568**, 279–301.

106 Z. Zhang, Y. Nie, Q. Zhang, X. Liu, W. Tu, X. Zhang and S. Zhang, *ACS Sustain. Chem. Eng.*, 2017, **5**, 2614–2622.

107 L. Cui, J. Gong, X. Fan, P. Wang, Q. Wang and Y. Qiu, *Eng. Life Sci.*, 2013, **13**, 149–155.

108 X. Mi, Y. Chang, H. Xu and Y. Yang, *Food Chem.*, 2019, **300**, 125181.

109 A. Idris, R. Vijayaraghavan, U. A. Rana, D. Fredericks, A. F. Patti and D. R. MacFarlane, *Green Chem.*, 2013, 525–534.

110 T. Fujii and D. Li, *J. Biol. Macromol*, 2008, **8**, 48–55.

111 V. Singh, S. Wang and K. W. Ng, in *Comprehensive Biomaterials II*, 2017, pp. 542–557.

112 A. Idris, R. Vijayaraghavan, A. F. Patti and D. R. Macfarlane, *ACS Sustain. Chem. Eng.*, 2014, **2**, 1888–1894.

113 A. Idris, R. Vijayaraghavan, U. A. Rana, A. F. Patti and D. R. MacFarlane, *Green Chem.*, 2014, **16**, 2857–2864.

114 J. E. Plowman, S. Clerens, E. Lee, D. P. Harland, J. M. Dyer and S. Deb-Choudhury, *Anal. Methods*, 2014, 7305–7311.

115 Y. Ji, J. Chen, J. Lv, Z. Li, L. Xing and S. Ding, *Sep. Purif. Technol.*, 2014, **132**, 577–583.

116 S. Zheng, Y. Nie, S. Zhang, X. Zhang and L. Wang, *ACS Sustain. Chem. Eng.*, 2015, **3**, 2925–2932.

117 A. Schindl, M. L. Hagen, S. Muzammal, H. A. D. Gunasekera and A. K. Croft, *Front. Chem.*, 2019, **7**, 1–31.

118 X. Liu, Y. Nie, X. Meng, Z. Zhang, X. Zhang and S. Zhang, *RSC Adv.*, 2017, **7**, 1981=1988.

119 C. Qin, H. Gao, X. Liu, X. Li, Y. Xie, Y. Bai and Y. Nie, *J. Mol. Liq.*, 2022, **349**, 1–8.

120 S. Rahayu, D. Syah and M. Thenawidjaja Suhartono, *Biocatal. Agric. Biotechnol.*, 2012, **1**, 152–158.

121 P. Ramnani, R. Singh and R. Gupta, *Can. J. Microbiol.*, 2005, **51**, 191–196.

122 US 2010/0012142 A1, 2010.

123 L. XiaoLi, *J. Am. Acad. Dermatol.*, 2011, **64**, 2414.

124 Z. J. Cao, Q. Zhang, D. K. Wei, L. Chen, J. Wang, X. Q. Zhang and M. H. Zhou, *J. Ind. Microbiol. Biotechnol.*, 2009, **36**, 181–188.

125 B. Vidmar and M. Vodovnik, *Food Technol. Biotechnol.*, 2018, **56**, 312–328.

126 Q. Li, *Front. Microbiol.*, 2021, **12**, 1–14.

127 A. Sharma and S. P. Gupta, in *Viral Proteases and Their Inhibitors*, ed. S. P. Gupta, Tenney, S, Elsevier., 2017, pp. 1–24.

128 M. S. Hossain and A. K. Azad, *J. Biol. Sci.*, 2007, **7**, 599–606.

129 A. B. Friedricht and G. Antranikian, *Appl. Environ. Microbiol.*, 1996, **62**, 2875–82.

130 G. W. Nam, D. W. Lee, H. S. Lee, N. J. Lee, B. C. Kim, E. A. Choe, J. K. Hwang, M. T. Suhartono and Y. R. Pyun, *Arch. Microbiol.*,

2002, **178**, 538–547.

131 C. Bernal, J. Cairó and N. Coello, *Enzyme Microb. Technol.*, 2006, **38**, 49–54.

132 C. G. Cai, J. S. Chen, J. J. Qi, Y. Yin and X. D. Zheng, *J. Zhejiang Univ. Sci. B*, 2008, **9**, 713–720.

133 B. Böckle and R. Müller, *Appl. Environ. Microbiol.*, 1997, **63**, 790–792.

134 L. Wang, Y. Zhou, Y. Huang, Q. Wei, H. Huang and C. Guo, *World J. Microbiol. Biotechnol.*, 2019, **35**, 1–9.

135 H. Hu, J. Gao, J. He, B. Yu, P. Zheng, Z. Huang, X. Mao, J. Yu, G. Han and D. Chen, *PLoS One*, 2013, **8**, 1–8.

136 Q. Huang, Y. Peng, X. Li, H. Wang and Y. Zhang, *Curr. Microbiol.*, 2003, **46**, 169–173.

137 CN102614104B, 2013.

138 X. Lin, C.-G. Lee, J. C. H. Shih, E. S. Casale and J. C. H. Shih, *Appl. Environ. Microbiol.*, 1992, **58**, 3271–3275.

139 S. Radha and P. Gunasekaran, *Protein Expr. Purif.*, 2009, **64**, 24–31.

140 Y. Huang, P. K. Busk, F. A. Herbst and L. Lange, *Appl. Microbiol. Biotechnol.*, 2015, **99**, 9635–9649.

141 H. Takami, T. Akiba and K. Horikoshi, *Appl. Microbiol. Biotechnol.*, 1990, **33**, 519–523.

142 Y. Yang, in *Side Reactions in Peptide Synthesis*, 2016, pp. 299–310.

143 J. J. Wang, J. D. Garlich and J. C. H. Shih, *J. Appl. Poult. Res.*, 2006, **15**, 544–550.

144 M. Cortezi, J. Contiero, C. J. B. De Lima, R. B. Lovaglio and R. Monti, 2008, **4**, 648–656.

145 R. Tatineni, K. K. Doddapaneni, R. C. Potumarthi, R. N. Vellanki, M. T. Kandathil, N. Kolli and L. N. Mangamoori, *Bioresour. Technol.*, 2008, **99**, 1596–1602.

146 H. J. Suh and H. K. Lee, *J. Protein Chem.*, 2001, **20**, 165–169.

147 S. Mitsuiki, M. Ichikawa, T. Oka, M. Sakai, Y. Moriyama, Y. Sameshima, M. Goto and K. Furukawa, *Enzyme Microb. Technol.*, 2004, **34**, 482–489.

148 CN102614104B, 2012.

149 WO/1999/026856, 2003.

150 WO2011050947A3, 2011.

151 US 2010 / 0247670 A1, 2009, 1, 1–6.

152 M. Fernandes and A. Cavaco-Paulo, *Biocatal. Biotransformation*, 2012, **30**, 10–19.

153 P. Ramnani, R. Singh and R. Gupta, *Can. J. Microbiol.*, 2005, **51**, 191–196.

154 H. K. Malviya, S. Parwekar, R. C. Rajak and S. K. Hasija, *Indian J. Exp. Biol.*, 1992, **30**, 103–6.

155 J. L. Mego, *BBA - Gen. Subj.*, 1985, **841**, 139–144.

156 R. Sharma and R. Gupta, *Bioresour. Technol.*, 2012, **120**, 314–317.

157 G. M. de Donatis, R. Moschini, M. Cappiello, A. del Corso and U. Mura, *Mol. Vis.*, 2010, **16**, 1025–1033.

158 M. H. Hanigan, *Adv. Cancer Res.*, 2014, **122**, 103–141.

159 H. Suzuki, K. Fukuyama, H. Kumagai and M. J. A. Teruhiko Beppu, *Proc. Japan Acad. Ser. B Phys. Biol. Sci.*, 2020, **96**, 440–469.

160 J. W. Keillor, R. Castonguay and C. Lherbet, *Methods Enzymol.*, 2005, **401**, 449–467.

161 M. Saini, A. Kashyap, S. Bindal, K. Saini and R. Gupta, *Front. Microbiol.*, 2021, **12**, 1–30.

162 J. Chen, S. Yang, S. Liang, F. Lu, K. Long and X. Zhang, *3 Biotech*, 2020, **10**, 1–7.

163 J. K. Lim, H. C. Jung, S. G. Kang and H. S. Lee, *Extremophiles*, 2017, **21**, 491–498.

164 H. Huber and K. O. Stetter, *J. Biotechnol.*, 1998, **64**, 39–52.

165 D. M. Brown, J. A. Upcroft and P. Upcroft, *Mol. Biochem. Parasitol.*, 1996, **83**, 211–220.

166 M. Berkmen, *Protein Expr. Purif.*, 2012, **82**, 240–251.

167 D. Yenugudhati, D. Prakash, A. K. Kumar, R. S. S. Kumar, N. H. Yennawar, H. P. Yennawar and J. G. Ferry, *Biochemistry*, 2016, **55**, 313–321.

168 A. Guagliardi, V. Nobile, S. Bartolucci and M. Rossi, *Int. J. Biochem.*, 1994, **26**, 375–380.

169 A. Guagliardi, D. De Pascale, R. Cannio, V. Nobile, S. Bartolucci and M. Rossi, *J. Biol. Chem.*, 1995, **270**, 5748–5755.

170 E. Pedone, M. Saviano, S. Bartolucci, M. Rossi, A. Ausili, A. Scirè, E. Bertoli and F. Tanfani, *J. Proteome Res.*, 2005, **4**, 1972–1980.

171 S. Bartolucci, D. de Pascale and M. Rossi, 2001, **334**, 62–73.

172 A. Vlamis-Gardikas and A. Holmgren, *Methods Enzymol.*, 2002, **347**, 286–296.

173 P. Wang, G. Ma, F. Gao and L. Liao, *China Particuology*, 2005, **3**, 304–309.

174 A. Holmgren, *Methods Enzymol.*, 1984, **107**, 295–300.

175 M. J. Parker, X. Zhu and J. Stubbe, *Biochemistry*, 2014, **53**, 766–776.

176 C. Berndt, C. H. Lillig and A. Holmgren, *Biochim. Biophys. Acta - Mol. Cell Res.*, 2008, **1783**, 641–650.

177 K. F. Discola, M. A. de Oliveira, J. R. Rosa Cussiol, G. Monteiro, J. A. Bárcena, P. Porras, C. A. Padilla, B. G. Guimarães and L. E. S. Netto, *J. Mol. Biol.*, 2009, **385**, 889–901.

178 M. A. Oliveira, K. F. Discola, S. V. Alves, F. J. Medrano, B. G. Guimaraìes and L. E. S. Netto, *Biochemistry*, 2010, **49**, 3317–3326.

179 K. F. Discola, S. V. Alves, M. A. De Oliveira, J. A. R. G. Barbosa, F. J. Medrano, L. E. S. Netto and B. G. Guimarães, *Acta Crystallogr. Sect. F Struct. Biol. Cryst. Commun.*, 2005, **61**, 387–390.

180 M. Akif, G. Khare, A. K. Tyagi, S. C. Mande and A. A. Sardesai, *J. Bacteriol.*, 2008, **190**, 7087–7095.

181 A. L. Olson, T. S. Neumann, S. Cai and D. S. Sem, *Proteins Struct. Funct. Bioinforma.*, 2013, **81**, 675–689.

182 A. P. Fernandes, M. Fladvad, C. Berndt, C. Andrésen, C. H. Lillig, P. Neubauer, M. Sunnerhagen, A. Holmgren and A. Vlamis-Gardikas, *J. Biol. Chem.*, 2005, **280**, 24544–24552.

183 K. Li, S. Hein, W. Zou and G. Klug, *J. Bacteriol.*, 2004, **186**, 6800–6808.

184 T. N. Gustafsson, M. Sahlin, J. Lu, B. M. Sjöberg and A. Holmgren, *J. Biol. Chem.*, 2012, **287**, 39686–39697.

185 K. J. Dietz, *Int. Rev. Cytol.*, 2003, **228**, 141–193.

186 A. Holmgren, *J. Biol. Chem.*, 1979, **254**, 9113–9119.

187 S. X. Tan, D. Greetham, S. Raeth, C. M. Grant, I. W. Dawes and G. G. Perrone, *J. Biol. Chem.*, 2010, **285**, 6118–26.

188 US4894223A, 1998.

189 K. Funane, H. Iwahashi and T. Nakamura, *Agric. Biol. Chem.*, 1987, **51**, 1247–1256.

190 T. Nakatani, I. Ohtsu, G. Nonaka, N. Wiriyathanawudhiwong, S. Morigasaki and H. Takagi, *Microb. Cell Fact.*, 2012, **11**, 1–9.

191 C. Hecklau, S. Pering, R. Seibel, A. Schnellbaecher, M. Wehsling, T. Eichhorn, J. von Hagen and A. Zimmer, *J. Biotechnol.*, 2016, **218**, 53–63.

192 L. Meng, J. H. Wong, L. J. Feldman, P. G. Lemaux and B. B. Buchanan, *Proc. Natl. Acad. Sci. U. S. A.*, 2010, **107**, 3900–3905.

193 E. M. Hanschmann, J. R. Godoy, C. Berndt, C. Hudemann and C. H. Lillig, *Antioxidants Redox Signal.*, 2013, **19**, 1539–1605.

194 S. Mondal and S. P. Singh, *Heliyon*, 2022, **8**, 1–17.

195 J. F. Collet and J. Messens, *Antioxidants Redox Signal.*, 2010, **13**, 1205–1216.

196 T. Tamura and T. C. Stadtman, *Methods Enzymol.*, 2002, **347**, 297–306.

197 C. H. Williams, L. David Arscott, S. Müller, B. W. Lennon, M. L. Ludwig, P. F. Wang, D. M. Veine, K. Becker and R. Heiner Schirmer, *Eur. J. Biochem.*, 2000, **267**, 6110–6117.

198 J. Kuriyan, T. S. R. Krishna, L. Wong, B. Guenther, A. Pahler, C. H. W. Jrll and P. Model, *Nature*, 1991, **352**, 172–174.

199 A. Kharin, B. Varghese, R. Verhagen and N. Uzunbajakava, *J. Biomed. Opt.*, 2009, **14**, 1–7.

200 R. L. Fagan and B. A. Palfey, in *Comprehensive Natural Products II: Chemistry and Biology*, 2010, vol. 7, pp. 65–68.

201 P. W. Huber and K. G. Brandt, *Biochemistry*, 1980, **19**, 4568–4575.

202 C. A. McDonald, R. L. Fagan, F. Collard, V. M. Monnier and B. A. Palfey, *J. Am. Chem. Soc.*, 2011, **133**, 16809–16811.

203 A. P. Fernandes and A. Holmgren, *Antioxid. Redox Signal.*, 2004, **6**, 63–74.

204 G. L. Newton, K. Arnold, M. S. Price, C. Sherrill, S. B. Delcardayre, Y. Aharonowitz, G. Cohen, J. Davies, R. C. Fahey and C. Davis, *J. Bacteriol.*, 1996, **178**, 1990–1995.

205 R. C. Fahey, W. C. Brown, W. B. Adams and M. B. Worsham, *J. Bacteriol.*, 1978, **133**, 1126–1129.

206 M. Wallenberg, E. Olm, C. Hebert, M. Björnstedt and A. P. Fernandes, *Biochem. J.*, 2010, **429**, 85–93.

207 I. A. Cotgreave and R. G. Gerdes, *Biochem. Biophys. Res. Commun.*, 1997, **242**, 1–9.

208 D. S. Berkholz, H. F. Faber, S. N. Savvides and P. A. Karplus, *J. Mol. Biol.*, 2008, **382**, 371–384.

209 D. Scott, M. Toney and M. Muzikár, *J. Am. Chem. Soc.*, 2008, **130**, 865–874.

210 L. D. Arscott, D. M. Veine and C. H. Williams, *Biochemistry*, 2000, **39**, 4711–4721.

211 M. Schwaller, B. Wilkinson and H. F. Gilbert, *J. Biol. Chem.*, 2003, **278**, 7154–9.

212 E. Pedone, G. Fiorentino, L. Pirone, P. Contursi, S. Bartolucci and D. Limauro, *Extremophiles*, 2014, **18**, 723–731.

213 *Medinas, D. B., Rozas, P., Hetz, C.*, 2022, **298**, 1–15.

214 EP0276547, 1992.

215 EP0272781, 1992.

216 J. Lundstrom and A. Holmgren, *J. Biol. Chem.*, 1990, **265**, 9114–9120.

217 M. Montazer, F. Alimohammadi, A. Shamei and M. K. Rahimi, *Colloids Surfaces B Biointerfaces*, 2012, **89**, 196–202.

218 K. Suzuta, S. Ogawa, Y. Takeda, K. Kaneyama and K. Arai, *J.*

Cosmet. Sci., 2012, **63**, 177–196.

219 T. Van Der Wijk, J. Overvoorde and J. Den Hertog, *J. Biol. Chem.*, 2004, **279**, 44355–61.

220 C. Du, Y. Huang, A. Borwankar, Z. Tan, A. Cura, J. C. Yee, N. Singh, R. Ludwig, M. Borys, S. Ghose, N. Mussa and Z. J. Li, *MAbs*, 2018, **10**, 500–510.

221 J. W. Weisel and R. I. Litvinov, *Blood*, 2013, **121**, 1712–9.

222 K. Natsuga, *Cold Spring Harb. Perspect. Med.*, 2014, **4**, 1–18.

223 A. Sandilands, C. Sutherland, A. D. Irvine and W. H. I. McLean, *J. Cell Sci.*, 2009, **122**, 1285–94.

224 M. O. Zemaitaitis, S. Y. Kim, R. A. Halverson, J. C. Troncoso, J. M. Lee and N. A. Muma, *J. Neuropathol. Exp. Neurol.*, 2003, **62**, 173–84.

225 M. P. Savoca, E. Tonoli, A. G. Atobatele and E. A. M. Verderio, *Micromachines*, 2018, **9**, 562–585.

226 R. Villalonga, M. Fernández, A. Fragoso, R. Cao, P. Di Pierro, L. Mariniello and R. Porta, *Biotechnol. Bioeng.*, 2003, **81**, 732–7.

227 C. L. Steffensen, M. L. Andersen, P. E. Degn and J. H. Nielsen, *J. Agric. Food Chem.*, 2008, **56**, 12002–12010.

228 M. C. R. Mano, P. N. Dos Santos and G. Molina, in *Value-Addition in Beverages through Enzyme Technology*, 2023, pp. 77–96.

229 J. Buchert, E. Nordlund, M. L. Mattinen and K. Kruus, in *Novel Enzyme Technology for Food Applications*, 2007, pp. 101–139.

230 R. P. Queirós, S. Gouveia, J. A. Saraiva and J. A. Lopes-da-Silva, *Food Res. Int.*, 2019, **115**, 73–82.

231 K. H. M. Gaffar Hossain, A. R. Juan and T. Tzanov, *Biocatal. Biotransformation*, 2008, **26**, 405–411.

232 H. Ando, M. Adachi, K. Umeda, A. Matsuura, M. Nonaka, R. Uchio, H. Tanaka and M. Motoki, *Agric. Biol. Chem.*, 1989, **53**, 2613–2617.

233 N. Chen, C. K. Liu and R. Ashby, *J. Nat. Fibers*, 2022, **19**, 10924–10934.

234 US5490980A, 1994.

235 M. I. Mattinen, M. Hellman, P. Permi, K. Autio, N. Kalkkinen and J. Buchert, *J. Agric. Food Chem.*, 2006, **54**, 8883–8890.

236 K. Agrawal, V. Chaturvedi and P. Verma, *Bioresour. Bioprocess.*, 2018, **5**, 1–12.

237 A. I. Cañas and S. Camarero, *Biotechnol. Adv.*, 2010, **28**, 694–705.

238 R. Hilgers, J. P. Vincken, H. Gruppen and M. A. Kabel, *ACS Sustain. Chem. Eng.*, 2018, **6**, 2037–2046.

239 Shraddha, R. Shekher, S. Sehgal, M. Kamthania and A. Kumar, *Enzyme Res.*, 2011, **3**, 1–11.

240 C. Felby, J. Hassingboe and M. Lund, *Enzyme Microb. Technol.*, 2002, **31**, 736–741.

241 A. Zerva, S. Simić, E. Topakas and J. Nikodinovic-Runic, *Catalysts*, 2019, **9**, 1023–1049.

242 S. Camarero, D. Ibarra, M. J. Martínez and Á. T. Martínez, *Appl. Environ. Microbiol.*, 2005, **71**, 1775–1784.

243 P. K. Chaurasia, R. S. S. Yadav and S. Yadava, *Res. Rev. Biosci.*, 2013, **7**, 66–71.

244 M. C. Terrón, M. López-Fernández, J. M. Carbajo, H. Junca, A. Téllez, S. Yagüe, A. Arana-Cuenca, T. González and A. E. González, *Biochimie*, 2004, **86**, 519–522.

245 M. M. Atalla, H. K. Zeinab, R. H. Eman, A. Y. Amani and A. A. E. A. Abeer, *Saudi J. Biol. Sci.*, 2013, **20**, 373–381.

246 S. M. Jones and E. I. Solomon, *Cell. Mol. Life Sci.*, 2015, **72**, 869–883.

247 M. Struch, D. Linke, A. Mokoonlall, J. Hinrichs and R. G. Berger, *Int. Dairy J.*, 2015, **49**, 89–94.

248 R. J. Martinie, P. I. Godakumbura, E. G. Porter, A. Divakaran, B. J. Burkhart, J. T. Wertz and D. E. Benson, *Metallomics*, 2012, **4**, 1037–1042.

249 M. S. Rogers, R. Hurtado-Guerrero, S. J. Firbank, M. A. Halcrow, D. M. Dooley, S. E. V. Phillips, P. F. Knowles and M. J. McPherson, *Biochemistry*, 2008, **47**, 10428–10439.

250 A. C. K. Sato, F. A. Perrechil, A. A. S. Costa, R. C. Santana and R. L. Cunha, *Food Res. Int.*, 2015, **75**, 244–251.

251 L. Arregui, M. Ayala, X. Gómez-Gil, G. Gutiérrez-Soto, C. E. Hernández-Luna, M. Herrera De Los Santos, L. Levin, A. Rojo-Domínguez, D. Romero-Martínez, M. C. N. Saparrat, M. A. Trujillo-Roldán and N. A. Valdez-Cruz, *Microb. Cell Fact.*, 2019, **18**, 1–33.

252 P. Zucca, G. Cocco, F. Sollai and E. Sanjust, *Biocatalysis*, 2015, **1**, 82–108.

253 S. Couto and L. Herrera, *Curr. Enzym. Inhib.*, 2006, **2**, 343–352.

254 S. Jianliang, H. Liu, W. Yang, S. Chen and S. Fu, *Molecules*, 2017, **22**, 1353–1367.

255 S. S. Nadar and V. K. Rathod, *Biocatal. Agric. Biotechnol.*, 2019, **18**, 1–8.

256 M. L. Mattinen, K. Kruus, J. Buchert, J. H. Nielsen, H. J. Andersen and C. L. Steffensen, *FEBS J.*, 2005, **272**, 3640–50.

257 Y. Gu, L. Yuan, L. Jia, P. Xue and H. Yao, *RSC Adv.*, 2021, **11**, 29498–29506.

258 L. Kupski, G. M. Salcedo, S. S. Caldas, T. D. de Souza, E. B. Furlong and E. G. Primel, *Environ. Sci. Pollut. Res.*, 2019, **26**, 5131–5139.

259 P. Mani, V. T. F. Kumar, T. Keshavarz, T. Sainathan Chandra and G. Kyazze, *Energies*, 2018, **11**, 3455–3467.

260 Y. Wang, N. Zhang, Q. Wang, Y. Yu and P. Wang, *Carbohydr. Polym.*, 2021, **252**, 117157–117168.

261 Y. Li, J. Su, T. G. Castro and A. Cavaco-paulo, *J. Nat. Fibers*, 2021, **10**, 543418.

262 Y. Li, J. Su and A. Cavaco-Paulo, *Int. J. Biol. Macromol.*, 2021, **166**, 798–805.

263 S. Y. Seo, V. K. Sharma and N. Sharma, *J. Agric. Food Chem.*, 2003, **51**, 2837–2853.

264 K. U. Zaidi, A. S. Ali and S. A. Ali, *Enzyme Res.*, 2014, **2014**, 120739–120745.

265 R. Lantto, J. Ellis, E. Fatarella and J. Cortez, *J. Text. Inst.*, 2012, **103**, 55–63.

266 S. Jus, V. Kokol and G. M. Guebitz, *J. Biomater. Sci. Polym. Ed.*, 2009, **20**, 253–69.

267 G. Faccio, O. Nivala and K. Kruus, 2011, **91**, 957–966.

268 B. Bogicevic, H. Berthoud, R. Portmann, L. Meile and S. Irmler, *Appl. Microbiol. Biotechnol.*, 2012, **94**, 1209–1220.

269 A. Susmitha, H. Bajaj and K. Madhavan Nampoothiri, *Cell Surf.*, 2021, **7**, 2468–2330.

270 B. Richts, J. Rosenberg and F. M. Commichau, *Front. Mol. Biosci.*, 2019, **6**, 1–19.

271 B. Renga, *Allergy*, 2011, **10**, 85–91.

272 T. Majtan, A. L. Pey, R. Fernández, J. A. Fernández, L. A. Martínez-Cruz and J. P. Kraus, *PLoS One*, 2014, **9**, 1–14.

273 P. Brzovic, E. L. Holbrook, I. R. C. Greene and M. F. Dunn, *Biochem. J.*, 1990, **29**, 442–451.

274 Y. Goto, B. Li, J. Claesen, Y. Shi, M. J. Bibb and W. A. van der Donk, *PLoS Biol.*, 2010, **8**, 1000339–49.

275 G. L. Ellman, *Arch. Biochem. Biophys.*, 1959, **82**, 70–77.

276 Y. Du, H. Zhang, J. Lu and A. Holmgren, *J. Biol. Chem.*, 2012, **287**, 38210–38219.

277 C. Che, T. Su, P. Sun, G. Li, J. Liu, Z. Wei and G. Yang, *J. Gen. Appl. Microbiol.*, 2020, **66**, 245–255.

278 Holmgren, *J. Biol. Chem.*, 1979, **254**, 9627–9632.

279 C. Cupp-Enyard and S. Aldrich, *J. Vis. Exp.*, 2008, **899**, 4–5.

280 M. Heinzkill, L. Bech, T. Halkier, P. Schneider and T. Anke, *Appl. Environ. Microbiol.*, 1998, **64**, 1601–1606.

281 A. J. Winder and H. Harris, *Eur. J. Biochem.*, 1991, **198**, 317–326.

282 P. W. Folk, J. E. and Cole, *Biochim. Biophys. Acta*, 1966, **122**, 244–264.

283 I. Elbalasy, N. Wilharm, E. Herchenhahn, R. Konieczny, S. G. Mayr and J. Schnauß, *Polymers (Basel).*, 2022, **14**, 1–13.

284 J. Kim, J. Y. Moon, W. J. Kim, D. G. Kim, B. H. Nam, Y. O. Kim, J. Y. Park, C. M. An and H. J. Kong, *Int. J. Mol. Sci.*, 2015, **16**, 19433–19446.

285 M. Gonzalo, R. Espersen, W. A. Al-Soud, F. Cristiano Falco, P. Hägglund, S. J. Sørensen, B. Svensson and S. Jacquiod, *Microb. Biotechnol.*, 2020, **13**, 984–996.

286 H. Takami, S. Nakamura, R. Aono and K. Horikoshi, *Biosci. Biotechnol. Biochem.*, 1992, **56**, 1667–1669.

287 H.-D. Weigmann, *J. Polym. Sci. Part A-1 Polym. Chem.*, 1968, **6**, 2033–2432.

288 US 2005/0124797 A1, 2005, 1–7.

289 US 2009/0111750 A1, 2009, 1–25.

290 G. Coward-Kelly, V. S. Chang, F. K. Agbogbo and M. T. Holtzapple, *Bioresour. Technol.*, 2006, **97**, 1337–43.

291 US 2021/0093538 A9, 2021, 1–9.

292 J. F. Osma, J. L. Toca-Herrera and S. Rodríguez-Couto, *Bioresour. Technol.*, 2010, **101**, 8509–8514.

293 P. Sathishkumar, M. Arulkumar and T. Palvannan, *J. Clean. Prod.*, 2012, **22**, 67–75.

294 NCBI, BLAST Homepage and Selected Search Pages, https://blast.ncbi.nlm.nih.gov/Blast.cgi, (accessed 5 May 2020).

295 S. Gullón, S. Marín and R. P. Mellado, *Microb. Cell Fact.*, 2019, **18**, 1–9.

296 C. M. Williams, C. S. Richter, J. M. Mackenzie and J. C. H. Shih, 1990, **56**, 1509–1515.

297 H. Takami, Y. Nogi and K. Horikoshi, *Extremophiles*, 1999, **3**, 293–296.

298 B. Galunsky, B. Bockle and R. Mu, *Appl. Environ. Microbiol.*, 1995, **61**, 3705–3710.

299 Y. peng Chao, F. hong Xie, J. Yang, J. hua Lu and S. jun Qian, *J. Environ. Sci.*, 2007, **19**, 1125–1128.

300 C. Zheng, S. Guo, W. G. Tennant, P. K. Pradhan, K. A. Black and P. C. Dos Santos, *Biochemistry*, 2019, **58**, 1892–1904.

301 B. Fischer, B. Perry, G. Phillips, I. Sumner and P. Goodenough, *Appl. Microbiol. Biotechnol.*, 1993, **39**, 537–40.

302 H. Takaki, T. Asae, M. Ryuji, N. Kazuo, K. Masakazu, F. Kazuko and I. Morio, *Gene*, 1987, **56**, 53–9.

303 G. L. Rosano and E. A. Ceccarelli, *Front. Microbiol.*, 2014, **5**, 1–17.

304 N. S. de Groot and S. Ventura, *FEBS Lett.*, 2006, **580**, 6471–6.

305 H. H. Hernandez, O. A. Jaquez, M. J. Hamill, S. J. Elliott and C. L. Drennan, *Biochemistry*, 2008, **47**, 9728–9737.

306 R. M. Buey, R. A. Schmitz, B. B. Buchanan and M. Balsera, *Antioxidants*, 2018, **7**, 166–77.

307 K. Schwinn, N. Ferré and M. Huix-Rotllant, *Phys. Chem. Chem. Phys.*, 2020, **22**, 12447–12455.

308 L. S. Erlendsson, M. Möller and L. Hederstedt, *J. Bacteriol.*, 2004, **186**, 6230–6238.

309 E. S. J. Arnér, L. Zhong and A. Holmgren, *Methods Enzymol.*, 1999, **300**, 226–239.

310 J. Lu and A. Holmgren, *Free Radic. Biol. Med.*, 2014, **66**, 75–87.

311 M. Shoor, I. Gudim, H. P. Hersleth and M. Hammerstad, *FEBS Open Bio*, 2021, **11**, 3019–3031.

312 Y. Nisimoto, H. Otsuka-Murakami and D. J. Lambeth, *J. Biol. Chem.*, 1995, **270**, 16428–16434.

313 Z. Zhang, J. Yu and R. C. Stanton, *Anal. Biochem.*, 2000, **285**, 163–7.

314 A. Holmgren and F. Aslund, *Methods Enzymol.*, 1995, **252**, 264–274.

315 F. Åslund, K. Nordstrand, K. D. Berndt, M. Nikkola, T. Bergman, H. Ponstingl, H. Jo, G. Otting and A. Holmgren, 1996, **271**, 6736–6745.

316 S. Luikenhuis, G. Perrone, I. W. Dawes and C. M. Grant, *Mol. Biol. Cell*, 1998, **9**, 1081–1091.

317 L. Coppo, S. J. Montano, A. C. Padilla and A. Holmgren, *Anal. Biochem.*, 2016, **499**, 24–33.

318 C. Espinosa-Diez, V. Miguel, D. Mennerich, T. Kietzmann, P. Sánchez-Pérez, S. Cadenas and S. Lamas, *Redox Biol.*, 2015, **6**, 183–97.

319 T. Scientific, Chemistry of Protein Assays, https://www.thermofisher.com/uk/en/home/life-science/protein-biology/protein-biology-learning-center/protein-biology-resource-library/pierce-protein-methods/chemistry-protein-assays.html#:~:text=For the standard BCA assay,room temperature for 5 minutes., (accessed 21 March 2023).

320 T. Togawa, Y. Akiyama, K. Kaneko, A. Nakamura and T. Imanari, *Anal. Sci.*, 1986, **2**, 477–480.

321 M. Buchacher, T. Bechtold and T. Pham, *Polym. Test.*, 2022, **106**, 107438–48.

322 A. Vlamis-Gardikas, F. Åslund, G. Spyrou, T. Bergman and A. Holmgren, *J. Biol. Chem.*, 1997, **272**, 11236–11243.

323 C. E. Outten and V. C. Culotta, *Biochem. J.*, 2004, **279**, 1–10.

324 M. Man and R. G. Bryant, *Anal. Biochem.*, 1974, **57**, 429–431.

325 C. Sadegh and R. P. Schreck, *Massachusetts Inst. Technol. Undergrad. Res. J.*, 2003, **8**, 39–43.

326 L. J. Wolfram and M. K. O. Lindemann, *J. Soc. Cosmet. Chem.*, 1971, **22**, 839–850.

327 A. Bindoli and M. P. Rigobello, *Methods Enzymol.*, 2002, **347**, 307–16.

328 M. P. Rigobello and A. Bindoli, *Methods Enzymol.*, 2010, **474**, 109–22.

329 J. M. May, *Methods Enzymol.*, 2002, **347**, 327–332.

330 A. C. McCarver and D. J. Lessner, *FEBS J.*, 2014, **281**, 4598–4611.

331 M. Schmid, T. K. Prinz, A. Stäbler and S. Sängerlaub, *Front. Chem.*, 2017, **4**, 1–15.

332 X. Yang and K. Ma, *J. Bacteriol.*, 2010, **192**, 1370–1376.

333 E. A. Badiea, A. A. Sayed, M. Maged, W. M. Fouad, M. M. Said and A. Y. Esmat, *PLoS One*, 2019, **14**, 1–20.

334 Y. Ghasemi, M. Shahbazi, S. Rasoul-Amini, M. Kargar, A. Safari, A. Kazemi and N. Montazeri-Najafabady, *Ann. Microbiol.*, 2012, **62**, 737–744.

335 W. L. Wu, M. Y. Chen, I. F. Tu, Y. C. Lin, N. Eswarkumar, M. Y. Chen, M. C. Ho and S. H. Wu, *Sci. Rep.*, 2017, **7**, 1–12.

336 M. V. R. Velasco, T. C. De Sá Dias, A. Z. De Freitas, N. D. V. Júnior, C. A. S. D. O. Pinto, T. M. Kaneko and A. R. Baby, *Brazilian J. Pharm. Sci.*, 2009, **45**, 153–162.

337 C. Nowogrodski, I. Simon, S. Magdassi and O. Shoseyov, *Polymers (Basel).*, 2020, **12**, 2568–81.

338 T. M. Florence, *Biochem. J.*, 1980, **189**, 507–520.

339 S. K. Garg, M. Suhail Alam, V. Soni, K. V. Radha Kishan and P. Agrawal, *Protein Expr. Purif.*, 2007, **52**, 422–432.

340 J. S. Kim, L. D. Kluskens, W. M. De Vos, R. Huber and J. Van Der Oost, *J. Mol. Biol.*, 2004, **335**, 787–97.

341 S. C. B. Gopinath, P. Anbu, T. Lakshmipriya, T.-H. Tang, Y. Chen, U. Hashim, A. R. Ruslinda and M. K. M. Arshad, *Biomed Res. Int.*, 2015, **2015**, 1–10.

342 N. Z. Jaouadi, H. Rekik, A. Badis, S. Trabelsi, M. Belhoul, A. B. Yahiaoui, H. Ben Aicha, A. Toumi, S. Bejar and B. Jaouadi, *PLoS One*, 2013, **8**, 76722–39.

343 H. S. Jin, S. Y. Park, K. Kim, Y. J. Lee, G. W. Nam, N. J. Kang and D. W. Lee, *PLoS One*, 2017, **12**, 1–18.

344 A. G. Kumar, S. Swarnalatha, S. Gayathri, N. Nagesh and G. Sekaran, *J. Appl. Microbiol.*, 2008, **104**, 411–419.

345 A. Ghosh, K. Chakrabarti and D. Chattopadhyay, *J. Ind. Microbiol. Biotechnol.*, 2008, **35**, 825–834.

346 J. Qiu, K. Barrett, C. Wilkens and A. S. Meyer, *N. Biotechnol.*, 2022, **68**, 19–27.

347 J. Tian, Z. Xu, X. Long, Y. Tian and B. Shi, *Int. J. Biol. Macromol.*, 2019, **135**, 119–126.

348 Y. Wang, M. Misto, J. Yang, N. Gehring, X. Yu and B. Moussian, *Toxicol. Reports*, 2021, **8**, 124–130.

349 AmericanBio, 1,4-Dithiothreitol (DTT) Safety Data Sheet, https://www.americanbio.com/sites/default/files/sds/AB00490.pdf, (accessed 15 March 2023).

350 C. Su, J. S. Gong, J. Qin, J. M. He, Z. C. Zhou, M. Jiang, Z. H. Xu and J. S. Shi, *J. Clean. Prod.*, 2020, **270**, 122092–122104.

351 S. Mowry and P. J. Ogren, *J. Chem. Educ.*, 1999, **76**, 970–974.

352 J. A. Scott and W. A. Untereiner, *Med. Mycol.*, 2004, **42**, 239–46.

353 A. M. Abdel-Fattah, M. S. El-Gamal, S. A. Ismail, M. A. Emran and A. M. Hashem, *J. Genet. Eng. Biotechnol.*, 2018, **16**, 311–318.

354 R. Gupta and P. Ramnani, *Appl. Microbiol. Biotechnol.*, 2006, **70**, 21–33.

355 K. Song, H. Xu, B. Mu, K. Xie and Y. Yang, *J. Clean. Prod.*, 2017, **150**, 214–223.

356 R. Puri, F. Bot, U. Singh and J. A. O'mahony, *Foods*, 2021, **10**, 3146–62.

357 M. Wu, Q. He, Y. Hong and S. Wang, *Lwt*, 2016, **65**, 816–822.

358 A. Basman, H. Köksel and P. K. W. Ng, *J. Food Sci.*, 2002, **67**, 2654–2658.

359 A. Verdnik, M. Čolnik, Ž. Knez and M. Škerget, *Acta Chim. Slov.*, 2021, **68**, 433–440.

360 M. P. Bönisch, M. Huss, K. Weitl and U. Kulozik, *Int. Dairy J.*, 2007, **17**, 1360–1371.

361 Y. F. Fan, S. X. Zhu, F. Bin Hou, D. F. Zhao, Q. S. Pan, Y. W. Xiang, X. K. Qian, G. B. Ge and P. Wang, *Biosensors*, 2021, **11**, 290.

362 J. Yang, Z. Wang, Y. Lin, T. B. Ng, X. Ye and J. Lin, *Sci. Rep.*, 2017, **7**, 16429–38.

363 A. Maadani Mallak, A. Lakzian, E. Khodaverdi, G. H. Haghnia and S. Mahmoudi, *Microb. Pathog.*, 2020, **149**, 104473–80.

364 E. Bari, N. Nazarnezhad, S. M. Kazemi, M. A. Tajick Ghanbary, B. Mohebby, O. Schmidt and C. A. Clausen, *Int. Biodeterior. Biodegrad.*, 2015, **104**, 231–237.

365 V. V. Kumar, S. Venkataraman, P. S. Kumar, J. George, D. S. Rajendran, A. Shaji, N. Lawrence, K. Saikia and A. K. Rathankumar, *Environ. Pollut.*, 2022, **309**, 119729.

366 P. J. Fernandez-Julia, J. Tudela-Serrano, F. Garcia-Molina, F. Garcia-Canovas, A. Garcia-Jimenez and J. L. Munoz-Munoz, *Biotechnol. Appl. Biochem.*, 2021, **68**, 823–831.

367 Z. Yang and F. Wu, *Biotechnology*, 2006, **5**, 344–348.

368 A. B. Lerner, *Arch. Biochem. Biophys.*, 1952, **36**, 473–81.

369 S. Zolghadri, A. Bahrami, M. T. Hassan Khan, J. Munoz-Munoz, F. Garcia-Molina, F. Garcia-Canovas and A. A. Saboury, *J. Enzyme Inhib. Med. Chem.*, 2019, **34**, 279–309.

370 J. E. O'Connell and C. G. De Kruif, *Colloids Surfaces A Physicochem. Eng. Asp.*, 2003, **216**, 75–81.

371 C. G. De Kruif and C. Holt, in *Advanced Dairy Chemistry—1 Proteins*, 2003, pp. 233–234.

372 T. Huppertz, P. F. Fox and A. L. Kelly, in *Proteins in Food Processing (Second Edition)*, 2018, pp. 49–92.

373 J. M. M. Mohamed, A. Alqahtani, A. Al Fatease, T. Alqahtani, B. A. Khan, B. Ashmitha and R. Vijaya, *Pharmaceuticals*, 2021, **14**, 1–15.

374 C. Sagné, M. F. Isambert, J. P. Henry and B. Gasnier, *Biochem. J.*, 1996, **316**, 825–31.

375 Croda, .

376 S. Takano and T. Tsukuda, in *Frontiers of Nanoscience, Volume 9*, 2015, pp. 9–38.

377 A. Pallares-Rusiñol, M. Bernuz, S. L. Moura, C. Fernández-Senac, R. Rossi, M. Martí and M. I. Pividori, in *Advances in Clinical Chemistry*, Elsevier Inc., 1st edn., 2023, vol. 112, pp. 69–117.

378 P. K. Deb, S. F. Kokaz, S. N. Abed, A. Paradkar and R. K. Tekade, in *Basic Fundamentals of Drug Delivery*, 2019, pp. 203–267.

379 K. J. Kirkwood, Y. Ahmad, M. Larance and A. I. Lamond, *Mol. Cell. Proteomics*, 2013, **12**, 3851–3873.

380 M. Sorci and G. Belfort, in *Bio-nanoimaging: Protein Misfolding and Aggregation*, 2014, pp. 233–245.

381 K. Štulík, V. Pacáková and M. Tichá, *J. Biochem. Biophys. Methods*, 2003, **56**, 1–13.

382 W. W. Yau, C. R. Ginnard and J. J. Kirkland, *J. Chromatogr. A*, 1978, **149**, 465–487.

383 E. R. S. Kunji, M. Harding, P. J. G. Butler and P. Akamine, *Methods*, 2008, **46**, 62–72.

384 P. Hong, S. Koza and E. S. P. Bouvier, *J. Liq. Chromatogr. Relat. Technol.*, 2012, **35**, 2923–2950.

385 S. Simon, B. Païro, M. Villain, P. D'Abzac, E. Van Hullebusch, P. Lens and G. Guibaud, *Bioresour. Technol.*, 2009, **100**, 6258–6268.

386 C. R. Cammarata, M. E. Hughes and C. M. Ofner, *Mol. Pharm.*, 2015, **12**, 783–793.

387 H. M. Powell and S. T. Boyce, *Biomaterials*, 2006, **27**, 5821–5827.

388 M. P. Wickramathilaka and B. Y. Tao, *J. Biol. Eng.*, 2019, **13**, 1–10.

389 S. Lauber, T. Henle and H. Klostermeyer, *Eur. Food Res. Technol.*, 2000, **210**, 305–309.

390 S. N. Lim and J. S. Park, *J. Digit. Converg.*, 2019, **17**, 447–452.

391 Y. Yu, W. Yang, B. Wang and M. A. Meyers, *Mater. Sci. Eng. C*, 2017, **73**, 152–163.

392 R. R. Wickett, E. Kossmann, A. Barel, N. Demeester, P. Clarys, D. Vanden Berghe and M. Calomme, *Arch. Dermatol. Res.*, 2007, **299**, 499–505.

393 G. Y. Lee and B. S. Chang, *Korean J. Microsc.*, 2008, **38**, 251–257.

394 F. Franbourg, A., Hallegot, P., Baltenneck, F., Toutain, C., Leroy, *J Am Acad Dermatol*, 2003, **48**, 115–119.

395 C. Robbins and R. Crawford, *J Soc Cosmet Chem*, 1991, **42**, 49–58.

396 J. Huang, P. Fu, W. Li, L. Xiao, J. Chen and X. Nie, *RSC Adv.*, 2022, **12**, 23048–23056.

397 F. M. Maddar, D. Perry, R. Brooks, A. Page and P. R. Unwin, *Anal. Chem.*, 2019, **91**, 4632–4639.

398 R. M. Trüeb, *Int. J. Cosmet. Sci.*, 2015, **37**, 25–30.

399 M. Belén García-Alonso, J. Pena-Egido and C. García-Moreno, *J. Agric. Food Chem.*, 2001, **49**, 423–429.

400 I. G. Kim, N. K. Han, S. Y. Kim and J. S. Han, *J. Soc. Cosmet. Sci. Korea*, 2016, **42**, 279–284.

401 I. A. Cotgreave, M. Berggren, T. W. Jones, J. Dawson and P. Moldéus, *Biopharm. Drug Dispos.*, 1987, **8**, 377–386.

402 H. A. Khan and B. Mutus, *Front. Chem.*, 2014, **2**, 1–9.

403 F. Chu, D. T. Thornton and H. T. Nguyen, *Methods*, 2018, **15**, 53–63.

404 M. Götze, C. Iacobucci, C. H. Ihling and A. Sinz, *Anal. Chem.*, 2019, **91**, 10236–10244.

405 OpenWetWare, E. coli genotypes, https://openwetware.org/wiki/E._coli_genotypes, (accessed 16 August 2019).

406 J. Lim, C., J. S. Takagi, N. Ida, M. Tokushige, H. Sakamoto and Y. Shimura, *Nucleic Acids Res.*, 1985, **13**, 2063–2074.

407 J. YU and C. Z. ZHOU, *Wiley Liss, Inc.*, 2007, **68**, 972–979.

8. Appendix

General information

Bacillus subtilis thioredoxin and thioredoxin reductase sequences

pET21a::*trxa* sequence

TGGCGAATGGGACGCGCCCTGTAGCGGCGCATTAAGCGCGGCGGGT
GTGGTGGTTACGCGCAGCGTGACCGCTACACTTGCCAGCGCCCTAGC
GCCCGCTCCTTTCGCTTTCTTCCCTTCCTTTCTCGCCACGTTCGCCGG
CTTTCCCCGTCAAGCTCTAAATCGGGGGCTCCCTTTAGGGTTCCGATT
TAGTGCTTTACGGCACCTCGACCCCAAAAAACTTGATTAGGGTGATGG
TTCACGTAGTGGGCCATCGCCCTGATAGACGGTTTTTCGCCCTTTGAC
GTTGGAGTCCACGTTCTTTAATAGTGGACTCTTGTTCCAAACTGGAAC
AACACTCAACCCTATCTCGGTCTATTCTTTTGATTTATAAGGGATTTTG
CCGATTTCGGCCTATTGGTTAAAAAATGAGCTGATTTAACAAAAATTTA
ACGCGAATTTTAACAAAATATTAACGTTTACAATTTCAGGTGGCACTTT
TCGGGGAAATGTGCGCGGAACCCCTATTTGTTTATTTTTCTAAATACAT
TCAAATATGTATCCGCTCATGAGACAATAACCCTGATAAATGCTTCAAT
AATATTGAAAAAGGAAGAGTATGAGTATTCAACATTTCCGTGTCGCCCT
TATTCCCTTTTTTGCGGCATTTTGCCTTCCTGTTTTTGCTCACCCAGAA
ACGCTGGTGAAAGTAAAAGATGCTGAAGATCAGTTGGGTGCACGAGT
GGGTTACATCGAACTGGATCTCAACAGCGGTAAGATCCTTGAGAGTTT
TCGCCCCGAAGAACGTTTTCCAATGATGAGCACTTTTAAAGTTCTGCTA
TGTGGCGCGGTATTATCCCGTATTGACGCCGGGCAAGAGCAACTCGG
TCGCCGCATACACTATTCTCAGAATGACTTGGTTGAGTACTCACCAGT
CACAGAAAAGCATCTTACGGATGGCATGACAGTAAGAGAATTATGCAG
TGCTGCCATAACCATGAGTGATAACACTGCGGCCAACTTACTTCTGAC
AACGATCGGAGGACCGAAGGAGCTAACCGCTTTTTTGCACAACATGG
GGGATCATGTAACTCGCCTTGATCGTTGGGAACCGGAGCTGAATGAA
GCCATACCAAACGACGAGCGTGACACCACGATGCCTGCAGCAATGGC
AACAACGTTGCGCAAACTATTAACTGGCGAACTACTTACTCTAGCTTC
CCGGCAACAATTAATAGACTGGATGGAGGCGGATAAAGTTGCAGGAC
CACTTCTGCGCTCGGCCCTTCCGGCTGGCTGGTTTATTGCTGATAAAT
CTGGAGCCGGTGAGCGTGGGTCTCGCGGTATCATTGCAGCACTGGG
GCCAGATGGTAAGCCCTCCCGTATCGTAGTTATCTACACGACGGGGA
GTCAGGCAACTATGGATGAACGAAATAGACAGATCGCTGAGATAGGT
GCCTCACTGATTAAGCATTGGTAACTGTCAGACCAAGTTTACTCATATA
TACTTTAGATTGATTTAAAACTTCATTTTTAATTTAAAAGGATCTAGGTG
AAGATCCTTTTTGATAATCTCATGACCAAAATCCCTTAACGTGAGTTTT
CGTTCCACTGAGCGTCAGACCCCGTAGAAAAGATCAAAGGATCTTCTT
GAGATCCTTTTTTTCTGCGCGTAATCTGCTGCTTGCAAACAAAAAAACC
ACCGCTACCAGCGGTGGTTTGTTTGCCGGATCAAGAGCTACCAACTCT
TTTTCCGAAGGTAACTGGCTTCAGCAGAGCGCAGATACCAAATACTGT
CCTTCTAGTGTAGCCGTAGTTAGGCCACCACTTCAAGAACTCTGTAGC
ACCGCCTACATACCTCGCTCTGCTAATCCTGTTACCAGTGGCTGCTGC
CAGTGGCGATAAGTCGTGTCTTACCGGGTTGGACTCAAGACGATAGTT
ACCGGATAAGGCGCAGCGGTCGGGCTGAACGGGGGGTTCGTGCACA

CAGCCCAGCTTGGAGCGAACGACCTACACCGAACTGAGATACCTACA
GCGTGAGCTATGAGAAAGCGCCACGCTTCCCGAAGGGAGAAAGGCG
GACAGGTATCCGGTAAGCGGCAGGGTCGGAACAGGAGAGCGCACGA
GGGAGCTTCCAGGGGGAAACGCCTGGTATCTTTATAGTCCTGTCGGG
TTTCGCCACCTCTGACTTGAGCGTCGATTTTTGTGATGCTCGTCAGGG
GGGCGGAGCCTATGGAAAAACGCCAGCAACGCGGCCTTTTTACGGTT
CCTGGCCTTTTGCTGGCCTTTTGCTCACATGTTCTTTCCTGCGTTATCC
CCTGATTCTGTGGATAACCGTATTACCGCCTTTGAGTGAGCTGATACC
GCTCGCCGCAGCCGAACGACCGAGCGCAGCGAGTCAGTGAGCGAGG
AAGCGGAAGAGCGCCTGATGCGGTATTTTCTCCTTACGCATCTGTGCG
GTATTTCACACCGCATATATGGTGCACTCTCAGTACAATCTGCTCTGAT
GCCGCATAGTTAAGCCAGTATACACTCCGCTATCGCTACGTGACTGG
GTCATGGCTGCGCCCCGACACCCGCCAACACCCGCTGACGCGCCCT
GACGGGCTTGTCTGCTCCCGGCATCCGCTTACAGACAAGCTGTGACC
GTCTCCGGGAGCTGCATGTGTCAGAGGTTTTCACCGTCATCACCGAAA
CGCGCGAGGCAGCTGCGGTAAAGCTCATCAGCGTGGTCGTGAAGCG
ATTCACAGATGTCTGCCTGTTCATCCGCGTCCAGCTCGTTGAGTTTCT
CCAGAAGCGTTAATGTCTGGCTTCTGATAAAGCGGGCCATGTTAAGG
GCGGTTTTTTCCTGTTTGGTCACTGATGCCTCCGTGTAAGGGGGATTT
CTGTTCATGGGGGTAATGATACCGATGAAACGAGAGAGGATGCTCAC
GATACGGGTTACTGATGATGAACATGCCCGGTTACTGGAACGTTGTGA
GGGTAAACAACTGGCGGTATGGATGCGGCGGGACCAGAGAAAAATCA
CTCAGGGTCAATGCCAGCGCTTCGTTAATACAGATGTAGGTGTTCCAC
AGGGTAGCCAGCAGCATCCTGCGATGCAGATCCGGAACATAATGGTG
CAGGGCGCTGACTTCCGCGTTTCCAGACTTTACGAAACACGGAAACC
GAAGACCATTCATGTTGTTGCTCAGGTCGCAGACGTTTTGCAGCAGCA
GTCGCTTCACGTTCGCTCGCGTATCGGTGATTCATTCTGCTAACCAGT
AAGGCAACCCCGCCAGCCTAGCCGGGTCCTCAACGACAGGAGCACG
ATCATGCGCACCCGTGGGGCCGCCATGCCGGCGATAATGGCCTGCTT
CTCGCCGAAACGTTTGGTGGCGGGACCAGTGACGAAGGCTTGAGCG
AGGGCGTGCAAGATTCCGAATACCGCAAGCGACAGGCCGATCATCGT
CGCGCTCCAGCGAAAGCGGTCCTCGCCGAAAATGACCCAGAGCGCT
GCCGGCACCTGTCCTACGAGTTGCATGATAAAGAAGACAGTCATAAGT
GCGGCGACGATAGTCATGCCCCGCGCCCACCGGAAGGAGCTGACTG
GGTTGAAGGCTCTCAAGGGCATCGGTCGAGATCCCGGTGCCTAATGA
GTGAGCTAACTTACATTAATTGCGTTGCGCTCACTGCCCGCTTTCCAG
TCGGGAAACCTGTCGTGCCAGCTGCATTAATGAATCGGCCAACGCGC
GGGGAGAGGCGGTTTGCGTATTGGGCGCCAGGGTGGTTTTTCTTTTC
ACCAGTGAGACGGGCAACAGCTGATTGCCCTTCACCGCCTGGCCCTG
AGAGAGTTGCAGCAAGCGGTCCACGCTGGTTTGCCCCAGCAGGCGAA
AATCCTGTTTGATGGTGGTTAACGGCGGGATATAACATGAGCTGTCTT
CGGTATCGTCGTATCCCACTACCGAGATATCCGCACCAACGCGCAGC
CCGGACTCGGTAATGGCGCGCATTGCGCCCAGCGCCATCTGATCGTT
GGCAACCAGCATCGCAGTGGGAACGATGCCCTCATTCAGCATTTGCA
TGGTTTGTTGAAAACCGGACATGGCACTCCAGTCGCCTTCCCGTTCCG
CTATCGGCTGAATTTGATTGCGAGTGAGATATTTATGCCAGCCAGCCA
GACGCAGACGCGCCGAGACAGAACTTAATGGGCCCGCTAACAGCGC
GATTTGCTGGTGACCCAATGCGACCAGATGCTCCACGCCCAGTCGCG
TACCGTCTTCATGGGAGAAAATAATACTGTTGATGGGTGTCTGGTCAG
AGACATCAAGAAATAACGCCGGAACATTAGTGCAGGCAGCTTCCACA
GCAATGGCATCCTGGTCATCCAGCGGATAGTTAATGATCAGCCCACTG

ACGCGTTGCGCGAGAAGATTGTGCACCGCCGCTTTACAGGCTTCGAC
GCCGCTTCGTTCTACCATCGACACCACCACGCTGGCACCCAGTTGAT
CGGCGCGAGATTTAATCGCCGCGACAATTTGCGACGGCGCGTGCAG
GGCCAGACTGGAGGTGGCAACGCCAATCAGCAACGACTGTTTGCCCG
CCAGTTGTTGTGCCACGCGGTTGGGAATGTAATTCAGCTCCGCCATC
GCCGCTTCCACTTTTTCCCGCGTTTTCGCAGAAACGTGGCTGGCCTG
GTTCACCACGCGGGAAACGGTCTGATAAGAGACACCGGCATACTCTG
CGACATCGTATAACGTTACTGGTTTCACATTCACCACCCTGAATTGACT
CTCTTCCGGGCGCTATCATGCCATACCGCGAAAGGTTTTGCGCCATTC
GATGGTGTCCGGGATCTCGACGCTCTCCCTTATGCGACTCCTGCATTA
GGAAGCAGCCCAGTAGTAGGTTGAGGCCGTTGAGCACCGCCGCCGC
AAGGAATGGTGCATGCAAGGAGATGGCGCCCAACAGTCCCCCGGCC
ACGGGGCCTGCCACCATACCCACGCCGAAACAAGCGCTCATGAGCCC
GAAGTGGCGAGCCCGATCTTCCCCATCGGTGATGTCGGCGATATAGG
CGCCAGCAACCGCACCTGTGGCGCCGGTGATGCCGGCCACGATGCG
TCCGGCGTAGAGGATCGAGATCTCGATCCCGCGAAATTAATACGACT
CACTATAGGGGAATTGTGAGCGGATAACAATTCCCCTCTAGAAATAAT
TTTGTTTAACTTTAAGAAGGAGATATA**CATATG**GCGATTGTGAAAGCGAC
CGATCAGAGCTTTAGCGCGGAAACGAGCGAAGGCGTGGTGCTGGCG
GATTTTTGGGCGCCGTGGTGCGGCCCGTGCAAAATGATTGCGCCGGT
GCTGGAAGAACTGGATCAAGAAATGGGCGATAAACTGAAAATTGTGAA
AATTGATGTGGATGAAAACCAAGAAACCGCGGGCAAATATGGCGTGAT
GAGCATTCCGACCCTGCTGGTGCTGAAAGATGGCGAAGTGGTGGAAA
CGAGCGTGGGCTTTAAACCGAAAGAAGCGCTGCAAGAACTGGTGAAC
AAACATCTG**CTCGAG**CACCACCACCACCACCACTGAGATCCGGCTGCTA
ACAAAGCCCGAAAGGAAGCTGAGTTGGCTGCTGCCACCGCTGAGCAA
TAACTAGCATAACCCCTTGGGGCCTCTAAACGGGTCTTGAGGGGTTTT
TTGCTGAAAGGAGGAACTATATCCGGAT

pET21a::*trxb* sequence

TGGCGAATGGGACGCGCCCTGTAGCGGCGCATTAAGCGCGGCGGGT
GTGGTGGTTACGCGCAGCGTGACCGCTACACTTGCCAGCGCCCTAGC
GCCCGCTCCTTTCGCTTTCTTCCCTTCCTTTCTCGCCACGTTCGCCGG
CTTTCCCCGTCAAGCTCTAAATCGGGGGCTCCCTTTAGGGTTCCGATT
TAGTGCTTTACGGCACCTCGACCCCAAAAAACTTGATTAGGGTGATGG
TTCACGTAGTGGGCCATCGCCCTGATAGACGGTTTTTCGCCCTTTGAC
GTTGGAGTCCACGTTCTTTAATAGTGGACTCTTGTTCCAAACTGGAAC
AACACTCAACCCTATCTCGGTCTATTCTTTTGATTTATAAGGGATTTTG
CCGATTTCGGCCTATTGGTTAAAAAATGAGCTGATTTAACAAAAATTTA
ACGCGAATTTTAACAAAATATTAACGTTTACAATTTCAGGTGGCACTTT
TCGGGGAAATGTGCGCGGAACCCCTATTTGTTTATTTTTCTAAATACAT
TCAAATATGTATCCGCTCATGAGACAATAACCCTGATAAATGCTTCAAT
AATATTGAAAAAGGAAGAGTATGAGTATTCAACATTTCCGTGTCGCCCT
TATTCCCTTTTTTGCGGCATTTTGCCTTCCTGTTTTTGCTCACCCAGAA
ACGCTGGTGAAAGTAAAAGATGCTGAAGATCAGTTGGGTGCACGAGT
GGGTTACATCGAACTGGATCTCAACAGCGGTAAGATCCTTGAGAGTTT
TCGCCCCGAAGAACGTTTTCCAATGATGAGCACTTTTAAAGTTCTGCTA
TGTGGCGCGGTATTATCCCGTATTGACGCCGGGCAAGAGCAACTCGG
TCGCCGCATACACTATTCTCAGAATGACTTGGTTGAGTACTCACCAGT
CACAGAAAAGCATCTTACGGATGGCATGACAGTAAGAGAATTATGCAG

TGCTGCCATAACCATGAGTGATAACACTGCGGCCAACTTACTTCTGAC
AACGATCGGAGGACCGAAGGAGCTAACCGCTTTTTTGCACAACATGG
GGGATCATGTAACTCGCCTTGATCGTTGGGAACCGGAGCTGAATGAA
GCCATACCAAACGACGAGCGTGACACCACGATGCCTGCAGCAATGGC
AACAACGTTGCGCAAACTATTAACTGGCGAACTACTTACTCTAGCTTC
CCGGCAACAATTAATAGACTGGATGGAGGCGGATAAAGTTGCAGGAC
CACTTCTGCGCTCGGCCCTTCCGGCTGGCTGGTTTATTGCTGATAAAT
CTGGAGCCGGTGAGCGTGGGTCTCGCGGTATCATTGCAGCACTGGG
GCCAGATGGTAAGCCCTCCCGTATCGTAGTTATCTACACGACGGGGA
GTCAGGCAACTATGGATGAACGAAATAGACAGATCGCTGAGATAGGT
GCCTCACTGATTAAGCATTGGTAACTGTCAGACCAAGTTTACTCATATA
TACTTTAGATTGATTTAAAACTTCATTTTTAATTTAAAAGGATCTAGGTG
AAGATCCTTTTTGATAATCTCATGACCAAAATCCCTTAACGTGAGTTTT
CGTTCCACTGAGCGTCAGACCCCGTAGAAAAGATCAAAGGATCTTCTT
GAGATCCTTTTTTTCTGCGCGTAATCTGCTGCTTGCAAACAAAAAAACC
ACCGCTACCAGCGGTGGTTTGTTTGCCGGATCAAGAGCTACCAACTCT
TTTTCCGAAGGTAACTGGCTTCAGCAGAGCGCAGATACCAAATACTGT
CCTTCTAGTGTAGCCGTAGTTAGGCCACCACTTCAAGAACTCTGTAGC
ACCGCCTACATACCTCGCTCTGCTAATCCTGTTACCAGTGGCTGCTGC
CAGTGGCGATAAGTCGTGTCTTACCGGGTTGGACTCAAGACGATAGTT
ACCGGATAAGGCGCAGCGGTCGGGCTGAACGGGGGGTTCGTGCACA
CAGCCCAGCTTGGAGCGAACGACCTACACCGAACTGAGATACCTACA
GCGTGAGCTATGAGAAAGCGCCACGCTTCCCGAAGGGAGAAAGGCG
GACAGGTATCCGGTAAGCGGCAGGGTCGGAACAGGAGAGCGCACGA
GGGAGCTTCCAGGGGGAAACGCCTGGTATCTTTATAGTCCTGTCGGG
TTTCGCCACCTCTGACTTGAGCGTCGATTTTTGTGATGCTCGTCAGGG
GGGCGGAGCCTATGGAAAAACGCCAGCAACGCGGCCTTTTTACGGTT
CCTGGCCTTTTGCTGGCCTTTTGCTCACATGTTCTTTCCTGCGTTATCC
CCTGATTCTGTGGATAACCGTATTACCGCCTTTGAGTGAGCTGATACC
GCTCGCCGCAGCCGAACGACCGAGCGCAGCGAGTCAGTGAGCGAGG
AAGCGGAAGAGCGCCTGATGCGGTATTTTCTCCTTACGCATCTGTGCG
GTATTTCACACCGCATATATGGTGCACTCTCAGTACAATCTGCTCTGAT
GCCGCATAGTTAAGCCAGTATACACTCCGCTATCGCTACGTGACTGG
GTCATGGCTGCGCCCCGACACCCGCCAACACCCGCTGACGCGCCCT
GACGGGCTTGTCTGCTCCCGGCATCCGCTTACAGACAAGCTGTGACC
GTCTCCGGGAGCTGCATGTGTCAGAGGTTTTCACCGTCATCACCGAAA
CGCGCGAGGCAGCTGCGGTAAAGCTCATCAGCGTGGTCGTGAAGCG
ATTCACAGATGTCTGCCTGTTCATCCGCGTCCAGCTCGTTGAGTTTCT
CCAGAAGCGTTAATGTCTGGCTTCTGATAAAGCGGGCCATGTTAAGG
GCGGTTTTTTCCTGTTTGGTCACTGATGCCTCCGTGTAAGGGGGATTT
CTGTTCATGGGGGTAATGATACCGATGAAACGAGAGAGGATGCTCAC
GATACGGGTTACTGATGATGAACATGCCCGGTTACTGGAACGTTGTGA
GGGTAAACAACTGGCGGTATGGATGCGGCGGGACCAGAGAAAAATCA
CTCAGGGTCAATGCCAGCGCTTCGTTAATACAGATGTAGGTGTTCCAC
AGGGTAGCCAGCAGCATCCTGCGATGCAGATCCGGAACATAATGGTG
CAGGGCGCTGACTTCCGCGTTTCCAGACTTTACGAAACACGGAAACC
GAAGACCATTCATGTTGTTGCTCAGGTCGCAGACGTTTTGCAGCAGCA
GTCGCTTCACGTTCGCTCGCGTATCGGTGATTCATTCTGCTAACCAGT
AAGGCAACCCCGCCAGCCTAGCCGGGTCCTCAACGACAGGAGCACG
ATCATGCGCACCCGTGGGGCCGCCATGCCGGCGATAATGGCCTGCTT
CTCGCCGAAACGTTTGGTGGCGGGACCAGTGACGAAGGCTTGAGCG

AGGGCGTGCAAGATTCCGAATACCGCAAGCGACAGGCCGATCATCGT
CGCGCTCCAGCGAAAGCGGTCCTCGCCGAAAATGACCCAGAGCGCT
GCCGGCACCTGTCCTACGAGTTGCATGATAAAGAAGACAGTCATAAGT
GCGGCGACGATAGTCATGCCCCGCGCCCACCGGAAGGAGCTGACTG
GGTTGAAGGCTCTCAAGGGCATCGGTCGAGATCCCGGTGCCTAATGA
GTGAGCTAACTTACATTAATTGCGTTGCGCTCACTGCCCGCTTTCCAG
TCGGGAAACCTGTCGTGCCAGCTGCATTAATGAATCGGCCAACGCGC
GGGGAGAGGCGGTTTGCGTATTGGGCGCCAGGGTGGTTTTTCTTTTC
ACCAGTGAGACGGGCAACAGCTGATTGCCCTTCACCGCCTGGCCCTG
AGAGAGTTGCAGCAAGCGGTCCACGCTGGTTTGCCCCAGCAGGCGAA
AATCCTGTTTGATGGTGGTTAACGGCGGGATATAACATGAGCTGTCTT
CGGTATCGTCGTATCCCACTACCGAGATATCCGCACCAACGCGCAGC
CCGGACTCGGTAATGGCGCGCATTGCGCCCAGCGCCATCTGATCGTT
GGCAACCAGCATCGCAGTGGGAACGATGCCCTCATTCAGCATTTGCA
TGGTTTGTTGAAAACCGGACATGGCACTCCAGTCGCCTTCCCGTTCCG
CTATCGGCTGAATTTGATTGCGAGTGAGATATTTATGCCAGCCAGCCA
GACGCAGACGCGCCGAGACAGAACTTAATGGGCCCGCTAACAGCGC
GATTTGCTGGTGACCCAATGCGACCAGATGCTCCACGCCCAGTCGCG
TACCGTCTTCATGGGAGAAAATAATACTGTTGATGGGTGTCTGGTCAG
AGACATCAAGAAATAACGCCGGAACATTAGTGCAGGCAGCTTCCACA
GCAATGGCATCCTGGTCATCCAGCGGATAGTTAATGATCAGCCCACTG
ACGCGTTGCGCGAGAAGATTGTGCACCGCCGCTTTACAGGCTTCGAC
GCCGCTTCGTTCTACCATCGACACCACCACGCTGGCACCCAGTTGAT
CGGCGCGAGATTTAATCGCCGCGACAATTTGCGACGGCGCGTGCAG
GGCCAGACTGGAGGTGGCAACGCCAATCAGCAACGACTGTTTGCCCG
CCAGTTGTTGTGCCACGCGGTTGGGAATGTAATTCAGCTCCGCCATC
GCCGCTTCCACTTTTTCCCGCGTTTTCGCAGAAACGTGGCTGGCCTG
GTTCACCACGCGGGAAACGGTCTGATAAGAGACACCGGCATACTCTG
CGACATCGTATAACGTTACTGGTTTCACATTCACCACCCTGAATTGACT
CTCTTCCGGGCGCTATCATGCCATACCGCGAAAGGTTTTGCGCCATTC
GATGGTGTCCGGGATCTCGACGCTCTCCCTTATGCGACTCCTGCATTA
GGAAGCAGCCCAGTAGTAGGTTGAGGCCGTTGAGCACCGCCGCCGC
AAGGAATGGTGCATGCAAGGAGATGGCGCCCAACAGTCCCCCGGCC
ACGGGGCCTGCCACCATACCCACGCCGAAACAAGCGCTCATGAGCCC
GAAGTGGCGAGCCCGATCTTCCCCATCGGTGATGTCGGCGATATAGG
CGCCAGCAACCGCACCTGTGGCGCCGGTGATGCCGGCCACGATGCG
TCCGGCGTAGAGGATCGAGATCTCGATCCCGCGAAATTAATACGACT
CACTATAGGGGAATTGTGAGCGGATAACAATTCCCCTCTAGAAATAAT
TTTGTTTAACTTTAAGAAGGAGATATA**CATATG**GTGAGCGAAGAAAAAA
TTTATGATGTGATTATTATTGGCGCGGGCCCGGCGGGCATGACCGCG
GCGGTGTATACGAGCCGCGCGAACCTGAGCACCCTGATGATTGAACG
CGGCATTCCGGGCGGTCAGATGGCGAACACCGAAGATGTGGAAAACT
ATCCGGGCTTTGAAAGCATTCTGGGCCCGGAACTGAGCAACAAAATG
TTTGAACATGCGAAAAAATTTGGCGCGGAATATGCGTATGGCGATATT
AAAGAAGTGATTGATGGAAAGGAGTATAAAGTAGTTAAAGCGGGCAGC
AAAGAATATAAAGCGCGTGCGGTGATTATCGCGGCTGGTGCGGAATA
CAAGAAGATAGGCGTGCCGGGCGAAAAAGAACTGGGCGGCCGCGGC
GTGAGCTATTGCGCGGTGTGCGATGGCGCGTTTTTTAAAGGCAAAGA
ACTGGTGGTGGTGGGCGGCGGCGATAGCGCGGTGGAAGAAGGCGTG
TATCTGACCCGCTTTGCGAGCAAAGTGACCATTGTGCATCGCCGCGAT
AAACTGCGCGCGCAGAGCATTCTGCAAGCGCGCGCGTTTGATAACGA

AAAAGTGGATTTTCTGTGGAACAAAACCGTGAAAGAAATTCATGAAGA
AAACGGCAAAGTGGGCAACGTGACCCTGGTGGATACCGTGACCGGC
GAAGAAAGCGAATTTAAAACCGATGGCGTGTTTATTTATATTGGCATG
CTGCCGCTGAGCAAACCGTTTGAAAACCTGGGCATTACCAACGAAGA
AGGCTATATTGAAACCAACGATCGCATGGAAACCAAAGTGGAAGGCAT
TTTTGCGGCCGGAGATATTCGCGAAAAAAGCCTGCGTCAGATTGTGAC
CGCGACCGGCGATGGCAGCATTGCGGCGCAGAGCGTGCAGCATTAT
GTGGAAGAACTGCAAGAAACCCTGAAAACCCTGAAA**CTCGAG**CACCA
CCACCACCACCACTGAGATCCGGCTGCTAACAAAGCCCGAAAGGAAG
CTGAGTTGGCTGCTGCCACCGCTGAGCAATAACTAGCATAACCCCTTG
GGGCCTCTAAACGGGTCTTGAGGGGTTTTTTGCTGAAAGGAGGAACT
ATATCCGGAT

trxa Gene Sequence (optimised for *E. coli*)

GCGATTGTGAAAGCGACCGATCAGAGCTTTAGCGCGGAAACGAGCGA
AGGCGTGGTGCTGGCGGATTTTTGGGCGCCGTGGTGCGGCCCGTGC
AAAATGATTGCGCCGGTGCTGGAAGAACTGGATCAAGAAATGGGCGA
TAAACTGAAAATTGTGAAAATTGATGTGGATGAAAACCAAGAAACCGC
GGGCAAATATGGCGTGATGAGCATTCCGACCCTGCTGGTGCTGAAAG
ATGGCGAAGTGGTGGAAACGAGCGTGGGCTTTAAACCGAAAGAAGCG
CTGCAAGAACTGGTGAACAAACATCTG

trxa Amino Acid Sequence

MAIVKATDQSFSAETSEGVVLADFWAPWCGPCKMIAPVLEELDQEMGDK
LKIVKIDVDENQETAGKYGVMSIPTLLVLKDGEVVETSVGFKPKEALQELV
NKHL

trxb Gene Sequence (optimised for *E. coli*)

GTGAGCGAAGAAAAAATTTATGATGTGATTATTATTGGCGCGGGCCCG
GCGGGCATGACCGCGGCGGTGTATACGAGCCGCGCGAACCTGAGCA
CCCTGATGATTGAACGCGGCATTCCGGGCGGTCAGATGGCGAACACC
GAAGATGTGGAAAACTATCCGGGCTTTGAAAGCATTCTGGGCCCGGA
ACTGAGCAACAAAATGTTTGAACATGCGAAAAAATTTGGCGCGGAATA
TGCGTATGGCGATATTAAAGAAGTGATTGATGGAAAGGAGTATAAAGT
AGTTAAAGCGGGCAGCAAAGAATATAAAGCGCGTGCGGTGATTATCG
CGGCTGGTGCGGAATACAAGAAGATAGGCGTGCCGGGCGAAAAAGA
ACTGGGCGGCCGCGGCGTGAGCTATTGCGCGGTGTGCGATGGCGCG
TTTTTTAAAGGCAAAGAACTGGTGGTGGTGGGCGGCGGCGATAGCGC
GGTGGAAGAAGGCGTGTATCTGACCCGCTTTGCGAGCAAAGTGACCA
TTGTGCATCGCCGCGATAAACTGCGCGCGCAGAGCATTCTGCAAGCG
CGCGCGTTTGATAACGAAAAAGTGGATTTTCTGTGGAACAAAACCGTG
AAAGAAATTCATGAAGAAAACGGCAAAGTGGGCAACGTGACCCTGGT
GGATACCGTGACCGGCGAAGAAAGCGAATTTAAAACCGATGGCGTGT
TTATTTATATTGGCATGCTGCCGCTGAGCAAACCGTTTGAAAACCTGG
GCATTACCAACGAAGAAGGCTATATTGAAACCAACGATCGCATGGAAA
CCAAAGTGGAAGGCATTTTTGCGGCCGGAGATATTCGCGAAAAAAGC
CTGCGTCAGATTGTGACCGCGACCGGCGATGGCAGCATTGCGGCGC
AGAGCGTGCAGCATTATGTGGAAGAACTGCAAGAAACCCTGAAAACC
CTGAAA

trxb Amino Acid Sequence

MSEEKIYDVIIIGAGPAGMTAAVYTSRANLSTLMIERGIPGGQMANTEDVE
NYPGFESILGPELSNKMFEHAKKFGAEYAYGDIKEVIDGKEYKVVKAGSK
EYKARAVIIAAGAEYKKIGVPGEKELGGRGVSYCAVCDGAFFKGKELVVV
GGGDSAVEEGVYLTRFASKVTIVHRRDKLRAQSILQARAFDNEKVDFLWN
KTVKEIHEENGKVGNVTLVDTVTGEESEFKTDGVFIYIGMLPLSKPFENLGI
TNEEGYIETNDRMETKVEGIFAAGDIREKSLRQIVTATGDGSIAAQSVQHY
VEELQETLKTLK

Plasmid maps:

1.

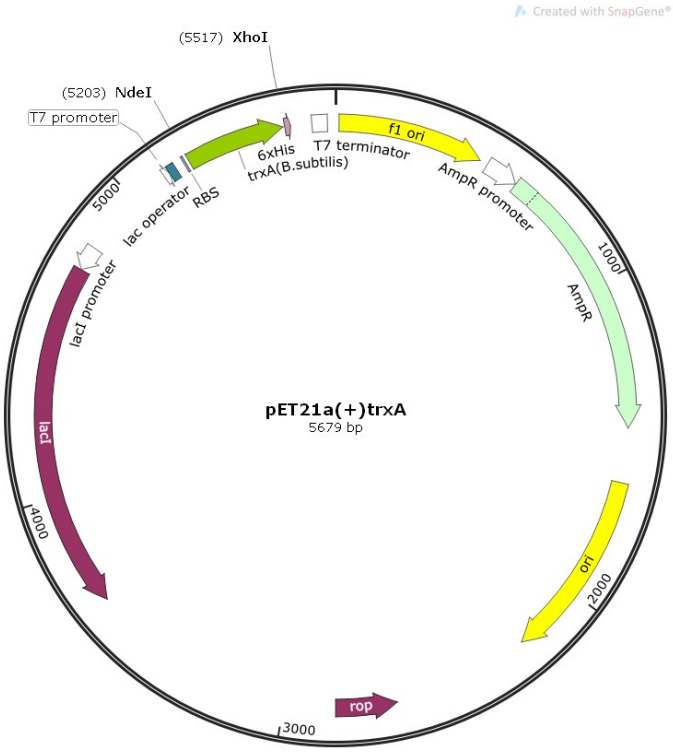

2.

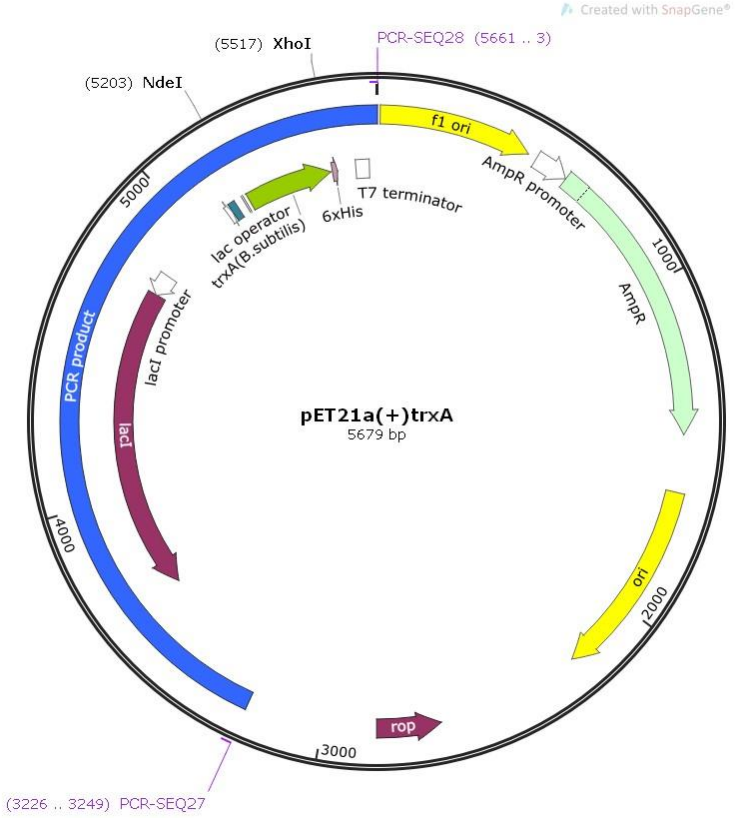

Figure A. pET21a::*trxA* plasmid map, without (1.) and with (2.) PCR primers.

1.

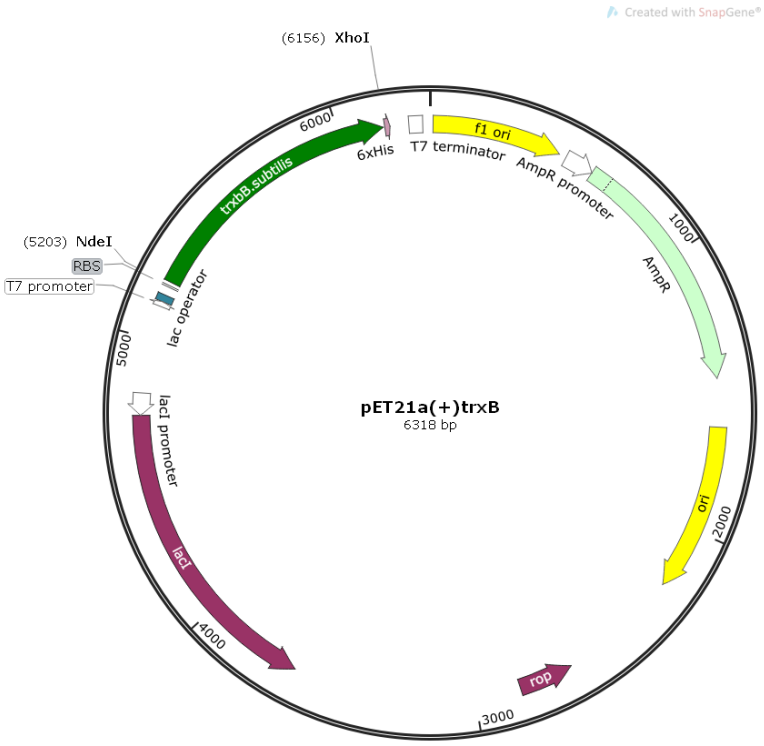

2.

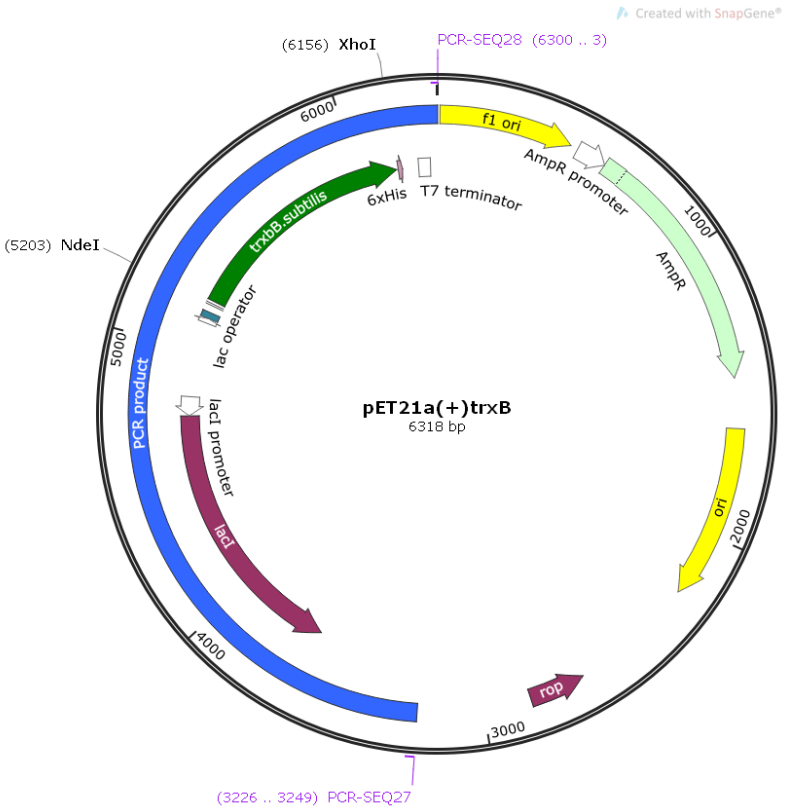

Figure B. pET21a::*trxB* plasmid map, without (1.) and with (2.) PCR primers.

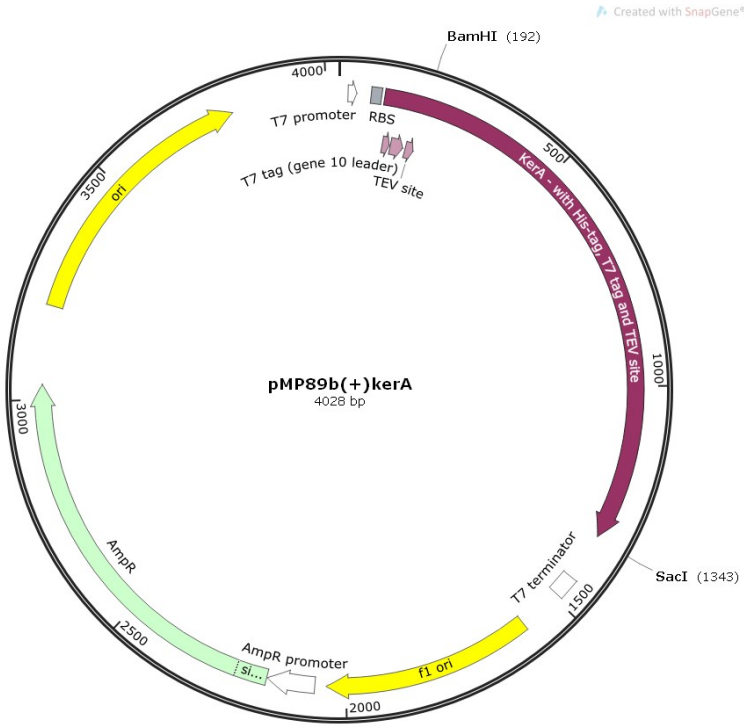

Figure C. pMP89b::*kerA* plasmid map.

3. Materials and methods

Table 3.1 Primers used in this study.

Primer name	***Sequence***	***Source***
Oligo-CF-F1	ATGGATCCGATGATGCGCAA	Sigma-Aldrich
Oligo-CF-R1	AGCCCAGTAAGAGCTCAGT	Sigma-Aldrich
T7 promoter, forward primer	TAATACGACTCACTATAGGG	Source Bioscience
T7 terminator, reverse primer	GCTAGTTATTGCTCAGCGG	Source Bioscience
PCR-SEQ27	5'-ATTCATTCTGCTAACCAGTAAGGC-3'	Unknown
PCR-SEQ28	5'-CCAATCCGGATATAGTTCCTCC-3'	Unknown

Table 3.2 Plasmids used or constructed in this study.

Plasmid name	***Description***	***Antibiotic resistance gene***	***Source***

pMP89b	T7 Expression vector	Ampicillin/carbenicillin	AddGene
pUC::*kerA*	High copy number vector containing a custom synthesised *kerA* gene	Ampicillin	Invitrogen (GeneArt Synthesis)
pMP89b::*kerA*	pMP89b expression vector with *kerA* cloned into it	Ampicillin/carbenicillin	This Study
pET21a(+)	T7 Expression vector	Ampicillin/carbenicillin	Novagen
pUC-GW-Kan::*trxA*::*trxB*	High copy number vector containing custom synthesised *trxA* and *trxB* genes	Kanamycin	Genewiz
pET21a::*trxA*	pET21a expression vector with trx*A* cloned into it	Ampicillin/carbenicillin	This study
pET21a::*trxB*	pET21a expression vector with trxB cloned into it	Ampicillin/carbenicillin	This study

Table 3.3 Strains used in this study.

E. coli strains	***Genotype***	***Source***
DH5α	F$^-$ *endA1 glnV44 thi-1 recA1 relA1 gyrA96 deoR nupG purB20* φ80d*lacZ*ΔM15 Δ(*lacZYA-argF*)U169, hsdR17($r_K^-m_K^+$), λ^{-405}	Merck
BL21	B F$^-$ *ompT gal dcm lon hsdS$_B$*(r_B^- m_B^-) [*malB*$^+$]$_{K-12}$(λ^S)	Merck
BL21 (DE3)	B F$^-$ *ompT gal dcm lon hsdS$_B$*($r_B^-m_B^-$) λ(DE3 [*lacI lacUV5-T7p07 ind1 sam7 nin5*]) [*malB*$^+$]$_{K-12}$(λ^S)	Merck

Rosetta (DE3)	F$^-$ *ompT hsdS*$_B$(r_B^- m_B^-) *gal dcm* (DE3) pRARE (Cam^R)	Merck
BL21 (DE3)-RIPL	*B F– ompT hsdS(rB – mB –) dcm+ Tetr gal λ(DE3) endA Hte*	Merck
BL21 STAR (DE3)	F$^-$*ompT hsdS*$_B$ (r_B^-, m_B^-) *galdcmrne*131 *(DE3)*	Merck

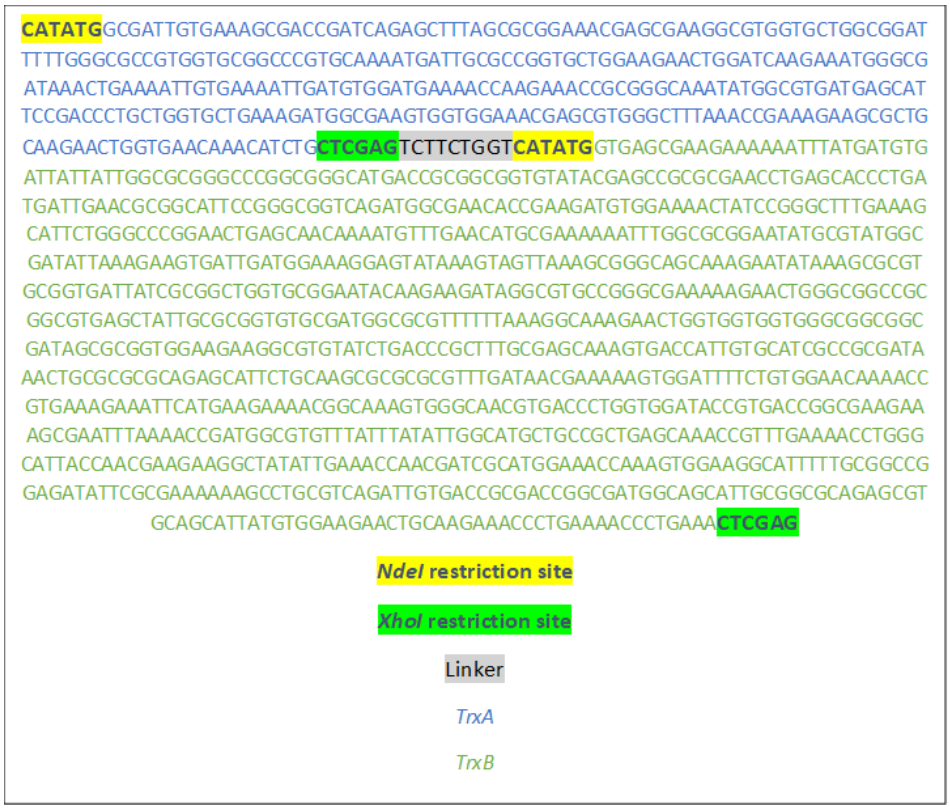

Figure 3.1 Synthetised trxA::trxB gene sequence with a linker (GeneWiz)

4. Reduction of keratin disulfide bonds by the thioredoxin system from *Bacillus subtilis*

Table 4.1 **Homology analysis of N-terminal amino acid sequences of enzyme 1 from *Bacillus halodurans.***

Name	Origin	N-terminal amino acid sequence	Identity with Enzyme 1 (%)
Enzyme 1 (query)	*Bacillus halodurans*	QPNDPADDWN	100%
Protein-disulfide reductase	*Bradyrhizobium* sp. BTAi1	QPNDQAQIDAW	64%

Glutathione-disulfide reductase	*Rhodobacter sphaeroides*	PVDDW	80%
Glutathione reductase	*Francisella tularensis* subsp. *mediasiatica*	PANEW	60%

Table 4.2 Enzymes selected following sequence BLAST based of enzymes described by Prakash et al. (2010).[29,294]

Name	Organism	Cysteine motif	Identity (%)	Length (*k*Da)
Thioredoxin family protein (A)	*Bradyrhizobium* sp. BTAi1	CVTC	100 %	73.55
Protein disulfide reductase (A1)	*Bradyrhizobiaceae* bacterium	CVTC	99 %	73.82
Thioredoxin family protein (A2)	*Escherichia coli*	CVTC	42 %	57.51
Thioredoxin family protein (A3)	*Bacillus sp. SRB_336*	CVTC	37%	101.94
Thioredoxin (A4)	*Bacillus* sp, Y1	CPPC	29%	11.64
Thioredoxin reductase (A5)	*Myobacterium tuberculosis*	CATC	18%	35.65
Glutathione reductase (B)	*Rhodobacter azotoformans*	CVIRGC	100%	48.29
Glutathione reductase (B1)	*Rhodobacter sp. JA983*	CVIRGC	98%	48.42
Glutathione reductase (B2)	*Rhodobacter spjaeroides*	CVIRGC	94%	48.18
Glutathione reductase (B3)	*Cereibacter changlensis*	CVIRGC	84%	48.45
Glutathione reductase (C)	*Francisella tularensis*	CVNRGC	100%	49.45
Glutathione reductase (C1)	*Francisella tularensis*	CVNRGC	99%	49.52
Glutathione reductase (C2)	*Francisella sp. TX07-6608*	CVNRGC	98%	49.54

Glutathione reductase (C3)	*Bacillus sp. 18070*	CVNVGC	49%	48.46
Glutathione reductase (C4)	*Bacillus sp. 2B10*	CVIRGC	37%	48.31
Glutathione reductase (C5)	*Bacillus sp. SB49*	CPNRGC	32%	49.22

Table 4.3 Potential disulfide reducing enzyme candidates (all enzymes were expressed in *E. coli* unless otherwise stated).

Name / accession number	Organism	Cysteine motif	More info
Thioredoxin 1 (trxa) - P0AA25	*E. coli* strain K12	CGPC	Assayed: DTNB (insulin, GSSG)[98,278,406] Structure: 1F6M PDB
Thioredoxin reductase (trxb) - P0A9P4	*E. coli* strain K12	CATC	Assayed: DTNB (trxa, NADPH)[98,278]
Thioredoxin 1 (trx1) - P22217	*Saccharomyces cerevisiae*	CGPC	Expressed Assayed: DTNB[178] Structure: 2I9H PDB
Thioredoxin 2 (trx2) - P22803	*Saccharomyces cerevisiae*	CGPC	Assayed: DTNB[178] Structure: 2FA4 PDB
Thioredoxin reductase (trr1) - P29509	*Saccharomyces cerevisiae*	CAVC	Expressed[179] Assayed: DTNB (NADPH, trx1, trx2)[178] Structure: 3D8X PDB
Thioredoxin B (trxb) - L7N664	*Mycobacterium tuberculosis*	CGPC	Expressed Assayed: DTNB[180]
Thioredoxin reductase - P9WHH1	*Mycobacterium tuberculosis*	CATC	Expressed Assayed: DTNB[180] Structure: 4GCM PDB
Thioredoxin (trxa) - P14949	*Bacillus subtilis* strain 168	CGPC	Expressed Assayed: DTNB, (insulin, GSSG, cysteine)[98] Structure: 2GZY PDB
Thioredoxin reductase (trxc) - P80880	*Bacillus subtilis* strain 168	CAVC	Expressed Assayed: DTNB, (trxa, NADPH)[98]

			Structure: 4GCM PDB
Glutaredoxin 2 (grxb) - P0AC59	*E. coli* strain K12	CPYC	Expressed Assayed: NADPH monitoring (HED, insulin) & NADPH[322] Structure: 1G7O
Glutathione reductase (gor) - P06715	*E. coli* strain K12	CVNVGC	Expressed Assayed: NADPH monitoring (grx2, GSH)[322] Structure: 1GER PDB
Glutaredoxin 1 (grx1) - P25373	*Saccharomyces cerevisiae*	CPYC	Expressed Assayed: NADPH monitoring (HED & GSH mixed disulfide)[48] Structure: 2JAC PDB
Glutaredoxin 2 (grx2) - P17695	*Saccharomyces cerevisiae*	CPYC	Expressed Assayed: NADPH monitoring (HED & GSH mixed disulfide)[48] Structure: 3CTF PDB
Glutathione reductase (GLR1) - P41921	*Saccharomyces cerevisiae*	CVNVGC	Expressed (*Pichia pastoris*), Assayed: NADPH monitoring & DTNB[316,407] *Structure: 2HQM PDB*

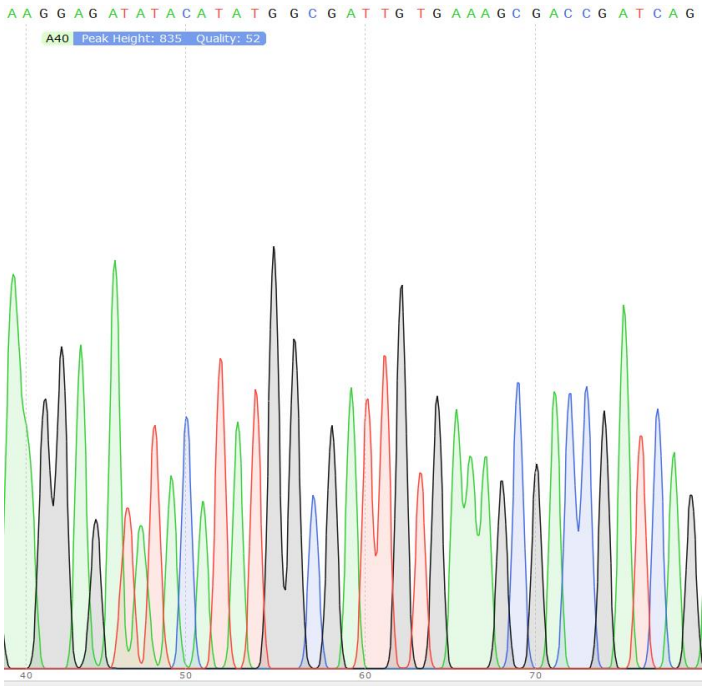

Figure 4.1 Sanger sequencing example displaying good peak resolution (thioredoxin from Bacillus subtilis forward sequencing).

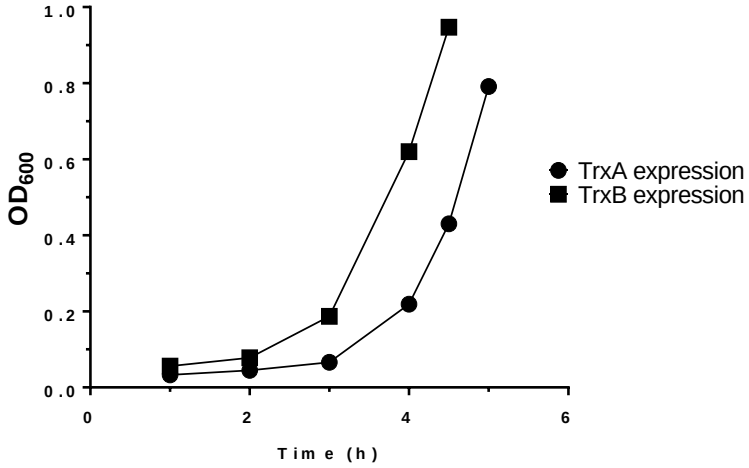

Figure 4.2 Pre-induction cell growth curves for TrxA and TrxB expression in BL21(DE3) cells in LB media. Induction at 5 h and 4.5 h respectively. For both thioredoxin and thioredoxin reductase expressions, the associated cell growth curves displayed similar proliferation patterns. The lag phases, which seem to have lasted between 2 and 3 hours, correspond to cells adapting to the culture conditions. This is then followed by the logarithmic growth phase, where cells actively proliferate at an exponential rate.

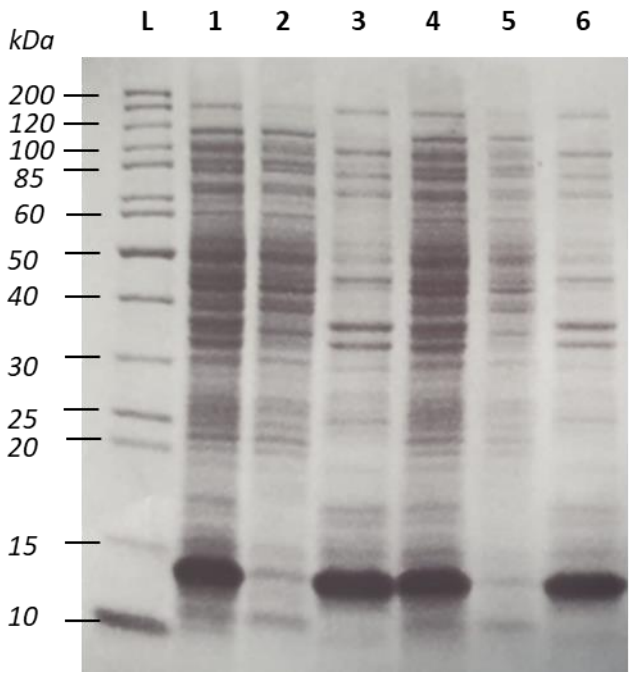

Figure 4.3 SDS PAGE analysis of trxA and trxB overnight expression at 30 °C, with 0.1 mM IPTG. L: protein ladder, lanes 1 and 4: trxA and trxB lysates, lanes 2 and 5: trxA and trxb cell-free extracts, lanes 3 and 6: trxA and trxB insoluble fractions.

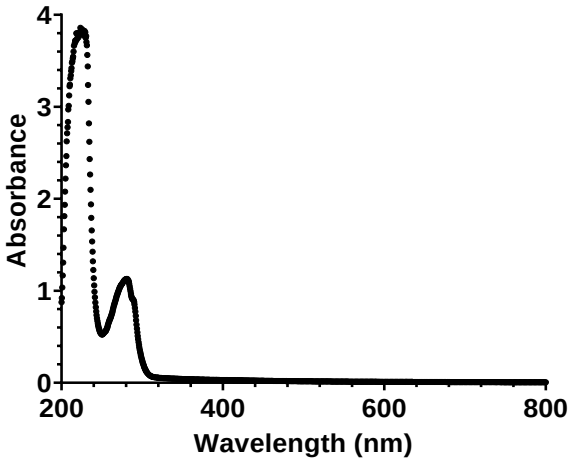

Figure 4.4 200-800 nm absorbance spectrum recorded for purified thioredoxin from Bacillus subtilis, 4x diluted in deionised water. C=A/E= 1.1273x4=4.5092/12700 (E 280nm 12700, Parker et a. (2014)) = 0.000355 M x 11393 = 4.05 mg/mL.

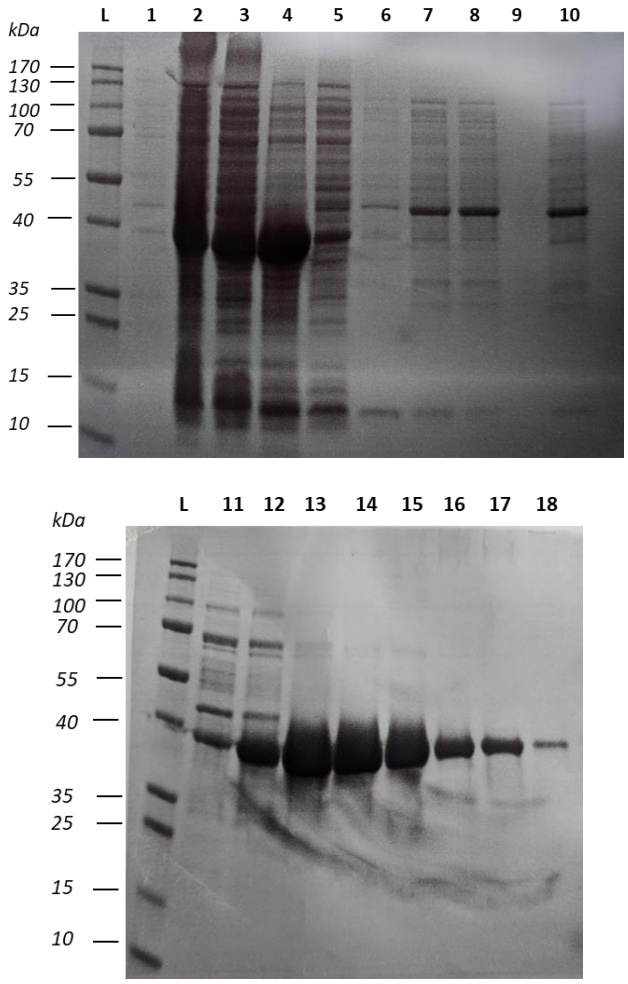

Figure 4.5 SDS PAGE analyses of TrxB HisTag IMAC purification. L: ladder, lane 1: pre-induction control, lane 2: lysate, lane 3: cell-free extract, lane 4: insoluble fraction, lanes 5-10: flow-through fractions, lane 11: B2 fraction, lane 12: B1 fraction, lanes 13-18: C1-C6 fractions.

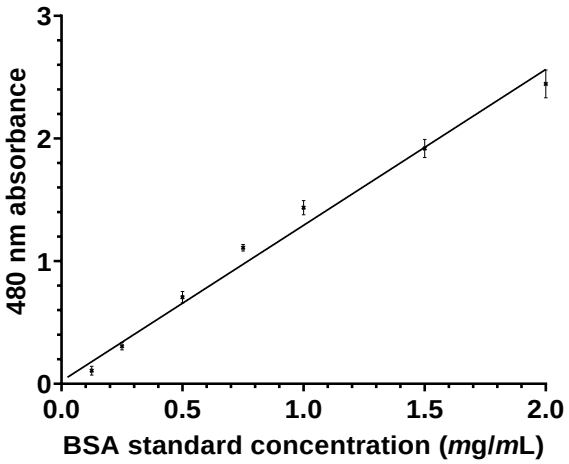

Figure 4.6 BSA (0-2.0 mg/mL) standard curve for BCA assay of purified thioredoxin reductase from *Bacillus subtilis*, triplicate measurements, line of best fit generated using GraphPad Pryzm, where y = 1.271x + 0.02125.

Table 4.4 BCA assay of purified thioredoxin reductase from Bacillus subtilis, with protein concentrations calculated using a BSA (0-2.0 mg/mL) standard curve.

Sample	480 nm absorbance	Protein concentration / *m*g/*m*L	Dilution-corrected protein concentration / *m*g/*m*L
1xBS-trxR	1.091667	0.842184632	**0.842185**
0.5xBS-trxR	0.525667	0.396865985	**0.793732**
0.1xBS-trxR	0.050667	0.023144506	**0.231445**

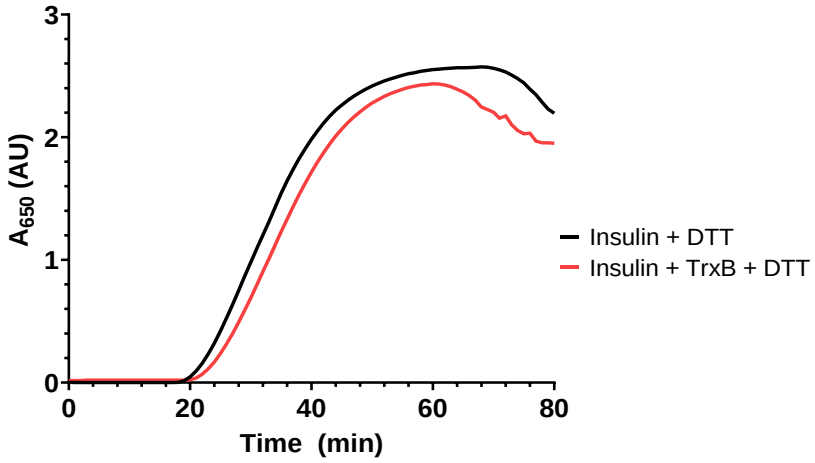

Figure 4.7 Insulin disulfide bond reduction assay using thioredoxin reductase and DTT via turbidity measurements at 660 nm over 80 minutes. TrxB (1.4 µg/mL or 0.041 µM) incubated with insulin (1 mg/mL) and DTT (3 mM) in 0.1 M sodium phosphate buffer pH 7 at 25 °C - maybe address much higher absorbances.

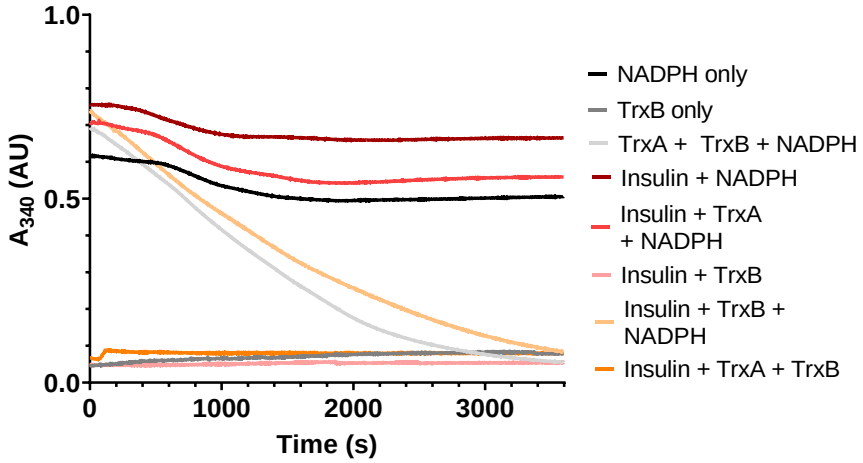

Figure 4.8 - NADPH degradation assay of thioredoxin system with insulin (further controls). insulin (1.22 mg/mL or 213 µM), Trx1 (39.3 µg/mL or 3.33 µM) or TrxA (44.6 µg/mL or 3.92 µM) and TrxB (111.9 µg/mL or 3.25 µM) were added to 0.50 mM Tris-HCl pH 7.5, 1 mM EDTA mL or 0.213 mM). The decrease in absorbance at 340 nm was then immediately monitored for up to one hour at 25 °C.

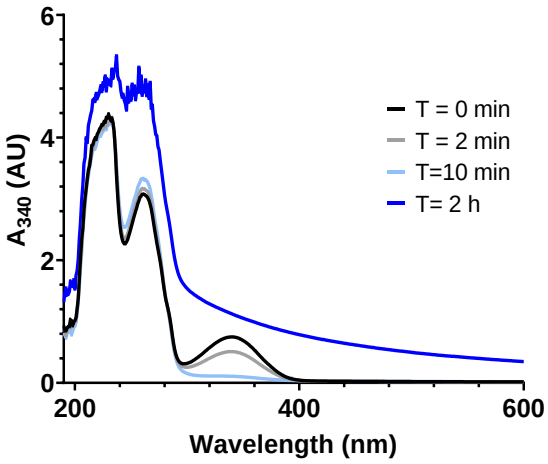

Figure 4.9 NADPH degradation assay on insulin - absorbance spectra recorded over time to understand the increase in absorbance noticed. Insulin (1.22 mg/mL or 213 µM) was incubated with TrxA (7.8 µM) and TrxB (6.5 µM) were added to 0.50 mM Tris-HCl pH 7.5, 1 mM EDTA. In the same way, the reaction (1 mL) was then initiated by addition of NADPH (0.213 mM). The decrease in absorbance at 340 nm was then immediately monitored for up to one hour at 25 °C and 200-600 nm spectra were recorded at different time points.

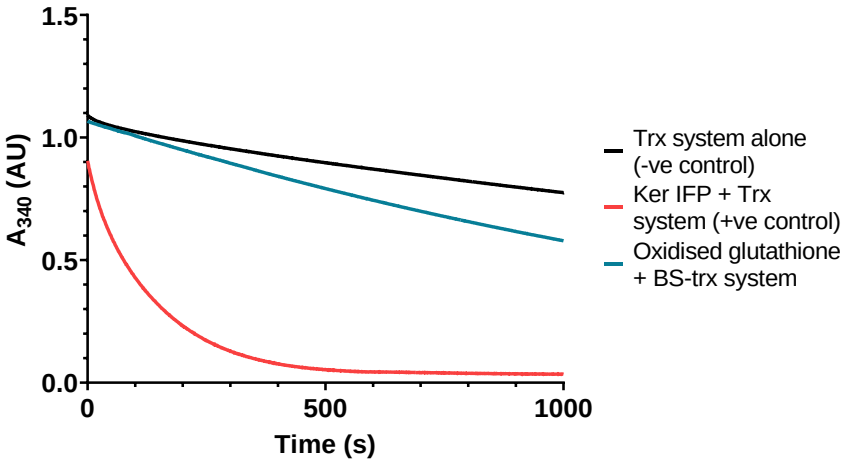

Figure 4.10 NADPH degradation assay using the thioredoxin system from Bacillus subtilis on oxidised glutathione. Oxidised glutathione (6.53 µM), TrxA (11.3 µL of 3.1 mg/mL stock, final concentration of 35.0 µg/mL or 3.11 µM) and TrxB (68.1 µL of 0.8 mg/mL stock, final concentration of 54.5 µg/mL or 1.58 µM) were added to 0.50 mM Tris-HCl pH 7.5, 1 mM EDTA. The reaction (up to 0.75 mL) was then initiated by addition of NADPH (10 µL of 16.7 mg/mL stock, final concentration of 0.17 mg/mL or 0.20 mM). The decrease in absorbance at 340 nm was then immediately monitored for up to one hour at 25 °C. Absorbances taken prior to NADPH addition were subtracted.

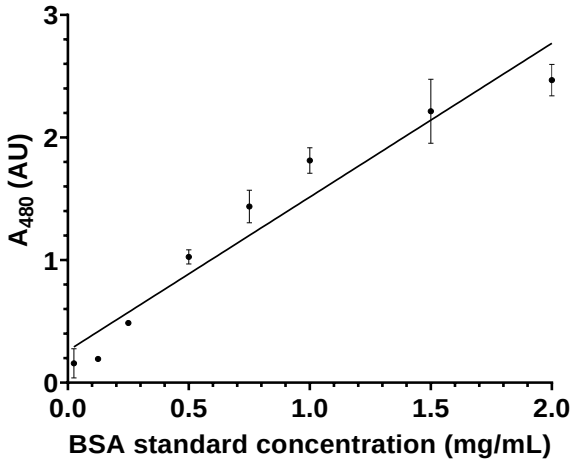

Figure 4.11. BSA standard curve for Keratec™ IFP protein concentration analysis using the BCA assay. Non-linear fit equation: y=1.271x + 0.02125 - data given as average values of triplicate absorbance measurements and shown ± the standard deviation.

Table 4.5. Keratec™ IFP protein concentration calculations from a BSA standard curve using the BCA assay.

Sample	*480 nm absorbance*	*Protein conc. (mg/mL)*	*Dilution-corrected protein conc. (mg/mL)*
1 in 500 Ker IFP	2.33	1.65	82.4
1 in 1000 Ker IFP	1.6	1.08	107.8

a.

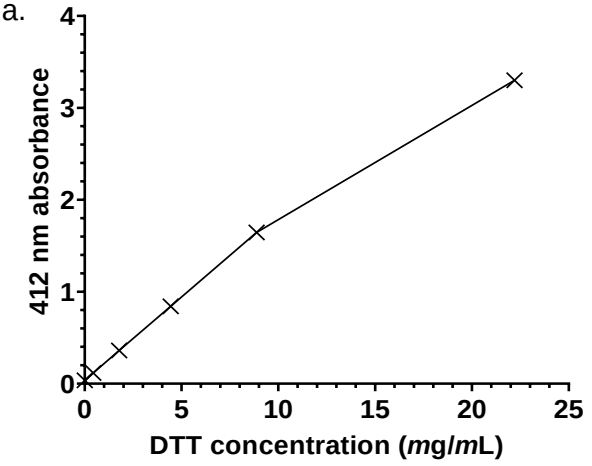

b.

DTT concentration in *m*g/*m*L	**412 nm absorbances**
22.2	3.301
8.88	1.645
4.44	0.841
1.78	0.361
0.44	0.116
0	0.036

Figure 4.12. Evaluation of DTT interference with Ellman's assay. 0-22.2 mg/mL DTT solutions were made up in deionised water an analysed by 412 nm absorbance measurements.

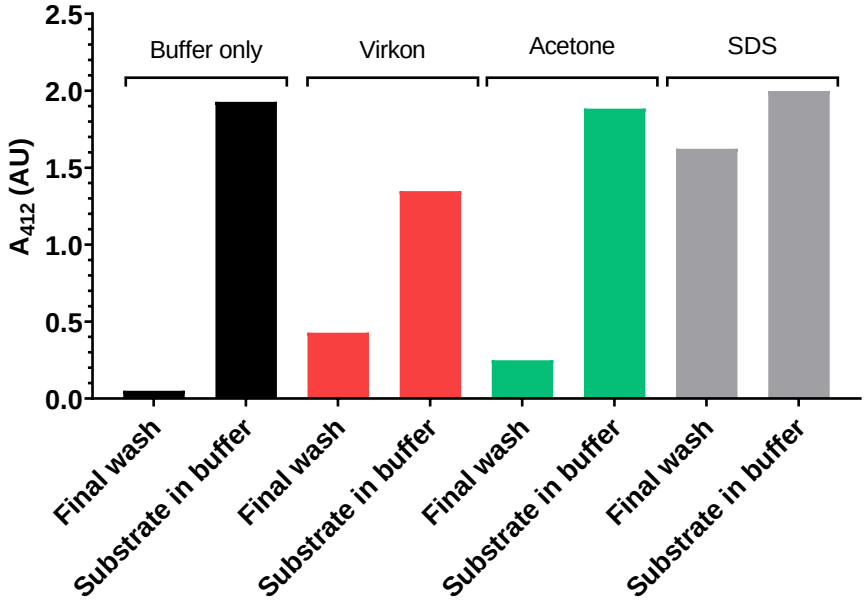

Figure 4.13. Investigation of various substrate rinsing methods to avoid interferences with Ellman's assay. Incubation of keratin azure (8 mg/mL) with DTT (49.7 mg/mL) in Ellman's buffer for 1 hour at 37 °C, 250 rpm, followed by washes using 0.2 M SDS, acetone or Virkon with 5 subsequent buffer rinsings before incubation of both the substrate and final wash with DTNB (0.08 mg/mL or 0.20 µM) and 412 nm absorbance measurements.

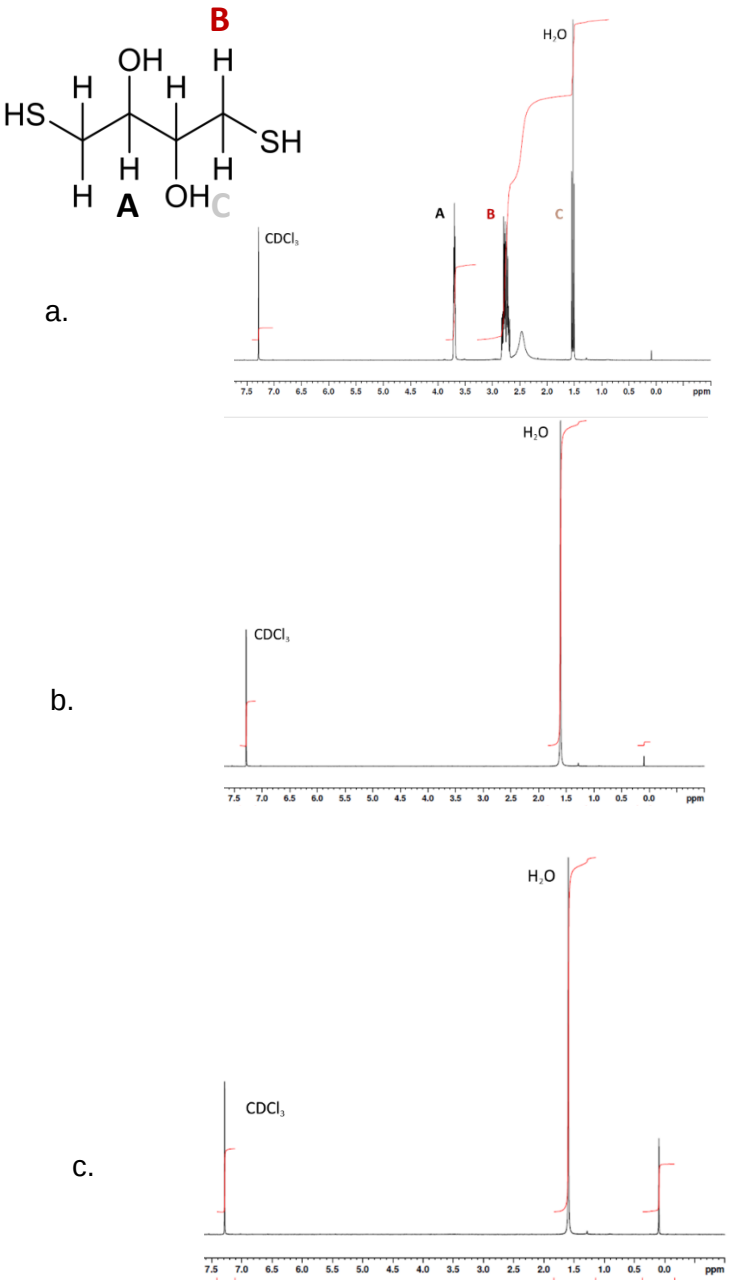

Figure 4.14. NMR analysis of DTT-rinsing from hair using five consecutive buffer rinsings, a. DTT only control, b. Hair only control & c. Hair + DTT sample, 5x buffer rinsed.

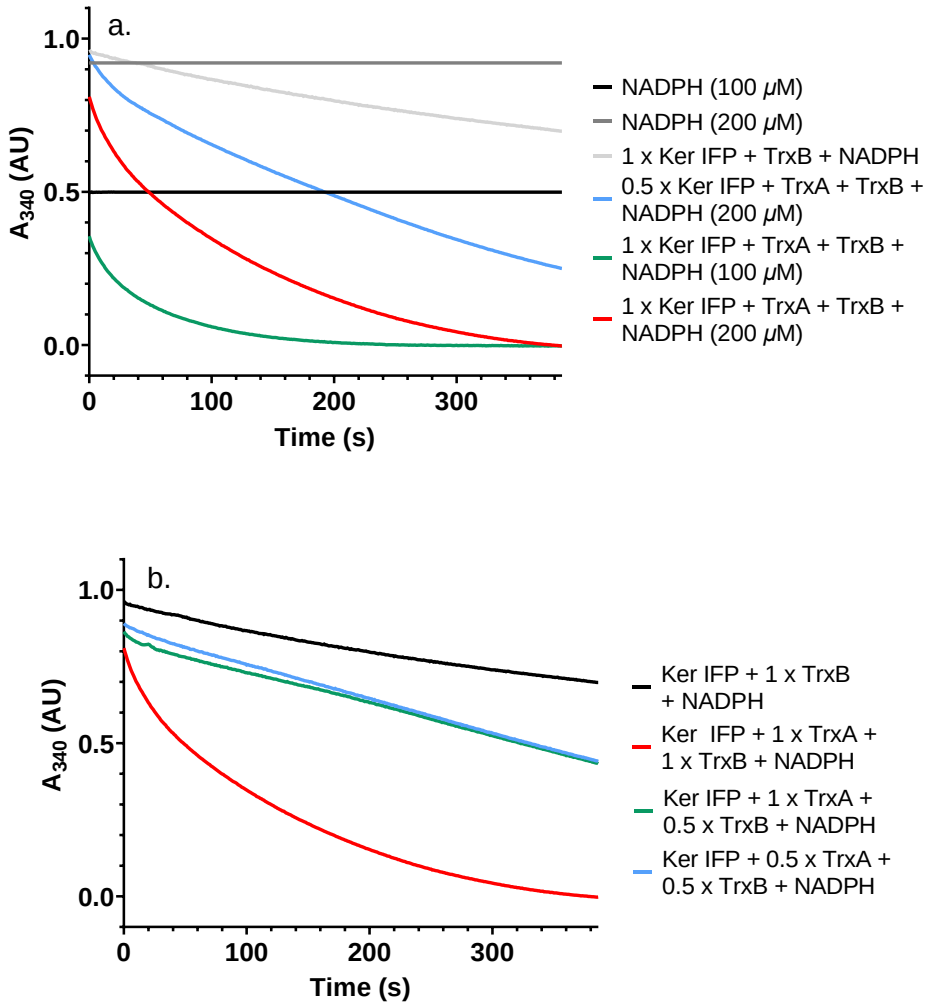

Figure 4.15. Optimisation of NADPH degradation assay on Keratec™ IFP using the *Bacillus subtilis* thioredoxin system, looking at NADPH and substrates (a.) and enzyme concentrations (b.). Keratec™ IFP (Ker IFP, 1.63-3.25 mg/mL) was incubated with TrxA (0.070 mg/mL or 6.02 µM) and TrxB (0.17 mg/mL or 4.93 µM) were added to 0.50 mM Tris-HCl pH 7.5, 1 mM EDTA. In the same way, the reaction (1 mL) was then initiated by addition of NADPH (0.1-0.2 mM). (b.) Keratec IFP™ (3.25 mg/mL) was incubated with TrxA (0.035-0.070 mg/mL or 3.01-6.02 µM) and TrxB (0.085-0.17 mg/mL or 2.47-4.93 µM) were added to 0.50 mM Tris-HCl pH 7.5, 1 mM EDTA. In the same way, the reaction (1 mL) was then initiated by addition of NADPH (0.2 mM). The decrease in absorbance at 340 nm was then immediately monitored for up to one hour at 25 °C. Absorbances taken prior to NADPH addition were subtracted.

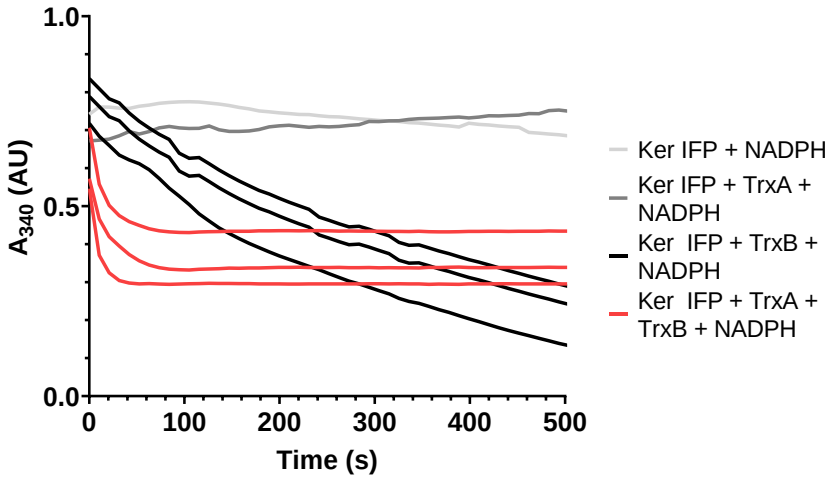

Figure 4.16. NADPH degradation assay of *Bacillus subtilis* thioredoxin system on Keratec™ IFP in triplicates. Keratec™ IFP (Ker IFP, 3.25 mg/mL) was incubated with Trxa (0.14 mg/mL or 12.3 µM) and TrxB (0.34 mg/mL or 9.8 µM) were added to 0.50 mM Tris-HCl pH 7.5, 1 mM EDTA. The reaction (1 mL) was then initiated by addition of NADPH (10 µL of 16.7 mg/mL stock, final concentration of 0.167 mg/mL or 0.200 mM). The decrease in absorbance at 340 nm was then immediately monitored for up to one hour at 25 °C. Absorbances taken prior to NADPH addition were subtracted.

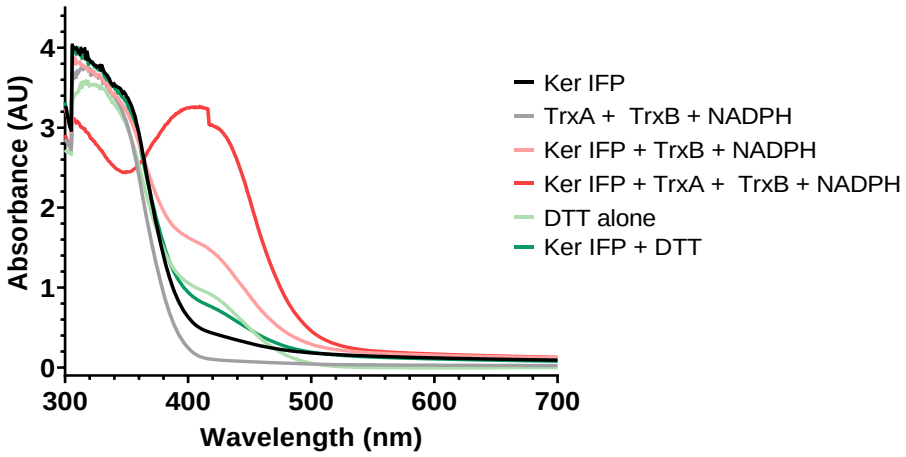

Figure 4.17. Ellman's assay of *Bacillus subtilis* thioredoxin system on Keratec™ IFP, absorbance spectra. Keratec™ IFP (Ker IFP, 3.25 mg/mL) incubated with DTT (3.24 mM) or TrxA (0.14 mg/mL or 12.3 µM), TrxB (0.34 mg/mL or 9.8 µM)) and NADPH (200 µM) in 100 mM Sodium Phosphate buffer with 1 mM EDTA, pH 8 up to 1 mL, at 37 °C. A range of controls were included and volumes were adjusted using buffer. DTNB (0.08 mg/mL or 0.20 µM) was then added, followed by 15 minute-incubation at room temperature and 300-700 nm absorbance spectra recordings

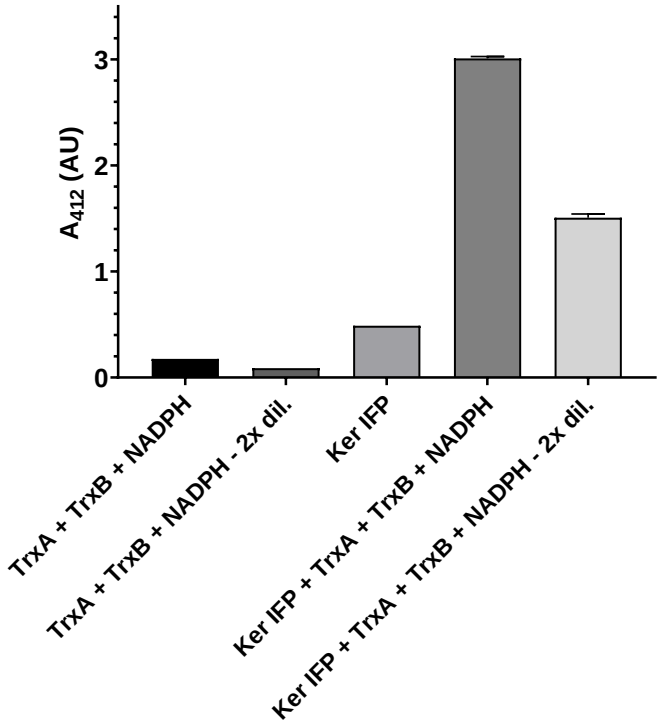

Figure 4.18. Ellman's assay of *Bacillus subtilis* thioredoxin system on Keratec™ IFP. Keratec™ IFP (Ker IFP, 3.25 mg/mL) incubated with TrxA (0.070 mg/mL or 6.2 µM), TrxB (0.17 mg/mL or 4.92 µM)) and NADPH (200 µM) in 100 mM Sodium Phosphate buffer with 1 mM EDTA, pH 8 up to 1 *m*L, at 37 °C. A range of controls were included and volumes were adjusted using buffer. DTNB (0.08 mg/mL or 0.20 µM) was then added, followed by 15 minute incubation at room temperature and 412 nm absorbance measurements – where relevant, - data given as average values of triplicate absorbance measurements and shown ± the standard deviation.

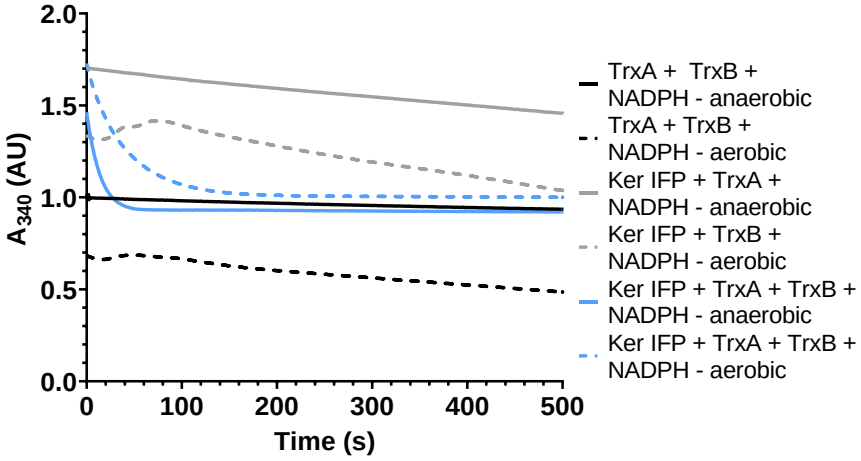

Figure 4.19. Anaerobic NADPH degradation assay of *Bacillus subtilis* thioredoxin system on Keratec™ IFP. Keratec™ IFP (Ker IFP, 3.25 mg/mL) was incubated with TrxA (0.14 mg/mL or 12.3 µM) and TrxB (0.34 mg/mL or 4.93 µM) in 0.50 mM Tris-HCl pH 7.5, 1 mM EDTA. The reaction (1 mL) was then initiated by addition of NADPH (0.167 mg/mL or 0.200 mM). The decrease in absorbance at 340 nm was then immediately monitored for up to one hour at 25 °C.

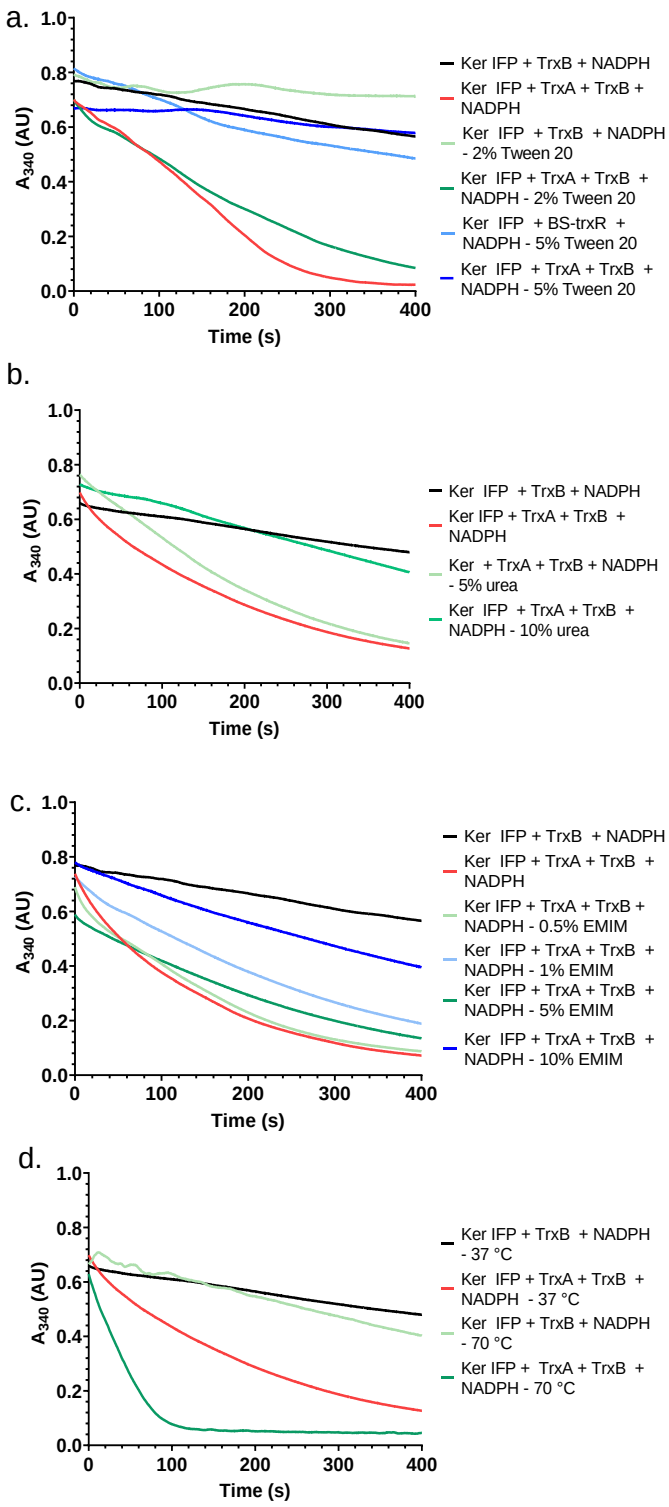

Figure 4.20. NADPH consumption monitoring of Keratec^{TM} IFP disulfide bond reduction by *Bacillus subtilis* thioredoxin system and effect of additives and temperature. a. Tween 20, b.urea, c.[EMIM]ESO_4, d. high incubation temperature. Keratec^{TM} IFP (Ker IFP, 3.25 mg/mL) was incubated with TrxA (0.17 U/mL, 0.035 mg/mL), TrxB (0.085 mg/mL) and NADPH (0.200 mM) in 0.50 mM Tris-HCl pH 7.5, 1 mM EDTA, up to 1 mL at 25 °C (a.-c.) or 50 °C (d.), in the presence or absence of Tween 20 (2-5% v/v), urea (5-10% w/v) or [EMIM]ESO4 (0.5-10%). Absorbances taken prior to NADPH addition were subtracted.

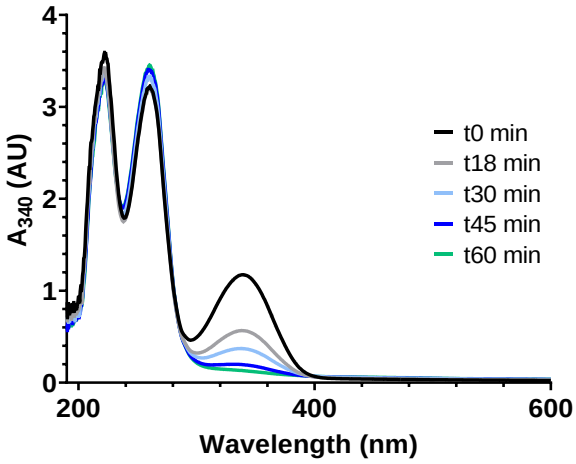

Figure 4.21. NADPH degradation assay of *Bacillus subtilis* thioredoxin system on solid human hair, absorbance spectra taken at different time intervals. Hair (0.02 g/mL) was incubated with TrxA (0.14 mg/mL or 12.3 µM) and TrxB (0.34 mg/mL or 9.8 µM) were added to 0.50 mM Tris-HCl pH 7.5, 1 mM EDTA. The reaction (1 mL) was then initiated by addition of NADPH (66.6 µL of 4.5 mg/mL stock, final concentration of 0.30 mg/mL or 0.36 mM). The decrease in absorbance at 340 nm was then monitored at regular intervals for up to one hour at 25 °C, by pipette the sample supernatant into the quartz cuvette prior to every measurement.

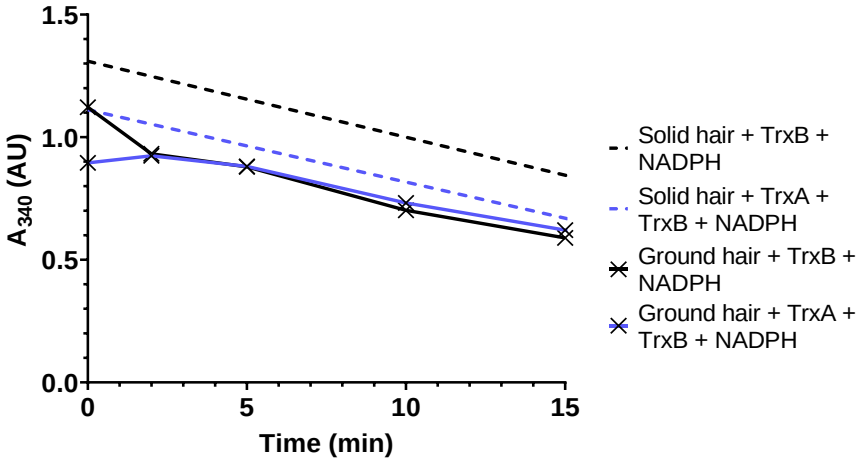

Figure 4.22. NADPH consumption monitoring of ground hair disulfide bond reduction by *Bacillus subtilis* thioredoxin system. Ground hair (0.02 g/mL) was incubated with TrxA (0.70 U/mL, 0.14 mg/mL), TrxB (0.34 mg/m), NADPH (0.213 mM) and Tween20 (0.5% v/v) in 0.50 mM Tris-HCl pH 7.5, 1 mM, up to 1 mL. The decrease in absorbance at 340 nm was then monitored at regular intervals for up to one hour at 25 or 50 °C, by pipetting the sample supernatant into the quartz cuvette prior to every measurement.

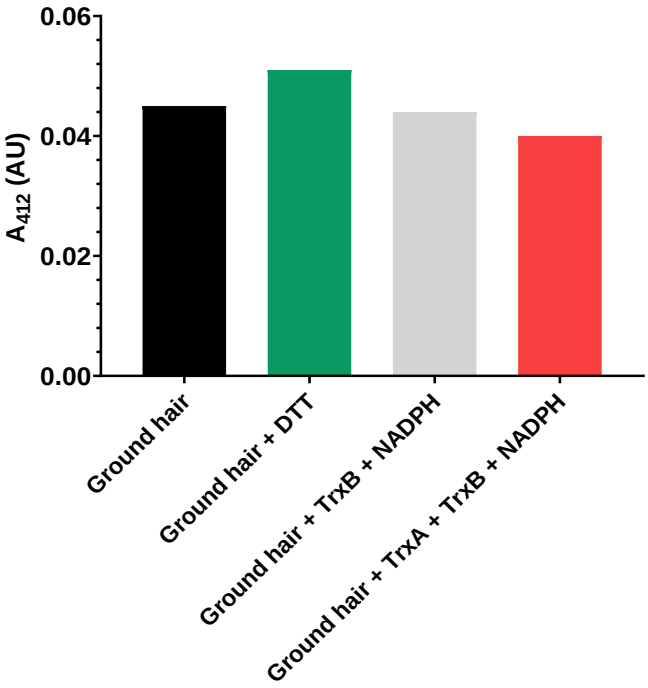

4.23. Ellman's assay of ground hair disulfide bond reduction by *Bacillus subtilis* thioredoxin system. Ground hair (8.0 mg/mL) incubated with DTT (0.5 mM) or TrxA (0.70 U/mL, 0.14 mg/mL), TrxB (0.34 mg/mL) and NADPH (213 µM) in 100 mM Sodium Phosphate buffer with 1 mM EDTA, pH 8 up to 1 mL, for one hour at 37 °C. Following dialysis or Buchner filtration, DTNB (0.20 µM) was added and incubated for 15 minutes at room temperature. 412 nm absorbances were then recorded.

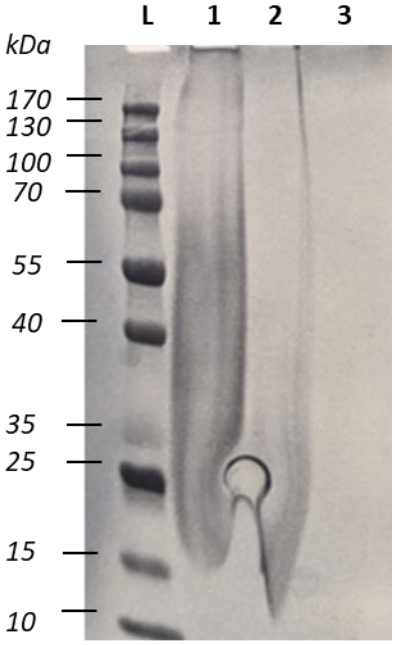

Figure 4.24. SDS PAGE analysis of [EMIM]ESO_4-solubilised hair at various dilutions. L: BioRad protein ladder, lane 1: undiluted substrate, lane 2: 1 in 2 diluted substrate, 3: 1 in 4 diluted substrate.

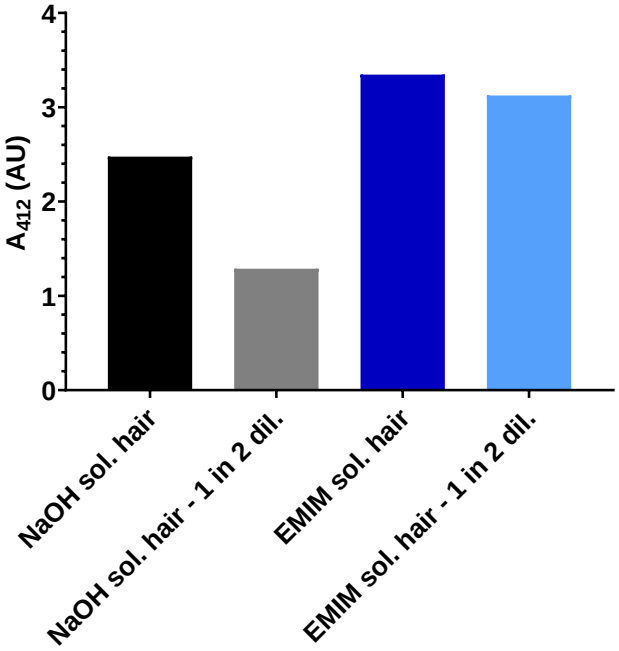

Figure 4.25. Evaluation of solubilised hair compatibility with Ellman's assay. 412 nm absorbance measurements prior to DTNB addition.

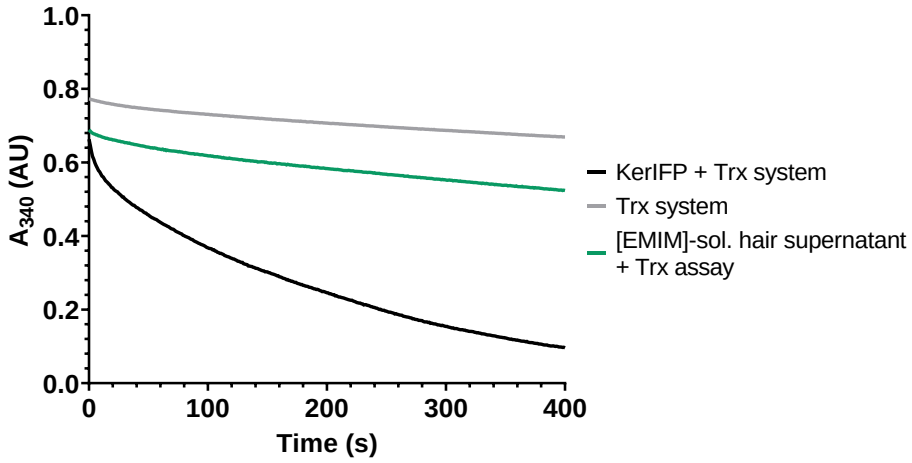

Figure 4.26. NADPH degradation assay of *Bacillus subtilis* thioredoxin system on centrifuged [EMIM]ESO_4- solubilised human hair. [EMIM]ESO_4 solubilised human hair (0.02 g/mL eq.) was centrifuged and the supernatant incubated with TrxA (0.14 mg/mL or 12.3 µM), TrxB (0.34 mg/mL or 9.8 µM) in 0.50 mM Tris-HCl pH 7.5, 1 mM EDTA buffer. The reaction (1 mL) was then initiated by addition of NADPH (0.213 mM). The decrease in absorbance at 340 nm was then monitored over time for up to one hour at 25 °C.

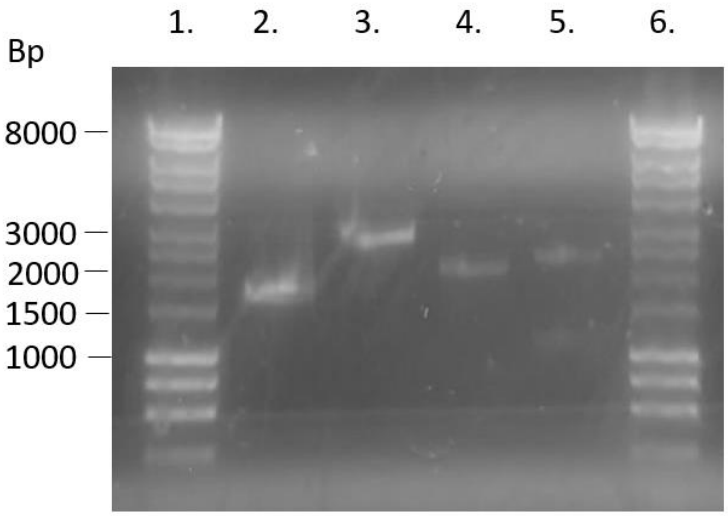

Figure 4.27. Agarose gel analysis of double digested pMP89b and pUC::*KerA*. Lanes 1 & 6: ladder, lane 2: undigested pMP89b, lane 3: double-digested pMP89b, lane 4: undigested kerA and lane 5: double-digested *kerA*.

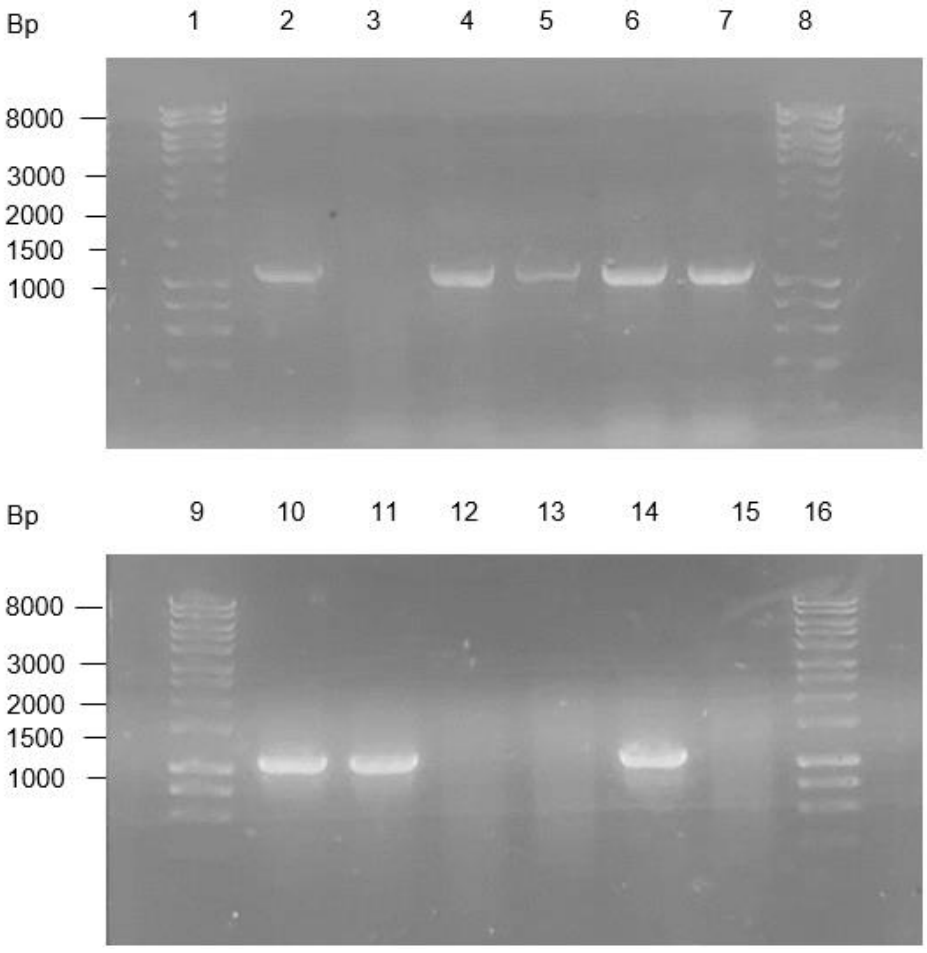

Figure 4.28. Ligation mix Colony PCR Agarose Gel Analysis of ligation mix. DNA ladder: lanes 1, 8, 9 &16, E. coli DH5α pMP89b::*kerA* colonies: lanes 2-7 & 10-15 - Bands corresponding to *kerA* can be seen at 1100 bp in lanes 2, 4-7, 10,11 and 14, confirming successful *E. coli* DH5α transformation with pMP89b-*kerA* ligation mix.

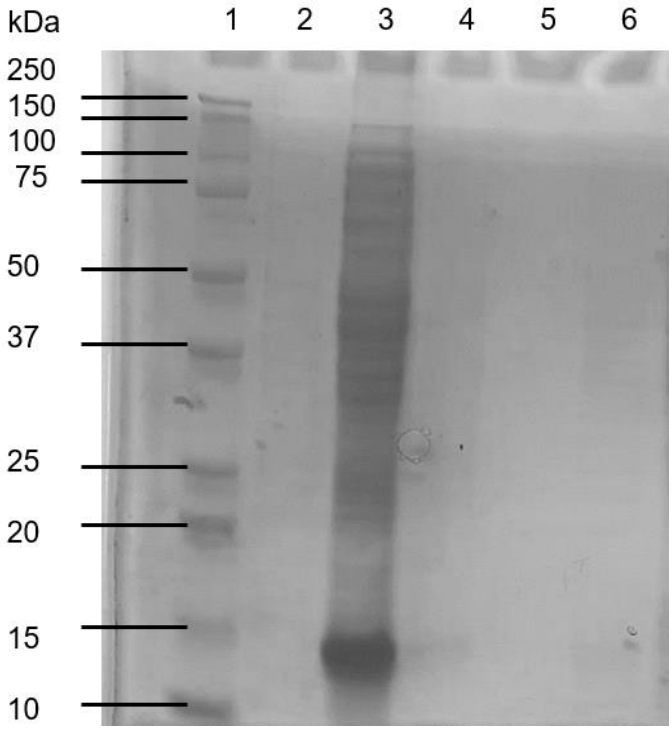

Figure 4.29. SDS PAGE analysis of initial keratinase expression conditions (protein ladder: lane 1, 4.5 hour post-induction: lane 2, lysate: lane 3, 10x diluted cell-free extract: lane 4, 100x diluted cell-free extract: : lane 5, insoluble: lane 6).

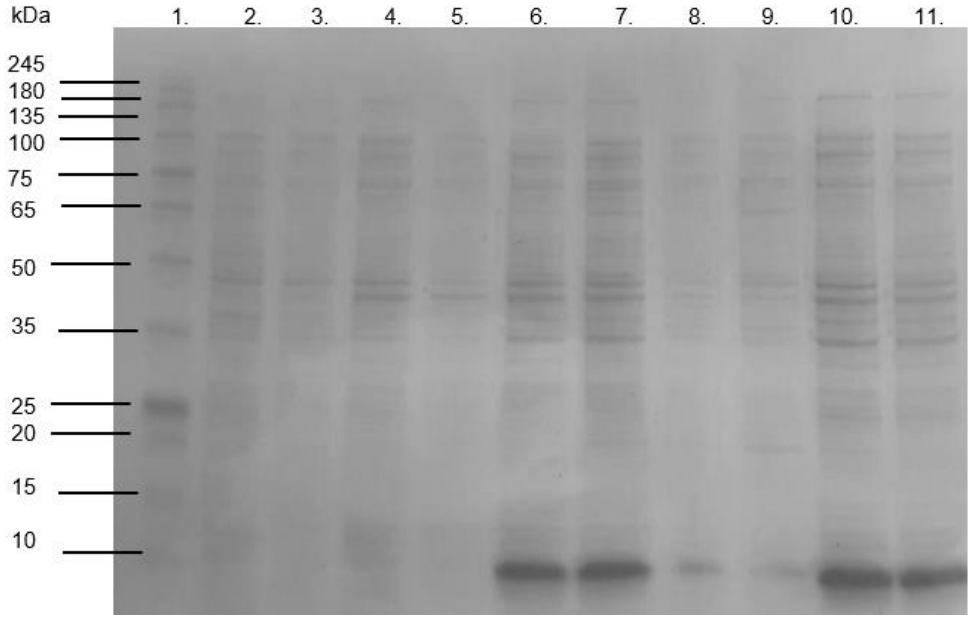

Figure 4.30. SDS PAGE analysis of keratinase expression in the presence of glucose at 30 or 37 °C, lane 1: protein ladder, lane 2: 30 °C pre-induction control, lane 3: 37 °C pre-induction control, lane 4: 4.5 hour post-induction 30 °C, lane 5: 4.5 hour post-induction 37 °C, lane 6: total protein (lysate) 30 °C, lane 7: total protein 37 °C, lane 8: soluble protein (cell-free extract) 30 °C, lane 9: soluble protein 37 °C, lane 10: insoluble protein washes 30 °C, lane 11: insoluble protein washes 37 °C.

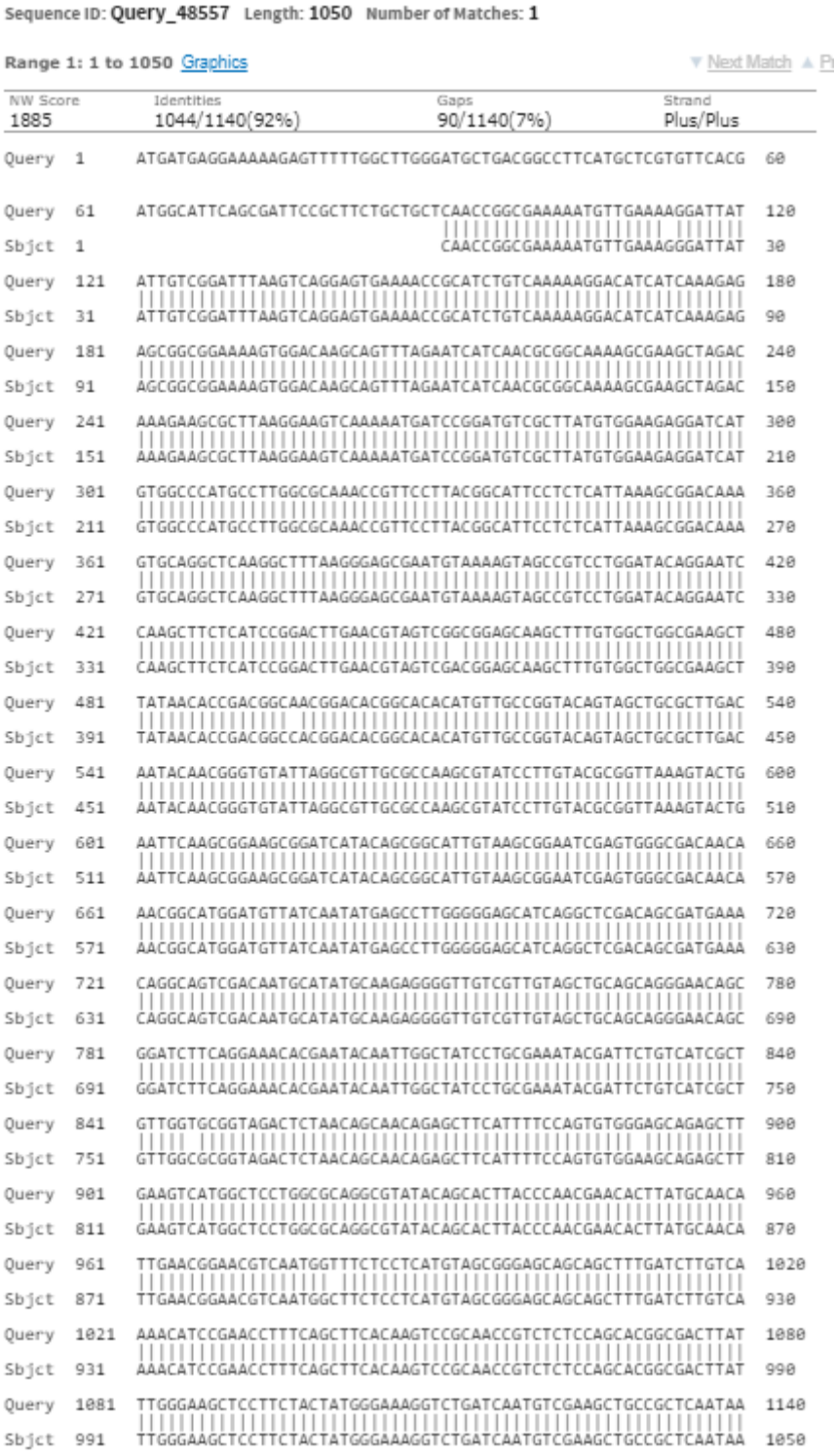

Figure 4.31. Sequence alignment between kerA from *Bacillus licheniformis* PWD-1 (Query 1, Lin 1992)[31] **and S90** (Subject 1, Hu 2013)[32], showing 68% identity. The BLAST function from the NCBI database was used.[294]

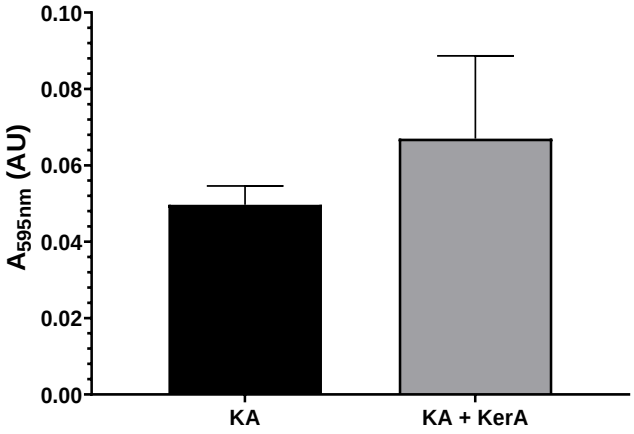

Figure 4.32. Keratin azure assay of keratinase from *Bacillus licheniformis*. Keratin azure (KA, 0.04 mg/mL) was incubated with KerA (3.0 U/mL or 8.8 µg/mL) for 20h incubation at 37 °C – data given as average values of triplicate reactions and shown ± the standard deviation.

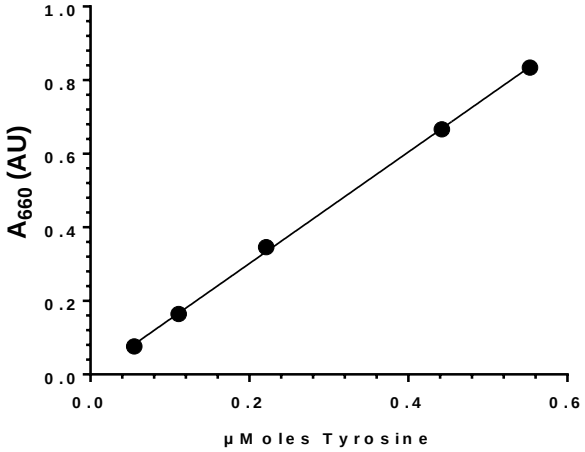

Figure 4.33. L-tyrosine standard curve (0.055-0.553 µmol) from *Bacillus licheniformis* keratinase proteolytic assay on casein.

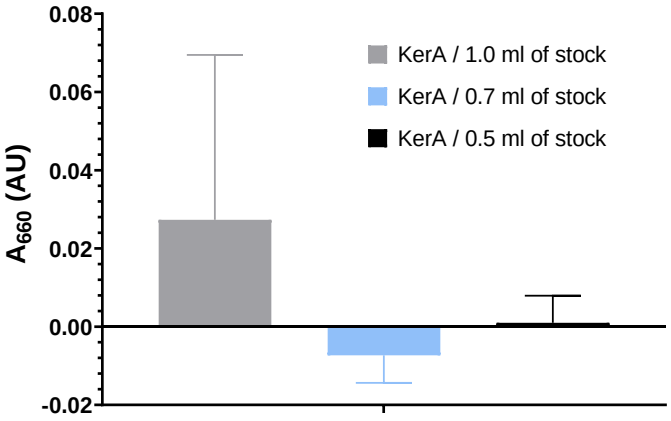

Figure 4.34. Casein assay of keratinase from *Bacillus licheniformis* (blank absorbances subtracted from test absorbances). KerA (0.01-0.02 U/mL or 0.03-0.06 µg/mL) incubated with

casein (2.9 mg/mL) for 10 minutes at 37 °C before TCA (8.2 mg/mL) addition. Casein digestion was monitored at 660 nm absorbance.

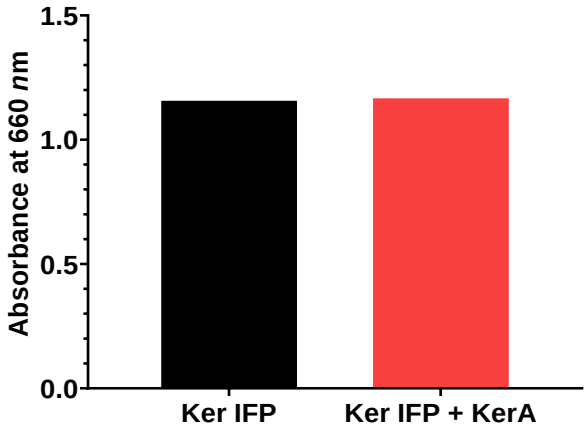

Figure 4.35. Keratinase activity assay based on Merck's casein assay using Keratec™ IFP as the substrate. KerA (0.05 Us/mL or 0.15 µg/mL) incubated with Keratec™ IFP (Ker IFP, 5.8 mg/mL) for 10 minutes at 37 °C before TCA (8.2 mg/mL final conc.) addition. Casein digestion was monitored at 660 nm absorbance. An untreated control was included, where the volume was made up using buffer.

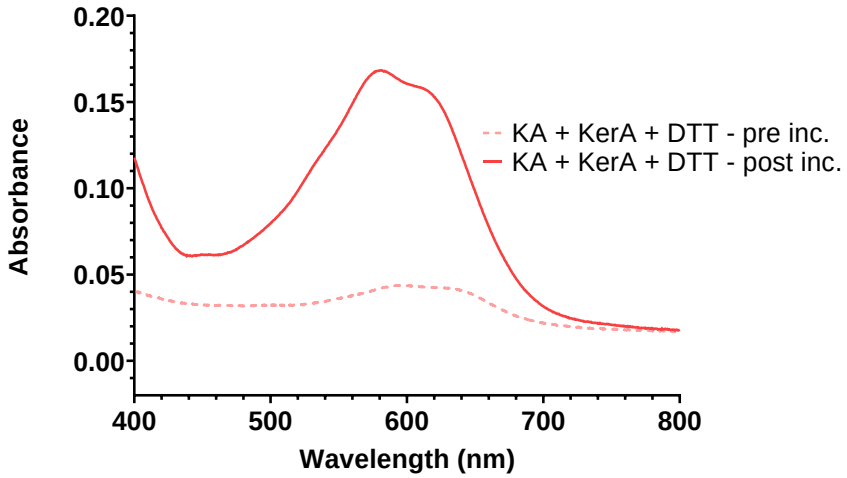

Figure 4.36. Absorbance spectrum of keratin azure incubation with keratinase and DTT. Keratin azure (KA, 4 mg/mL) was incubated with KerA (3.0 U/mL or 8.8 µg/mL) and DTT (20.8 mg/mL) in Tris buffer pH 7.5 for 20h at 37 °C – 400-800 nm spectra recorded before and after incubation.

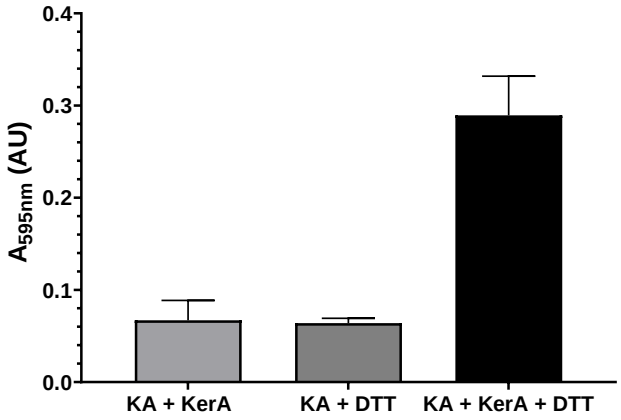

Figure 4.37. Keratin azure assay of keratinase in the presence of DTT. Keratin azure (KA, 4 mg/mL) was incubated with KerA (3.0 U/mL or 8.8 µg/mL) and/or DTT (20.8 mg/mL) in Tris buffer pH 7.5 for 20h at 37 °C – data given as average values of triplicate reactions and shown ± the standard deviation.

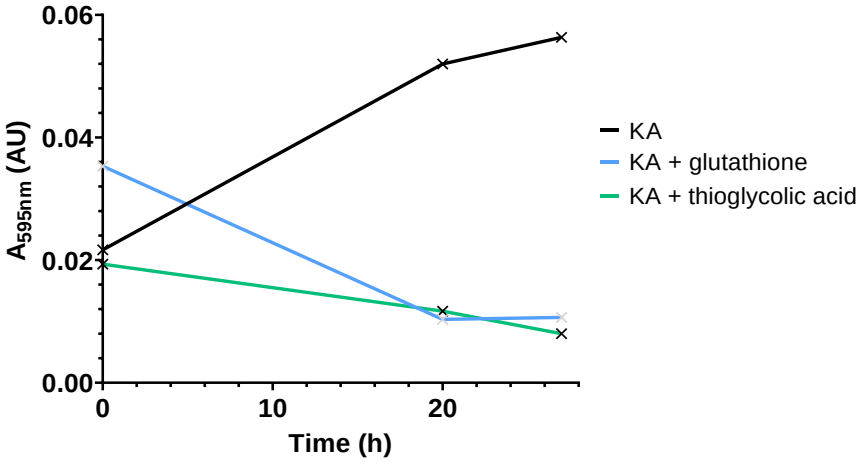

Figure 4.38. Keratin azure assay exploring dye degradation by glutathione and TGA. Keratin azure (KA, 4 mg/mL) incubated with KerA (3.0 U/mL or 8.8 µg/mL) and reducing agents (5% w/v, 49.7 mg/mL or glutathione: 0.16 mM, thioglycolic acid: 0.54 mM) in Tris buffer pH 7.5 for 24 h incubation at 37 °C, 250 rpm.

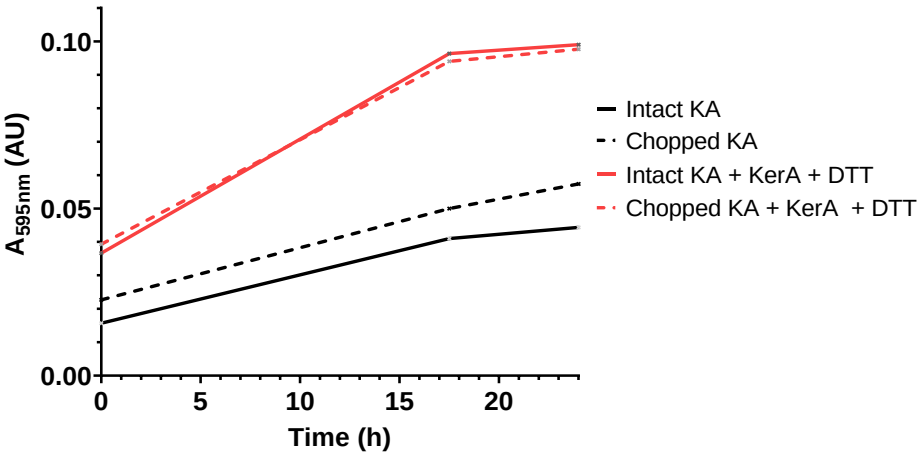

Figure 4.39. Keratin azure assay on chopped keratin azure. Chopped Keratin Azure (Chopped KA, 4 mg/ml) incubated with KerA (0.95 U/mL or 2.8 µg/mL) and DTT (49.7 mg/ml, 5% w/v) in Tris buffer pH 7.5, 24 h incubation at 37 °C, 250 rpm.

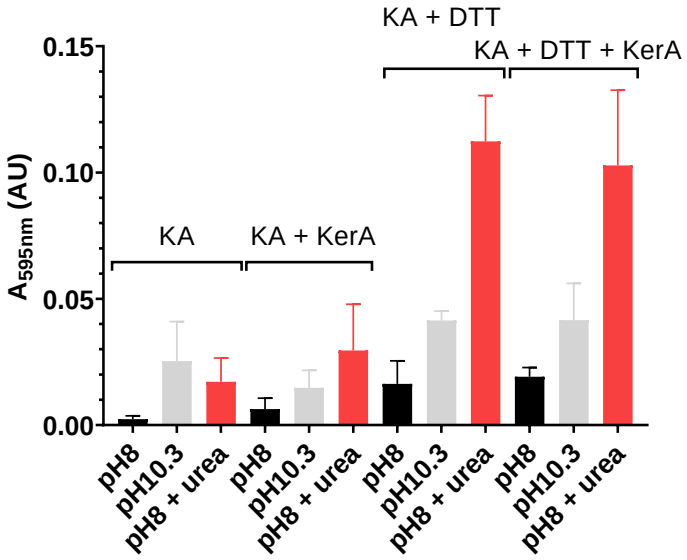

Figure 4.40. Effect of pH and urea on keratin azure assay. Keratin azure (KA, 4 mg/mL) was incubated with KerA (0.95 U/mL or 2.8 µg/mL) and DTT (49.7 mg/mL, 5% w/v) in the presence or absence of urea (4 M) in Tris buffer pH 8-10.3 for 1 hour at 37 °C, 250 rpm.

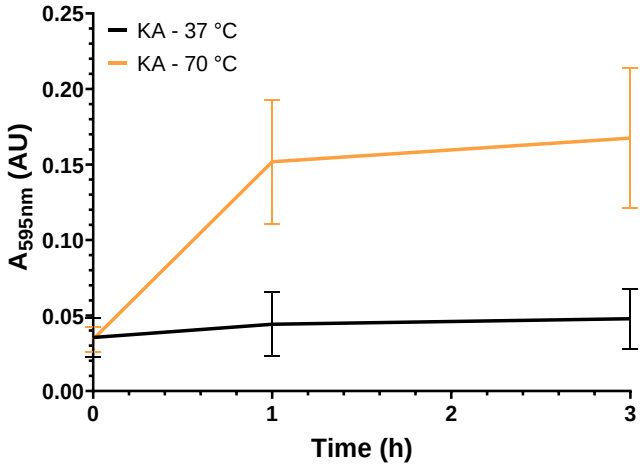

Figure 4.41. Keratin azure assay exploring the effect of incubation temperature on keratin azure. Keratin azure (KA, 4 mg/mL) incubated in Tris buffer pH 7.5 for 3 h at 37-70 °C, 250 rpm.

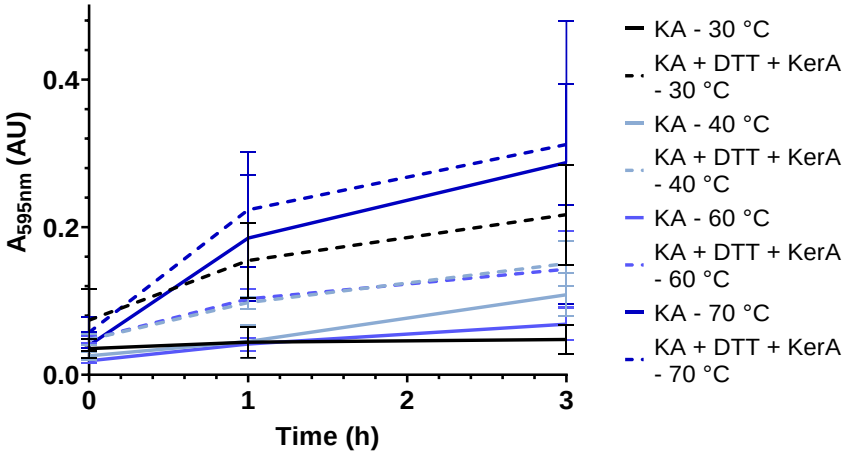

Figure 4.42. Temperature studies showcasing keratinase activity in the presence of DTT. Keratin azure (KA, 4 mg/mL) incubated with KerA (3.0 U/mL or 8.8 µg/mL) and DTT (49.7 mg/mL) in Tris buffer pH 8 for 3 h, 250 rpm at 30-70 °C.

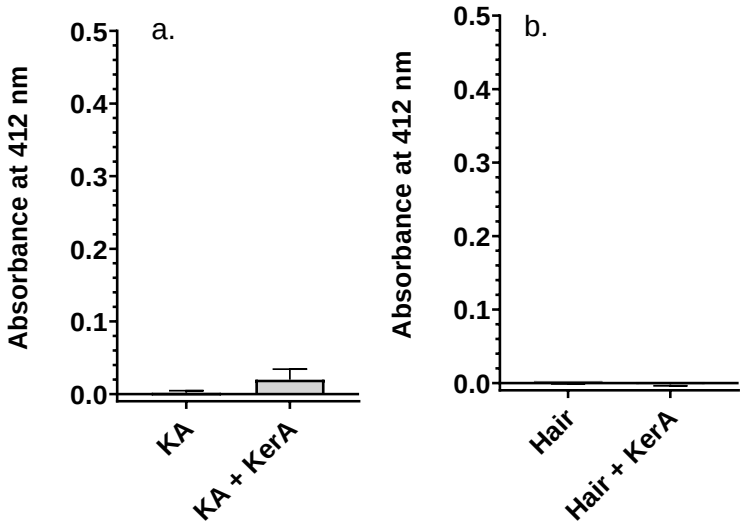

Figure 4.43. Ellman's assay of keratinase on keratin azure and human hair, (a) Keratin azure (KA, 4 mg/mL) incubated with KerA (0.75 U/mL or 2.2 µg/mL) in Ellman's buffer for 24 hours at 37 °C, 250 rpm, followed by 5 buffer rinsings and 30 min incubation with DTNB (0.08 mg/mL or 0.20 µM) and 412 nm absorbance measurements, (b) hair (8 mg/mL) incubated with KerA (1.5 U/mL or 4.4 µg/mL) in Ellman's buffer for 17 hours at 37 °C, 250 rpm, followed by 5 buffer rinsings and 30 min incubation with DTNB (0.08 mg/mL or 0.20 µM) in buffer and 412 nm absorbance measurements - data given as average values of triplicate reactions (final wash subtracted from sample absorbance) and shown ± the standard deviation.

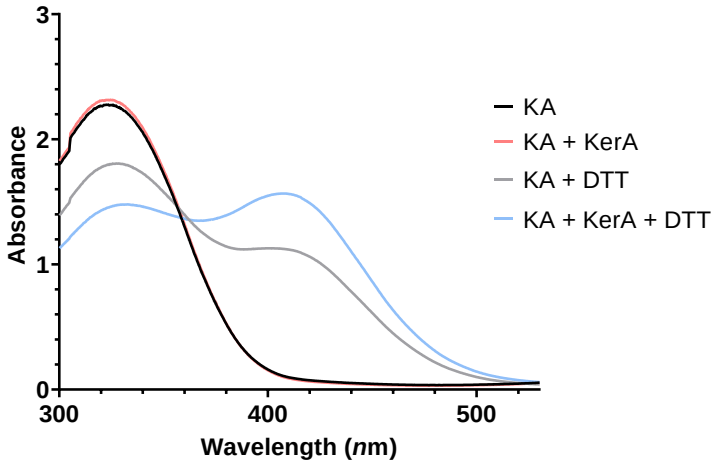

Figure 4.44. Absorbance spectra for keratin azure treated with keratinase and DTT. Keratin azure (KA, 4 mg/mL) incubated with KerA (1.5 U/mL or 4.4 µg/mL) and DTT (49.7 mg/mL, 0.31 M) in Ellman's buffer 24 hour at 37 °C, 250 rpm, followed by 5 buffer rinsings and 30 min incubation with DTNB (0.08 mg/mL or 0.20 µM) and 412 nm absorbance measurements – final wash not subtracted from sample absorbance.

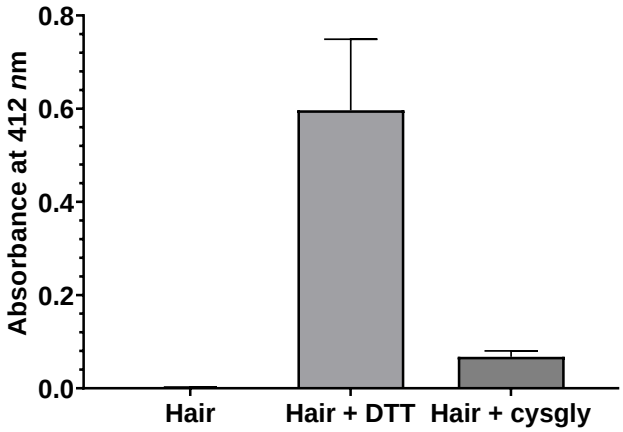

Figure 4.45. Elman's assay on human hair in the presence of DTT or cysteinyl glycine reducing agents. Hair (8 mg/mL) was incubated with reducing agents (DTT or cysteinyl glycine - 1 mM) in 100 mM sodium phosphate buffer with 1 mM EDTA, pH 8 (2.5 mL) for 1 hour at 37 °C, 250 rpm. Following thorough rinsing, DTNB (0.2 mg/mL) was added to the substrate in 2.5 mL buffer and incubated at room temperature for 15 minutes before 412 nm absorbance measurements - data given as average values of triplicate absorbance measurements (final wash absorbances were subtracted) and shown ± the standard deviation.

5. Enzymatic crosslinking of keratin

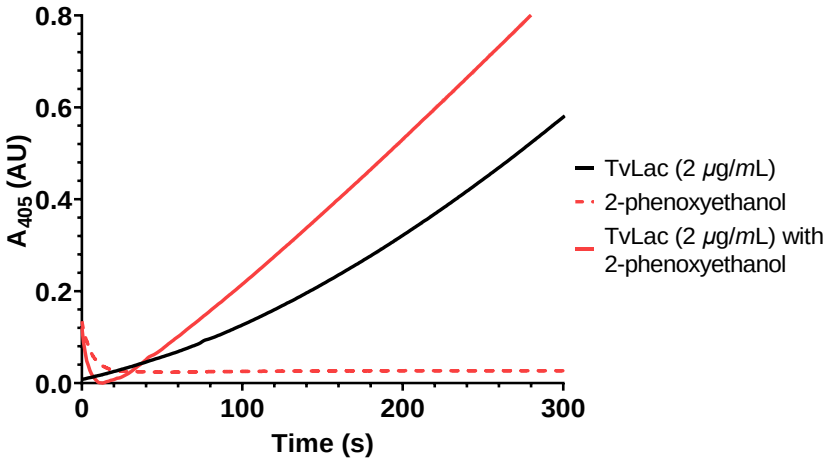

Figure 5.1. Effect of 2-phenoxyethanol on *Trametes versicolor* laccase activity assay. TvLac (6.82 mU/mL or 2 µg/ml) was incubated with ABTS (1 mM) and 2-phenoxyethanol (80 mM) in dH_2O at 25 °C and 405 nm absorbance monitored over time.

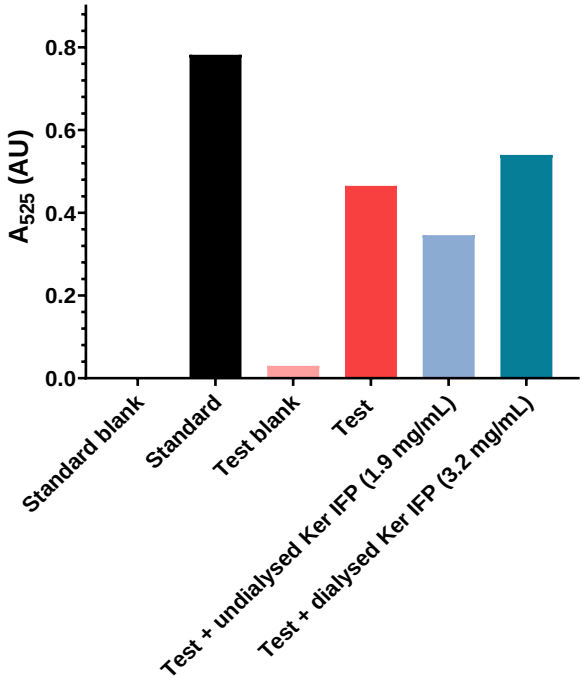

Figure 5.2. Effect of undialysed and dialysed Keratec™ IFP on microbial transglutaminase *via* Cbz-Gln-Gly assay. Test composed of Tg (0.097 U/mL or 6.86 µg/mL) with Cbz-Gln-Gly (31 mM), hydroxylamine (87 mM), reduced glutathione (8.7 mM), calcium chloride (4 mM) and undialysed Keratec™ IFP (Ker IFP, 1.9 mg/mL) or dialysed Keratec™ IFP (Ker IFP, 3.2 mg/mL) in Tris buffer pH6 and deionised water, at pH 6 at 37 °C (test blank without transglutaminase). Standard made from L-Glutamic Acid γ-monohydroxamate (1mM) in deionised water (standard blank without L-Glutamic Acid γ-monohydroxamate). Absorbances were recorded at 525 nm.

Table 5.1. Turbidity analysis of casein at different incubation temperatures via 660 nm absorbance measurements. Casein (6 mg/mL) incubated in potassium phosphate buffer pH 7.5 at 5-55 °C for 30 minutes.

Incubation temperature / °C	*600 nm absorbance*
5	1.539
25	1.479
55	1.832

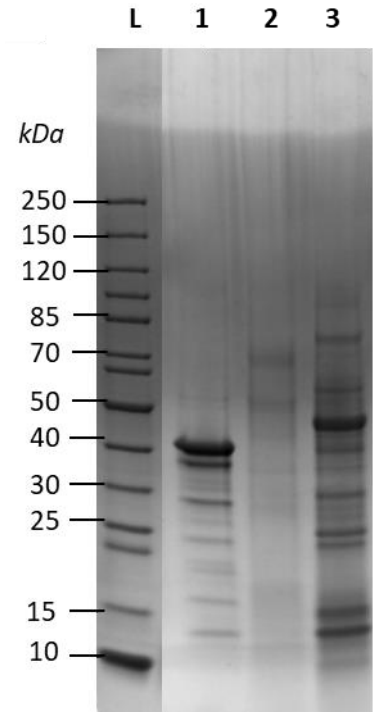

Figure 5.3. SDS PAGE analysis of TvLac (97 kDa), Tyr (119.5 kDa) & Tg (38 kDa). L = Ladder, 1 = Tg, 2 = TvLac and 3 = Tyr (15 µg per well)

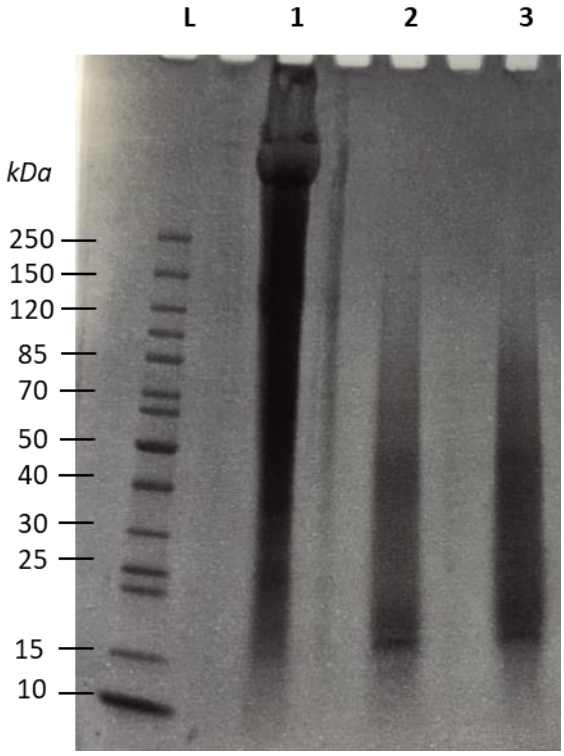

Figure 5.4. SDS PAGE analysis of gelatine crosslinking by laccase from *Trametes versicolor* - Gelatine (10 mg/mL) was incubated in the presence or absence of TvLac (1.71 U/mL or 0.5 mg/mL) in dH_2O with or without ABTS (1mM) overnight at 37°C, 250 rpm – L=protein ladder, 1=Gelatine alone sample, 2=Gelatine + laccase, 3=Gelatine + laccase + ABTS.

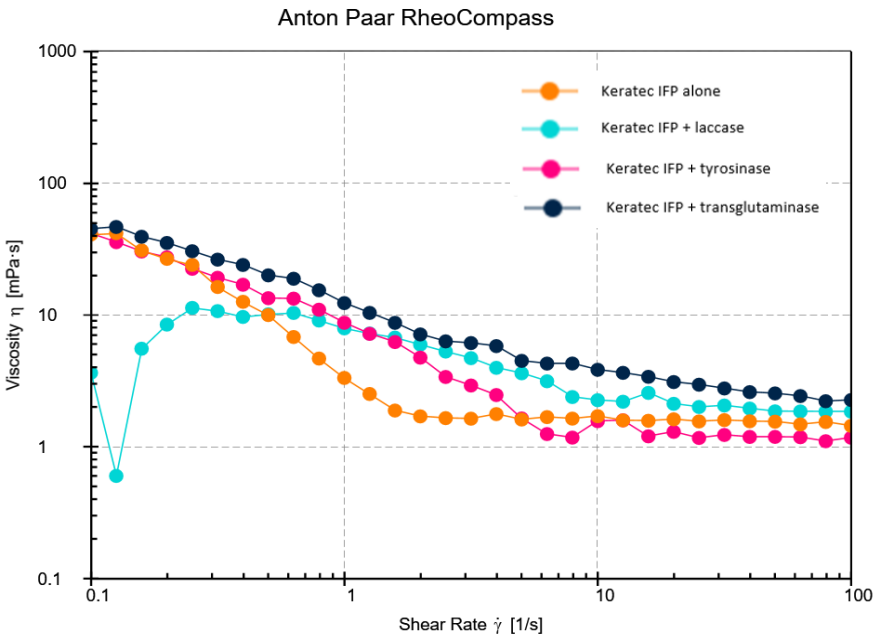

Figure 5.5. Enzymatic crosslinking monitoring *via* viscosity analysis over sheer rate. TvLac (0.204 U/mL or 60 µg/mL), Tyr (0.66 U/mL or 60 µg/mL) or Tg (0.045 U/mL or 3.15 µg/mL) incubated with Keratec™ IFP (32.5 mg/mL) in acetate pH 5 (TvLac), Tris pH 7.5 (Tyr) and Tris pH 6 (Tg) buffers overnight at 37 °C, 250 rpm before viscosity measurements.

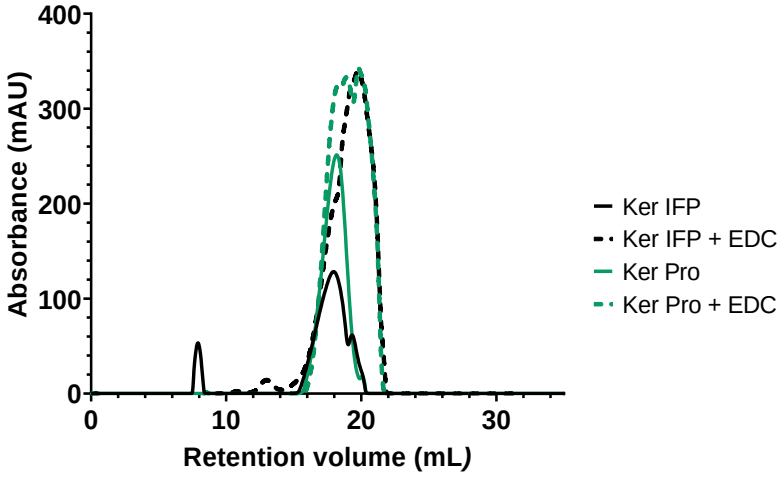

Figure 5.6. SEC analysis of dialysed Keratec™ IFP and Keratec™ ProSina crosslinking with EDC. Dialysed Keratec™ IFP (Ker IFP, 19.9 mg/mL) and Keratec™ ProSina (Ker Pro, 7.3 mg/mL) in dH_2O incubated overnight at 37°C, 250 rpm in the presence or absence of EDC (56 mM) crosslinker and injected into SEC column.

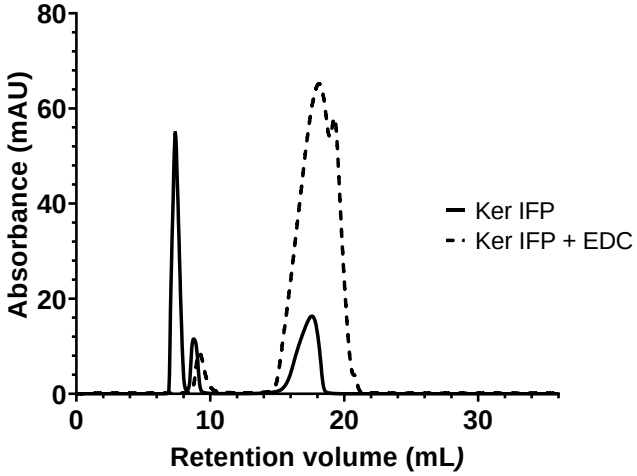

Figure 5.7. SEC analysis of EDC-crosslinking of dialysed Keratec™ IFP. Dialysed Keratec™ IFP (Ker IFP, 17.7 mg/mL) incubated for 4 hours in dH_2O at 37 °C, 250 rpm in the presence or absence of EDC (56 mM) crosslinker.

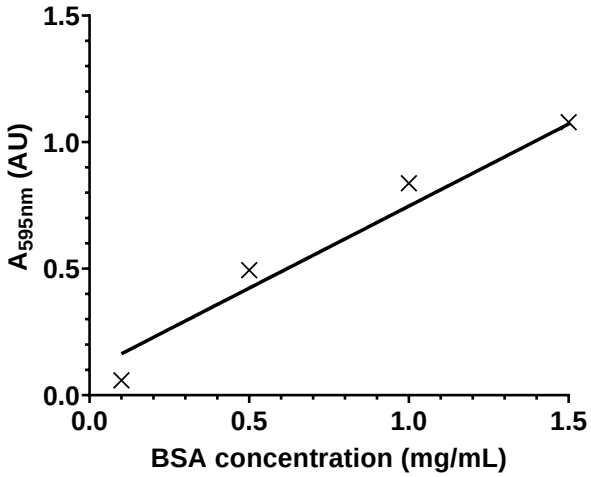

Figure 5.8. Bradford assay of SEC fractions– BSA standard curve.

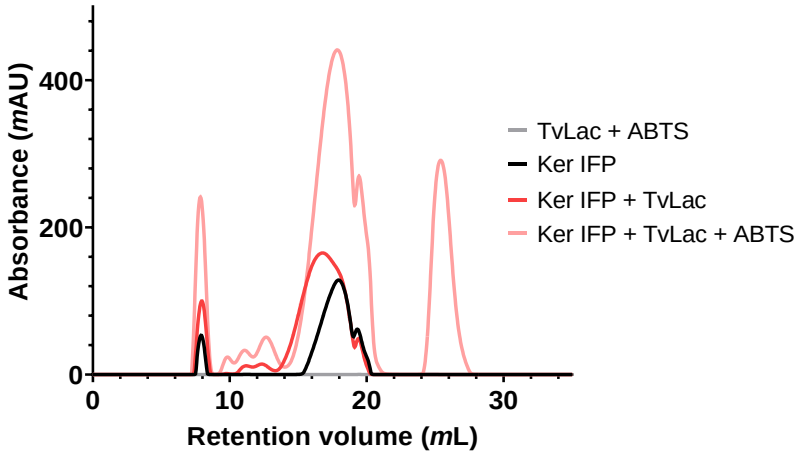

Figure 5.9. Effect of ABTS on Keratec™ IFP crosslinking by laccase from *Trametes versicolor via* SEC. TvLac (1.71 U/mL or 0.5 mg/mL) incubated with dialysed Keratec™ IFP

(Ker IFP, 11.1 mg/mL) in the presence or absence of ABTS (1mM) in dH_2O, overnight at 37°C, 250 rpm.

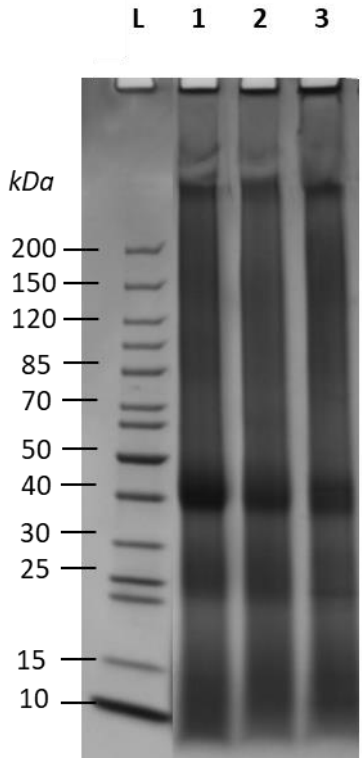

Figure 5.10. SDS PAGE analysis of undialysed Keratec™ IFP crosslinking by laccase from *Trametes versicolor.* TvLac (1.71 U/mL or 0.5 mg/mL) was incubated with undialysed Keratec™ IFP (6.5 mg/mL) in dH_2O overnight at 37°C, 250 rpm, in the presence or absence of vanillin (1mM) – L=protein ladder, 1=Undialysed keratec IFP, 2=Undialysed keratec IFP + TvLac, 3=Undialysed IFP + TvLac + vanillin.

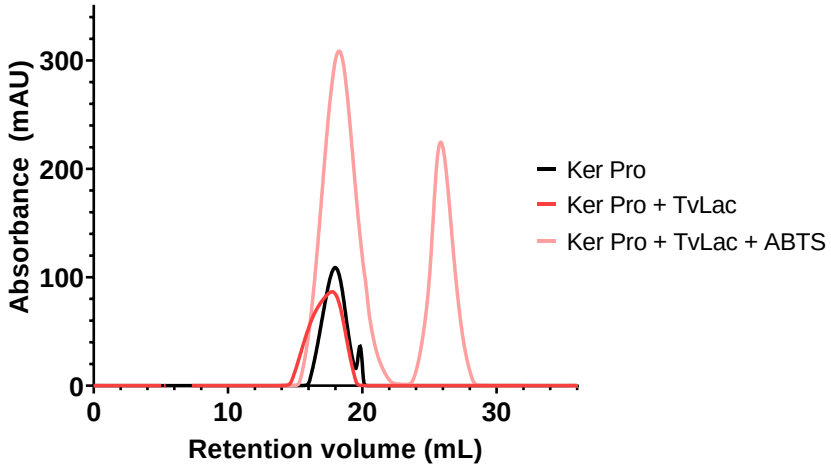

Figure 5.11. SEC analysis of laccase from *Trametes versicolor* on dialysed Keratec™ ProSina. TvLac (1.71 U/mL or 0.5 mg/mL) was incubated with dialysed Keratec™ ProSina (Ker Pro, 7.3 mg/mL) in dH_2O, overnight at 37°C, 250 rpm, in the presence or absence of ABTS (1 mM).

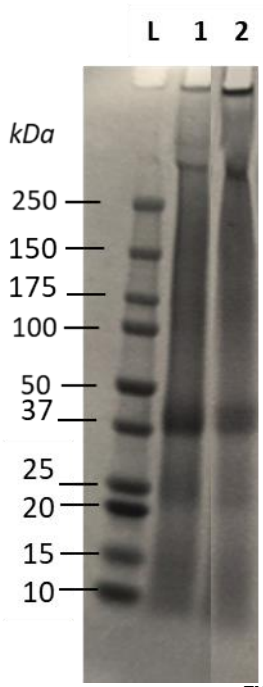

Figure 5.12. SDS PAGE analysis of dialysed Keratec™ IFP crosslinking by tyrosinase from mushroom. Tyr (5.47 U/mL or 0.5 mg/mL) was incubated with dialysed Keratec™ IFP (11.1 mg/mL) in dH_2O at 37°C, 250 rpm - L=protein ladder, 1=Dialysed Keratec™ IFP, 2=Dialysed Keratec™ IFP + Tyr

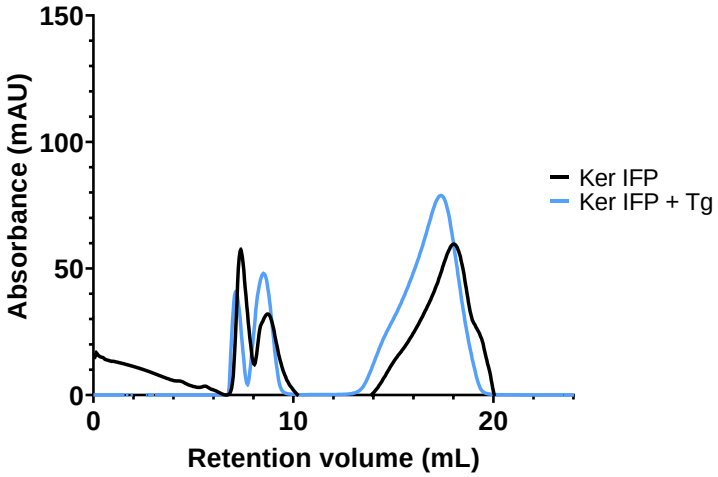

Figure 5.13. SEC analysis of microbial transglutaminase activity on dialysed Keratec™ IFP. TG (0. 5 U/mL or 13.15 µg/mL) was incubated with dialysed Keratec™ IFP (Ker IFP,11.1 mg/mL) in Tris buffer pH 6 overnight at 37°C, 250 rpm.

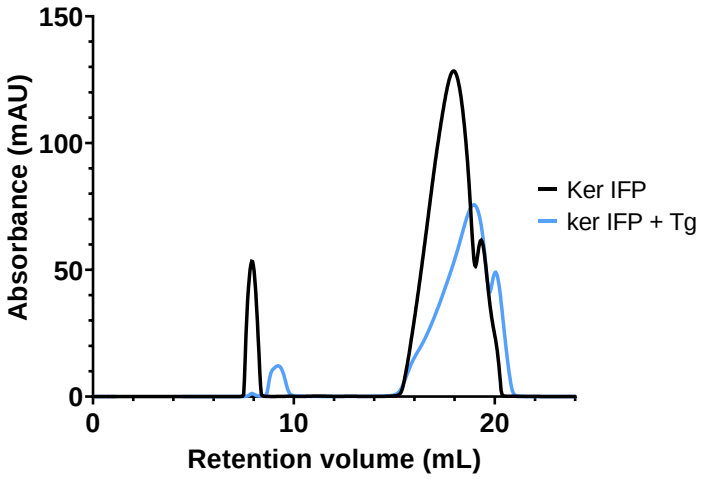

Figure 5.14. SEC analysis of microbial transglutaminase activity on dialysed Keratec™ IFP. Tg (0. 5 U/mL or 13.15 µg/mL) was incubated with dialysed Keratec™ IFP (Ker IFP,11.1 mg/mL) in Tris buffer pH 6 overnight at 37°C, 250 rpm.

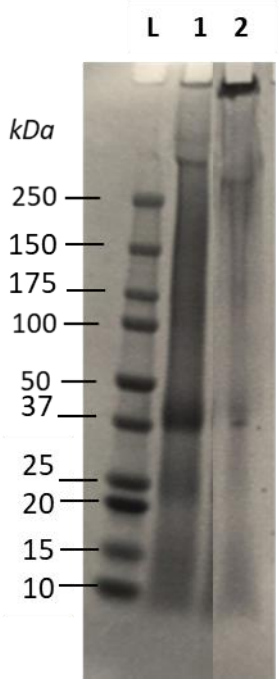

Figure 5.15. SDS PAGE analysis of dialysed Keratec™ IFP crosslinking by microbial transglutaminase. Tg (0. 5 U/mL or 13.15 µg/m) was incubated overnight with Keratec™ IFP (11.1 mg/mL)) in Tris buffer, pH6 at 37°C, 250 rpm – L=ladder, 1=Dialysed Keratec™ IFP, 2=Dialysed Keratec™ IFP + Tg.

9. Covid statement

During the first year of my PhD, I was faced with a change of supervisors, research group and faculty, which resulted in a lack of access to labs between October and December 2019. Following this disruption, I adapted to the new lab, and started to work towards my readjusted experimental goals. The pandemic then occurred and led to lab closures between March and August 2020. This of course greatly hindered my progress due to my project being entirely experimental. I re-focused my work in order to best use that time outside of the lab. I learned about bioinformatic technologies to identify more enzyme sequences and used them to conduct a literature review and sequence search towards identifying potential disulfide bond reducing enzyme candidates. I also planned exact expression and assay protocols to be used when labs reopened and familiarised myself with useful data analysis and protein visualisation software. Despite my best efforts to mitigate the impacts of covid lab closures, I still accumulated severe delays to my research objectives. Once the lab reopened (on a 1 week on, 1 week off basis) in August 2020, I immediately resumed experimental work. However, the efficiency of the work was greatly reduced and access to equipment was limited, which went on until the end of 2020. As a result, I readjusted my experimental targets, having to drop some planned experiments, and have since worked against the clock to meet the clear objectives of my project, designed in collaboration with the industrial partner at the start of the PhD.

Due to the pandemic and the restricted visitor access that ensued, I was unable to do a placement with my industrial partner. I believe that working within a team specialised in hair care would have been very valuable towards

gaining a more industry-based insight to my project and its impact beyond my own research. I was luckily able to spend a day within the Croda labs more recently to conduct tensile strength experiments on hair samples, however a much more thorough approach could have been taken by having more time there.

Overall, while I believe that this thesis would have benefited from further crosslinking assays on hair at the Croda labs, as well as increased robustness towards work conducted with keratinase, I have done my best to mitigate the impact the pandemic had on my research outcomes.